AD NUMBER

AD857263

NEW LIMITATION CHANGE

TO

Approved for public release, distribution unlimited

FROM

Distribution authorized to U.S. Gov't. agencies and their contractors; Critical Technology; MAR 1969. Other requests shall be referred to Air Force Materials Laboratory, ATTN: MAAE, Wright-Patterson AFB, Oh 45433.

AUTHORITY

AFML ltr dtd 12 Jan 1972

AFML-TR-68-163
Volume II

TENSILE PROPERTIES AND FRACTURE TOUGHNESS OF 6Al-4V TITANIUM

C. E. Hartbower
W. G. Reuter
P. P. Crimmins

Aerojet-General Corporation
Sacramento, California 95813

Technical Report AFML-TR-68-163, Volume II
March 1969

This Document Contains
Missing Page/s That Are
Unavailable In The
Original Document

OR are
Blank pgs.
that have
Been Removed

AFML-TR-68-163
Volume II

TENSILE PROPERTIES AND FRACTURE TOUGHNESS OF 6Al-4V TITANIUM

C. E. Hartbower
W. G. Reuter
P. P. Crimmins

Technical Report AFML-TR-68-163, Volume II
March 1969

Air Force Materials Laboratory
Research and Technology Division
Air Force Systems Command
Wright-Patterson Air Force Base, Ohio

FOREWORD

This report was prepared by Aerojet-General Corporation, Sacramento, California, under USAF Contract F33615-67-C-1358. The contract was initiated under Project No. 7381, a Materials Applications, Task No. 738106, "Engineering and Design Data", and administered under the direction of the Air Force Materials Laboratory, Wright-Patterson Air Force Base, Ohio, with Mr. A. W. Gunderson (MAAE) as Project Engineer.

The study program at the Aerojet-General Corporation was performed under the management of P. P. Crimmins, Manager of Structural Metals Research and Development, Materials Advanced Technology Department, with C. E. Hartbower as Principal Investigator.

The authors gratefully acknowledge the many helpful comments and suggestions made by A. W. Gunderson of the Air Force Materials Laboratory during the conduct of this program. The authors are also indebted to Mrs. Mary W. Fong of the Aerojet Computing Sciences Division for her assistance in statistical analysis of the data.

This report covers the period April 1968 to March 1969. The report was submitted by the authors in March 1969.

This technical report has been reviewed and approved.

A. Olevitch
Chief, Materials Engineering Branch
Systems Support Division
Air Force Materials Laboratory

ABSTRACT

Material taken from 6Al-4V titanium rocket motor cases was tested with precrack Charpy impact specimens to evaluate the following as factors affecting plane-stress crack toughness and/or chamber performance: (1) anisotropy and inhomogeneity, (2) forging practice (die, ring-roll and extrusion), (3) interstitial-element chemistry, and (4) test temperature. The material was obtained from 14 hydroburst Minuteman chambers, nine of which were premature-proof-test failures, four were successfully hydroburst chambers, and one failed after 11 proof-test cycles. Material sampling included the immediate vicinity of fracture origins in an attempt to correlate fracture toughness and chamber performance.

Significant differences in precrack Charpy W/A values were found between (1) the two chamber wall thicknesses tested, (2) forgings, (3) forging practices and (4) test temperatures. Some individual cylinders appeared to have a marked difference in W/A value from end-to-end in both the membrane wall and the reinforced sections. However, analysis of variance did not show a significant difference from end-to-end of the cylinders. Multiple regression and correlation analysis indicate carbon and oxygen to have a significant effect on toughness in the Minuteman chemistry. In four out of six chambers with secondary fractures in the hoop direction, the W/A values in the hoop direction were either very low or lower than those in the axial direction. Variable response to temperature and forging-to-forging differences necessitate fracture testing of every forging in critical service applications.

Relationships between fracture toughness and chamber performance were evaluated. Because of the relatively low plane-stress crack toughness of the material, Irwin's leak-before-burst criterion was not met. Thus, the chambers failed as a result of plane-strain pop-in. In chambers with semi-elliptical surface flaws, an attempt was made to predict the hoop stress at failure on the basis of the measured flaw dimensions and the mean K_{Ic} value as determined from 109 forgings in Phase I; viz, 39 ksi-in.$^{1/2}$ with a standard deviation of 1.6 ksi-in.$^{1/2}$. The prediction was in close agreement in five out of six cases based on a two-sigma spread in K_{Ic} value.

TABLE OF CONTENTS

APPENDIXES

LIST OF TABLES

LIST OF TABLES

LIST OF TABLES

LIST OF ILLUSTRATIONS

LIST OF ILLUSTRATIONS (cont.)

LIST OF ILLUSTRATIONS (cont.)

SECTION I

INTRODUCTION

Phase I, a MIL-HDBK-5 data collection program, has been completed to provide room- and elevated-temperature-tensile and fracture-toughness data on 6Al-4V titanium at a 0.2% offset yield strength of approximately 160 ksi. The data were presented in Technical Report AFML-TR-68-163, Volume I, September 1968, entitled "Tensile Properties and Fracture Toughness of 6Al-4V Titanium" (378 pages, including five appendices). The material was from 44- and 52-in.-dia second-stage Minuteman rocket-motor cases. The elevated-temperature tensile data were for temperatures up to 330°F. The fracture toughness data included plane-strain K_{Ic} from 540 part-through-crack (PTC) tensile tests of 109 forgings, plane-stress K_c from 75 fatigue-precracked center-notch (CN) tensile tests of 18 forgings, and precrack Charpy slow-bend and impact tests of specimens cut from fractured CN-tensile specimens. The 18 forgings were from nine hydroburst chambers, four of which were premature proof-test failures and five were successfully hydroburst in the Minuteman development program.

The uniaxial tensile-data means were determined for each temperature and plots of percent-of-room temperature tensile-properties versus temperature were constructed for input to MIL-HDBK-5. For room temperature, the A-basis values of ultimate strength, yield strength, and percent elongation were 166.3 ksi, 153.0 ksi, and 10.2%, respectively; the B-basis values were 168.8 ksi and 156.4 ksi, respectively. The PTC-tensile specimens were oriented in the hoop direction; i.e., the flaw was propagating in the axial direction of the cylinder. The PTC-tensile K_{Ic} data were examined for the variation in fracture toughness attributable to between-forging, between-heat, and between-test-laboratory variability, first on the basis of engineering plots of data from individual laboratories, forgings, billets, and heats, and then by statistical-analysis techniques. Based on the engineering plots, tests of multiple forgings from a single heat of titanium and multiple forgings from a single billet of titanium revealed differences in K_{Ic} from forging to forging when the surface precrack was deep (approximately 50% of specimen thickness) but little or no difference in K_{Ic} with a shallow crack (approximately 25% of specimen thickness). Comparisons between laboratories revealed differences between test results in some forgings but not all. Based on statistical analysis, a significant difference was indicated between K_{Ic} values at the two crack depths investigated. However, statistically, there was not a significant difference between forgings or between heats with shallow cracks, whereas, with deeper cracks there was a significant difference between heats but not a significant difference between forgings. When the data from the shallow cracks were pooled and plotted on probability paper, the population mean was 39.1 ksi-in.$^{1/2}$ with a standard deviation of 1.6 ksi-in.$^{1/2}$. On the basis of all 540 tests, treated as a non-normal distribution, the A-basis value was 30.6 ksi-in.$^{1/2}$ and the B-basis value was 35.2 ksi-in.$^{1/2}$.

I, Introduction (cont.)

The CN-tensile specimens were oriented in the axial direction; i.e., the flaw was propagating in the hoop direction. The CN-tensile K_{Ic} values ranged from 31.2 to 74.6 ksi-in.$^{1/2}$; thus, the K_{Ic} values in some forgings were appreciably higher than any values measured in the PTC-tensile tests of 109 forgings tested with a different crack orientation. Precrack Charpy slow-bend W/A values were found to provide a good estimate of the CN-tensile K_{Ic} values through the relationship

$$K_{Ic} = 170\ (W/A)_{PCSB} + 16200$$

where $(W/A)_{PCSB}$ is the precrack Charpy slow-bend value in in.-lb/in.^{2}. The CN-tensile K_c data based on the onset of crack instability as determined by an acoustical technique ranged from 71 to 137 ksi-in.$^{1/2}$ for the 18 forgings tested. Precrack Charpy impact W/A values were found to provide a good estimate of the CN-tensile K_c values through the relationship

$$K_c = 100\ (W/A)_{PCI} + 6700$$

In the Phase I data collection, the orientation of the CN-tensile specimen was such that the crack was propagating in the chamber hoop direction; i.e., at 90 degrees to the principal direction of fracture in the premature proof-test failures of full-scale chambers. No attempt was made in Phase I of the data collection to correlate the laboratory test results with full-scale Minuteman chamber performance because (1) anisotropy in the forgings precluded correlation between CN-notch tensile specimens oriented for fracture in the hoop direction and chamber performance with fracture in the axial direction; and (2) reliable axial-crack-propagation CN-tensile data could not be obtained in the reinforced (increased-thickness) region containing the chamber girth welds where fracture usually initiated in premature proof-test failures of full-scale chambers. Thus, Phase II, as described in the following paragraphs, sought correlation with full-scale chamber performance using the fatigue-precracked Charpy impact test specimen.

The material for Phase II of the data collection was obtained from 14 full-scale hydroburst Minuteman chambers, including eight of the nine chambers investigated in Phase I. Nine of the 14 chambers were premature proof-test failures, four were successfully hydroburst chambers and one was cycled 11 times before it failed in proof test. Closures, skirts, and cylinders from the 14 chambers provided data on 69 forgings, involving three forging practices; viz, die, ring roll and extrusion. The small size of the precrack Charpy specimen permitted testing with the specimen oriented so as to fracture in the chamber-axial direction. The Charpy specimens were located in both the 0.19-in.-thick reinforced section adjacent to the girth

welds and the 0.10-in.-thick walls on either side of the girth-weld reinforced sections. Selected forgings in each chamber were tested at -40, RT, 200, and 320°F. Particular attention was directed to the material in the immediate vicinity of the fracture origin in each of the chambers that failed in proof test.

The objectives of the Phase II data collection were as follows: (1) correlation of fracture toughness and chamber performance; (2) evaluation of anisotropy and inhomogeneity in chamber components as factors affecting chamber performance; (3) evaluation of forging practice (metal processing) as a factor affecting crack toughness; (4) evaluation of chemistry as a factor affecting crack toughness; (5) evaluation of test reproducibility (between Phases I and II and replicate tests); and (6) evaluation of the effect of temperature as an environmental factor affecting crack toughness.

SECTION II

TEST PROCEDURE

A. MATERIAL SAMPLING

Phase I of this study indicated a variation in toughness both with crack direction (anisotropy) and with specimen location in a given forging (inhomogeneity). Thus, in Phase II of the data collection, the material sampling procedure was designed to determine the extent of variability from location to location in a given forging as well as to evaluate toughness in the immediate vicinity of the fracture origin. Because fracture in the full-scale chambers usually propagated in the chamber-axial direction, and because several of the premature failures initiated in the reinforced section at a girth weld, it was necessary to machine the Charpy specimens in the hoop direction (crack propagating in the chamber-axial direction) and in the immediate vicinity of the girth welds. The combination of (1) dimensions of the reinforced wall at the girth welds, (2) the inherent curvature in the material cut from the 52-in.-dia chamber, and (3) the direction of fracture in the full-scale chambers, individually and collectively, precluded the use of specimens larger than the precrack Charpy. Obviously, if the 3-in.-wide center-notched panel (used in Phase I of the collection) were machined with the notch centered on the weld reinforcement, the $2a_o$ crack length would have exceeded the width of the reinforced section and, moreover, the test section in the path of fracture would have been of variable thickness. Taking these limitations into account, the widest CN-tensile that could have been used to test the reinforced section of the Minuteman girth welds was approximately 1 in. Also, the curvature in the CN-tensile would have produced a bending stress that would have been a complication in calculating the fracture toughness; and, furthermore, if the material had been heat-straightened preparatory to testing, the properties of the material could have been substantially changed by the plastic deformation introduced in the flattening operation.

In premature proof-test failures originating from girth-weld reinforced sections, the crack origin was often found to be transverse to the weld and located in the base metal adjacent to the weld, bounded on one side by weld heat-affected zone and on the other by parent metal. In other words, the initiating cracks were usually outside the weld fusion zone but close enough to the weld to extend partially into the weld heat-affected zone.

The size of the Charpy specimen allowed it to be positioned in the reinforced section with the V-notch in the weld metal and the fatigue precrack extending into the heat-affected base metal. Figure 1 shows the position of the Charpy in the reinforced section adjacent to a girth weld; Figure 1 also shows the macrostructure as contained in a typical specimen. Note the location of the V-notch and fatigue precrack with respect to the darkly etched weld heat-affected zone. In an occasional test specimen, because of irregularities in the width of the weld deposit, the weld metal extended somewhat below the fatigue precrack; in such cases, both the fracture appearance and the magnitude of the toughness values made the discrepancy apparent.

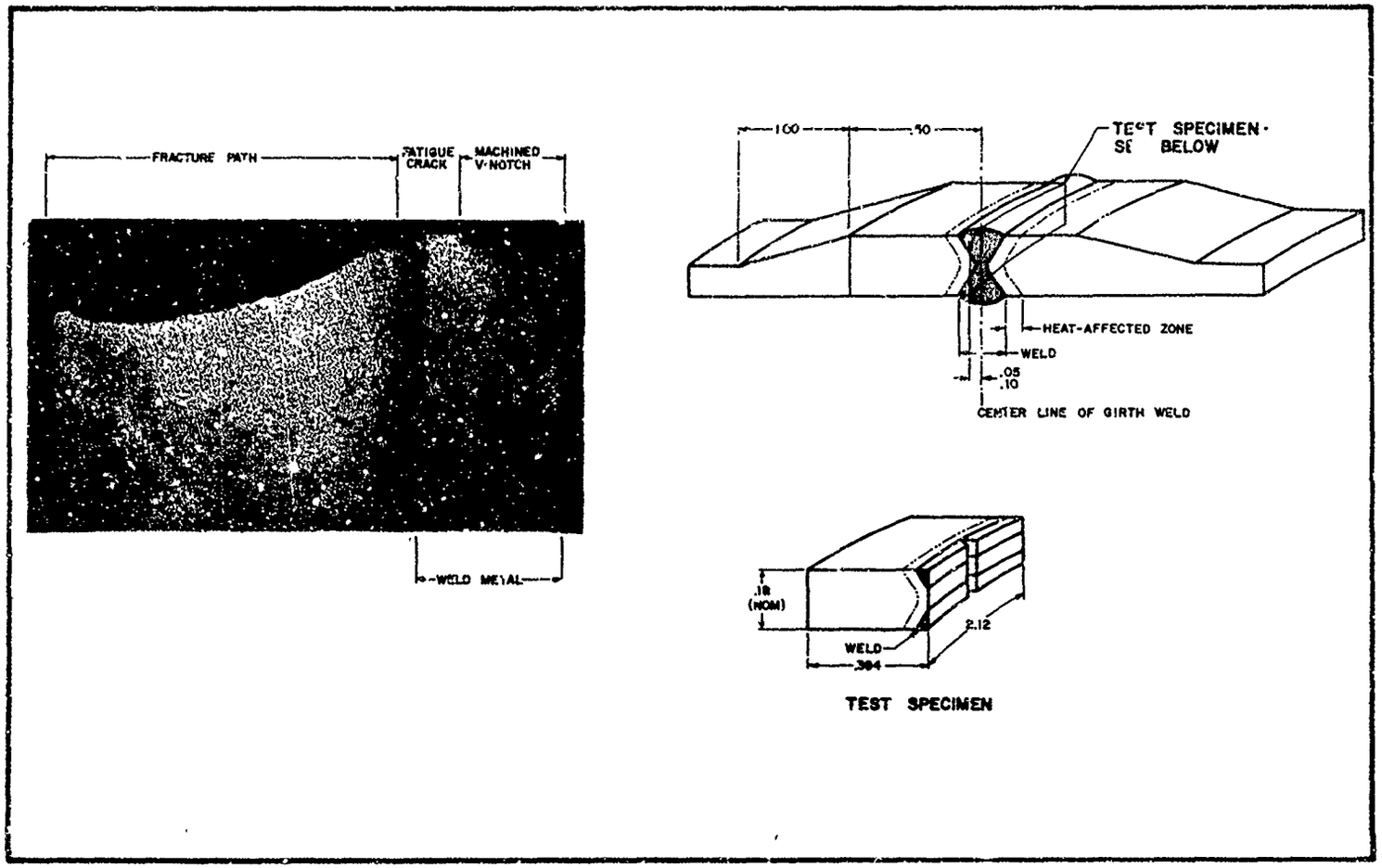

Figure 1. Location of Precrack Charpy Impact Specimens in Reinforced Section at Chamber Girth Welds

II, A, Material Sampling (cont.)

From Figures 2 and 3 (44-in. and 52-in.-dia chambers), it will be seen that one major difference between the 44-in.-dia and the 52-in.-dia chambers was in the interstage connection. In the 44-in.-dia chamber, the skirts were an integral part of the closure die-forgings; whereas, in the 52-in.-dia chamber, the skirts were ring-rolled forgings joined to the closure die-forgings by welding. The cylinders in the 52-in.-dia chambers were, in each case, extrusions; whereas, in the 44-in.-dia chambers, they were sometimes extrusions and sometimes ring-rolled forgings. In all chambers, the cylinders were welded to the forward and aft closures. The adapter, or flange, in both the 44-in.-dia and the 52-in.-dia chambers is an integral part of the closure die-forgings.

The general test plan called for fracture tests of each forging type. In some chambers, material was not available from all components. Tables I and II show the test plan for the chambers. Wherever possible, the specimens to be tested over a range of temperature were machined from material in the immediate vicinity of the fracture origin. Figure 4 schematically shows the location of test specimens in the 44-in. and 52-in.-dia chambers. In some chambers, secondary fracturing occurred in the hoop direction. Additional specimens were taken from these chambers as close as possible to the intersection of the main (axial) and the secondary (hoop) fracture paths; the additional specimens were machined to test with crack propagation in the axial and hoop directions.

The elevated test temperatures were selected to coincide with the temperatures used in hydroburst testing. Note that these temperatures, together with a -40°F test, resulted in approximately uniform increments of 120°F; viz, -40, RT, 200, and 320°F.

B. PRECRACK CHARPY IMPACT TEST

The precrack Charpy test* is similar to the standard V-notch Charpy impact test, except that (1) the machined notch in the specimen is sharpened by fatigue cracking, (2) the width of the test piece is generally the material thickness (the width may be as small as 0.03 in. in testing high-strength sheet and as large as 0.8 in., a limit imposed by the design of most impact-testing machines) and (3) the test result is expressed in terms of energy absorbed per unit of fracture area (W/A - in.-lb/in.^{2}).

The precracking of Charpy specimens is best accomplished by fatigue cycling. A special machine is commercially available for precracking Charpy specimens. Crack depths are normally held to approximately 0.025 in., but may vary considerably without significantly affecting the results. Since the

*Hartbower, C. E. and Orner, G. M.; Welding Journal, Vol 36(11), p.494-s (Nov 1957); ASTM Proceedings, Vol 58(1958), p.623; Welding Journal, Vol 33(4), p.147-s (Apr 1960); Ibid. Vol 40(9), p.405-s (Sept 1961); ASD-TDR-62-868, June 1963.

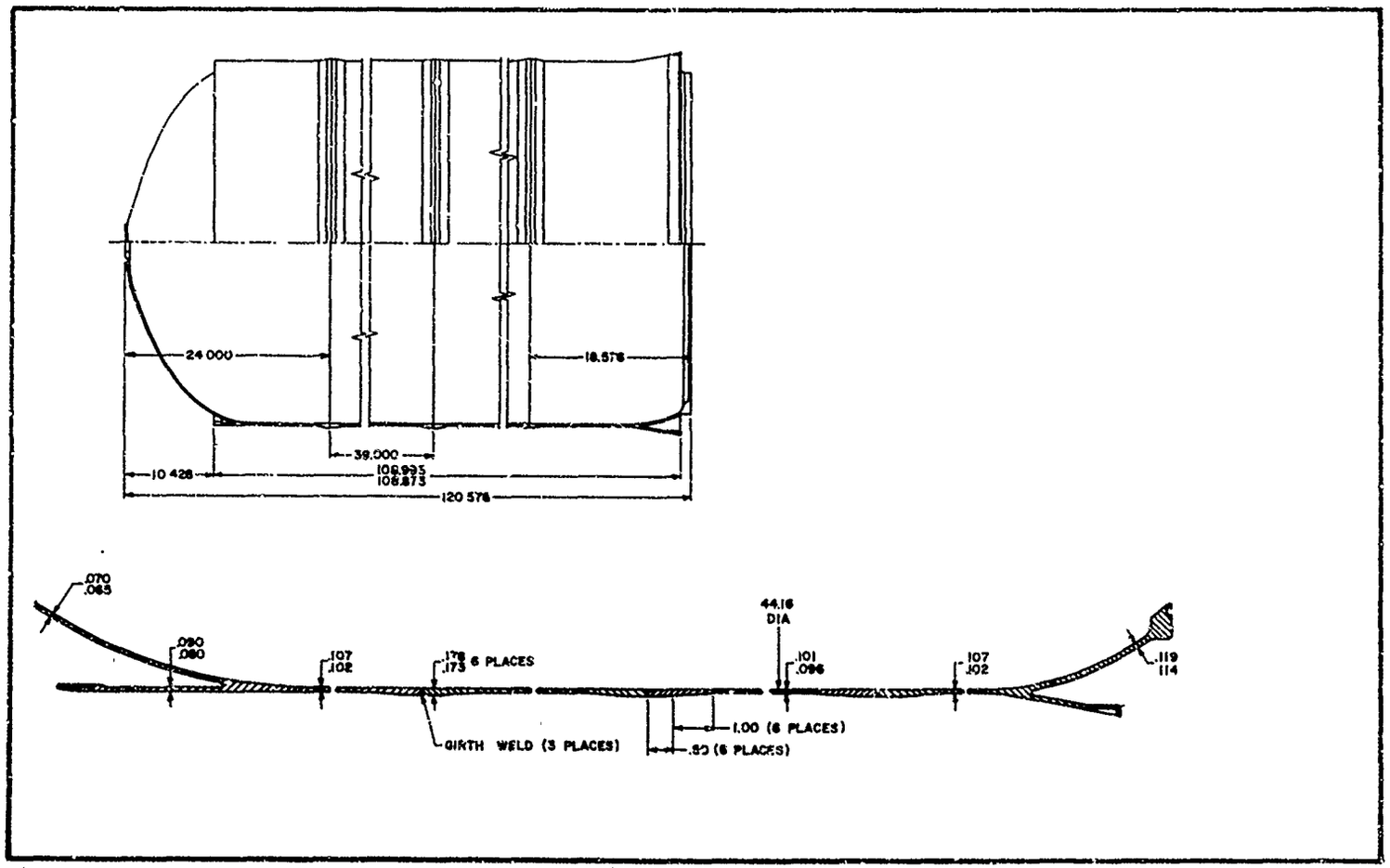

Figure 2. Design of the 44-in.-dia Second-Stage Minuteman Chamber

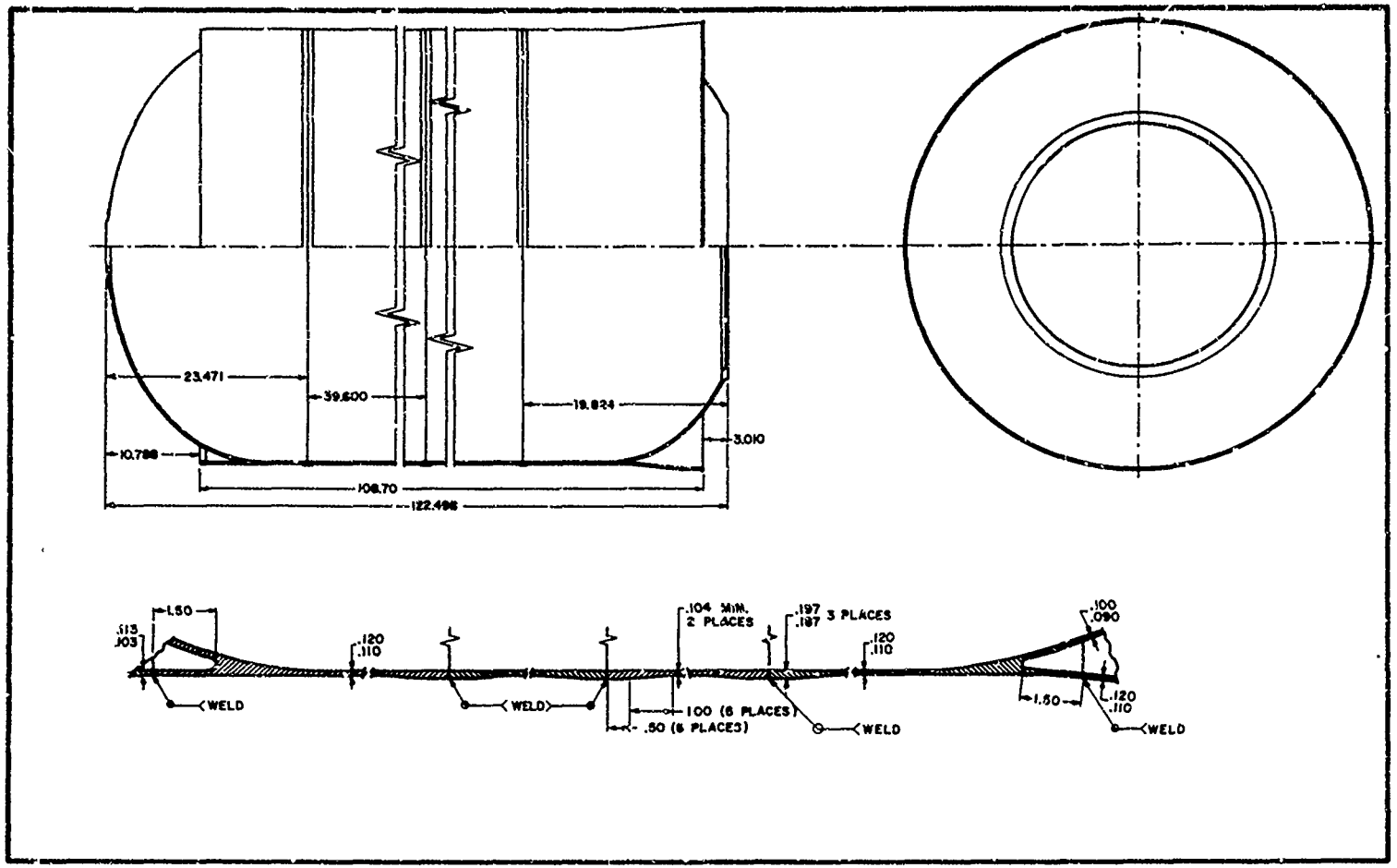

Figure 3. Design of the 52-in.-dia Second-Stage Minuteman Chamber

TABLE I

TEST PLAN FOR MINUTEMAN CHAMBERS
R26, R41, BL26 and 2191456

Chamber Component		Specimen Location	Total Specimens	Test Temperature, °F -40	RT	200	320
Chambers R26, R41, and 2191456							
Dome		(a)	12	3	3	3	3
Adapters -	Fwd	(a)	12	3	3	3	3
	Aft	(a)	12	3	3	3	3
Cylinders -	Fwd	(a)	12	3	3	3	3
	Aft	(a)	12	3	3	3	3
Chamber BL26							
Adapter -	Fwd	At G1 weld	4		4		
		thin wall	12	2	3	3	2
	Aft	At G3 weld	4		4		
		thin wall	12	3	3	3	3
Cylinders -	Fwd	At G1 weld	4		4		
		thin wall	4		4		
	Aft	At G3 weld	4		4		
		thin wall	12	3	3	3	3

*Exact location within the chamber component not known.

TABLE II

TEST PLAN FOR MINUTEMAN CHAMBERS
R490, R369, R512, R516, R543, 673078, 673095, 673122, 674514, and 2192109

Chamber Component	Specimen Location	Total Specimens	Test Temperature, °F			
			-40	RT	200	320
Dome	-	12	3	3	3	3
Adapter - Fwd	At G1 weld	12	3	3	3	3
	thin wall	3		3		
Aft	At G3 weld	12	3	3	3	3
	thin wall	3		3		
Cylinders - Fwd	At G1 weld	3		3		
	thin wall	3		3		
	At G2 weld	12	3	3	3	3
	thin wall	3		3		
Aft	At G2 weld	12	3	3	3	3
	thin wall	3		3		
	At G3 weld	3		3		
	thin wall	3		3		
Skirts - Fwd	-			3		
Aft	-			3		
Weld (R490 only)	-	12	3	3	3	3

Note: In all cases, three specimens were fabricated so the flaw was growing in the hoop direction. These specimens were located adjacent to one of the sets of three taken from the thin wall of the cylinders.

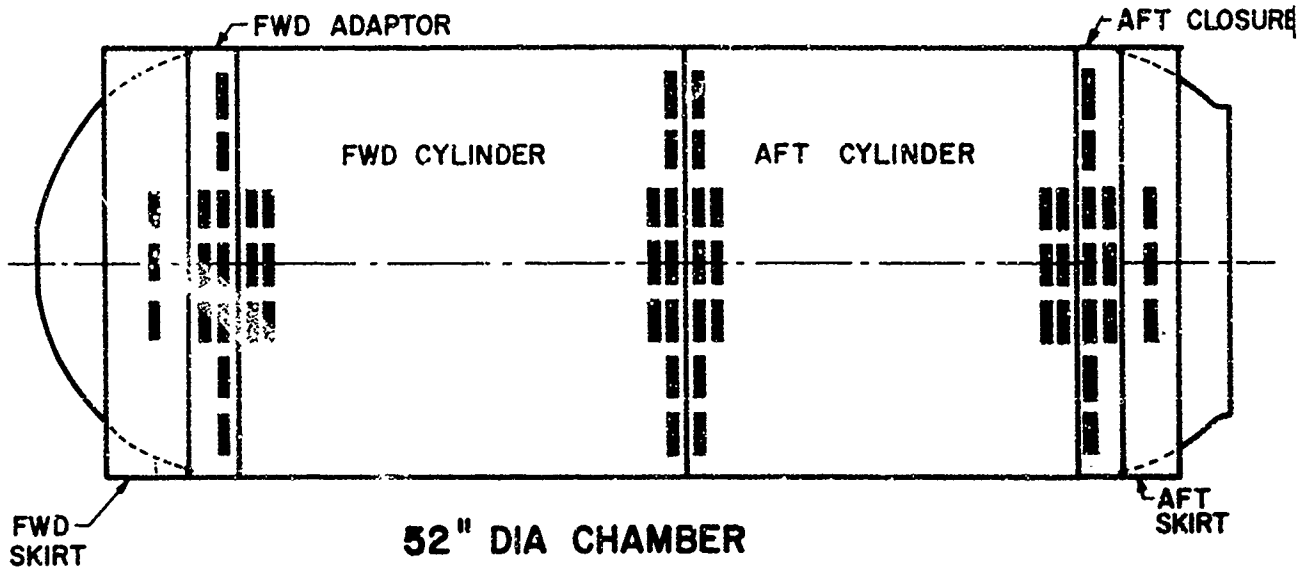

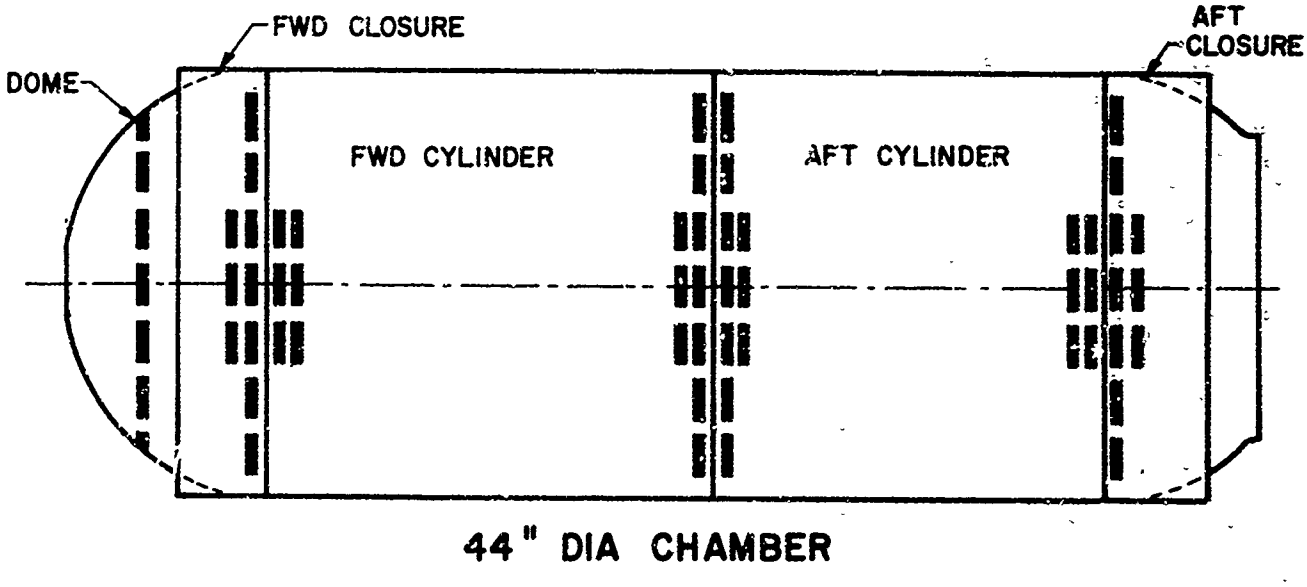

Figure 4. Schematic of Specimen Location in the 44-in.-dia and 52-in.-dia Chambers

test results are expressed in terms of work divided by fracture area, the lower energy values resulting from more deeply cracked specimens are compensated by the decrease in fracture area. Thus, within practical limits, the measurement of W/A is largely insensitive to precrack depth.

Impact testing precracked specimens is conducted using standard Charpy techniques; however, because of the low energy values often encountered in precracked high-strength materials, a sub-size impact-testing machine is used which reads in small energy increments. This machine and the precracking machine are shown in Figure 5.

In the MIL-HDBK-5 data collection described in this report, precracking was accomplished in approximately 3 min (at 1725 cpm) using a fatigue precracking machine. Loading was in tension-zero-tension, and the outer fiber stress was nominally 45 ksi. The precrack Charpy specimens were tested in a MANLABS CIM-24 Impact Tester. Impact testing at room and elevated temperature was conducted using standard Charpy techniques. The elevated temperatures were obtained in a bath of silicone-base oil, the room temperature tests were made in air, and the -40°F temperature was obtained in acetone and dry ice. The test pieces were soaked for a minimum of 15 min within ±2°F of the desired temperature; the maximum time for testing a specimen was 3 sec.

C. PLANE STRESS (K_c) CRACK TOUGHNESS MEASUREMENT

There is as yet no generally accepted, standardized test for measuring the crack toughness of sheet materials. Most of the work done up to this time has been based on linear-elastic fracture-mechanics concepts as developed by Irwin and the ASTM Special Committee on Fracture Testing of High Strength Metallic Materials*.

In the early work of the ASTM Committee (now designated E24), emphasis was placed on K_c measurements and, after the necessity for using fatigue cracked specimens was realized and improved methods for measuring crack growth came into use, such as displacement gages and electrical potential measurements, reasonably satisfactory procedures for K_c measurements were developed. The emphasis on plane-stress (K_c) crack toughness was the direct result of problems with premature failures in thin-skinned, roll-and-weld missiles that were being built at that time. The goal was a critical defect size of at least twice the thickness; it was found that when this criterion was met, a satisfactory service performance was generally assured**.

*"Fracture Testing of High Strength Sheet Materials," ASTM Bulletin, January 1960, pp 29-40, and February 1960, pp 18-28; also "The Slow Growth and Rapid Propagation of Cracks," Materials Research Standards, May 1961, pp 389-393.

**Irwin, G. R., "Structural Aspects of Brittle Fracture," Applied Materials Research, Vol. 3, pp 65, April 1964.

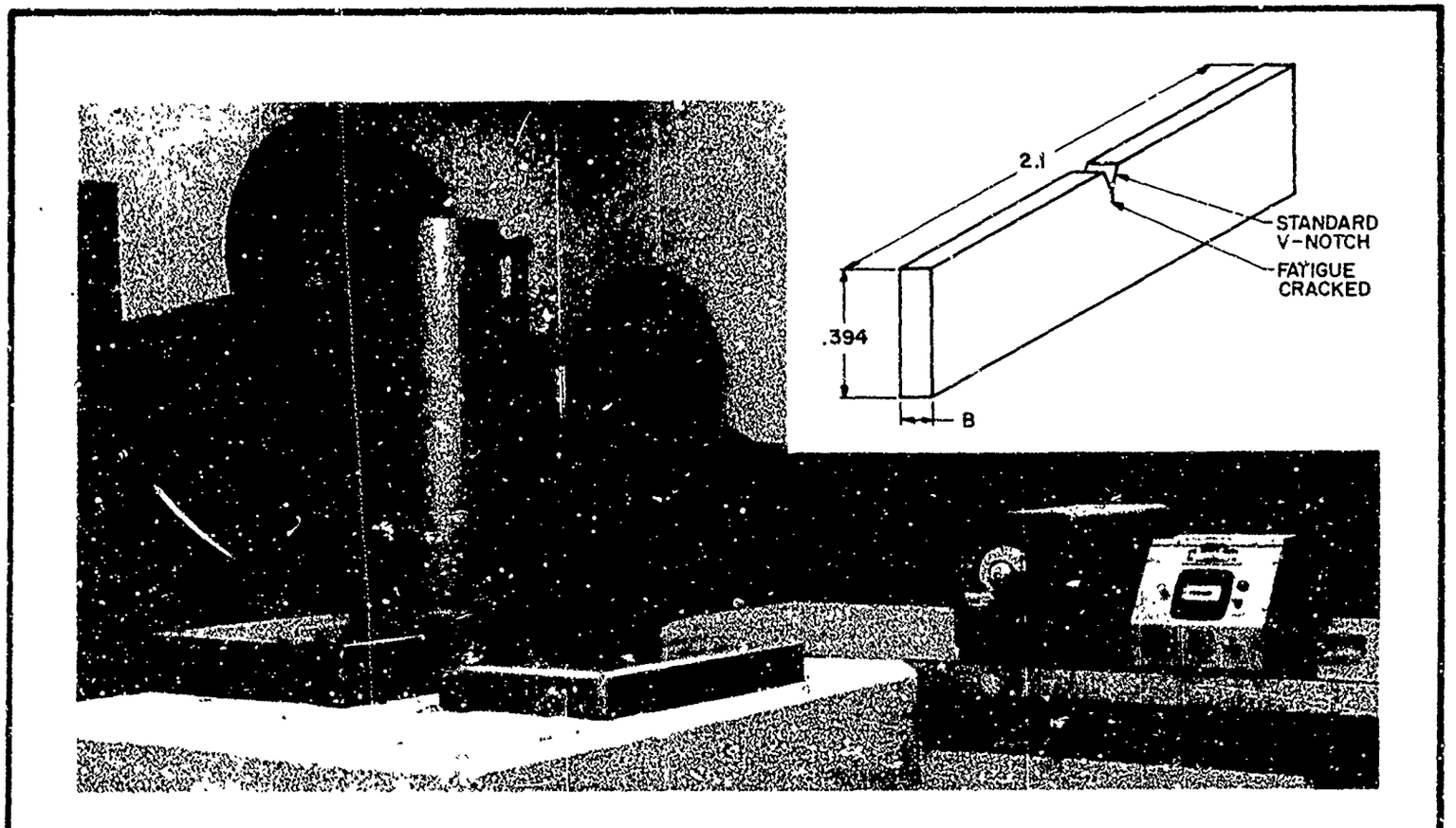

Figure 5. Fatigue-Precracking and Impact-Testing Machines for the Precrack Charpy Test (Specimen Superimposed)

II, C, Plane Stress (K_c) Crack Toughness Measurement (cont.)

As the plane-stress fracture toughness studies progressed, experimental data were obtained by various investigators showing a marked variation in K_c with material thickness. From this, it became apparent that the applicability of K_c results would be markedly dependent upon the thickness of the material and might be significant only at the specific thickness of the test specimen. This limited applicability of the plane-stress measurement, together with the realization that the K_{Ic} values as determined from thick specimens were generally applicable regardless of thickness, were predominant factors in the switch to plane-strain fracture toughness testing which has dominated E24 Committee activities over the last three years or so.

Unfortunately, because of the later emphasis on plane-strain crack toughness, many people appear to have concluded that the K_c measurement is less meaningful than K_{Ic} and, therefore, have concentrated on the plane-strain K_{Ic} measurement in lieu of K_c crack toughness measurements, even for sheet applications. This trend has been strengthened by the realization that although plane-strain fracture conditions are most nearly approached in thick sections, this condition may be approached by shallow surface cracks propagating in the thickness direction of sheet materials. However, as will be shown in following paragraphs, in sheet thicknesses and even in some plate materials, exclusive use of the K_{Ic} crack-toughness measurement leads to an overly conservative design for some service applications.

Irwin has pointed out that there are two lines of defense against crack propagation. The first line of defense is based on an adequate K_{Ic} crack toughness. When the crack is spreading as an embedded crack, if the stresses are high, very small cracks must be regarded as dangerous. Thus, the first line of defense is based on minimizing the working stresses and stress concentrations in design, improving nondestructive inspection to eliminate small cracks and notches, and using material of optimum K_{Ic} crack toughness. Sometimes, on reaching plane-strain instability (pop-in), the crack extension across the sheet will be arrested by an increasing resistance to crack propagation under plane-stress conditions. This increasing resistance to propagation as the crack spreads laterally in the sheet is associated with a fracture-appearance transition as the fracture surface changes from square in the pop-in region to an increasing percentage of slant fracture as the plane-stress condition is approached.

The practical importance of the plane-stress K_c crack toughness measurement is further substantiated by the fact that in some materials and material conditions, there is no correlation between the K_c and K_{Ic} measurements. Some investigators have been willing to focus their attention on K_{Ic} to the exclusion of K_c, based on the assumption that a material with low K_{Ic} will also have low K_c values. Thermal-mechanically treated 0.250" H-11 steel is a notable example where K_{Ic} is relatively low and invariant, whereas K_c varies over a wide range*.

---

*Berberich, W. W., "A Discussion of Slow Crack Growth Associated with Plane-Strain Instability," ASTM Transactions, Vol. 59(4), December 1966.

II, C, Plane Stress (K_c) Crack Toughness Measurement (cont.)

In work by Kaufman of the Alcoa Research Laboratories*, it has been shown that even in 1-in.-thick, wide-plate, through-crack, center-notch tension tests, there was stable, slow crack growth after plane-strain pop-in, with K_c controlling the ultimate fracture of the panels. In other words, the thick plate demonstrated considerably more crack toughness than was indicated by the plane-strain stress-intensity factor. In the Alcoa study, ten combinations of alloy and temper were investigated using 20-in.-wide, center-notch tension panels, single-edge-notch specimens and notch-bend specimens. Only the large center-notch panels provided information on the critical instability of the alloys in terms of K_c for the thickness tested. This is an important observation because, of the eight alloy compositions tested, all except two exhibited values of K_c considerably higher than K_{Ic} in the cracking direction tested. As a result, the use of the K_{Ic} value in design could be overly conservative in materials where mixed-mode fracture prevails and where leak-before-burst is an acceptable service condition**. If fatigue-sharpened notches had been used in the study rather than machined sharp notches, an even greater difference between the K_{Ic} and K_c values might have been expected (i.e., lower K_{Ic} values).

Similar results were obtained in studies of eight candidate alloys for the supersonic commercial transport (SST)***. In 1-in.-thick panels, slow crack growth of as much as 1.1 in. occurred before the crack reached critical length. The data in Table III were obtained from 9-in.-wide, center-notch panels of 1-in.-thick plate, tested at room temperature (the fracture toughness values include a plastic-zone correction). The values of percent shear (slant) were measured in the fracture surfaces at a distance of 2 in. from the outside edge of the panel. The critical crack length was determined by motion-picture photography. Pop-in was detected by crack-opening displacement and by accelerometer.

Thus, it has been shown that a variety of materials are capable of stable slow crack growth after plane-strain pop-in, even in plate thicknesses up to 1 in. In such materials, rapid (unstable) crack propagation occurs only

*Kaufman, J.G., Nelson, F.G. Jr., and Holt, M, "Fracture Toughness of Aluminum Alloy Plate Determined with Center-Notch Tension, Single-Edge-Notch Tension and Notch-Bend Tests," presented at the National Symposium on Fracture Mechanics, Lehigh University, June 20, 1967.

**Obviously, in some service applications, say a fuel tank, one cannot tolerate a leak (pop-in through the thickness) and, therefore, plane-strain fracture toughness is the only consideration.

***Thick Section Fracture Toughness, Air Force Materials Laboratory Tech. Doc. Report No. ML-TDR-64-236, October 1964, prepared under Contract AF 33(657) 11461 by Boeing-North American in a joint venture.

TABLE III

CENTER-NOTCH-PANEL TESTS OF 1-IN.-THICK SST MATERIALS

Alloy	1/2 Crack Length, in.		Slant Fracture, %	Fracture Toughness, ksi-in.$^{1/2}$	
	Initial	Critical		K_{Ic}	K_c
4340	1.50	1.55	8	98	100
	1.50	1.50	7	99	99
9Ni-4Co	1.50	2.0	18	*	109
	1.50	2.0	10	*	109
AM 355	1.50	2.25	13	71	129
	1.50	1.69	7	55	79
Maraging 250	1.50	1.86	15	*	107
	1.50	1.97	14	86	113
INCO 718	1.50	1.89	25	*	341**
	1.50	1.99	27	*	404**
Ti 6Al-4V	1.50	2.60	18	*	105
Ti 6Al-6V-2Sn	1.50	1.75	20	54	90
	1.50	1.79	17	60	91
PH 13-8 Mo	1.50	1.60	5	98	107
	1.50	1.65	3	79	87

*No pop-in detected.
**Ratio of σ_N/σ_{ys} exceeded 0.8

II, C, Plane Stress (K_c) Crack Toughness Measurement (cont.)

when the stress-intensity factor of the stress field surrounding the crack reaches the value of K_c. The data show that with as little as 10 to 15% slant fracture, slow crack growth can still occur after the plane-strain pop-in, requiring a continuous increase in the applied stress to drive the crack, with the eventual unstable fracturing controlled by the K_c value.

1. The Leak-Before-Burst Fracture Toughness Criterion

For a crack length 2a in a large sheet, the K_c value permits an estimation of the critical crack for unstable crack propagation through the relationship

$$K_c^2 = \pi \sigma^2 a_1 \qquad \text{(Eq 1)}$$

where a_1 is the "effective" half-length of the crack. When the effective half-crack length is expressed in terms of the plastic-zone correction and the actual half-crack length, the effective half-crack length becomes

$$a_1 = a + K_c^2/2 \pi \sigma_{ys}^2 \qquad \text{(Eq 2)}$$

Substituting in Equation 1 and solving for K_c in terms of the actual half-length a,

$$K_c^2 = \pi \sigma^2 a/[1 - 1/2 (\sigma/\sigma_{ys})^2] \qquad \text{(Eq 3)}$$

When the working stresses approach the yield strength, $\sigma = \sigma_{ys}$, Equation 3 becomes

$$K_c^2/\pi \sigma_{ys}^2 = 2a \qquad \text{(Eq 4)}$$

The fracture-toughness criterion suggested by Irwin is, in effect, that if the quantity

$$K_c^2/\pi \sigma_{ys}^2$$

exceeds twice the wall thickness, a small surface crack is unlikely to develop to the stage of unstable fracturing under stresses which do not exceed the yield strength. This quantity is the critical crack length at the yield strength for a through-the-thickness crack, so the criterion suggested is that the critical crack length for the material should exceed twice the wall thickness.

II, C, Plane Stress (K_c) Crack Toughness Measurement (cont.)

The usefulness of the leak-before-burst concept has received a large amount of study and trial in connection with steel rocket motor cases*.

2. Precrack Charpy Impact for Approximating K_c

In Appendix D of Volume I of AFML-TR-68-163, the merits and limitations of the precrack Charpy impact test are discussed. The chief objection to the precrack Charpy test has come from those who have considered the test only in terms of a quantitative measure of fracture toughness. It has been suggested** that the basic limitation in the precracked Charpy test is the small size of the test specimen. In Appendix D of Volume I, it is shown that the small size of the test precrack Charpy specimen has not been a serious limitation and, in fact, can be its chief advantage. Moreover, because of the small specimen size and the inherent simplicity of impact testing, the Charpy test is easily and inexpensively conducted over a wide range of temperatures. Charpy test results have shown the importance of testing over a range of temperatures, particularly in K_c determinations where testing at a single temperature, as is often done when using much more expensive test methods, can be seriously misleading. Two points should be made clear with regard to the use of the precrack Charpy test; viz, (1) the principal advantage of the precrack Charpy is in its use as a screening test where an approximate fracture toughness value is desired; and (2) the precrack Charpy impact test provides a good approximation of K_c through the relationship

$$K_c^2 = E(W/A)$$

where the K_c instability is associated with a running crack under plane-stress conditions.

Examples of the correlation of precrack Charpy impact data and center-notch tensile data were presented in Appendix D of Volume I, together with a discussion of certain metallurgical complications in correlation studies. Correlation between the tests was obtained when the Charpy specimens were machined from the broken halves of the larger test specimen and, thus, the test material had identically the same heat-treatment history and notch orientation. Over the last several years a limited number of precrack Charpy tests have been made from prematurely burst Minuteman chambers. However, the data were not always taken from the immediate vicinity of the fracture origin, nor were the test specimens oriented to propagate fracture in the chamber-axial direction. In the following Phase II study, the Charpy specimens were oriented to propagate fracture in the chamber-axial direction and were machined from various locations, including a position as close to the fracture origin as possible.

*Irwin, G. R., Applied Materials Research, Vol. 3, pp 65, April 1964; Irwin, G. R. and Sullivan, A. M., Proc. Roy. Soc., A285, pp 141(1965); Gerberich, W. W., Metals Engr. Quarterly, Vol. 4(4), pp 23, November 1964 and Application of Fracture Toughness Parameters to Structural Metals, AIME Met. Soc. Conf., Vol. 31(1966) pp 86.

**Brown and Srawley, Plane-Strain Crack Toughness Testing, ASTM STP 410, pp 33.

SECTION III

DATA COMPILATION

The precrack Charpy impact data compiled from 69 forgings as contained in 14 second-stage Minuteman 6Al-4V titanium rocket motor cases are tabulated. The data from the individual tests are presented in Appendix I, together with summary tabulations of the form shown in Table IV. From Table IV, it will be seen that the data are presented as a function of: (1) test location within the chamber (forging-to-forging differences), (2) test location within a given forging (effect of thickness and end-to-end homogeneity), and (3) test temperature (at 120°F increments encompassing the range anticipated in service). The data obtained over a range of temperature were plotted as shown in Figure 6; these plots are presented in Appendix II.

TABLE IV

SUMMARY OF PRECRACK CHARPY IMPACT DATA FROM 6Al-4V TITANIUM CHAMBER 673122

Minuteman Chamber SN	Component	Specimen Location	Wall Thickness	Test Temperature, °F -40	RT	200	320
673122	Fwd Closure	2-in. fwd of G1 weld	0.102		532 - 631 Avg(3) 573		
		G1 reinforced section	0.177	280 - 452 Avg(3) 375	656 - 693 Avg(3) 679	753 - 1100 Avg(3) 964	1250 - 1340 Avg(3) 1293
	Fwd Cyl	G1 reinforced section	0.171		334 - 578 Avg(3) 439		
		2-in. aft of G1 weld	0.102		396 - 412 Avg(3) 406		
		2-in. fwd of G2 weld	0.100		498 - 588 Avg(3) 549		
		G2 reinforced section	0.170	352 - 359 Avg(3) 355	408 - 554 Avg(3) 484	289 - 875 Avg(3) 638	1080 - 1330 Avg(3) 1167
	Aft Cyl	G2 reinforced section	0.171	378 - 464 Avg(3) 409	593 - 634 Avg(3) 619	719 - 865 Avg(3) 815	1130 - 1300 Avg(3) 1200
		2-in. aft of G2 weld	0.097		550 - 620 Avg(3) 585		
		2-in. fwd of G3 weld	0.094		441 - 548 Avg(3) 484		
		G3 reinforced section	0.170		387 - 631 Avg(3) 507		
	Aft Closure	G3 reinforced section	0.179	169 - 468 Avg(3) 329	601 - 640 Avg(3) 624	770 - 1060 Avg(3) 874	1140 - 1200 Avg(3) 1163
		2-in. aft of G3 weld	0.106		487 - 519 Avg(3) 503		

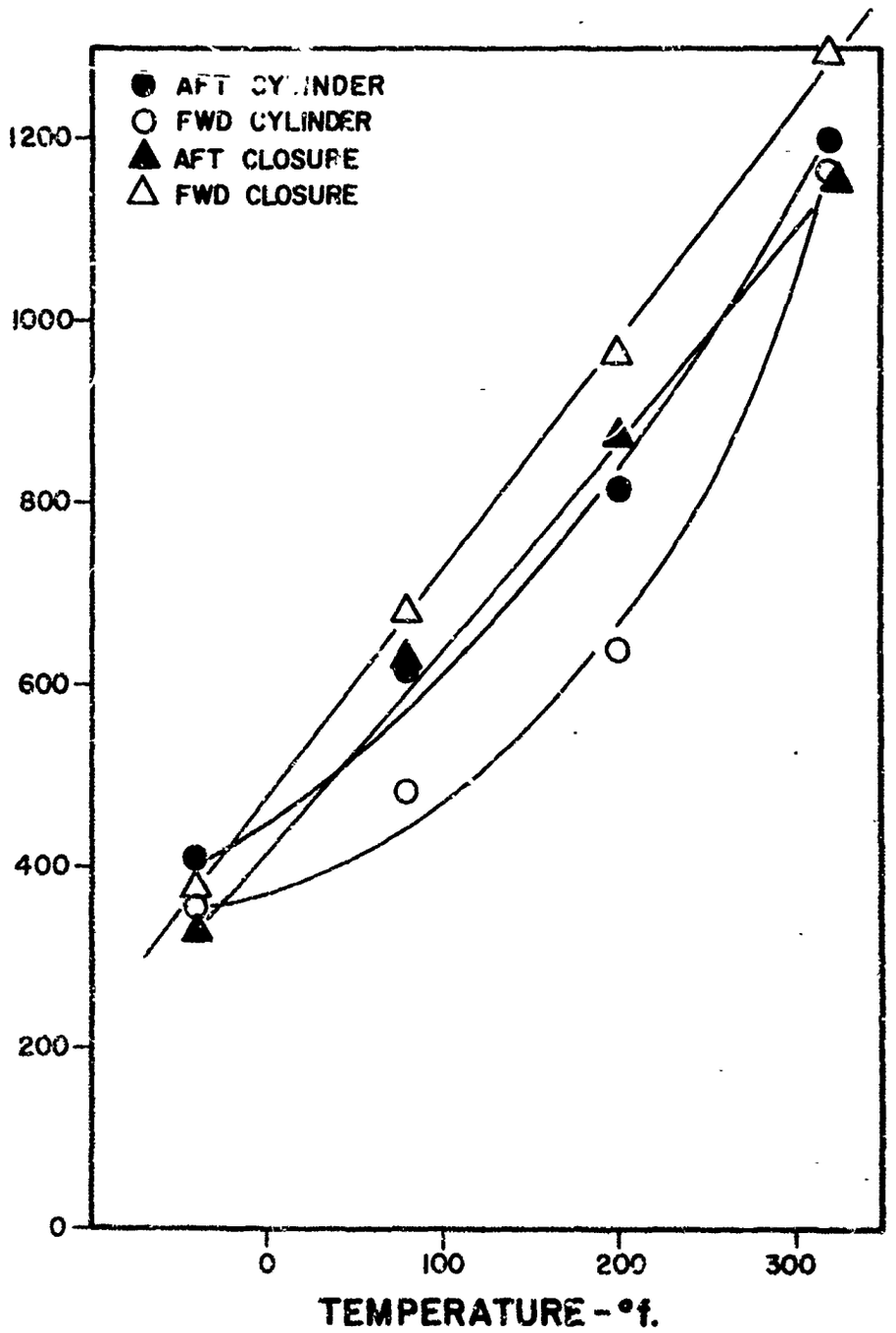

Figure 6. Effect of Test Temperature on the Precrack Charpy Impact W/A Values in 6Al-4V Titanium Chamber 673122

SECTION IV

DISCUSSION OF RESULTS

A. TEST REPRODUCIBILITY

Twenty-four tests were run from a single closure forging, with 12 specimens taken from the closure flange (0.110 in. thick) and 12 from the dome (0.070 in. thick). The fatigue crack depths for both sets ranged from approximately 0.05 to 0.10 in., with an average depth (24 specimens) of 0.072 in. From Figure 7, it will be seen that the variation in fatigue-crack depth had no discernible effect on the W/A value.

Each set of data was statistically tested. With the W/A values from the 12 dome specimens as input to the computer and a typical class interval of 440-540, the computer printout was as shown in Table V. Likewise, with the W/A values from 12 flange specimens as input to the computer and a typical class interval of 405-485, the computer printout was as shown in Table VI.

From a simple analysis of covariance, it was determined that there was a highly significant difference between the means of the flange and dome sections (significance level 0.0019). It is reasonable to assume that the highly significant difference between the means of the flange and dome is due to the difference in thickness and/or possible anisotropy due to a difference in specimen orientation. Multiple linear regression and correlation analysis was then employed to determine if crack depth had an effect on the two sets of 12 tests. The analysis showed that there was no correlation between the W/A value and net section within the limits investigated.

Table VII presents data on variability in the precrack Charpy impact W/A value as measured in Minuteman 6Al-4V titanium. The data presented in Table VII are for the body cylinders in each chamber without regard for possible differences between forgings or possible differences from end-to-end in a given forging. The variability is intended for use as a yardstick against which the seeming difference between averages is assessed. In this report, the following measures of variability are used: the variance, the standard deviation and the range of a sample. Table VII presents the sample variance (s^2), the sample standard deviation (s) and the sample mean. Note that the standard deviations for the individual chambers ranged from 54 to 174 in.-lb/in.^{2}, and when the data from all 26 forgings were tested for variability, the standard deviations were very large.

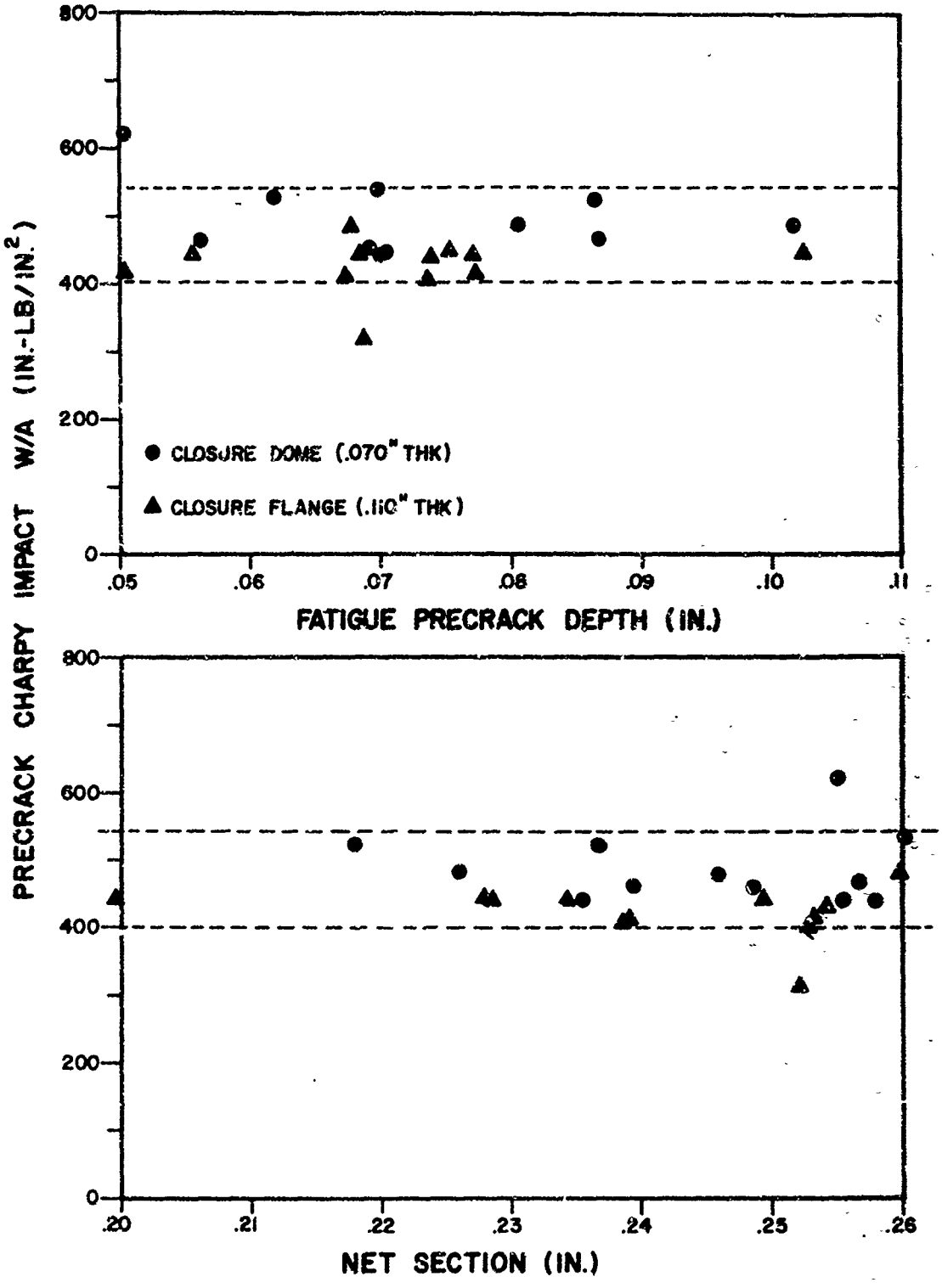

Figure 7. Effect of Crack Depth (Net Section) on Precrack Charpy W/A Values

TABLE V

COMPUTER PRINTOUT FOR REPLICATE TESTS OF CHAMBER R26 DOME MATERIAL

DATA 472,486,463,540,483,456,448,443,465,524,526,623

S U M M A R Y S T A T I S T I C S

NUMBER OF VARIATES	= 12
ARITHMETIC MEAN	= 494.083
STANDARD DEVIATION	= 49.4241
VARIANCE	= 2442.74
COEFF OF VAR (PCT)	= 10.003
STANDARD SKEWNESS	= 1.342
STANDARD EXCESS	= 1.159

O R D E R S T A T I S T I C S

SMALLEST VARIATE	= 443
LOWER DECILE	= 444.5
FIRST QUARTILE	= 457.75
MEDIAN	= 477.5
THIRD QUARTILE	= 525.5
UPPER DECILE	= 598.1
LARGEST VARIATE	= 623
TOTAL RANGE	= 180
DECILE RANGE	= 153.6
SEMI-QUARTILE RANGE	= 33.875
BOWLEY'S SKEWNESS	= .417
PEARSON SKEWNESS	= 1.007

F R E Q U E N C Y D I S T R I B U T I O N

FROM	UP TO BUT NOT INCLUDING	FREQUENCY	PERCENT FREQUENCY
440	540	10	83.333
540	640	2	16.667

C U M U L A T I V E D I S T R I B U T I O N

VALUE	NUMBER LESS THAN VALUE	PERCENT LESS THAN VALUE	VARIATE SUM - PCT LESS THAN VALUE
540	10	83.333	80.385
640	12	100.	100.

O R D E R E D A R R A Y

443	463	483	526
448	465	486	540
456	472	524	623

TABLE VI

COMPUTER PRINTOUT FOR REPLICATE TESTS OF CHAMBER R26 FLANGE MATERIAL

DATA 419,410,484,446,415,443,449,437,443,318,445,407

S U M M A R Y S T A T I S T I C S

NUMBER OF VARIATES	= 12
ARITHMETIC MEAN	= 426.333
STANDARD DEVIATION	= 38.5170
VARIANCE	= 1483.56
COEFF OF VAR (PCT)	= 9.034
STANDARD SKEWNESS	= -1.541
STANDARD EXCESS	= 2.669

O R D E R S T A T I S T I C S

SMALLEST VARIATE	= 318
LOWER DECILE	= 344.7
FIRST QUARTILE	= 411.25
MEDIAN	= 440
THIRD QUARTILE	= 445.75
UPPER DECILE	= 473.5
LARGEST VARIATE	= 484
TOTAL RANGE	= 166
DECILE RANGE	= 128.8
SEMI-QUARTILE RANGE	= 17.25
BOWLEY'S SKEWNESS	= -.667
PEARSON SKEWNESS	= -1.064

F R E Q U E N C Y D I S T R I B U T I O N

FROM	UP TO BUT NOT INCLUDING	FREQUENCY	PERCENT FREQUENCY
245	325	1	8.333
325	405	0	0
405	485	11	91.667

C U M U L A T I V E D I S T R I B U T I O N

VALUE	NUMBER LESS THAN VALUE	PERCENT LESS THAN VALUE	VARIATE SUM - PCT LESS THAN VALUE
325	1	8.333	6.216
405	1	8.333	6.216
485	12	100.	100.

O R D E R E D A R R A Y

318	415	443	446
407	419	443	449
410	437	445	484

TABLE VII

VARIABILITY IN THE PRECRACK CHARPY IMPACT W/A VALUE IN MINUTEMAN 6A1-4V TITANIUM

Chamber	$\Sigma(W/A)$	$\Sigma(W/A)^2$ x 10^6	$(\Sigma W/A)^2$ x 10^6	n	n-1	$(\Sigma W/A)^2/n$ x 10^6	$[\Sigma(W/A)^2-(\Sigma W/A)^2/n]$ SS x 10^6	$[SS/n-1]$ s^2 x 10^5	Std. Devia. s	Sample Mean in.-lb/in.^{2}
226										
0.10 in.	18173	10.8910	330.2580	33	32	10.0078	0.8832	0.0276	166	551
R41										
0.10 in.	7927	4.4281	62.8373	15	14	4.1891	0.2390	0.0170	130	528
2191456										
0.10 in.	8589	5.1850	73.7709	15	14	4.9180	0.2670	0.0190	138	573
BL26										
0.10 in.	6311	3.1010	39.8287	13	12	3.0637	0.0373	0.0031	56	485
0.18 in.	6464	3.0481	41.7833	14	13	2.9845	0.0636	0.0048	69	462
2192109										
0.10 in.	4649	1.9273	21.6132	12	11	1.8011	0.1262	0.0114	107	387
0.18 in.	2163	0.9503	4.6786	5	4	0.9357	0.0146	0.0036	60	541
R369										
0.10 in.	11375	5.6535	129.3906	24	23	5.3913	0.2622	0.0114	107	474
0.18 in.	5752	1.9990	33.0855	17	16	1.9462	0.0528	0.0033	58	338
R490										
0.10 in.	9131	3.9460	83.3752	22	21	3.7897	0.1563	0.0074	86	415
0.18 in.	6553	2.4350	42.9418	18	17	2.3856	0.0494	0.0029	54	364
R512										
0.10 in.	13513	7.9465	182.6012	24	23	7.6083	0.3382	0.0147	121	563
0.18 in.	7674	3.4390	58.8903	18	17	3.2716	0.1674	0.0098	99	426

TABLE VII (cont.)

Chamber	$\sum(W/A)$	$\sum(W/A)^2$ x 10^6	$(\sum W/A)^2$ x 10^6	n	n-1	$(\sum W/A)^2/n$ x 10^6	$[\sum(W/A)^2-(\sum W/A)^2/n]$ SS x 10^6	$[SS/n-1]$ s^2 x 10^6	Std. Devia. s	Sample Mean in.-lb/in.^{2}
R516										
0.10 in.	11412	6.0482	130.2337	24	23	5.4264	0.6218	0.0270	164	476
0.18 in.	7189	2.9541	51.6817	18	17	2.8712	0.0829	0.0048	69	399
R543										
0.10 in.	11939	6.6815	142.5397	23	22	6.1973	0.4842	0.0220	148	519
0.18 in.	6774	2.6523	45.8871	18	17	2.5492	0.1031	0.0060	78	376
673078										
0.10 in.	12966	8.1633	168.1172	21	20	8.0056	0.1577	0.0079	89	617
0.18 in.	8779	4.7125	77.0708	17	16	4.5336	0.1789	0.0112	106	516
673095										
0.10 in.	9490	5.0418	90.0601	19	18	4.7400	0.3018	0.0167	129	499
0.18 in.	8766	4.5357	76.8428	18	17	4.2690	0.2667	0.0156	125	487
673122										
0.10 in.	9304	4.8956	86.5644	18	17	4.8091	0.0865	0.0050	71	517
0.18 in.	10056	5.8040	101.1231	18	17	5.6179	0.1861	0.0109	105	559
674514										
0.10 in.	5989	2.4850	35.8681	15	14	2.3912	0.0938	0.0067	82	399
0.18 in.	5540	2.7262	30.6916	13	12	2.3608	0.3654	0.0304	174	426
Composite										
All Chambers										
0.10 in.	140768	76.3941	19815.6298	278	277	71.2792	5.1149	0.0184	136	506
0.18 in.	75710	35.2563	5732.0041	174	173	32.9425	2.3138	0.0133	115	435
Both Thick.	215478	111.6504	46430.7685	452	451	102.7229	8.9275	0.0197	140	477

IV, A, Test Reprcducibility (cont.)

Composite (All Chambers)	W/A	Standard Deviation
0.10-in.	506	± 136
0.18-in.	435	± 115
Combined Thickness	477	± 140

On the other hand, when standard deviations were determined for a single forging at two thickness levels (from Tables V and VI), the standard deviations were small

R26 Forward Closure	W/A	Standard Deviation
0.072-in.	494	± 49
0.110-in.	426	± 38

The large standard deviations as obtained with composite data suggest the possibility of a large forging-to-forging variability in the W/A value. In contrast, the plane-strain (K_{Ic}) crack toughness as measured in 109 forgings was 39 ksi-in.$^{1/2}$ with a standard deviation of only 1.6 ksi-in.$^{1/2}$

B. FORGING ANISOTROPY AND INHOMOGENEITY

1. Anisotropy

In Phase I of this contract, a comparison between axial- and hoop-direction fracture using the precrack Charpy impact test revealed marked anisotropy in some forgings (see Figure 25, page 52 of Volume I). Therefore, in Phase II, wherever secondary hoop fracture developed in a chamber, the material at the junction of the hoop and axial fractures was tested for anisotropy. As noted in Table II a large number of forgings also were examined for anisotropy where there was no hoop-direction fracture.

The fracture in chamber R490 originated in the center girth weld and propagated forward and aft in the chamber with a single secondary fracture starting in the membrane wall near the aft grith weld and doubled back at approximately 45 degrees toward the center girth weld. Precrack Charpy impact specimens were machined from the two body cylinders on either side of the center girth weld (not at the juncture of the axial and 45 degree fractures). From summary Table VIII, it will be seen that the crack toughness in both cylinders was higher in the hoop direction.

TABLE VIII

SUMMARY OF PRECRACK CHARPY IMPACT TESTS FOR ANISOTROPY IN 6Al-4V TITANIUM FORGINGS

Minuteman Chamber S/N	Component	Thickness, in.	W/A Values ($in.\text{-}lb/in.^2$) Crack Propagation Direction: Axial	Hoop
490	Fwd Cyl	0.109	321 - 466 Avg(3) 410	654 - 703 Avg(3) 680
	Aft Cyl	0.110	379 - 388 Avg(3) 382	403 - 439 Avg(3) 426
R512	Fwd Cyl	0.108	526 - 532 Avg(3) 529	388 - 468 Avg(3) 436
	Aft Cyl	0.109	386 - 443 Avg(3) 414	414 - 539 Avg(3) 467
R516	Fwd Cyl	0.105	315 - 375 Avg(3) 349	393 - 501 Avg(3) 459
	Aft Cyl	0.106	384 - 482 Avg(3) 444	345 - 400 Avg(3) 374
R543	Fwd Cyl	0.106	401 - 500 Avg(3) 447	361 - 507 Avg(3) 450
	Aft Cyl	0.105	336 - 351 Avg(3) 343	546 - 646 Avg(3) 602
673078	Aft Flange*	0.107	567 - 642 Avg(3) 614	492 - 539 Avg(3) 519
	Aft Cyl	0.105	519 - 608 Avg(6) 569	611 - 702 Avg(6) 652
673095	Aft Cyl*	0.102	334 - 401 Avg(4) 379	280 - 325 Avg(3) 301
	Phase I	0.100	406 - 522 Avg(3) 460	303 - 416 Avg(9) 348
674514	Aft Cyl*	0.098	295 - 324 Avg(3) 306	274 - 320 Avg(3) 304
	Phase I	0.099	343 - 396 Avg(6) 366	274 - 330 Avg(6) 308
2192109	Fwd Cyl*	0.105	242 - 276 Avg(3) 263	340 - 381 Avg(3) 365
	Phase I	0.103	398 - 454 Avg(6) 432	459 - 516 Avg(6) 489

*Specimens taken at junction of hoop and axial fracture.

IV, B, Forging Anisotropy and Inhomogeneity (cont.)

The fracture in chamber R512 originated in the forward cylinder approximately 3-1/2 in. from the center girth weld and propagated forward and aft in the chamber with no secondary fracture. Precrack Charpy impact specimens were machined from the two body cylinders on either side of the center girth weld. From summary Table VIII it will be seen that the crack toughness in the hoop direction was lower in the forward cylinder, but higher in the aft cylinder as compared with the axial direction.

The fracture in chamber R516 originated in the aft-cylinder reinforced section of the center girth weld, and propagated forward and aft in the chamber, with a single secondary fracture starting in the membrane wall near the aft girth weld and doubling back at approximately 45 degrees toward the center girth weld. Precrack Charpy impact specimens were machined from the two body cylinders on either side of the center girth weld (not at the juncture of the axial and 45° fractures). From summary Table VIII it will be seen that the crack toughness in the aft cylinder containing the 45 degree fracture was lower in the hoop direction than in the axial direction; in the forward cylinder, the crack toughness was higher in the hoop direction than in the axial direction.

The fracture in chamber R543 originated in the aft cylinder, 18 in. forward of the aft girth weld, and propagated forward and aft in the chamber with no secondary fracture. Precrack Charpy impact specimens were machined from the two body cylinders at the ends closest to the forward and aft girth welds. From summary Table VIII, it will be seen that the crack toughness in the hoop direction was higher than that in the axial direction in both cylinders.

The fracture in chamber 673078 originated in the center girth weld and propagated forward and aft, terminating in the aft skirt and propagating through the entire diameter of the forward dome. After crossing the aft girth weld, a secondary hoop fracture developed in the aft flange. Precrack Charpy impact specimens were machined from the junction of the hoop and axial fractures. From summary Table VIII, it will be seen that the crack toughness in the hoop direction of the aft flange of chamber 673078 was appreciably lower than that in the axial direction. In the aft cylinder, on the other hand, the data obtained in Phase I showed greater resistance to propagation in the hoop direction than in the axial direction. Likewise, from Phase I of the contract, the forward cylinder had greater toughness in the hoop direction (629 in.-lb/in.^{2}) than in the axial direction (528 in.-lb/in.^{2}).

Rupture of room-temperature-hydroburst chamber 673095 extended longitudinally from the aft Y-joint to the forward girth weld where it split and continued through the forward Y-joint at two locations. Two hoop-direction rips occurred in the aft barrel. The first extended 270 degrees in a clockwise

direction at the midpoint of the barrel section; the second extended 200 degrees in a counter-clockwise direction near the center girth weld.* Precrack Charpy impact specimens were machined from the junction of the hoop and axial fractures just aft of the center girth weld, and the test results compared with those obtained from Phase-I material cut from a different location. From the summary Table VIII, it will be seen that the crack toughness in the hoop direction of chamber 673095 was lower than that in the axial direction at the junction of the hoop and axial fractures and, moreover, the toughness was lower at the juncture than at the location tested in Phase I.

The rupture of room-temperature-hydroburst chamber 674514 extended longitudinally from the aft Y-joint, through the forward Y-joint and and through the forward dome. A hoop-direction rip occurred in the aft barrel and extended approximately 330 degrees.* Precrack Charpy impact specimens were machined from the junction of the hoop and axial fractures in the aft cylinder, and the test results compared with those obtained from Phase-I material cut from a different location. From summary Table VIII, it will be seen that the crack toughness at the juncture of the fracture paths was approximately equal and, moreover, the hoop-direction data obtained in Phase I and Phase II were identical for all practical purposes. The crack toughness in the axial direction in the material location tested in Phase I had higher toughness than at the junction of the hoop and axial fracture.

The rupture of chamber 2192109 (tested at 212°F) originated in the aft cylinder at a point, as determined by break wires and stress-wave analysis, approximately 72 in. aft of the forward skirt. A hoop-direction rip occurred in the forward cylinder approximately 12 in. aft of the forward girth weld. Precrack Charpy impact specimens were machined from the forward cylinder at the junction of the hoop and axial fractures, and the test results compared with those obtained from Phase-I material cut from a different location. From summary Table VIII, it will be seen that the crack toughness in the axial direction, as tested at room temperature, was lower than that in the hoop direction and, therefore, did not explain the hoop-direction rip. However, the hoop direction data obtained at the juncture of the fractures was appreciably lower than those obtained from Phase-I material cut from a different location. Moreover, data were not obtained at the 212°F hydroburst test temperature and, therefore, it is possible that at 212°F the crack toughness in the hoop direction may have been lower than that in the axial direction.

2. Forging Inhomogeneity

Table IX summarizes the body-cylinder data that were taken to determine the variation in toughness from end-to-end in any given cylinder

*R. H. Powell, "Burst Test of High-Strength Minuteman Wing II, Second-Stage Motor Cases", Report No. 999M-FR-1 and 2, 18 September 1963; and Report No. 999M-R, 23 October 1963.

TABLE IX

SUMMARY OF PRECRACK CHARPY IMPACT TESTS FOR INHOMOGENEITY IN 6Al-4V TITANIUM FORGINGS

Minuteman Chamber		Reinforced Section*		Membrane Section*	
S/N	Component	Fwd	Aft	Fwd	Aft
R369 52-in. Dia	Fwd Cyl	286 - 303 Avg(3) 295	207 - 216 Avg(2) 211	316 - 330 Avg(3) 324	332 - 349 Avg(3) 342
	Aft Cyl	359 - 385 Avg(3) 374	350 - 377 Avg(3) 368	432 - 489 Avg(3) 455	472 - 514 Avg(3) 490
R490 52-in. Dia	Fwd Cyl	346 - 421 Avg(3) 378	323 - 366 Avg(3) 347	343 - 435 Avg(3) 393	321 - 466 Avg(3) 410
	Aft Cyl	315 - 380 Avg(3) 343	260 - 303 Avg(3) 289	379 - 388 Avg(3) 382	256 - 311 Avg(3) 284
R512 52-in. Dia	Fwd Cyl	362 - 456 Avg(3) 420	340 - 409 Avg(3) 368	468 - 540 Avg(3) 509	526 - 532 Avg(3) 529
	Aft Cyl	316 - 341 Avg(3) 326	368 - 372 Avg(3) 370	386 - 443 Avg(3) 414	405 - 436 Avg(3) 424
R516 52-in. Dia	Fwd Cyl	373 - 644 Avg(3) 465	328 - 405 Avg(3) 358	404 - 428 Avg(3) 415	315 - 375 Avg(3) 349
	Aft Cyl	389 - 457 Avg(3) 429	338 - 381 Avg(3) 362	384 - 482 Avg(3) 444	426 - 493 Avg(3) 469
R543 52-in. Dia	Fwd Cyl	394 - 436 Avg(3) 419	289 - 393 Avg(3) 352	401 - 500 Avg(3) 447	351 - 496 Avg(3) 445
	Aft Cyl	247 - 302 Avg(3) 280	269 - 361 Avg(3) 303	360 - 371 Avg(2) 366	336 - 351 Avg(3) 343
673078 44-in. Dia	Fwd Cyl	530 - 564 Avg(3) 543	442 - 738 Avg(3) 617	518 - 701 Avg(3) 630	655 - 824 Avg(3) 727
	Aft Cyl	422 - 482 Avg(3) 456	462 - 512 Avg(3) 484	445 - 494 Avg(3) 476	555 - 643 Avg(3) 608
673095 44-in. Dia	Fwd Cyl	543 - 674 Avg(3) 603	541 - 696 Avg(3) 634	608 - 783 Avg(3) 684	452 - 677 Avg(3) 598
	Aft Cyl	352 - 444 Avg(3) 386	352 - 392 Avg(3) 375	334 - 401 Avg(4) 379	355 - 419 Avg(3) 389
673122 44-in. Dia	Fwd Cyl	334 - 578 Avg(3) 439	408 - 554 Avg(3) 484	396 - 412 Avg(3) 406	498 - 588 Avg(3) 549
	Aft Cyl	593 - 634 Avg(3) 619	387 - 631 Avg(3) 507	550 - 620 Avg(3) 585	441 - 548 Avg(3) 484

*Reinforced section nominally 0.18-in. thick and membrane wall nominally 0.10-in. thick, tested in their respective thicknesses.

forging. Note that in a given section, there was sometimes a marked difference from end-to-end of a cylinder. For example, in chamber R369, in the reinforced section of the forward cylinder:

Aft	Forward
207 to 216	286 to 303
Av (2) 211	Av (3) 295

Note that the higher value obtained from the two tests at the aft end of the chamber (216 in.-lb/in.^{2}) was appreciably lower than the lowest value obtained from the forward end of the cylinder (286 in.-lb/in.^{2}); thus, from an engineering viewpoint, there was a significant difference between the arithmetic mean values (211 for the aft end and 295 for the forward end of the cylinder). Differences in toughness from end-to end of a given cylinder could be the result of a difference in the forging working-temperature and/or thickness effects.

With regard to thickness, it should be noted that differences between the two thicknesses of Charpy specimens tested may be the result of one or a combination of three factors; viz, (1) a difference in lateral restraint in the test specimen per se due to thickness (width of test specimen); (2) a gradient of microstructure in the chamber wall due to the limitations of 6Al-4V titanium hardenability (cylinders were solution treated with a 1/2-in. wall and then machined to the nominal 0.10-in. wall); and (3) a difference in interstitial content due to a gradient of chemistry in the thickness direction (surfaces of the 1/2-in.-thick cylinders were badly contaminated as the result of solution treating in air; out-of-roundness after water quenching can result in local sections of higher-than-average interstitial content in the finish-machined part). Thus, any one or a combination of the above factors could have caused a variable "thickness" effect from cylinder to cylinder. Consider, for example, a comparison between the W/A values obtained from the two sections at the aft end of the aft cylinder of chamber R369:

Reinforced	Membrane
350 to 377	472 to 514
Av (3) 368	Av (3) 490

Note that the highest value obtained from the three tests of the reinforced section (377 in.-lb/in.^{2}) was appreciably lower than the lowest value obtained from the three tests of the membrane wall (472 in.-lb/in.^{2}); thus, from an engineering viewpoint, there was a significant difference between the arithmetical mean values (368 for the thicker wall and 490 in.-lb/in.^{2} for the membrane wall). This trend is consistent with the effect of thickness usually observed in plane-stress fracture testing. From an examination of Table IX, it will be seen that

the scatter bands obtained in the two thicknesses sometimes overlapped and, therefore, there was uncertainty from an engineering viewpoint as to whether the difference in arithmetical mean between the two thicknesses tested was significant; this question will be reconsidered in subsequent paragraphs dealing with a statistical evaluation of the data. However, it should be noted from Table IX when there was no overlap of the W/A values, as illustrated above for chamber R369, the data always showed the reinforced section to have the lower toughness.

Figure 8 presents, in bar graph form, the data of Table IX. A comparison of adjacent bars (solid versus stippled) shows the difference between reinforced and membrane walls, and a comparison of adjacent pairs of bars shows the variation, if any, from end-to end-of any given forging. The top of any given bar represents the highest W/A values measured, and the top of the solid (or stippled) part of any given bar represents the lowest value measured; the solid point is the arithmetical mean of the W/A values for any given bar. Note that with few exceptions, the reinforced (thicker) sections had lower arithmetical mean values than the membrane sections. The exceptions generally involved differences of less than 50 in.-lb/in.^{2} Figure 8 also shows the marked differences in toughness that existed from forging to forging in a given chamber. Note, for example, the difference between the forward and aft cylinders in chamber R369. Other chambers, for example 673095, had even greater differences in toughness from forging to forging.

An analysis of variance was made to determine if there was a statistically significant difference (1) between cylinders, (2) between ends of cylinders, and (3) between thicknesses in a given cylinder. On the basis of an analysis of variance of the data from the body cylinders of eight chambers, it was determined that (1) there was a highly significant difference between cylinders (significance level 0.0001), and (2) there was a highly significant difference between the reinforced sections and the membrane walls (significance level 0.0002), but there appeared to be no significant difference between ends of cylinders (significance level 0.3120).

When the data were divided into two sets, one for membrane-wall and one for reinforced-section samples, the analysis of variance showed for the reinforced-section samples a highly significant difference between cylinders (significance level 0.0004), but, again, there appeared to be no significant difference between ends of cylinders (significance level 0.1384). For the membrane-wall samples, there was a highly significant difference between cylinders (significance level 0.0004) and a highly significant difference between ends of cylinders (significance level 0.0021).

C. EFFECT OF CHEMISTRY AND FORGING PRACTICE

The precrack Charpy impact W/A values tabulated in Appendix A were analyzed statistically to determine the effect of interstitials (C, N_2, H_2,

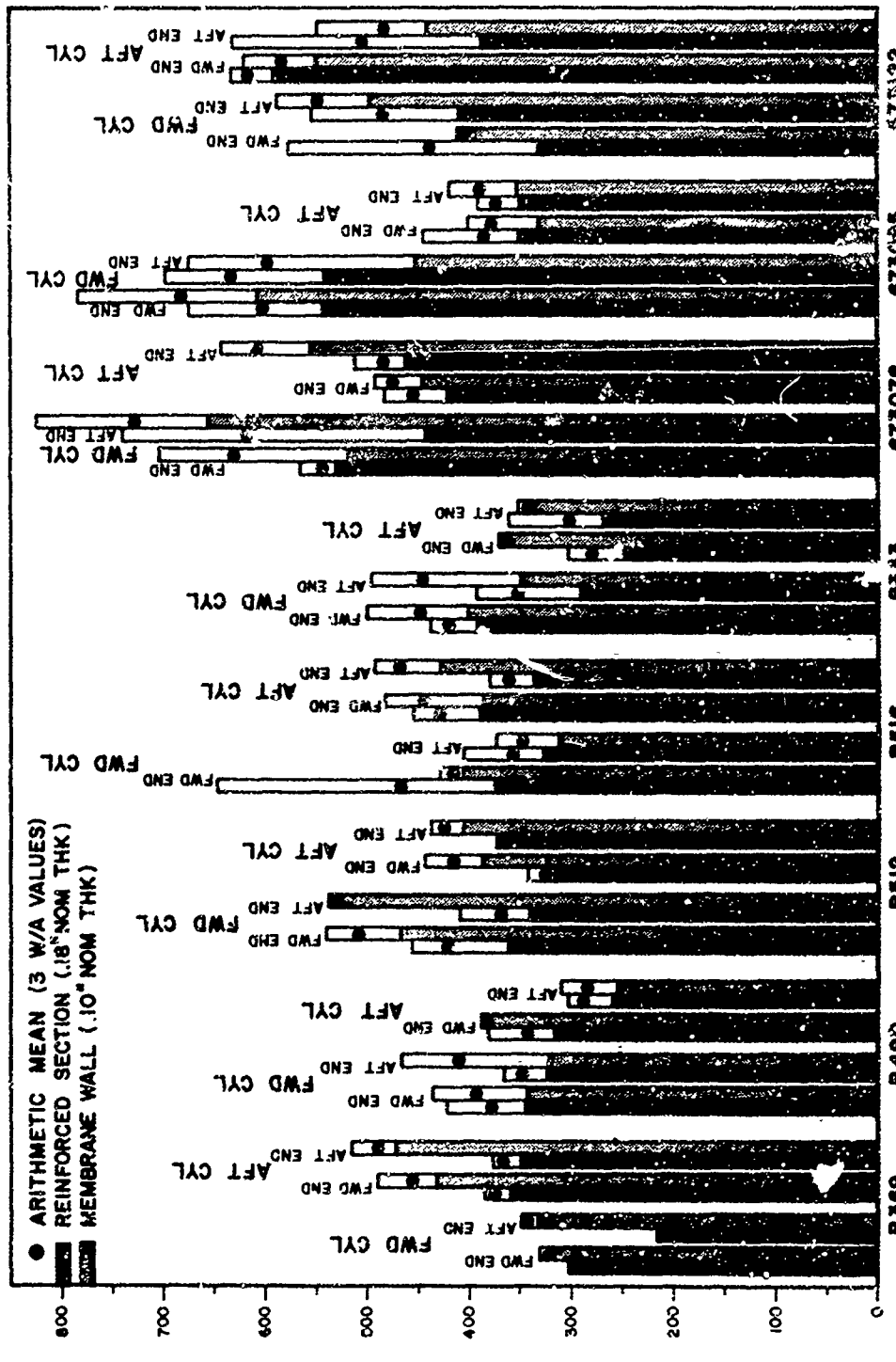

Figure 8. Inhomogeneity and Thickness Effects in 6Al-4V Titanium Forgings

and O_2) on W/A values. It must be pointed out that the statistical results are valid only for materials having the chemistry of 6Al-4V titanium comparable to that of these data. The data were separated according to whether they were taken from the membrane wall or reinforced section; i.e., one set was for a nominal 0.10-in. thickness and the other set for a nominal 0.18-in. thickness.

From Table X, it is obvious that there are basically three types of forgings and several aging temperatures involved in the data collection. Before the W/A values could be tested for dependence on chemistry, it was necessary to determine the effect of the type of forging and/or aging temperature on the W/A values.

1. Membrane 0.10-in.-Thick Material

When the data were separated into three categories, one for each type of forging, and analyzed by one-way multiple covariance analysis, it was found that there were significant differences in the means among forging types. The data were again separated, this time into two categories, one for those specimens aged at temperatures below or at 1000°F, and the other for those specimens aged above 1000°F. When the data were analyzed by analysis of variance, it was found that there was no difference between the means for the aging temperatures. Also, it was found that there were no forging-temperature interactions.

Since the W/A values were dependent on the type of forging, the data were separated into three categories, one for each type of forging. Multiple regression and correlation analyses were used to determine if the W/A values, for each forging type, were a function of carbon, oxygen, hydrogen, and/or nitrogen. The method of least squares was used to develop equations which gave the best fit to the data for each combination of interstitials. The hypothesis was made that the slope of each curve was zero and the "T" test was used to test the hypothesis. In Table XI, those instances where the hypothesis was false, i.e., where there was a dependence of W/A on chemistry, an asterisk is used to identify the elements that influence the W/A value. The results as presented in Table XI, may be summarized as follows: for closed-die forgings there is a correlation between W/A and O_2, and for ring-rolled forgings and extrusions, the strongest correlation was between W/A and C. The reason for this may be contained in the range of interstitial elements found in each forging type, as shown in the following tabulations:

TABLE X

CHEMISTRY OF MINUTEMAN CHAMBER COMPONENTS

Chamber/ Component	Type of Forging	Al	V	Fe	C	N_2	H_2	O_2	Solution Temp., °F	Aging Temp. °F
R26										
Fwd Clos	Closed Die								1780	1000
Fwd Cyl	Ring Roll								1750	1000
Aft Cyl	Ring Roll								1750	1000
Aft Fla	-								1780	1000
2191456										
Fwd Clos	Closed Die	6.12	4.02	0.30	0.03	0.014	0.008	0.20	1750	1100
Fwd Cyl	Ring Roll	6.22	4.15	0.18	0.04	0.007	0.006	0.17	1750	1050
Aft Cyl	Ring Roll	6.52	4.15	0.158	0.02	-	0.006	0.14	1750	1100
Aft Fla	Closed Die	6.40	4.08	0.17	0.01	0.024	0.0098	0.12	1750	1100
BL26										
Fwd Clos	Closed Die	6.38	4.18	0.18	0.08	0.028	0.0010	0.166	1050	1125
Fwd Cyl	-	6.18	4.33	0.19	0.05	0.039	0.0015	0.150	1750	1100
Aft Cyl	-	6.09	4.34	0.19	0.03	0.024	0.0022	0.183	1750	1000
Aft Fla	Closed Die	6.08	4.13	0.19	0.07	0.029	0.0041	0.168	1750	1125
673078										
Fwd Clos	Closed Die	6.30	4.06	0.16	0.04	0.017	0.0024	0.184	1750	1000
Fwd Cyl	Extrusion	6.55	4.02	0.23	0.05	0.011	0.0023	0.174	1750	1000
Aft Cyl	Extrusion	6.35	4.08	0.21	0.02	0.016	0.0030	0.192	1750	1000
Aft Fla	Closed Die	6.40	4.16	0.13	0.003	0.016	0.0025	0.11	1750	1000
673095										
Fwd Clos	Closed Die	6.35	4.16	0.14	0.06	0.013	0.0017	0.16	1775	1000
Fwd Cyl	Ring Roll	6.10	3.96	0.19	0.02	0.014	0.0033	0.19	1775	1000
Aft Cyl	Ring Roll	6.48	3.62	0.18	0.08	0.019	0.0034	0.22	1775	1000
Aft Fla	Closed Die	6.39	3.90	0.18	0.03	0.018	0.0027	0.19	1750	1000
673122										
Fwd Clos	Closed Die	6.18	3.98	0.08	0.03	0.040	0.0036	0.162	1800	1000
Fwd Cyl	Ring Roll	6.26	4.13	0.08	0.05	0.031	0.0077	0.165	1800	950
Aft Cyl	Ring Roll	6.10	4.02	0.07	0.05	0.018	0.0055	0.171	1830	1000
Aft Fla	Ring Roll	6.38	4.13	0.08	0.04	0.026	0.0044	0.170	1810	900
674514										
Fwd Clos	Closed Die	6.07	4.09	0.07	0.05	0.049	0.0003	0.134	1750	1000
Fwd Cyl	Extrusion	5.95	4.12	0.10	0.04	0.034	0.0031	0.162	1750	1000
Aft Cyl	Extrusion	6.00	4.18	0.10	0.03	0.031	0.0010	0.157	1750	1000
Aft Fla	Ring Roll	6.15	4.17	0.09	0.04	0.045	0.0082	0.148	1750	1000
2192109										
Fwd Clos	Closed Die	6.42	4.33	0.24	0.023	0.017	0.0021	0.185	1750	1000
Fwd Cyl	Extrusion	6.31	4.41	0.15	0.021	0.011	0.0016	0.17	1750	1000
Aft Cyl	Extrusion	6.42	4.48	0.15	0.027	0.007	0.0015	0.19	1750	1000

TABLE X (cont.)

Chamber/ Component	Type of Forging	Al	V	Fe	C	N_2	H_2	O_2	Solution Temp., °F	Aging Temp., °F
R369										
Fwd Skrt	Ring Roll	6.50	3.90	0.13	0.025	0.032	0.0054	0.16	1800	1000
Fwd Clos	Closed Die	6.65	4.30	0.24	0.031	0.007	0.0019	0.15	1750	1050
Fwd Cyl	Extrusion	6.3	4.25	0.18	0.024	0.010	0.005	0.185	1775	1075
Aft Cyl	Extrusion	6.5	4.1	0.18	0.24	0.013	0.0075	0.17	1775	1075
Aft Clos	Closed Die	6.70	4.00	0.15	0.030	0.010	0.0047	0.19	1750	1000
Aft Skrt	Ring Roll	6.52	4.33	0.30	0.039	0.009	0.0051	0.17	1750	1050
R490										
Fwd Skrt	Ring Roll	6.53	4.10	0.16	0.013	0.011	0.0043	0.18	1750	1050
Fwd Clos	Closed Die	6.64	3.87	0.17	0.017	0.011	0.0019	0.17	1750	1000
Fwd Cyl	Extrusion	6.25	4.1	0.175	0.022	0.014	0.003	0.18	1750	1025
Aft Cyl	Extrusion	6.4	4.15	0.19	0.022	0.011	0.0035	0.18	1750	1025
Aft Clos	Closed Die	6.54	3.97	0.15	0.046	0.013	0.0021	0.16	1750	1000
Aft Skrt	Ring Roll	6.62	3.89	0.16	0.031	0.011	0.0021	0.14	1750	1000
R512										
Fwd Skrt	Ring Roll	6.64	3.95	0.13	0.021	0.008	0.0065	0.15	1750	1000
Fwd Clos	Closed Die	6.68	3.60	0.13	0.019	0.011	0.0033	0.14	1750	1000
Fwd Cyl	Extrusion	6.2	4.15	0.16	0.022	0.010	0.0065	0.185	1750	1025
Aft Cyl	Extrusion	6.1	4.05	0.155	0.024	0.010	0.0045	0.175	1750	1025
Aft Clos	Closed Die	6.50	4.01	0.20	0.018	0.013	0.0019	0.17	1750	1000
Aft Skrt	Ring Roll	6.58	3.99	0.16	0.017	0.013	0.0032	0.14	1750	1000
R516										
Fwd Skrt	Ring Roll	6.53	4.10	0.16	0.013	0.011	0.0043	0.18	1750	1050
Fwd Clos	Closed Die	6.57	4.00	0.20	0.019	0.009	0.0036	0.16	1750	1050
Fwd Cyl	Extrusion	6.55	4.15	0.21	0.024	0.012	0.0085	0.19	1750	1025
Aft Cyl	Extrusion	6.3	4.2	0.21	0.021	0.014	0.0085	0.185	1750	1025
Aft Clos	Closed Die	6.66	3.83	0.16	0.016	0.013	0.0020	0.19	1750	1050
Aft Skrt	Ring Roll	6.57	3.96	0.14	0.048	0.010	0.0031	0.13	1750	1100
R543										
Fwd Skrt	Ring Roll	6.24	4.01	0.15	0.020	0.013	0.0023	0.15	1780	1000
Fwd Clos	Closed Die	6.14	4.15	0.17	0.026	0.010	0.0016	0.18	1750	1100
Fwd Cyl	Extrusion	6.5	4.45	0.08	0.02	0.012	0.0058	0.174	1750	1025
Aft Cyl	Extrusion	6.3	4.25	0.19	0.024	0.012	0.007	0.195	1750	1025
Aft Clos	Closed Die	6.49	3.61	0.18	0.027	0.012	0.0044	0.12	1750	1050
Aft Skrt	Ring Roll	6.55	4.08	0.15	0.016	0.012	0.0049	0.14	1750	1050

TABLE XI

SUMMARY OF MULTIPLE REGRESSION AND CORRELATION ANALYSIS FOR MEMBRANE-WALL MATERIAL

Interstitial Combinations Investigated	Closed-Die Forgings		Ring-Rolled Forgings		Extrusions	
	Correlation Coefficient	Regression Coefficient	Correlation Coefficient	Regression Coefficient	Correlation Coefficient	Regression Coefficient
C, N_2, H_2, O_2	*	O_2	*	C	*	C
C	-	-	*	C	*	C
N_2	-	-	*	N_2	-	-
H_2	-	-	-	-	-	-
O_2	*	O_2	*	O_2	-	-
(N_2+O_2)	*	(N_2+O_2)	*	(N_2+O_2)	-	-
(H_2+O_2)	*	(H_2+O_2)	*	(H_2+O_2)	-	-
C, N_2	-	-	*	C, N_2	*	C
C, H_2	-	-	*	C, H_2	*	C
C, O_2	*	O_2	*	C	*	C
N_2, H_2	-	-	*	N_2	-	-
N_2, O_2	*	O_2	*	N_2, O_2	-	-
H_2, O_2	*	O_2	*	H_2, O_2	-	-
C, N_2, H_2	-	-	*	C	*	C
C, N_2, O_2	-	-	*	C, N_2	*	C
C, H_2, O_2	*	O_2	*	C	*	C
N_2, H_2, O_2	*	O_2	*	H_2, O_2	-	-

* Significance Level 0.05

IV, C, Effect of Chemistry and Forging Practice (cont.)

FORGINGS TESTED IN MEMBRANE WALL

	No. Forgings	Carbon	Nitrogen	Hydrogen	Oxygen
Closed-die Forgings	19	0.010 to 0.050	0.009 to 0.024	0.0016 to 0.0047	0.110 to 0.200
Ring-rolled Forgings	18	0.013 to 0.050	0.008 to 0.032	0.0021 to 0.0065	0.130 to 0.190
Extrusions	16	0.020 to 0.030	0.007 to 0.016	0.0010 to 0.0075	0.157 to 0.195

Note that for the closed-die forgings there was a considerable spread, within the limits, in the amount of carbon and oxygen, and relatively little spread in the amount of nitrogen and hydrogen. For ring-rolled forgings, the spread in carbon is approximately the same as for the closed-die forgings, but there was a smaller spread in oxygen and a slight increase in spread for nitrogen and hydrogen as compared with the closed-die forgings. In the extrusions, the spread for all four interstitials was appreciably smaller than in either the closed-die or ring-rolled forgings. The statistical-analysis results in Table XI are generally consistent with the above observations. For closed-die forgings, W/A was found to be dependent on oxygen, and there was no interaction with the other three elements. For ring-rolled forgings, W/A was dependent primarily on carbon and to a lesser degree on nitrogen and oxygen. For extrusions, W/A was solely dependent on carbon content. For the conditions investigated, the above results indicate that the W/A value may be more dependent on carbon, within prescribed limits, than on oxygen with the exception of those instances when oxygen varied widely.

On the basis of the available data, equations were developed whereby W/A was given as a function of interstitial content. The equations, determined by the computer program, were as follows:

Closed-die Forgings: $W/A = 658.0 - 914.0(C) + 677.7(N_2) + 737.4(H_2) - 928.8(O_2)$

Ring-roll Forgings: $W/A = 869.6 - 3810.8(C) - 3057.1(N_2) - 784.5(H_2) - 622.3(O_2)$

Extrusions: $W/A = 19.3 + 8072.6(C) - 2303.8(N_2) + 165.9(H_2) + 1360.2(O_2)$

Note that the equation for ring-rolled forgings was of the form that might be expected, where the toughness value decreases by the addition of interstitials.

2. Reinforced-Section Material

When the data were separated into three categories, one for each type of forging, and analyzed by one-way multiple covariance analysis, it was found that there was no significant difference in the means among forging types. The data were again separated, this time into two categories; one for

those specimens aged at temperatures below or at 1000°F, and the other for those specimens aged above 1000°F. When the data were analyzed by analysis of variance, it was found that there was a difference in the means for the two temperature levels. However, it was found that there was no forging-temperature interaction. The range of interstitial elements found in each forging type is shown in the following tabulation:

FORGINGS TESTED IN THE REINFORCED SECTION

	No. Forgings	Carbon	Nitrogen	Hydrogen	Oxygen
Closed-die Forgings	19	0.010 to 0.046	0.007 to 0.024	0.0016 to 0.0047	0.110 to 0.190
Ring-roll Forgings	6	0.040 to 0.050	0.007 to 0.045	0.0044 to 0.0077	0.140 to 0.170
Extrusions	1	0.020 to 0.040	0.010 to 0.019	0.0010 to 0.0075	0.150 to 0.195

Since the W/A values were dependent on the aging temperature, the data were separated into two categories, one for each temperature range. Multiple regression and correlation analysis was used to determine if the W/A values, for each temperature range, were a function of carbon, oxygen, hydrogen, or nitrogen. The results of the multiple regression and correlation analysis are summarized in Table XII. The method of least squares was used to develop equations for each combination of interstitials which gave the best fit to the data. The hypothesis was made that the slope of each curve was zero and the "T" test was used to test the hypothesis. In Table XII, those instances where the hypothesis was false; i.e., where there was a dependence of W/A on chemistry, and asterisk was used to identify the elements that influence the W/A value. The data in Table XII show that for each aging temperature range, the W/A value was dependent on oxygen content.

On the basis of the available data, equations were developed whereby W/A was given as a function of interstitial content. The equations determined by the computer program were as follows:

For aging temperature $\leq$ 1000°F

$$W/A = 915.4 + 278.8(C) - 1207.2(N_2) + 9047.4(H_2) - 2614.6(O_2)$$

For aging temperature > 1000°F

$$W/A = 716.5 - 3421.8(C) + 4905.6(N_2) - 178.0(H_2) - 1851.7(O_2)$$

The range of interstitial elements found in the forgings that fall into the two categories of aging temperature is shown in the following tabulation:

TABLE XII

SUMMARY OF MULTIPLE REGRESSION AND CORRELATION ANALYSIS FOR REINFORCED-SECTION MATERIAL

Interstitial Combinations Investigated	Aging Temperature (°F) ≤1000 Correlation Coefficient	≤1000 Regression Coefficient	>1000 Correlation Coefficient	>1000 Regression Coefficient
C, N_2, H_2, O_2	*	O_2	*	O_2
C	-	-	-	-
N_2	-	-	-	-
H_2	-	-	-	-
O_2	*	O_2	*	O_2
(N_2+O_2)	*	(N_2+O_2)	*	(N_2+O_2)
(H_2+O_2)	*	(H_2+O_2)	*	(H_2+O_2)
C, N_2	-	-	-	-
C, H_2	-	-	-	-
C, O_2	*	O_2	*	C, O_2
N_2, H_2	-	-	-	-
N_2, O_2	-	-	*	O_2
H_2, O_2	*	O_2	*	O_2
C, N_2, H_2	-	-	-	-
C, N_2, O_2	*	O_2	*	O_2
C, H_2, O_2	*	O_2	*	C, O_2
N_2, H_2, O_2	*	O_2	*	O_2

*Significance Level 0.05

IV, C, Effect of Chemistry and Forging Practice (cont.)

	No. Forgings	Carbon	Nitrogen	Hydrogen	Oxygen
≤ 1000°F	34	0.017 to 0.050	0.010 to 0.040	0.0010 to 0.0055	0.134 to 0.192
> 1000°F	27	0.010 to 0.031	0.007 to 0.014	0.0016 to 0.0085	0.140 to 0.200

D. EFFECT OF TEST TEMPERATURE

The transition from high-energy oblique fracture to low-energy flat fracture with decreasing temperature is well established from both standard V-notch and precrack Charpy impact data. Figure 9 illustrates the variation in toughness and attending fracture appearance with temperature in the precrack Charpy impact test. The material is Minuteman 6Al-4V titanium tested in the 0.10-in. thickness, aged to two yield-strength levels. Note the increase from 45 to 90% oblique fracture as the temperature was increased from -40 to 320°F in the lower strength condition. The precrack Charpy impact and centernotch (CN) tensile data presented in Figure 10 are from the Supersonic Transport Research Program.* Note that many of the CN-tensile data were invalidated by excessive net-section stress and, consequently, had to be plotted as minimum values. The precrack Charpy impact test, on the other hand, indicated increasing fracture toughness with increasing temperature.

In Phase I of the current data collection, two chambers (SNs 2192109 and 673122) were evaluated by precrack Charpy impact tests at both room temperature and at 200 and 320°F. The test results are presented in Figure 11. Note that at room temperature, the slow bend test result was markedly lower than the impact test result; whereas, at elevated temperature, there was little or no difference between the slow-bend and impact test results. This difference in material behavior when tested in slow bend and impact is believed to be the result of a complex interplay of adiabatic deformation at the crack tip when tested in impact, and time-dependent metallurgical effects (such as the diffusion of hydrogen) when tested in slow bending.**

Additional plots of data based on tests of the body cylinders of three successfully hydrotested Minuteman 6Al-4V titanium chambers are presented in Figure 12. Note that in chamber 2191093, at room temperature the slow-bend

*"Thick-Section Fracture Toughness," a Boeing-North American joint venture, under Federal Aviation Contract AF 33(657)-11461.

**Hartbower, C. E., "Materials Sensitive to Slow Rates of Straining" Scheduled for Presentation at the ASTM Symposium on Testing by Impact, Annual Meeting, Atlantic City, June 1969.

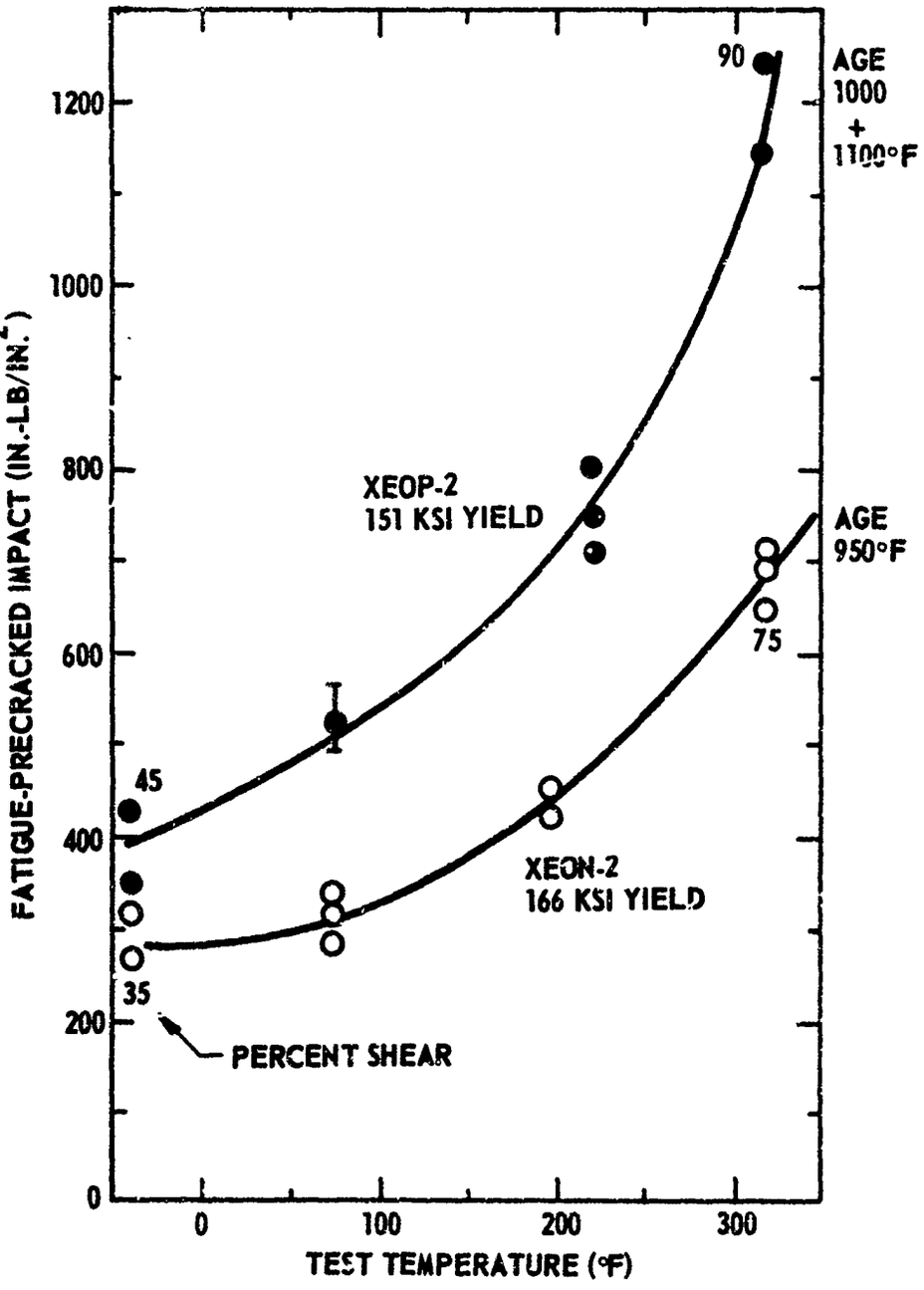

Figure 9. Effect of Temperature on the Precrack Charpy Impact W/A Value in 6Al-4V Titanium

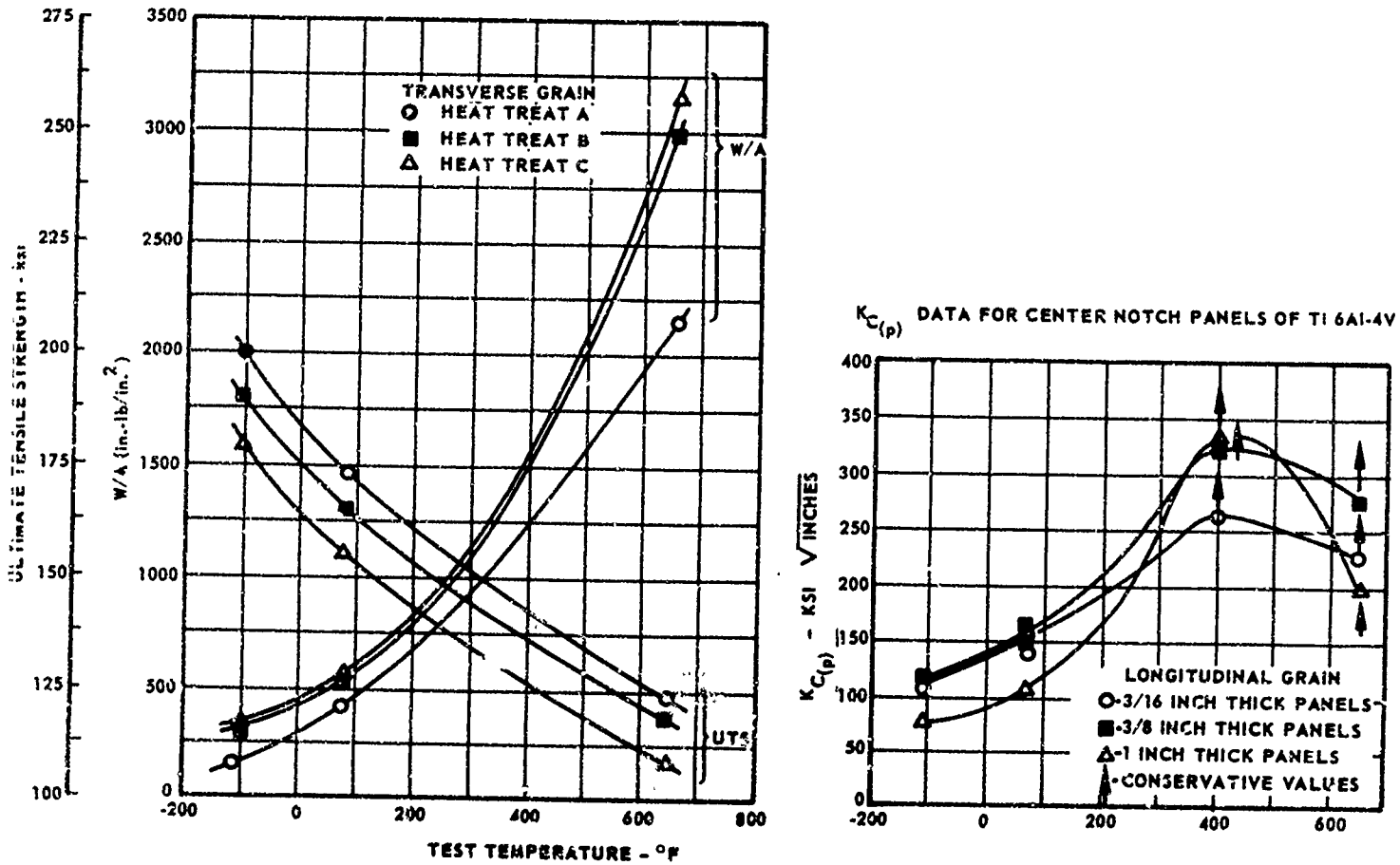

Figure 10. Effect of Temperature on Precrack Charpy Impact and CN-Tensile Tests in 6Al-4V Titanium

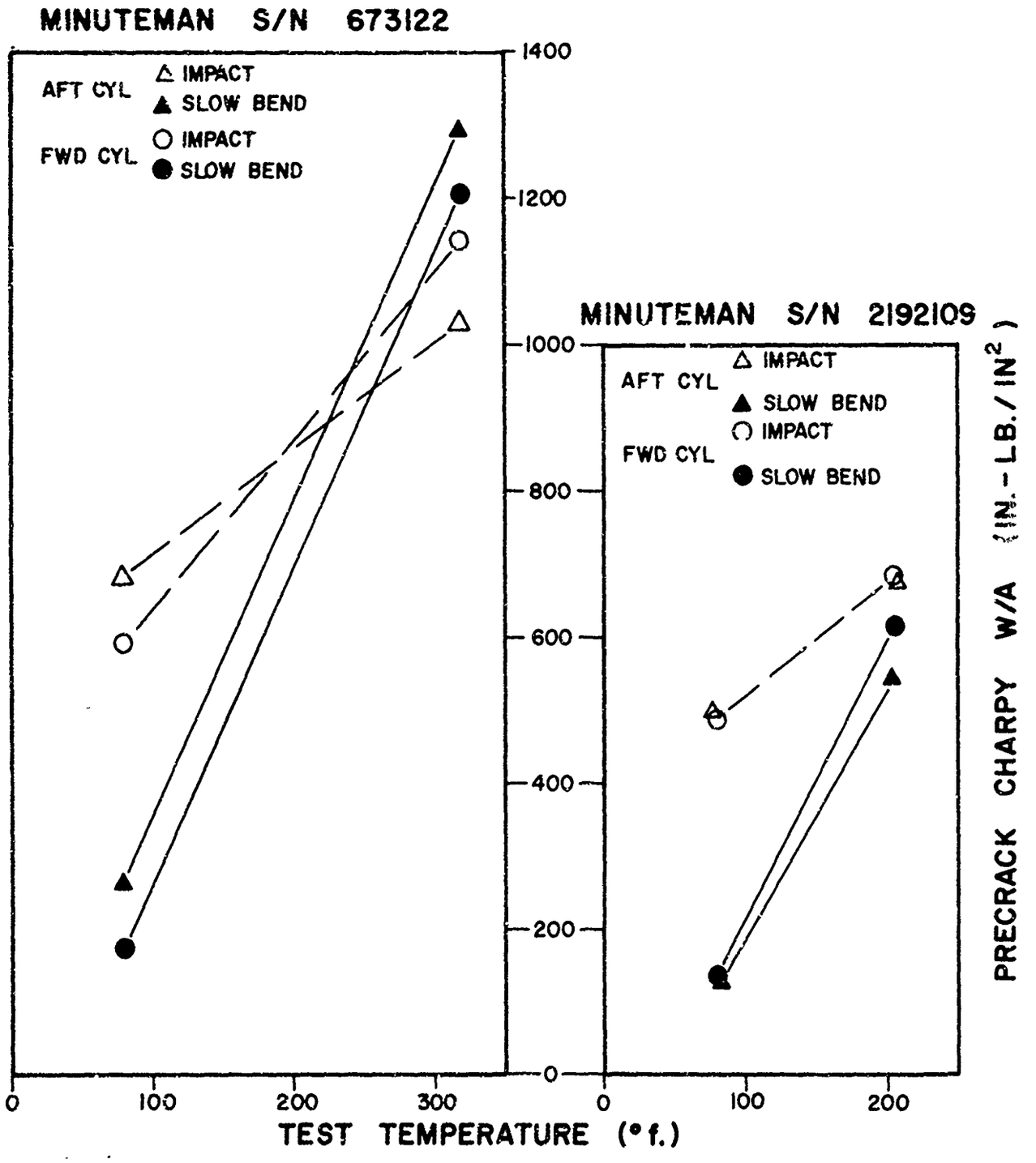

Figure 11. Effect of Temperature on Precrack Charpy Slow-Bend and Impact Tests of 6Al-4V Titanium Chambers 673122 and 2192109

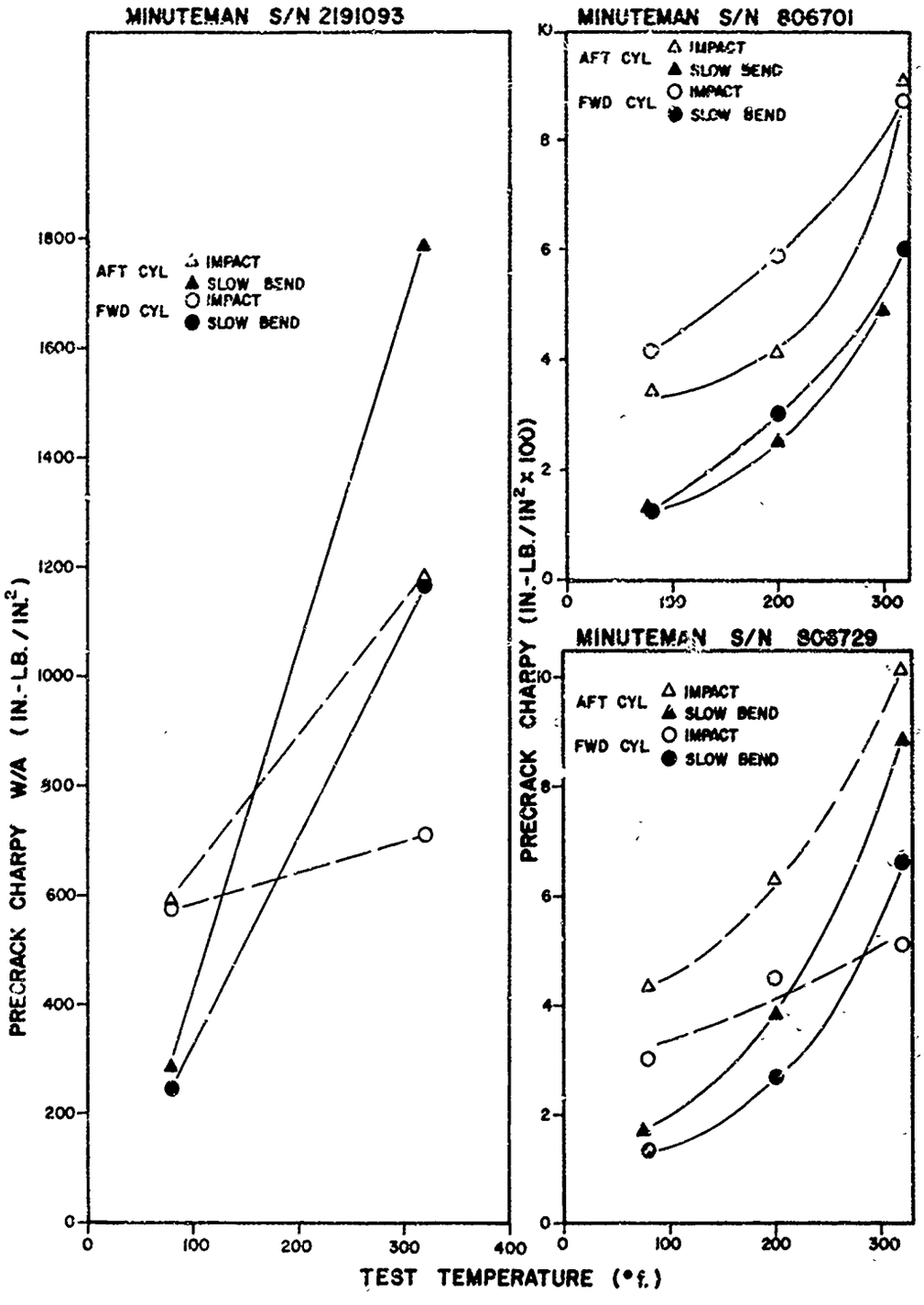

Figure 12. Effect of Temperature on the Toughness of Forgings in Chambers 2191093, and 806729

IV, D, Effect of Test Temperature (cont.)

W/A value was significantly lower than that obtained in impact; whereas, at 320°F, there was a complete reversal of the trend. In chambers 806701 and 806729, the behavior was different in that the slow-bend test result was lower than that obtained in impact in three out of the four body cylinders at all temperatures tested. It is suspected that the forging practice used in manufacturing the body cylinders of chambers 806701 and 806729 was different from that used for 2191093; however, information on the forging practice for these chambers was not available.

Figure 13 is a composite of the precrack Charpy impact transition curves for 55 chamber components tested in the current data collection. The curves for each individual forging will be found in Appendix I. From Figure 13, it will be noted that the band encompassing the data was wide, indicating considerable variation in toughness from component to component at any given temperature. At -40°F, the W/A values ranged from approximately 200 to 600 in.-lb/in.^{2}; at room temperature, from about 250 to 800 in.-lb/in.^{2}; at 200°F from about 400 to 1100 in.-lb/in.^{2}; and at 320°F, from about 600 to 1500 in.-lb/in.^{2}. The average W/A values at each temperature level are shown in the following summary tabulation:

Test Temperature, °F	Number Averaged	Arithmetical Mean
-40	51	380
RT	149	480
200	53	650
320	52	920

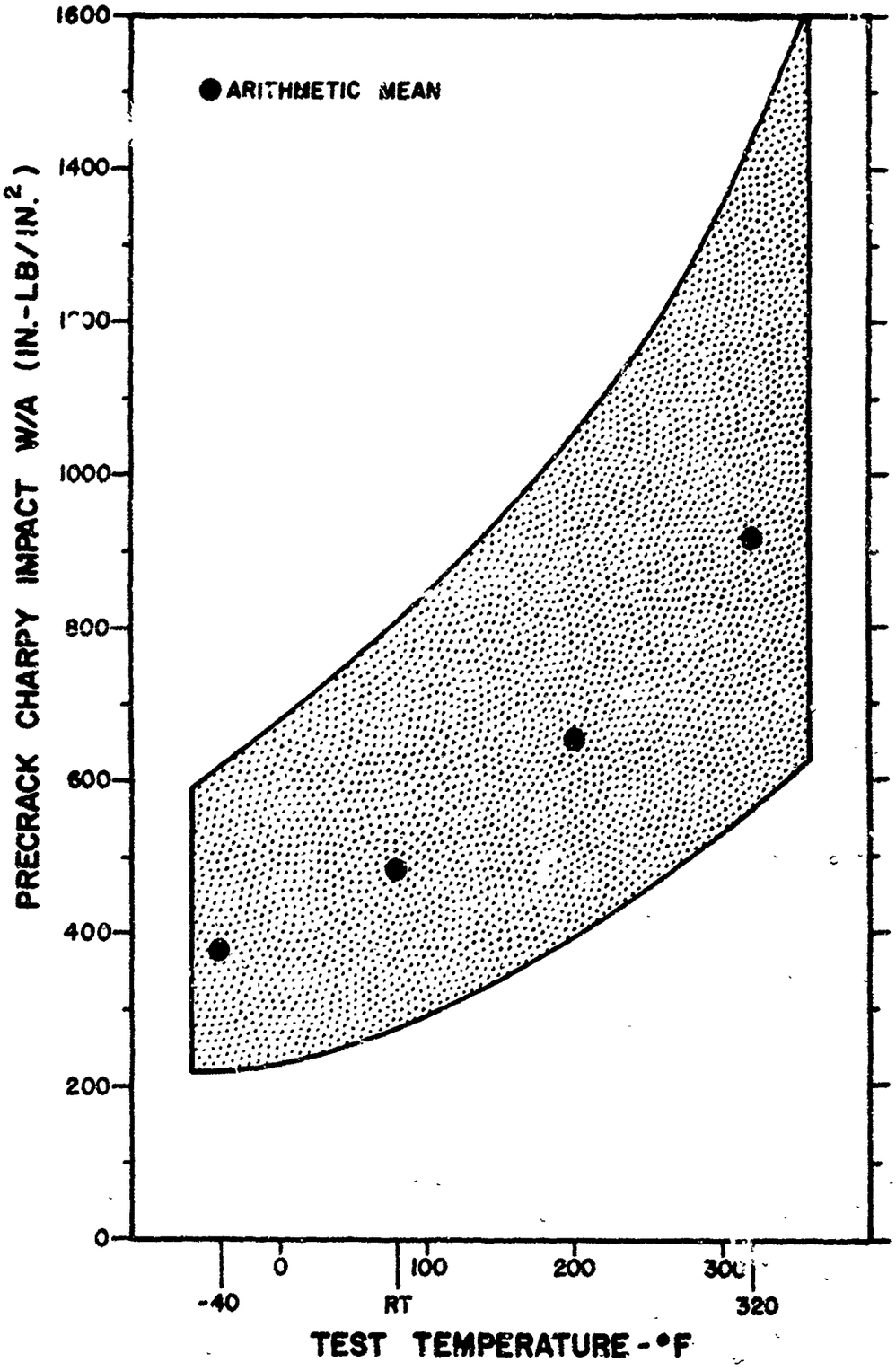

Figure 13. Composite Precrack Charpy Impact Transition Curves for 55 6Al-4V Titanium Forgings

IV, Discussion of Results (cont.)

E. CORRELATION OF FRACTURE TOUGHNESS AND CHAMBER PERFORMANCE

1. Correlation Concepts

When an existing flaw reaches the critical stress intensity under plane-strain conditions (K_{Ic}), the flaw will become unstable (pop-in) but then in some chambers be arrested by plane-stress crack toughness on penetrating the chamber wall ($c_{cr} > B$). The fact that there was relatively little variation in plane-strain crack toughness (K_{Ic}) as measured in 109 forgings, whereas, there was considerable variation in plane-stress crack toughness (K_c) suggests that K_c is the controlling property in 6Al-4V Minuteman chamber performance.

If a given chamber were to have a defect in each component, and if each defect were of the same size and orientation and equally stressed, on increasing the pressure the lowest-toughness component would reach a critical stress intensity first and fail the chamber. In a real situation, where some components contain flaws and others do not, the component with the highest stress-intensity flaw will fail the chamber, assuming the flawed components all have the same toughness. If the flawed components are of unequal toughness, the first component to reach a critical crack size will fail the chamber. Similarly, if only one component contains a defect, when that defect is stressed to the critical stress intensity, the chamber will fail. Thus, if a given chamber contains components of different fracture toughness, the component containing a flaw of critical size will fail the chamber even if that component has the highest toughness of any of the chamber components. On the other hand, if the critical crack size is not reached by the time the proof test is completed, the chamber will pass the proof test even though the crack may have been enlarged in the process.

Most of the prematurely failed Minuteman chambers contained a flaw which from discoloration was known to have existed before going into proof test. If the original flaw were to pop-in and then be arrested as a result of the plane-stress critical-crack-size being greater than twice the material thickness ($c > B$), there would have to be additional slow crack growth before catastrophic failure of the chamber. In other words, the arrested crack after pop-in would have to grow to the critical crack size under plane-stress conditions. The fact that some chambers failed while under constant load (at proof pressure) indicates that slow crack growth (probably stress corrosion cracking) did in fact occur. One way to verify this would be to calculate the failure hoop stress based on the heat-stained (original) defect dimensions and the mean plane-strain crack toughness (K_{Ic} = 39 ksi-in.$^{1/2}$) from the equation

$$K_{Ic}^2 = 1.21\pi F^2 a/Q$$

where F is the hoop stress at failure and a/Q the normalized crack depth. If the calculated value of stress were found to agree with failure hoop stress, it could be assumed that there was little, if any, slow crack growth. If, on the other hand, there were appreciable slow crack growth before plane-strain pop-in, the calculated value of hoop stress based on the heat-stained crack dimensions would be larger than the observed failure hoop stress. Because Q is a function of the ratio of failure stress to yield strength, iteration would have been required for calculating the failure hoop stress. To avoid this, the critical stress intensity (K_{Ic}) was calculated instead of the hoop stress, using the actual hoop stress at failure and the original flaw dimensions. With an appreciable amount of slow crack growth before pop-in, the calculated value of K_{Ic} would be low compared with the mean plane-strain crack toughness (K_{Ic} = 39 ksi-in.$^{1/2}$) as determined in Phase I of this contract.

Figures 14 and 15 provide a graphical solution of the equation

$$K_{Ic}^2 = 1.21\pi F^2 a/Q$$

for surface part-through cracks. Table XIII presents the yield strengths as measured from integral-ring material stress-relieved with the chamber.

2. Premature-Failure Case Histories

Of the 14 Minuteman chambers selected for the data collection, nine were premature proof-test failures. The following paragraphs present the salient facts relating to the failures, including the hoop stress at which failure occurred, and the nature and location of the originating defect. In some instances, a limited amount of precontract fracture testing was done on the casualty chamber; these data also are presented.

a. Chamber R26

In May 1962, chamber R26 failed during proof test with the fracture origin in the adapter of the forward closure. The failure occurred after 15 sec at maximum pressure (96-ksi hoop stress at the fracture origin). Examination of the fracture surfaces revealed a surface crack in the forward adapter 0.2 in. forward of the forward girth weld, near the heat-affected zone of the weld; the defect was approximately 0.10 in. deep and 0.18 in. long.

Uniaxial and PTC-tensile specimens were taken from the forward cylinder of chamber R26 across the forward girth weld opposite the origin of failure. The uniaxial tensile specimens from the forward cylinder

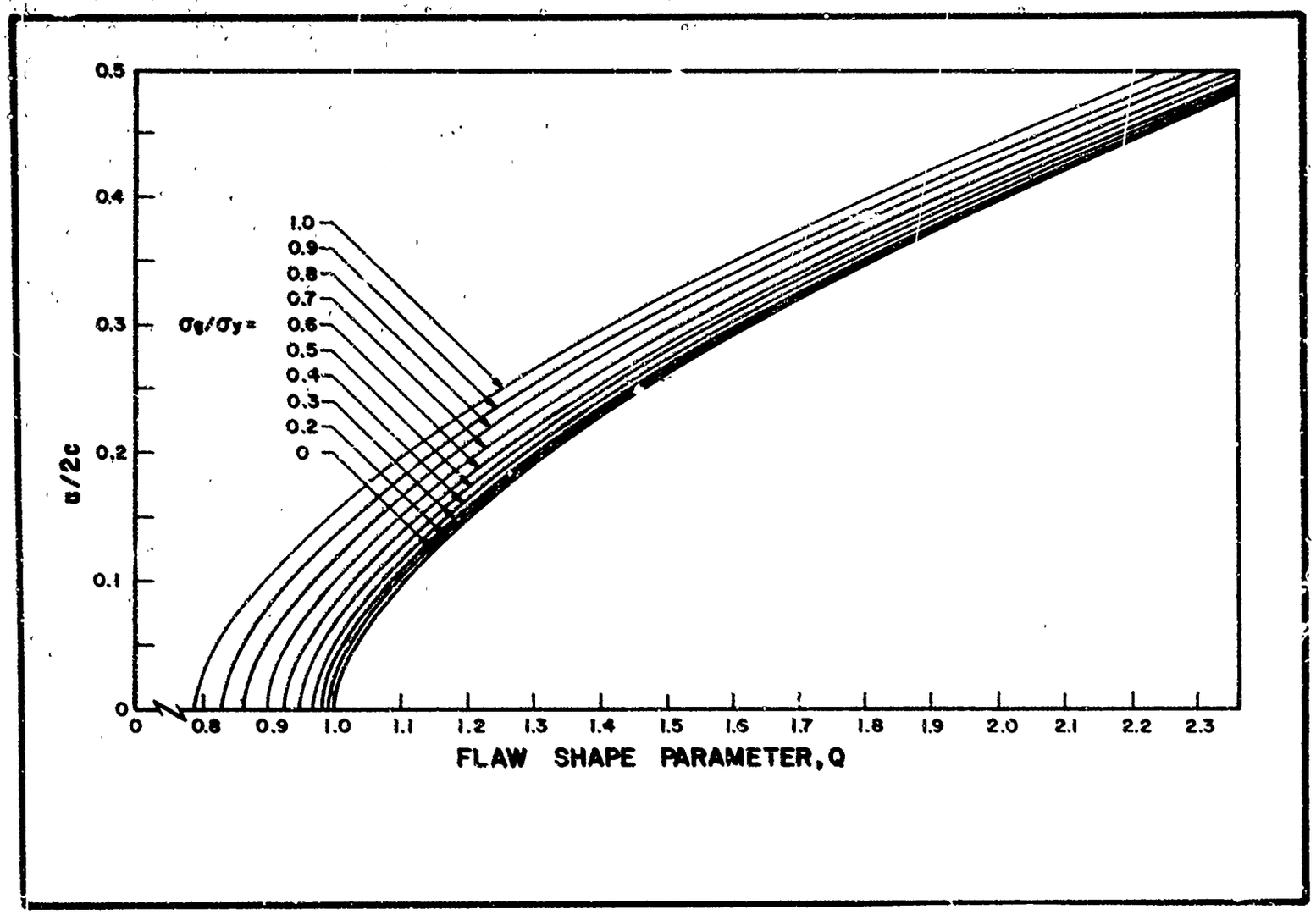

Figure 14. Flaw-Shape Parameter for Surface Embedded Flaws

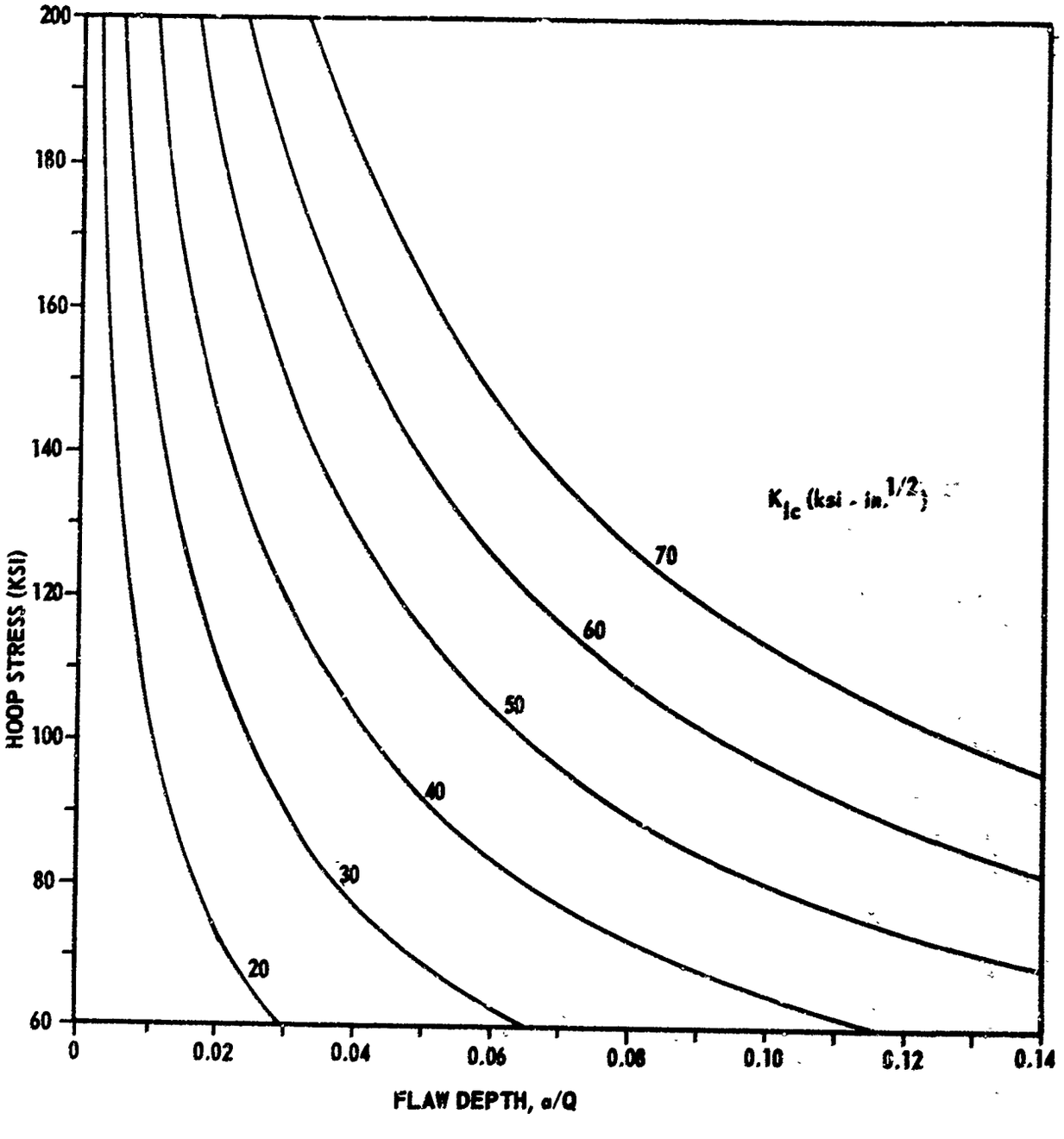

Figure 15. Hoop Fracture Stress as a Function of Normalized Flow Depth for Various Plane-Strain Critical-Stress-Intensity Levels

TABLE XIII

TENSILE PROPERTIES OF MINUTEMAN COMPONENTS AFTER CHAMBER STRESS RELIEF

Chamber	Fwd Closure		Fwd Cylinder		Aft Cylinder		Aft Flange	
	Yield ksi	Ult. ksi	Yield ksi	Ult. ksi	Yield ksi	Ult. ksi	Yield ksi	Ult. ksi
R26	167	178	165	173	165	177	168	174
BL26	160	170	158	167	164	175	166	175
R369	167	178	162	171	167	175	164	176
R490	164	176	161	172	168	176	162	174
R512	162	175	166	175	164	174	167	176
R516	164	177	165	176	165	174	162	174
R543	159	169	159	173	163	175	163	169
673078	168	183	170	184	164	176	164	180
2191456	169	179	166	177	158	168	164	176
2192109	166	176	167	174	165	173	166	173

near the fracture origin exhibited exceptionally low elongation*; examination of the tensile-specimen fracture surfaces revealed thumbnail-shaped spots of oxidation, surrounded by flat fracture. The defects were approximately 0.015 in. by 0.010 in. Metallography revealed no microstructural abnormality. The defects were in the surface corresponding to the ID surface of the chamber. In that the test specimens were heat-straightened (900°F for 2 hr) prior to testing, the defects could have been produced by the heat-straightening operation, or they could have been present in the ID surface of the chamber prior to heat-straightening the test specimens.

The results of the part-through-crack (PTC) tensile tests are presented in Table XIV, together with the K_{Ic} value calculated from the flaw dimensions and failure hoop stress in the prematurely burst chamber. If compared with the data from 109 forgings as reported in Appendix B of Volume I (K_{Ic} = 39.1 ksi-in.$^{1/2}$ with a standard deviation of 1.6 ksi-in.$^{1/2}$), the K_{Ic} values obtained from PTC-tensile tests of the body cylinders of chamber R26 were somewhat above the population mean value of 39 ksi-in.$^{1/2}$ (the upper limit for two sigma is 42.2 ksi-in.$^{1/2}$); whereas, the K_{Ic} value of 38.6 ksi-in.$^{1/2}$ calculated from the chamber itself was in agreement with the mean value.

The following summary of room-temperature precrack Charpy impact W/A values showed that the forward adapter (chamber fracture origin) had appreciably lower plane-stress fracture toughness than the body cylinders or the aft flange.

Forward Closure		Body Cylinders		
Dome	Adapter	Forward	Aft	Aft Flange
443 to 623	318 to 484	691 to 1010	663 to 938	719 to 883
Av (12) 494	Av (12) 426	Av (9) 841	Av (7) 847	Av (3) 822

The summary includes the axial-notch-direction precrack Charpy tests from Phase I (see Appendix D of Volume I).

b. Chamber R41

In November 1962, chamber R41 failed in the forward cylinder at 124-ksi hoop stress during rising load. Examination of the fracture surfaces revealed a metallurgical defect in the surface of the 0.10-in.-thick wall, which consisted of a void surrounded by massive alpha titanium; the embrittled zone was approximately 0.050 in. in diameter. Figure 16 shows the fracture surface containing the defect, together with a photomicrograph showing the massive alpha associated with the defect.

*Allison Monthly Status Report No. 8 for 15 March through 15 April 1963.

TABLE XIV

PTC-TENSILE TESTS OF 6Al-4V TITANIUM FROM MINUTEMAN CHAMBER R26

Component Tested	F_{ty}*	Crack Dimensions: Depth a	Crack Dimensions: Length 2c	Crack Dimensions: Shape a/2c	Gross Stress F	Ratio F/F_{ty}	Shape Parameter Q	Normalized Depth a/Q	Critical Stress Intensity K_{Ic} (ksi-in.$^{1/2}$)
Fwd Closure Origin**	167	0.10	0.18	0.56	99.6	0.60	2.55	0.039	38.6
Fwd Cyl Near Origin	165	0.042	0.100	0.420	151.6	0.92	1.92	0.022	43
		0.040	0.102	0.392	151.7	0.92	1.83	0.022	43
		0.050	0.203	0.246	126.8	0.77	1.32	0.038	48
		0.054	0.203	0.266	118.6	0.72	1.39	0.039	45
		0.050	0.200	0.250	126.5	0.77	1.33	0.038	47
Aft Cyl Location 1	165	0.040	0.107	0.374	156.4	0.95	1.71	0.023	46
		0.034	0.098	0.347	155.6	0.94	1.70	0.020	43
		0.056	0.205	0.273	135.8	0.82	1.40	0.040	52
		0.058	0.210	0.276	135.4	0.82	1.40	0.041	52
Aft Cyl Location 2	165	0.035	0.102	0.343	152.4	0.92	1.61	0.022	43
		0.037	0.108	0.343	152.8	0.93	1.61	0.023	45
		0.053	0.206	0.257	118.3	0.72	1.38	0.038	45
		0.055	0.207	0.266	117.9	0.71	1.42	0.039	45

*Yield strength in integral-test-ring material aged with the chamber.
**Calculation of critical stress intensity based on failure hoop stress and flaw dimensions as measured in the failed chamber.

8X

100X

Figure 16. Fracture Origin and Associated Microstructure in Chamber R41

IV, E, Correlation of Fracture Toughness and Chamber Performance (cont.)

An estimate was made of the plane-strain (K_{Ic}) fracture toughness on the basis of the flaw dimensions

$$a = 0.050 \text{ in.}, \quad 2c = 0.10 \text{ (estimated)}, \quad a/2c = 0.50$$

and the hoop stress at failure

$$F = 124 \text{ ksi}, \quad F/F_{ty} = 124/156.4 = 0.79$$

the flaw-shape parameter and normalized flaw depth were

$$Q = 2.28, \quad a/Q = 0.022$$

which give a plane-strain crack toughness from the chamber itself of

$$K_{Ic} = \underline{36 \text{ ksi-in.}^{1/2}}$$

This K_{Ic} value is reasonably close to the mean value reported in Volume I for 109 forgings (the lower limit for two sigma is 35.8 ksi-in.$^{1/2}$).

The following tabulation summarizes the room-temperature precrack Charpy impact W/A values obtained from chamber R41:

Forward Closure		Body Cylinder		
Dome	Adapter	Forward	Aft	Aft Flange
527 to 609	352 to 404	515 to 590	656 to 740	379 to 496
Av (3) 578	Av (3) 377	Av (3) 550	Av (3) 713	Av (3) 428

The impact test results from the forward cylinder (not from the immediate vicinity of the metallurgical defect) gave higher W/A values than either the forward or aft adapters. If there had been sizable defects in the latter components, they should have failed the chamber before the forward cylinder. The aft cylinder had the highest toughness of the various components in chamber R41.

c. Chamber BL26

In January 1964, chamber BL26 failed after a 4-sec hold at proof pressure (110-ksi hoop stress at the fracture origin). Examination of the fracture surfaces revealed a semielliptical crack on the inside of the aft adapter in the reinforced section adjacent to the aft girth weld, but outside the weld heat-affected zone; the defect initiating failure was 0.030 in. deep and 0.150 in. long. A second crack, 0.040 in. deep and 0.066 in. long,

was detected adjacent to the forward girth weld on the inside surface of the forward closure. From an examination of the fracture surfaces, it was postulated that the failure originated from the crack in the aft adapter, and proceeded forward and aft; and that the second crack originated a secondary failure in the weld-reinforced area of the forward dome. The two fractures intersected approximately 5 in. aft of the forward girth weld. After the failure, inspection revealed 16 additional cracks; all except one extended partially into weld heat-affected zone. The largest of these additional cracks was 0.040 in. deep and 0.060 in. long.

An estimate was made of the plane-strain (K_{Ic}) fracture toughness based on the measured crack dimensions in the fracture-origin component

$$a = 0.080 \text{ in.}, \quad 2c = 0.150, \quad a/2c = 0.534$$

and the chamber hoop stress at failure

$$F = 110 \text{ ksi}, \quad F/F_{ty} = 110/166 = 0.663$$

The flaw-shape parameter and normalized crack depth were

$$Q = 2.43, \quad a/Q = 0.0329$$

which gave a plane-strain crack toughness from the chamber itself of

$$K_{Ic} = \underline{39 \text{ ksi-in.}^{1/2}}$$

This K_{Ic} value is in agreement with the mean value reported in Volume I for 109 forgings.

The following tabulation summarizes the room-temperature precrack Charpy impact W/A values obtained from the reinforced sections next to the various girth welds:

	Body Cylinders		
Forward Adapter	Forward	Aft	Aft Adapter
405 to 432	429 to 559	418 to 541	380 to 623
Av (2) 419	Av (4) 486	Av (4) 461	Av (4) 460

Note that the Charpy tests of material from the reinforced sections adjacent to each of the girth welds gave W/A values that were not greatly different from one component to another.

IV, E, Correlation of Fracture Toughness and Chamber Performance (cont.)

With the fracture toughness of the various components nearly the same, the fracture origin was determined by the location of the largest defect present; the largest flaw was located in the reinforced section of the aft closure next to the G3 weld. It is interesting to note that all of the flaws were in the ID surface, all were oriented in the chamber-axial direction, and all except one extended partially into the HAZ of the girth welds.

d. Chamber 2191456

In March 1963, chamber 2191456 failed during rising load at a pressure of 457 psig (75-ksi hoop stress at the fracture origin). The failure origin as shown in Figure 17* was located in a repair of the forward girth weld. Examination of the fracture surfaces revealed porosity in the weld-repair area with two closely spaced pores (0.045-in.-dia and 0.020-in.-dia pores, one above the other, 0.004 in. apart) at approximately mid-thickness, resulting in an embedded flaw approximately 0.069 in. deep and 0.045 in. long in air-contaminated weld metal. Precrack Charpy tests were made at Aerojet-Sacramento of the weld metal in the forward girth weld both near the fracture origin and away from the fracture origin. The data presented in the following tabulation clearly show an embrittled condition near the fracture origin**.

	Precrack Charpy (in.-lb/in.^{2}) Tests of Weld-Fusion-Zone			
	Slow Bend		Impact	
	RT	320°F	RT	320°F
Near Origin	837 to 951 Av (2) 894	1024 to 1161 Av (2) 1092	721 to 757 Av (3) 742	1264 to 1816 Av (3) 1473
Away from Origin	1147 to 1164 Av (2) 1156	1663 to 1954 Av (2) 1808	1130 to 1370 Av (3) 1256	2010 to 2490 Av (3) 2210

*Metallurgical Failure Analysis of Second-Stage Minuteman Rocket Motor Case 2191456, Ti-6Al-4V Alloy, Hellmann, V. L., Allison Materials Research Lab Report 63FA4, 25 March 1963.

**The fracture-origin location in the forward girth weld of chamber 2191456 had appreciably lower toughness than any weld tested to date. The following table presents a comparison between the fracture origin in chamber 2191456 and welds in successfully hydrotested chambers.

Motor	Weld Yield, ksi	Fracture Toughness, in.-lb/in.^{2}
2191456	155	742
673196	147	1077
673097	144	1366
673122	123	1577

(Neg No. 8-09276) OD (Magn: 3X)

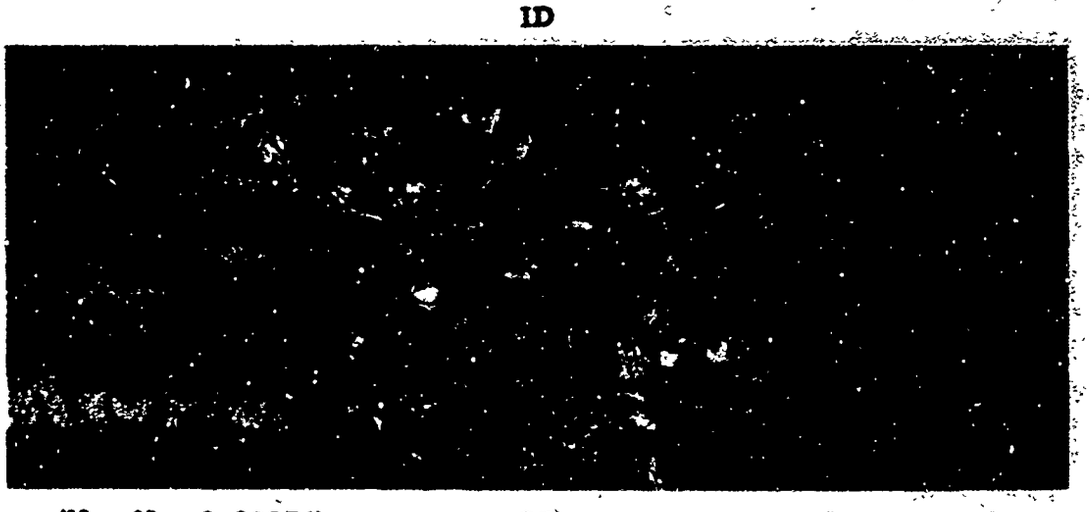

(Neg No. 8-09274) OD (Magn: 9X)

Figure 17. Fracture Origin in Forward Girth Weld of Chamber 2191456

IV, E, Correlation of Fracture Toughness and Chamber Performance (cont.)

An estimate was made of the plane-strain (K_{Ic}) fracture toughness assuming interaction of the porosity to form a single penny-shaped internal flaw of dimensions.

$$2a = 2c = 0.069,\ a/2c = 0.5$$

and a chamber hoop stress at failure

$$F \quad 75 \text{ ksi},\ F/F_{ty} = 75/155 = 0.484$$

the flaw-shape parameter and normalized crack depth were

$$Q = 2.36,\ a/Q = 0.0146$$

which gave a plane-strain crack toughness from the chamber itself of

$$K_{Ic} = \underline{16 \text{ ksi-in.}^{1/2}}$$

This value of K_{Ic} seems anomalously low; however, titanium weld metal in the vicinity of porosity can be expected to be contaminated*.

The following tabulation summarizes the PCI-test results obtained in chamber 2191456 (the body-cylinder data include the axial-notch-direction W/A values obtained in Phase I):

Forward Closure		Body Cylinder		Aft Closure
Dome	Adapter	Forward	Aft	Flange
484 to 564	411 to 435	418 to 537	674 to 814	638 to 725
Av (3) 530	Av (3) 423	Av (8) 481	Av (9) 756	Av (3) 674

Note that the precrack Charpy impact tests of the components on either side of the G1 weld showed the lowest fracture toughness in the chamber. Unfortunately, material was not available for testing the reinforced sections of the G1 weld.

a. Chamber R369

In September 1966, chamber R369 failed during rising load at a pressure of 380 psig (80-ksi hoop stress at the fracture origin).

*Hartbower, C. E., "Fusion Welding High-Strength Titanium Sheet", Proceedings of the 7th Sagamore Ordnance Materials Research Conference, 16-19 August 1960, p. III-101.

IV, E, Correlation of Fracture Toughness and Chamber Performance (cont.)

The fracture was located in the aft cylinder just outside the reinforced section of the aft (G3) weld, and was readily identified by a discolored semielliptical area at the ID surface approximately 0.25 in. long, which very nearly penetrated the wall thickness. The discoloration on the fracture face (Figure 18) showed the crack to have been open during one of the heat treatments.

An estimate was made of the plane-strain (K_{Ic}) fracture toughness on the basis of the measured flaw dimensions in the failed chamber

$$a = 0.10,\ 2c = 0.25,\ a/2c = 0.40$$

and the hoop stress in the chamber at failure

$$F = 80\ \text{ksi},\ F/F_{ty} = 0.49$$

the flaw-shape parameter and normalized crack depth were

$$Q = 1.92,\ a/Q = 0.052$$

which, with Smith's approximation of the stress-intensity magnification factor (M_K) for a deep surface flaw of $a/2c = 0.5$ ($M_K = 1.1$) gave a plane-strain crack toughness from the chamber liner of

$$K_{Ic} = 42\ \text{ksi}\sqrt{\text{in.}}$$

This value of K_{Ic} for the failure-origin component of chamber R369 is close to the mean value obtained for 109 forgings in Phase I of this study (two sigma upper limit 42.2 ksi-in.$^{1/2}$).

The following tabulation summarizes the data obtained from chamber R369, including the test results from the R369 body cylinders tested in Phase I.

Forward Skirt	Forward Closure	Body Cylinders Forward	Body Cylinders Aft	Aft Closure	Aft Skirt
615 to 636	474 to 486	302 to 403	432 to 528	487 to 496	606 to 628
Av (3) 629	Av (3) 446	Av (12) 340	Av (12) 480	Av (3) 492	Av (3) 615

Note that the precrack Charpy impact data for the failure-origin aft cylinder of chamber R369 was somewhat higher than the W/A values obtained from the forward cylinder. The ring-rolled skirts, on the other hand, had appreciably higher toughness than the body cylinders and closures.

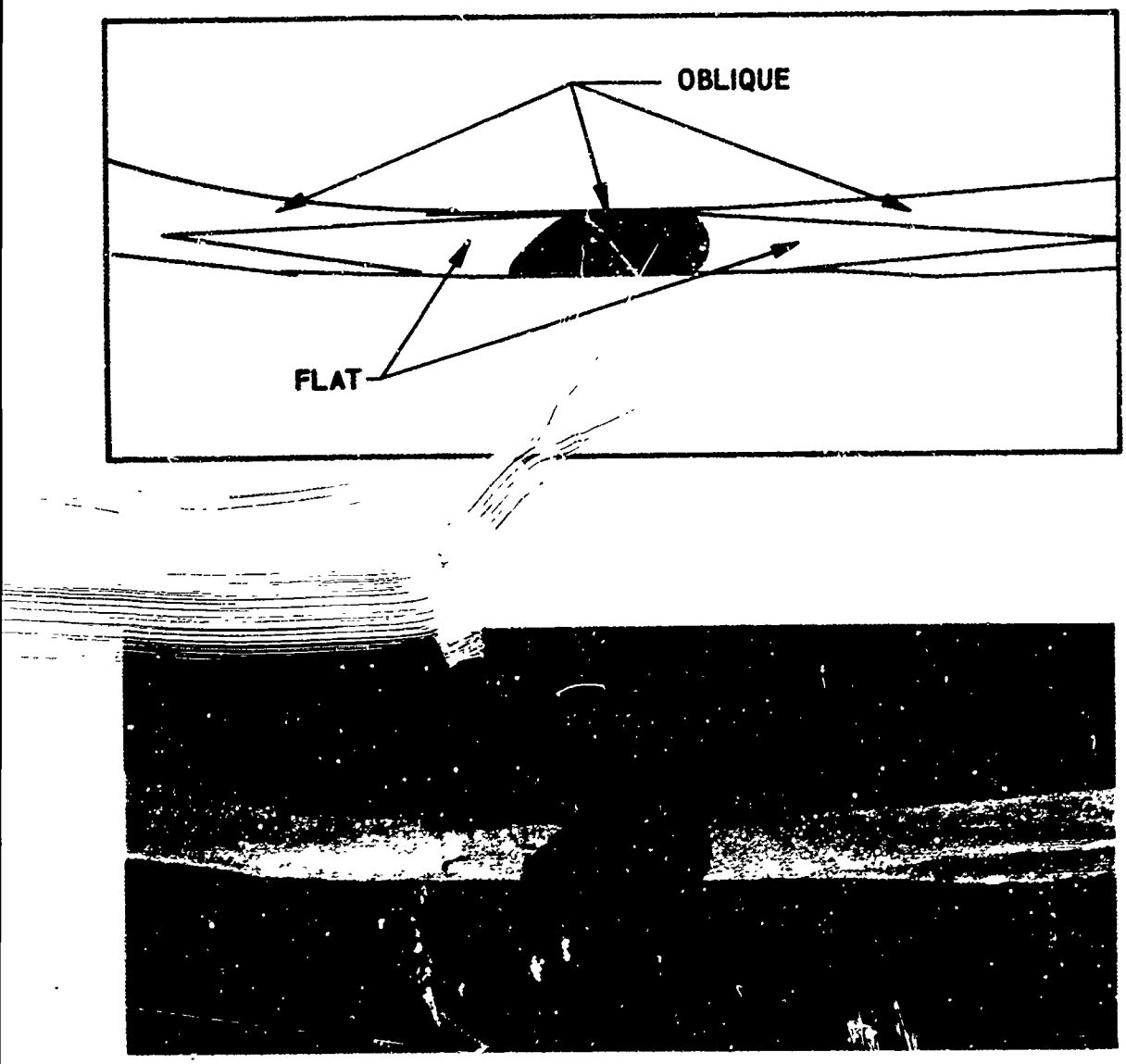

Figure 18. Fracture Origin in Chamber R369

IV, E, Correlation of Fracture Toughness and Chamber Performance (cont.)

The fact that chamber R369 contained a flaw that was very nearly a through crack is of particular interest from the standpoint of the leak-before-burst criterion. The discoloration, as seen in Figure 18, indicates that the flaw developed during heat treatment and, therefore, was in the chamber at the start of the proof test. A very thin shear lip at the OD surface and the tightness of the crack was all that prevented the chamber from leaking at the outset of pressurization. In the 0.10-in.-thick wall, at a yield strength of 166.7 ksi, a W/A value of approximately 1250 in.-lb/in.^{2} would have been required to meet the leak-before-burst criterion. However, this is a special case, in that a defect was already present of greater than "2t" length.

If the defect is treated as a through crack in a wide panel

$$K_c^2 = \pi c_1 F^2$$

where c_1 is the "effective" crack half-length

$$c_1 = c + K_c^2/2\pi F_{ty}^2$$

Substituting 100 (W/A) + 6700 for K_c (from Volume I), the measured value of half-crack length (c = 0.125 in.) and the yield strength (F_{ty} = 166.7 ksi), for W/A = 480 in.-lb/in.^{2}:

$$c_1 = 0.1421$$

Solving for the failure stress using the flat-sheet analysis

$$F^2 = K_c^2 / \pi c_1$$

$$= \underline{82 \text{ ksi}}$$

which is in excellent agreement with the chamber hoop stress at the fracture origin.

Sullivan and Pierce* in a study of the effect of radius on the bulging and fracture of through-cracked cylindrical pressure vessels, reported that when Irwin's flat-sheet analysis is applied to internally

*Sullivan, T. L. and Pierce, W. S., NASA TN D-4951. December 1968

pressured thin-wall, cylindrical vessels, the predicted failure stresses are greater than those obtained experimentally. An equation for predicting the critical hoop fracture stress (F) for an internally pressurized, through-cracked cylinder has been derived by Eiber, et al.* For plane-stress, the Eiber expression states

$$F^2 = K_c^2 / \left[\pi c \sec \left(\frac{\pi}{2} \frac{F}{F_u} \right) \right] \left(1 + \frac{5\pi}{32} \lambda^2 \right) \frac{1}{2} \left(4 - \frac{3-\nu}{1+\nu} \right)$$

where F_u is the biaxial ultimate strength, ν is Poisson's ratio and

$$\lambda^2 = c^2 \left[12 \, (1-\nu^2) \right]^{1/2} / r \, B$$

where r is the cylinder radius and B is the wall thickness. Substituting

$c = 0.125$

$\nu = 1/3$

$r = 26$ in., and $B = 0.10$ in.

$F_u = 1.15 \times F_{tu}$, where $F_{tu} = 175$ ksi

$K_c = 100 \, (W/A) + 6700$, where $W/A = 480$ in.-lb/in.^{2}

from Eiber's expression, by iteration the predicted critical hoop fracture stress is

$F = \underline{79 \text{ ksi}}$

which is in excellent agreement with the chamber hoop stress at the fracture origin.

f. Chamber R490

In June 1967, chamber R490 failed during rising load at a pressure of 600 psig (108-ksi hoop stress at the fracture origin). The failure origin was in the center (G2) girth weld and was attributed to weld contamination as the result of inadequate inert-gas shielding. Precrack

*Eiber, R. J., Maxey, W. A., Duffy, A. R., and McClure, G. M., "Behavior of Through-Wall and Surface Flaws in Cylindrical Vessels". Paper presented at the National Symposium on Fracture Mechanics, Lehigh University, Bethlehem, Pa., June 1968.

IV, E, Correlation of Fracture Toughness and Chamber Performance (cont.)

Charpy impact specimens were cut transverse to the weld, with the notch centered in the weld fusion zone. The specimens were approximately two feet from the fracture origin. The W/A value at this position in the weld was 1720 in.-lb/in.^{2}, which compares favorably with the toughness of the weld metal as measured in other chambers which were successfully hydroburst tested (see Figure 19). Unfortunately, weld metal from the immediate vicinity of the fracture origin was not available for testing. Chemical analysis of the weld metal in the immediate vicinity of the fracture origin revealed a high nitrogen content (1500 ppm).

g. Chamber R512

In September 1967, chamber R512 failed during rising load at a pressure of 590 psig (140 ksi hoop stress at the fracture origin). The fracture origin was located in the forward cylinder 3.5 in. from the center (G2) girth weld, and was readily identified by a discolored semi-elliptical area at the ID surface, approximately 0.03 in. deep and 0.2 in. long. The discoloration on the fracture surface showed the crack to have been open during one of the heat treatments (Figure 20). Examination of the metal in the thumbnail area revealed high interstitial content (approximately 1400 ppm nitrogen), but an essentially normal microstructure.

An estimate was made of the plane-strain (K_{Ic}) fracture toughness that was based on the measured crack dimensions

$$a = 0.03\text{-in.},\ 2c = 0.20\text{-in.},\ a/2c = 0.15$$

and the failure stress

$$F = 140\ \text{ksi},\ F/F_{ty} = 140/166 = 0.84$$

the flaw-shape parameter and normalized crack depth were

$$Q = 1.05,\ a/Q = 0.029$$

which gave a plane-strain crack toughness from the chamber itself of

$$K_{Ic} = \underline{46\ \text{ksi-in.}^{1/2}}$$

This K_{Ic} value is significantly higher than the population mean of 39 ksi-in.$^{1/2}$ (two sigma upper limit 42.2 ksi-in.$^{1/2}$) obtained for the 109 forgings reported in Volume I, and appears anomalously high considering that two laboratories measured 1400 ppm nitrogen in the immediate vicinity of the crack while it was only 112 ppm 1 in. away from the crack*. Figure 20 shows the heat-stained

*Motal, D., "Metallurgical Analysis of Hydrotest Failure R512," DM:cp:M-2139, 23 October 1967.

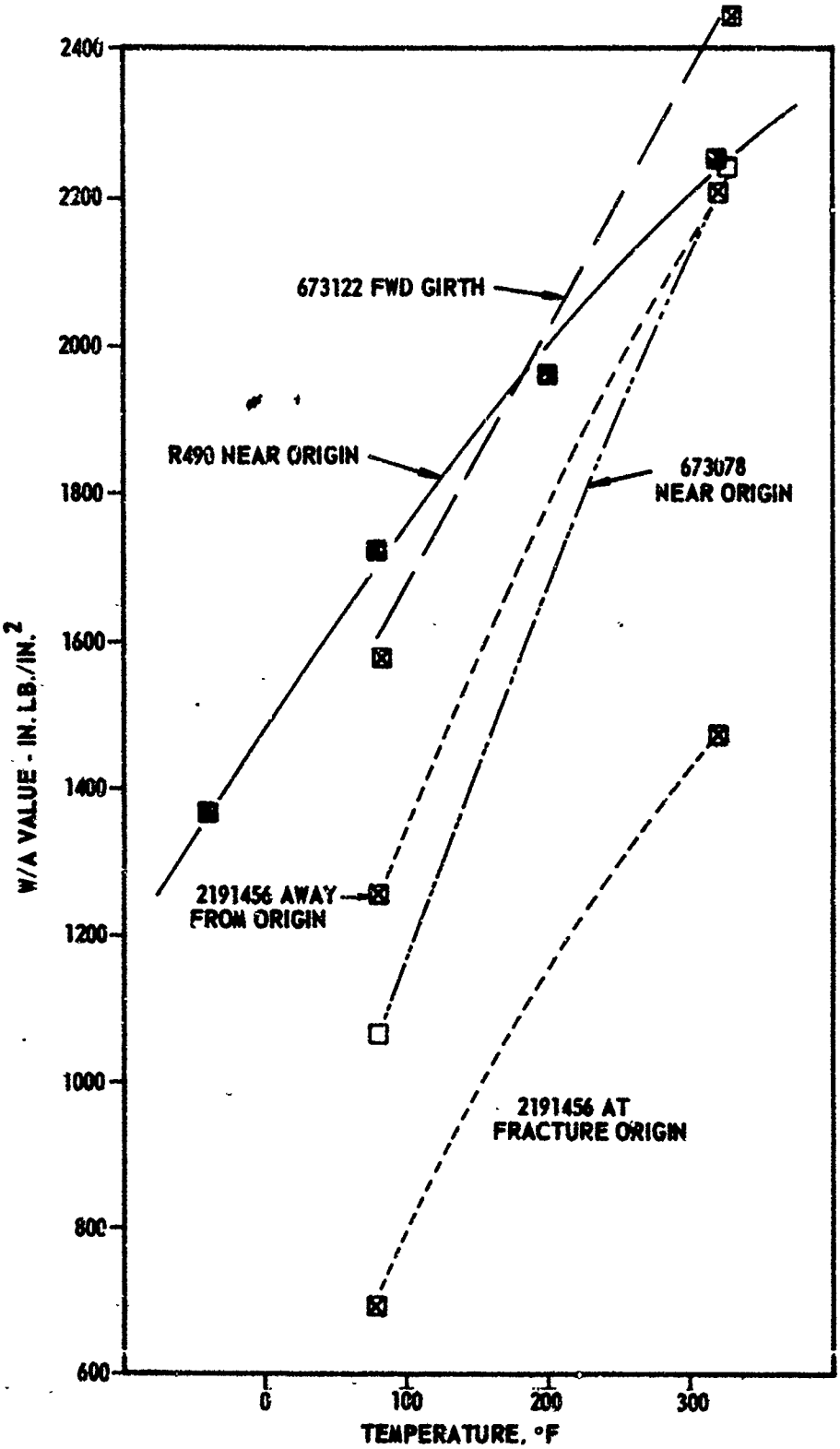

Figure 19. Precrack Charpy Impact Transition Curves for Welds in Minuteman Chambers

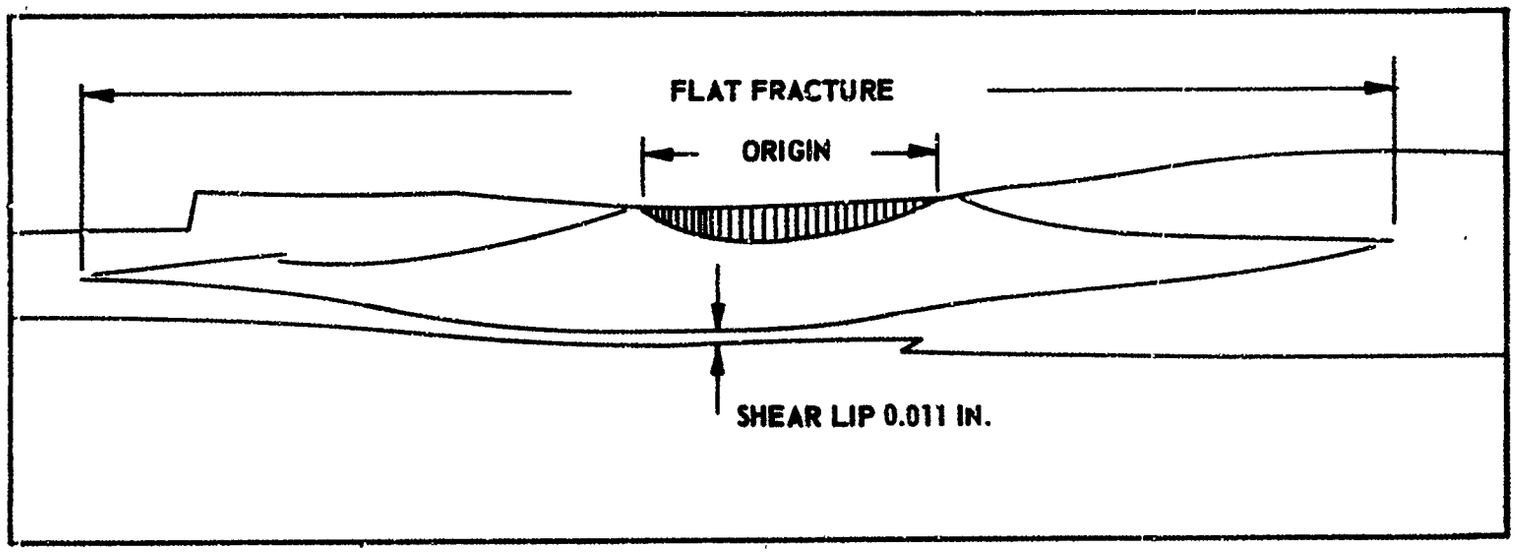

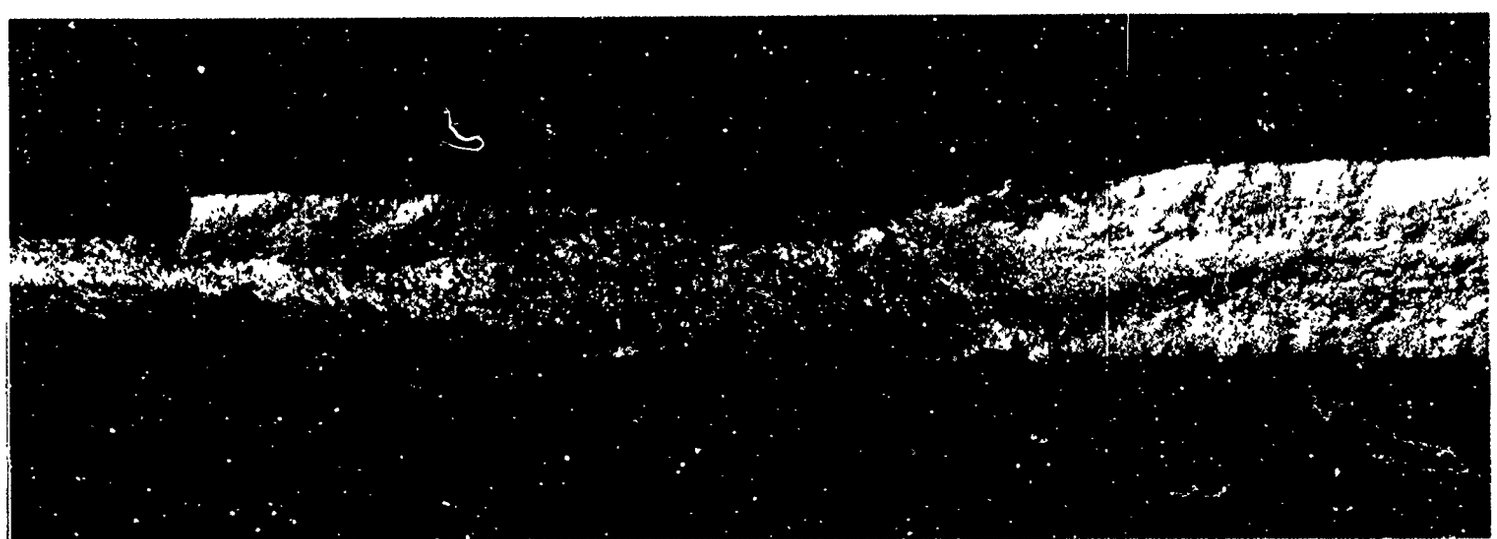

Figure 20. Fracture Origin in Chamber R512

fracture origin. Note that the flat-fracture region extended almost through the wall; the shear lip measured in the plane of the flat fracture was 0.011 in. wide at the OD surface of the chamber.

The following tabulation summarizes the W/A values for the 0.10-in.-thick body cylinders.

Forward Cylinder		Aft Cylinder	
Forward	Aft	Forward	Aft
468 to 540	526 to 532	386 to 443	414 to 539
Av (3) 509	Av (3) 529	Av (3) 414	Av (3) 467

Note that the precrack Charpy impact test results obtained from the forward cylinder approximately 3 in. from the center girth weld were not significantly different from those from the opposite end of the cylinder. Furthermore, the aft cylinder had significantly lower toughness than the failure-origin cylinder.

h. Chamber R516

In October 1967, chamber R516 failed while at the 625-psig proof pressure (112-ksi hoop stress), 45 sec into the hold period. The fracture origin appeared to be in the aft cylinder, in the reinforced section of the center (G2) girth weld; the defect presumed to have initiated the failure was discolored and roughly semicircular, approximately 0.05 in. dia.

An estimate was made of the plane-strain (K_{Ic}) fracture toughness that was based on the measured crack dimensions

$$a = 0.05 \text{ in.}, \quad 2c = 0.10 \text{ in.}, \quad a/2c = 0.5$$

and the failure stress

$$F = 112 \text{ ksi}, \quad F/F_{ty} = 112/163 = 0.69$$

the flaw-shape parameter and normalized crack depth were

$$Q = 2.3, \quad a/Q = 0.022$$

which gave a plane-strain crack toughness from the chamber itself of

$$K_{Ic} = \underline{32 \text{ ksi-in.}^{1/2}}$$

This value is somewhat below the mean K_{Ic} value reported in Volume I for 109 forgings (two-sigma lower limit 35.8 ksi-in.$^{1/2}$).

IV, E, Correlation of Fracture Toughness and Chamber Performance (cont.)

The following tabulation summarizes the reinforced-section precrack Charpy impact data from chamber R516:

Forward Closure	Forward* Cylinder	Aft* Cylinder	Aft Closure
356 to 428	328 to 405	389 to 457	320 to 381
Av (3) 394	Av (3) 358	Av (3) 429	Av (3) 355

Note that the precrack Charpy impact test results from the aft-cylinder reinforced section of the center girth weld were somewhat higher than those of the forward cylinder, but, in general there was little difference between the reinforced sections of various components in chamber R516.

1. Chamber R543

In December 1967, chamber R543 failed just after completing the 90-sec hold at the 627-psig proof pressure; failure occurred at 602 psig as the chamber was being depressurized. On the assumption that crack growth had become unstable just at the end of the 627-psig hold, the hoop stress at the onset of instability was 147 ksi. The fracture origin was in the aft cylinder, 18 in. forward of the aft (G3) girth weld. Examination of the metal in defect area revealed massive alpha in the microstructure and high interstitial content.

An estimate was made of the plane-strain (K_{Ic}) fracture toughness that was based on the flaw dimensions as measured in the fracture surface and the hoop fracture stress. In this chamber, the defect was not clearly defined. A void was observed in the ID surface near the center of the flat fracture identified as the fracture origin. The void was surrounded by massive alpha. This, then, constituted the lower bound of the initiating defect. The void was approximately 0.008 in. deep and 0.035 in. long.

$$a/2c = 0.23$$

$$F/F_{ty} = 147/163 = 0.90$$

$$Q = 1.23, \; a/Q = 0.0065$$

$$K_{Ic} = \underline{23 \text{ ksi-in.}^{1/2}}$$

*For the reinforced section at the center (G2) girth weld.

which appears fictitiously low. The upper bound of defect dimension was determined by the distance between the shear lips at the ID surface ($2c = 0.25$ in.) and the depth of the faceted area surrounding the void ($a = 0.04$ in.).

$$a/2c = 0.17$$

$$F/\bar{\sigma}_{ty} = 147/163 = 0.90$$

$$Q = 1.07,\ a/Q = 0.037$$

$$K_{Ic} = \underline{55\ \text{ksi-in.}^{1/2}}$$

which appears fictitiously high when compared with the mean value reported in Volume I for 109 forgings. Thus, it appears that the effective flaw dimensions were somewhere between the bounds used in making the above calculations.

The following tabulation summarizes the W/A test results obtained in the 0.10-in.-thick walls of chamber R543:

Forward Closure	Forward Cylinder	Aft Cylinder	Aft Closure
448 to 504	351 to 500	336 to 371	491 to 583
Av (3) 484	Av (6) 446	Av (5) 352	Av (3) 554

Note that the precrack Charpy impact test results obtained from the aft cylinder (fracture origin) were somewhat lower than those obtained in the other components of the chamber.

j. Chamber 673078

In August 1963, chamber 673078 failed under rising load in a special proof test preliminary to hydroburst testing. Chamber 673078 constituted a special case because it contained overstrength components (ultimate tensile strength of the forward closure was 182.6 ksi and the forward cylinder was 183.5 ksi) and involved a weld cracking problem. The girth welds consisted of one fusion pass and two filler passes, with all welding done from the outside. The chamber survived the proof test as specified for 42-in.-dia Minuteman cases; viz, three cycles of 90 sec each at 1.1 (MEOP) maximum engine operating pressure (590 psig) with inhibited water. However, after the proof test, cracks were found on the inside-diameter surface at the root of the girth welds. Consequently, the welds were partially routed out and rewelded with two passes on the inside diameter. After welding, the chamber was again stress relieved and then subjected to three additional proof-test cycles to 590 psig. The welds were reported to be free of cracks.

IV, E, Correlation of Fracture Toughness and Chamber Performance (cont.)

Because of the overstrength components, chamber 673078 was selected for hydroburst testing along with chambers 673095, 673147, and 674514.* However, because of a malfunctioning hydrotest rig (O-ring problems), the chamber was subjected to five additional cycles of pressurization, as summarized in the following tabulation:

Cycle Number	Pressure, psig	Time, sec	
		Rise Time	Hold
7(a)	600	548	0
8	530	400	0
9	630	638	96
	720(b)	328	0
10	620	616	120
	679(b)	156	0
11	690	360	Burst

(a) Counting six prior proof-test cycles.
(b) Rising to burst pressure.

Thus, the chamber withstood a total of ten cycles of pressurization and then failed on the eleventh cycle after having been previously subjected to higher pressure and extended periods at sustained load. Although the chamber was not instrumented with breakwires, fracture appearance indicated the failure origin to be at the center girth weld, with the flat fracture predominantly on the forward-cylinder side of the weld. After the burst, X-ray inspection of the welds revealed general, excessive porosity and two transverse cracks in the reinforced section of the center girth weld approximately 180 degrees from the fracture origin. The two cracks, 2 in. apart, were approximately 1/8 in. long and extended from the weld fusion line into the heat-affected base metal. It was not reported whether the cracks were in the forward or aft barrel.

Part-through-crack (PTC) tensile tests of both the forward and aft body cylinders gave the following K_{Ic} values:

*As a preliminary to hydroburst testing, these chambers were to receive an additional proof test consisting of one cycle with a 90-sec hold at 640 psig; see Section IV,E,3,a.

IV, E, Correlation of Fracture Toughness and Chamber Performance (cont.)

Chamber Component	PTC Tensile K_{Ic}, ksi-in.$^{1/2}$
Forward Cylinder	44.0 to 48.2 Av (6) 45.9
Aft Cylinder	39.3 to 43.0 Av (6) 40.8

Note that the measured K_{Ic} values for the forward cylinder were appreciably higher than the population mean of 39 ksi-in.$^{1/2}$ (1.6 ksi-in.$^{1/2}$ standard deviation) as determined for 109 forgings in Phase I; the K_{Ic} values for the aft cylinder, on the other hand, were in close agreement with the mean value.

The precrack Charpy impact data from the body cylinders on either side of the center girth weld together with data from the weld fusion zone are summarized in the following tabulation:

Forward Cylinder			Aft Cylinder	
Membr. Wall	Reinf. Sect.	Weld Deposit*	Reinf. Sect.	Membr. Wall
655 to 824 Av (3) 727	442 to 738 Av (3) 617	1005 to 1120 Av (2) 1062	422 to 482 Av (3) 456	446 to 494 Av (3) 476

*Specimens from near the fracture origin

Note that the toughness of the forward cylinder was appreciably higher than that of the aft cylinder. Note, also, that the toughness of the weld was comparable to that of other chambers which were successfully hydroburst tested (see Section IV,E,2,d). If a crack had escaped detection in the lower toughness aft cylinder, a crack large enough to fail the chamber at 590 psig, it almost certainly would have popped-in and failed the chamber on the first excursion to pressure greater than 590 psig. If, on the other hand, the crack was in the higher-toughness, forward cylinder, the crack could have popped-in, been arrested and then by slow crack growth, subsequently come to a critical size under plane-stress conditions. This concept will be elaborated on in the following paragraphs.

IV, E, Correlation of Fracture Toughness and Chamber Performance (cont.)

3. Discussion of the Leak-Before-Burst Crack-Arrest Concept

A graphical presentation of the leak-before-burst concept is shown in Figure 21. In establishing the curves of this figure, K_c was expressed in terms of precrack Charpy impact W/A values using the relationship established in Phase I; viz,

$$K_c = 100(W/A) + 6700$$

In Figure 21, when the property data plot to the right of the line representing a given thickness, the material complies with the leak-before-burst criterion. With room-temperature precrack Charpy impact W/A values ranging from approximately 300 to 800 in.-lb/in.^{2} (mean 480 in.-lb/in.^{2}) and 0.2% offset yield strengths ranging from approximately 155 to 170 ksi in Minuteman 6Al-4V titanium, it is obvious that the leak-before-burst criterion that was based on yield-strength-magnitude working stresses cannot be met in Minuteman chambers. Thus, any flaw of stress intensity exceeding K_{Ic} in either the membrane wall or the reinforced sections of the Minuteman chamber wall would be expected to burst the chamber during proof test. If, on the other hand, the leak-before-burst criterion were based on the actual hoop stress, the criterion might be met in some Minuteman chamber components.

Figure 22 shows the distribution of hoop stress in both 44- and 52-in.-dia Minuteman chambers at proof pressure. Figure 23 is a plot of hoop stress versus flaw dimension for a material with a yield strength of 165 ksi and a plane-strain crack toughness (K_{Ic}) of 39 ksi-in.$^{1/2}$ (three flaw shapes), and a plane-stress crack toughness of 300 in.-lb/in.^{2} (36.7 ksi-in.$^{1/2}$), 500 in.-lb/in.^{2} (56.7 ksi-in.$^{1/2}$) and 700 in.-lb/in.^{2} (76.7 ksi-in.$^{1/2}$). For the plane-strain crack-toughness curves, the flaw dimension on the abscissa is surface-crack depth; the flaw shape is described by the ratio of crack depth to length (a/2c). The linear-elastic fracture-mechanics equation used in plotting the curves was

$$K_{Ic}^2 = 1.21 \pi F^2 a/Q$$

as described by Tiffany*. The plane-strain crack toughness value of 39 ksi-in.$^{1/2}$ used in plotting the curves was the mean value (1.6 ksi-in.$^{1/2}$ standard deviation) obtained in Phase I from a study of 109 6Al-4V titanium Minuteman forgings. In plotting the plane-stress curves, the linear-elastic expression for a large, flat sheet containing a through crack was used

$$K_c^2 = \pi c_1 F^2$$

*ASTM Committee E-24, "Progress in the Measurement of Fracture Toughness and the Application of Fracture Mechanics to Engineering Problems," Materials Research and Standards Vol. 4(3), March 1964.

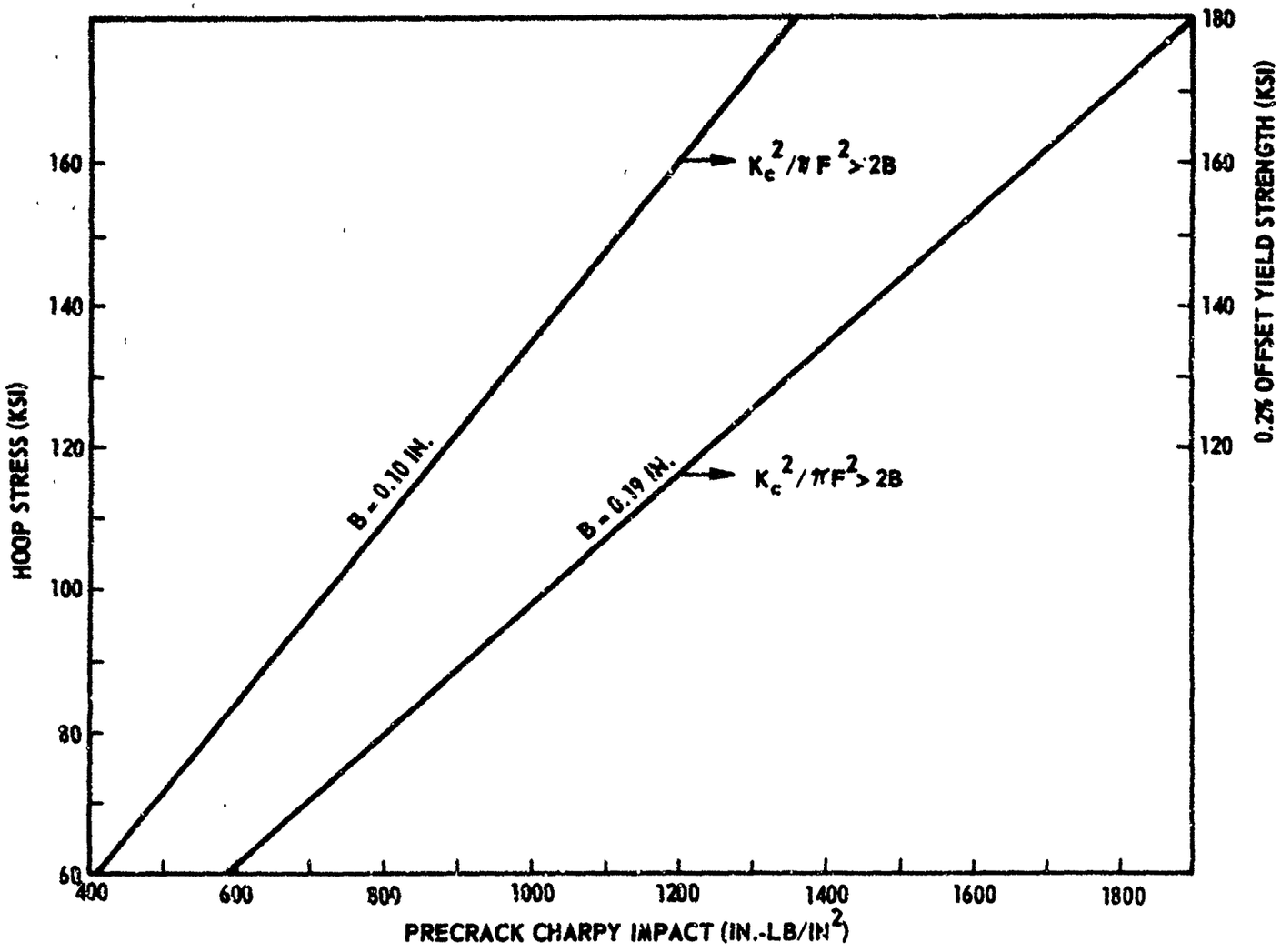

Figure 21. Leak-Before-Burst Criterion Limits for Minuteman 6Al-4V Titanium in Two Thicknesses

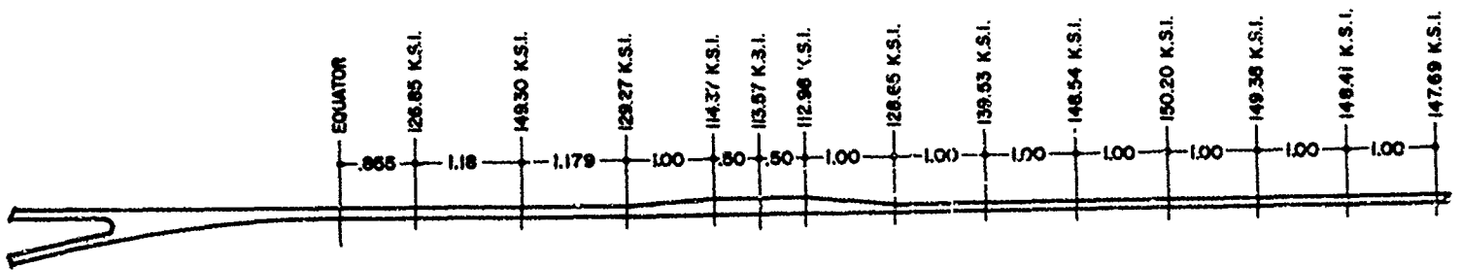

WING XI - 52" MOTOR

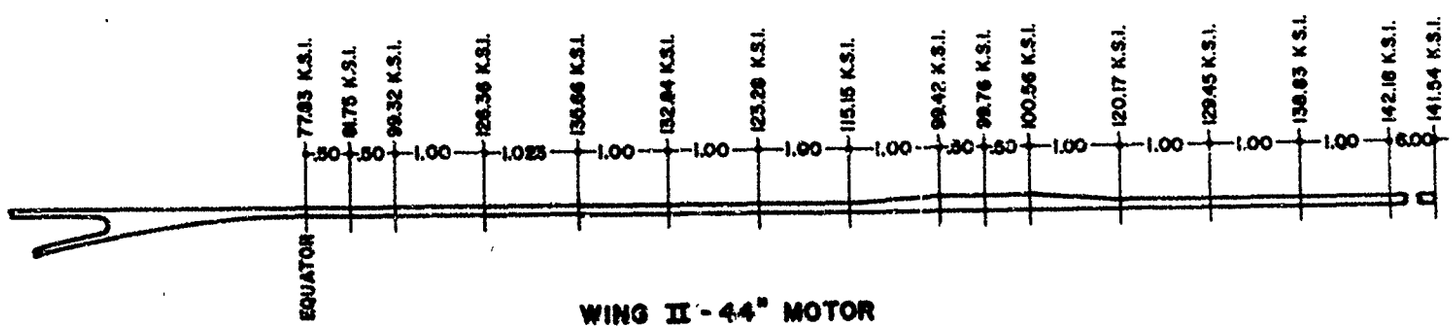

WING II - 44" MOTOR

Figure 22. Distribution of Hoop Stress in 44- and 52-in.-dia Chambers at Proof Pressure

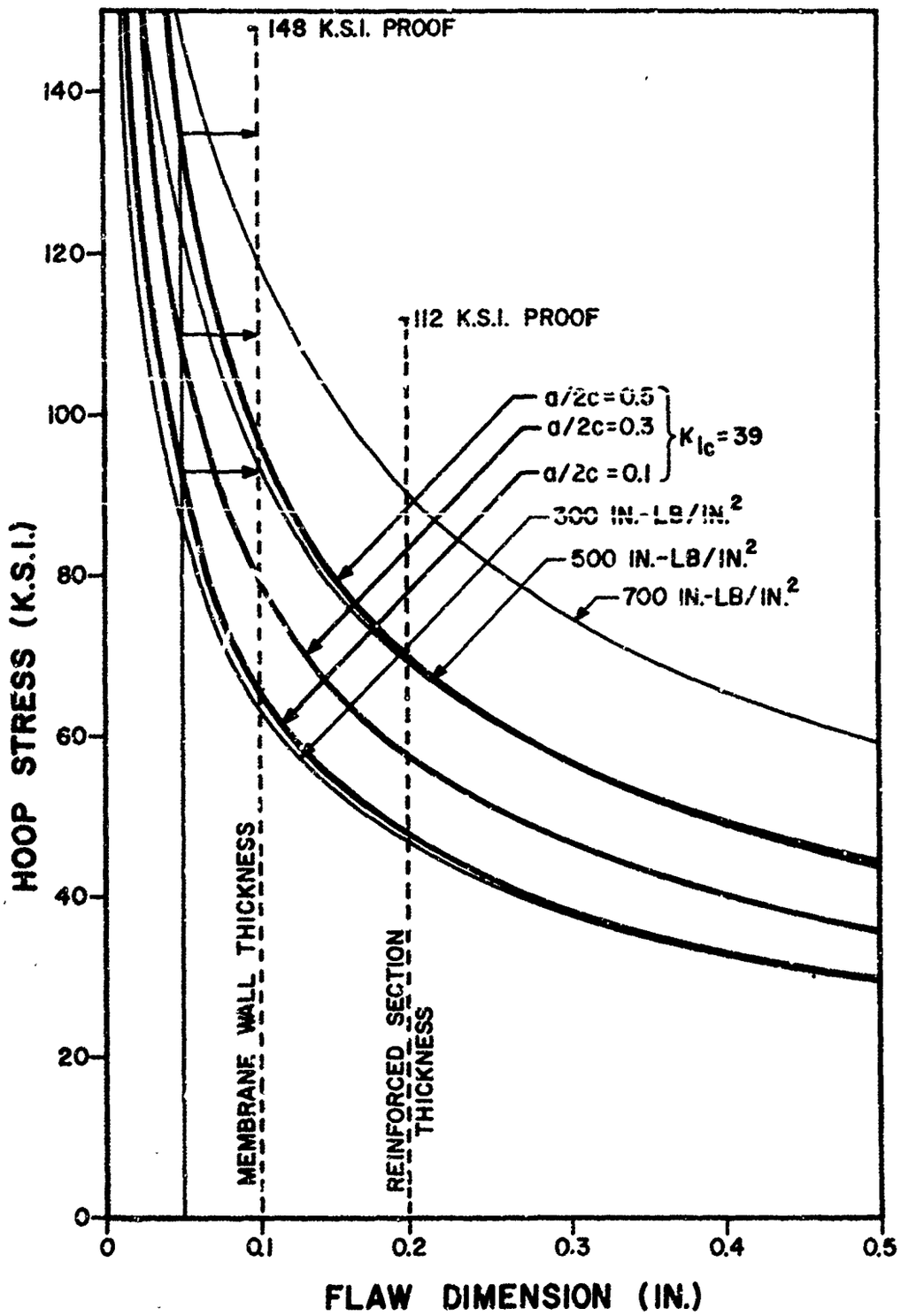

Figure 23. Hoop Fracture Stress as a Function of Flaw Dimension for Representative K_{Ic} and W/A Values in 6Al-4V Titanium at 165 ksi Yield Strength and 39 ksi-in. 1/2 Plane-Strain Fracture Toughness

where c_1 is the effective half-length of the crack. Expressed in terms of the actual half-crack length and a plastic-zone correction

$$c_1 = c + K_c^2/2 \pi F_{ty}^2$$

Thus, for the plane-stress curves, the flaw dimension plotted on the abscissa is half-crack length. The plane-stress crack toughness values used in plotting the curves (300, 500, and 700 in.-lb/in.^{2}) were generally representative of the range of W/A values measured in Minuteman chambers.

Consider now the interpretation of Figure 23 in terms of chamber performance. For example, with a semielliptical surface flaw 0.05 in. deep and 0.5 in. long ($\underline{a/2c = 0.1}$) in the 0.10-in.-thick membrane wall, on pressurization, the flaw would pop-in due to plane-strain instability at approximately 93-ksi hoop stress (see arrow). If the plane-stress crack toughness is 300 in.-lb/in.^{2} or less, there is no possibility of crack arrest and the chamber will fail catastrophically at pop-in. If, on the other hand, the same crack were in a material with markedly greater plane-stress crack toughness, say 700 in.-lb/in.^{2}, the pop-in could be arrested on reaching the biaxially stressed free surface at the chamber OD; i.e., the critical-crack half-length at this toughness level is greater than the wall thickness ($c > B$).

With a semielliptical surface flaw 0.05 in. deep and 0.15 in. long ($\underline{a/2c = 0.3}$) in the 0.10-in.-thick membrane wall, on pressurization, the plane-strain pop-in would occur at approximately 110 ksi hoop stress. If the initial plane-strain instability (pop-in) nearly penetrated the wall thickness, in a material of low-to-intermediate plane-stress toughness, say 300 to 500 in.-lb/in.^{2}, it would propagate catastrophically to the complete failure of the chamber ($c < B$) without arrest. In a material with a plane-stress crack toughness of 700 in.-lb/in.^{2}, the crack would be arrested on penetrating the thickness but would fail the chamber, nevertheless, when the rising pressure brought the hoop stress to 119 ksi.

With a semicircular surface flaw 0.05 in. deep and 0.10 in. long ($\underline{a/2c = 0.5}$) in the 0.10-in.-thick membrane wall, the chamber would almost reach proof pressure (148-ksi hoop stress) before plane-strain pop-in. However, if the pop-in instability enlarges the initial crack to a depth approaching the thickness of the material and therefore, an effective length of approximately twice the material thickness, the plane-stress critical crack size will be exceeded and the chamber will fail ($c < B$) corresponding to 700 in.-lb/in.^{2}.

In the preceding examples, even if the crack size had been small enough so that the pop-in instability would not occur until the proof-pressure hoop stress was reached, fracture of the Minuteman second-stage

chamber would still have occurred, regardless of whether the flaw were in the membrane wall or in the reinforced section. This is readily seen by noting the relative position of the dashed material-thickness lines in Figure 23 and the 700 in.-lb/in.^{2} crack toughness curve at the respective proof-pressure hoop stresses. For a material of K_{Ic} = 39 ksi-in.$^{1/2}$, it is of interest to note the maximum crack depths that can be tolerated in the reinforced section without plane-strain instability (pop-in) at proof pressure.

Flaw Shape, a/2c	Maximum Crack Depth 112-ksi Hoop Stress
0.1	0.030
0.3	0.045
0.5	0.070

In the membrane wall where the hoop stress is higher, even smaller cracks would cause pop-in instability and fail the chamber.

Consider the case of chamber 673078 as a specific example. On the premise that the flaw initiating failure was only slightly larger than the 1/8-in.-long cracks discovered by X-ray, the initiating flaw in all probability fell within the following range:

Assuming a 0.13-in. Flaw Length	
a/2c = 0.1,	Depth = 0.013
a/2c = 0.3,	Depth = 0.039
a/2c = 0.5,	Depth = 0.065

With the defects in the reinforced section of the center girth weld, Figure 23 shows that multiple excursions to proof pressure (112 ksi hoop stress) in the reinforced section) would not be expected to cause pop-in of such a crack, assuming a K_{Ic} of 39 ksi-in.$^{1/2}$ or higher. Actually, PTC-tensile tests showed that the K_{Ic} value in the forward cylinder was 46 ksi-in.$^{1/2}$. At 46 ksi-in.$^{1/2}$, the flaw dimensions tabulated above would have been smaller than the plane-strain critical crack size at the highest pressure (720 psig) seen by chamber 673078. The fact that the chamber withstood a total of ten cycles to proof pressure and then failed on the eleventh cycle after having been previously subjected to higher pressure and an extended period at sustained load, shows that there was slow crack growth in the chamber. When the initial flaw became a critical crack as a result of cycling and/or sustained load in a stress-corrosion-cracking environment, the pop-in instability further enlarged the crack to a depth approaching the material thickness and an effective length of approximately twice the thickness and consequently, the plane-stress critical crack dimension was exceeded and the chamber failed.

IV, E, Correlation of Fracture Toughness and Chamber Performance (cont.)

Any question as to whether the initiating defect was in the forward or aft cylinder is resolved by the above observations. If either the defect that initiated fracture of the chamber or the cracks discovered by X-ray had been contained in the reinforced section of the lower-toughness aft cylinder, pop-in certainly would have occurred in the cycle to 720 psig and failed the chamber.

4. Summary of Premature Burst Findings

Table XV summarizes the correlation of fracture toughness and chamber performance for the premature bursts. Four chambers were omitted; viz, 2191456 and R490, because they were weld fusion zone failures, and chamber 673078 and R543 because of insufficient information about the flaw dimensions. The prediction of flaw criticality was based on Figure 23. Pop-in was predicted on the basis of an assumption of K_{Ic} = 39 ksi-in.$^{1/2}$, using the measured crack depth and shape. The prediction of failure stress was based on consideration of the relative positions of the curves relating stress and flaw size in Figure 23, and the premise that pop-in will not be arrested until it penetrates, or nearly penetrates, the wall thickness; therefore, after pop-in, the half-crack dimension that has to be arrested by plane-stress crack toughness corresponds to the wall thickness. Figure 24 illustrates a case of crack arrest in a PTC-tensile test of 6Al-4V titanium heat treated to 160-ksi yield strength*. Note the shear lip at the free surface opposite the part-through-crack pop-in. The clearly delineated band beyond the fatigue precrack is the limit of the pop-in. Apparently, the crack was arrested at this point, and then failed under plane-stress conditions when the load and crack length corresponded to K_c. The plane-strain and plane-stress crack toughness were calculated to be 41 and 100 ksi-in.$^{1/2}$, respectively.

Pop-in was predicted to occur either on or before reaching proof pressure in all chambers investigated except R516. When failure occurred after reaching proof pressure (under sustained load), the prediction of pop-in was inconsistent with chamber performance, assuming a plane-strain critical stress intensity of 39 ksi-in.$^{1/2}$. There were two such cases; however, both involved very short times at load (4 and 15 sec) before failure occurred. Thus, apparently a small amount of slow-crack growth was necessary to reach the critical crack dimension. In chamber R516, pop-in was not predicted on the basis of the defect size; the fact that failure occurred after 45 sec at proof pressure indicates that approximately 0.025 in. of slow-crack growth occurred to make the initial 0.05-in. flaw critical. Again, this assumes a K_{Ic} of 39 ksi-in.$^{1/2}$.

The prediction of failure stress as shown in Table XV was either close or conservative in four out of the six cases. In chamber R41,

*Gerberich, W. W., "A Discussion of Slow Crack Growth Associated with Plane-Strain Instability," Trans. Quarterly, Vol. 59(4), pp 899, December 1966.

TABLE XV

SUMMARY OF TOUGHNESS - CHAMBER PERFORMANCE CORRELATION

Chamber S/N	Flaw Dimension a(in.)	Flaw Dimension a/2c	Flaw Location Component	Flaw Location Thick.(in.)	W/A at Origin (in.-lb/in.^{2})	Prediction of Flaw Criticality Pop-in	Prediction of Flaw Criticality Arrest	Failure Time (seconds)	Failure Hoop Stress Predicted (ksi)	Failure Hoop Stress Actual (ksi)
R26	0.10	0.56	Fwd Clos	0.19	426[a]	Yes[b]	No	15[c]	100	96
R41	0.05	0.50	Fwd Cyl	0.10	550	Yes	No	Loading[d]	135	124
2191456	Embedded flaw in deposited weld metal (see text)							Loading		
BL26	0.08	0.53	Aft Adpt	0.19	460	Yes	No	4	110	110
R369	0.10	0.40	Aft Cyl	0.10	480	Yes	No	Loading	88[e]	80
R490	Failure originated in the deposited weld metal (see text)							Loading		
R512	0.03	0.15	Fwd Cyl	0.10	509	Yes	No	Loading	120	140
R516	0.05	0.50	Aft Cyl	0.19	429	No	No	45	135	112
R543	Dimensions of defect uncertain (see text)							90+		

(a) W/A measured in the 0.1-in.-thick membrane wall.
(b) The prediction of pop-in in each case was based on the assumption of K_{Ic} = 39 ksi-in.$^{1/2}$.
(c) Time at proof pressure.
(d) Failure during rising load.
(e) No correction for deep flaw (see text).

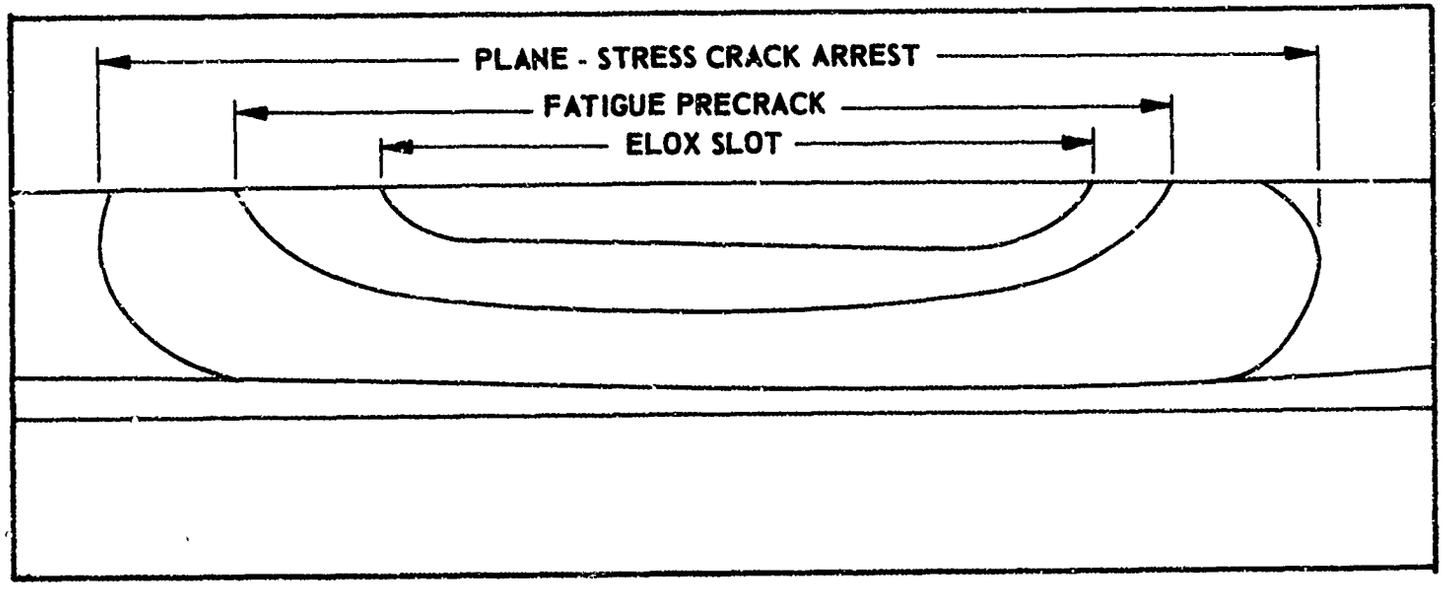

Figure 24. Plane-Stress Fracture Arrest in a PTC-Tensile Specimen of 1/8-in.-Thick 6Al-4V Titanium (160-ksi Yield Strength, 41 ksi-in.$^{1/2}$ K_{Ic} and 100 ksi-in.$^{1/2}$ K_c)

the calculated plane-strain crack toughness (K_{Ic}) was 36 ksi-in.$^{1/2}$, and, therefore, the use of Figure 23 which is based on K_{Ic} = 39 ksi-in.$^{1/2}$ would give a high prediction. Likewise, in chamber R516, the calculated value of plane-strain crack toughness (K_{Ic} = 32 ksi-in.$^{1/2}$) was appreciably lower than the value used in plotting the curves of Figure 23 and, therefore, again would be expected to give a high prediction.

The prediction of no crack arrest that is based on the leak-before-burst criterion does not constitute a verification of the criterion because none of the forgings investigated (not even in the successfully hydroburst chambers discussed in subsequent paragraphs) had sufficient plane-stress crack toughness to arrest pop-in in either the reinforced section or the membrane wall. If an arrested pop-in produced a leak that could be readily detected and the proof cycle interrupted before reaching the critical stress intensity under plane-stress conditions, the leak-before-burst criterion would have practical significance for the Minuteman chamber. However, a leak-before-burst has never been reported in proof testing Minuteman chambers. If the plane-stress crack toughness of the 6Al-4V titanium used in the Minuteman could be increased to a minimum of value of approximately 900 in.-lb/in.^{2} W/A in the membrane wall and approximately 800 in.-lb/in.^{2} W/A in the reinforced section, any pop-in occurring at or below proof stress would produce a crack depth of less than the critical half-length under plane-stress conditions ($c > B$). The leak-before-burst criterion would then be of practical significance for Minuteman titanium. An alternative would be to increase the plane-strain (K_{Ic}) crack toughness until the material could tolerate initial crack depths of much as the material thickness at proof stress; however, this would defeat the purpose of the proof test.

5. Successfully Hydroburst Chambers

Of the 14 Minuteman chambers selected for the data collection, two were successfully hydroburst tested at room temperature and two were successfully hydroburst tested at elevated temperature.

a. Room-Temperature Hydroburst Tests

Chambers 673078, 673095, 673147, and 674514 were selected for hydroburst testing as part of a qualification program originated by the Air Force Ballistic Systems Division (AFBSD) to evaluate motor cases with high-strength component sections (in excess of 180 ksi, ultimate tensile strength). Specific requirements were assigned to these discrepant chambers to prove the structural integrity of each unit. The first requirement was that the chambers be subjected to a hydrostatic proof-pressure test of one cycle with a 90-sec hold at 640 psig. The second requirement was that the

IV, E, Correlation of Fracture Toughness and Chamber Performance (cont.)

chambers be subjected to hydrostatic burst test, where the minimum burst pressure at room temperature would be 772 psig*, obtained as follows:

$$P_b(\text{Min}) = \frac{\text{MEOP} \times \text{FS} \times t\ (\text{Max})}{K_{tu}\ (320°\text{F}) \times t\ (\text{Min})}$$

$$= \frac{534 \times 1.15 \times 0.101}{0.835 \times 0.096}$$

$$= 772$$

where MEOP = Maximum Expected Operating Pressure

= 534 psig at 320°F

FS = Design Minimum Factor of Safety

= 1.15

t (Max)/(Min) = design thickness range

= 0.101/0.096 in.

$K_{tu}(320°\text{F})$ = ultimate strength degradation factor at 320°F

= 0.835

It was specified that to be successful, the hydroburst tests would have to demonstrate considerable radial deformation preceding burst and have a factor of safety of 1.15 or higher, on the basis of the above minimum burst pressure.

The performance of chamber 673078 was discussed in the previous section because of its failure in proof test.

(1) Chamber 673147

On 12 March 1964, chamber 673147 was successfully burst tested in spite of component sections which exceeded the maximum acceptable tensile strength as defined by Minuteman design.

Chamber Component	Ultimate Tensile Strength Minimum	Average
Forward Cylinder	181.1	181.9
Aft Cylinder	180.7	181.7

*This is a more severe requirement than usual. Minimum burst pressure at ambient temperature normally does not include the thickness ratio and is, therefore, only 737 psig.

This chamber was subjected to a proof test of one cycle at 657 psig for 90 sec prior to burst*. No yielding was observed during the proof-pressure test. The chamber was then taken to burst; the burst pressure was 860 psig, 88 psig above the minimum acceptable burst pressure. Maximum radial deformation computed from strain data was 0.384 in. The factor of safety was 1.28. There was no evidence that the motor case was degraded by the presence of the "overstrength" components.

The ability of chamber 673147 to successfully withstand pressure up to 860 psig indicates that the chamber was virtually free of sizable defects. Moreover, although there was insufficient material to measure the toughness in the reinforced sections of the girth welds, the data obtained from the 0.1-in.-thick membrane sections in Phase I of this contract showed the toughness of the body cylinders to be as follows:

Component	Toughness, W/A (in.-lb/in.^{2})	Yield Strength, ksi
Forward Cylinder	560 to 654 Av (6) 577	168.2
Aft Cylinder	498 to 663 Av (6) 547	168.6

Part-through-cracked (PTC) tensile tests of material from the forward and aft cylinders of chamber 673147 gave the following K_{Ic} values

Chamber Component	PTC-Tensile K_{Ic} (ksi-in.$^{1/2}$)
Forward Cylinder	31 to 44 Av (6) 40
Aft Cylinder	37 to 48 Av (6) 41

Note that these data were not significantly different from the population mean of 39 ksi-in.$^{1/2}$ (1.6 ksi-in.$^{1/2}$ standard deviation) as determined for 109 forgings in Phase I.

(2) Chamber 673095

On 18 September 1963, chamber 673095 was burst tested because it contained two components with ultimate tensile strength in excess of 180 ksi:

*Burst Test of a High-Strength Minuteman Wing II, Second-Stage Motor Case, Powell, R. H., Report 1091M-R, April 1964.

IV, E, Correlation of Fracture Toughness and Chamber Performance (cont.)

Chamber	Ultimate Tensile Strength Minimum	Average
Forward Dome	180.4	181.2
Forward Cylinder	173.3	174.9
Aft Cylinder	183.5	183.8
Aft Flange	177.4	178.0

Prior to the room-temperature hydrotest, the chamber was subjected to one cycle of 640 psig for 60 sec followed by a second cycle of 640 psig for 70 sec (a total time of 130 sec at proof pressure). The chamber was then pressurized until it burst at 895 psig, 123 psig above the minimum acceptable burst pressure. This pressure represented an ultimate biaxial strength of

$$F_h = PR/t = 895 \times 22.13/0.099$$
$$= 200.1 \text{ ksi}$$

Deformation in the cylinder sections was recorded by strain gages. A maximum radial deformation of 0.689 in. was recorded in the forward cylinder near the origin of failure; the maximum radial deformation, at burst, in the aft cylinder was 0.335 in. The factor of safety was 1.33. Thus, there was no evidence that the motor was degraded by the presence of the overstrength components.

The precrack Charpy impact data from the membrane wall of this chamber, as determined in Phases I and II, are summarized in the following tabulation:

Chamber Component	Room-Temperature Precrack Charpy Impact, in.-lb/in.^{2}
Forward Closure	476 to 613 Av (3) 529
Forward Cylinder	452 to 783 Av (12) 679*
Aft Cylinder	334 to 522 Av (10) 406*
Aft Flange	418 to 498 Av (3) 458

Note that the Charpy data showed the high-strength aft cylinder to have the lowest toughness; however, the high-strength forward closure had somewhat higher toughness than the lower-strength aft closure.

*Includes Phase I and Phase II data from both ends of the body cylinders.

IV, E, Correlation of Fracture Toughness and Chamber Performance (cont.)

The fact that the chamber withstood two excursions to proof pressure with a total of 130 sec at pressure, demonstrated that there were no defects in the chamber of critical size at 640-psig pressure. Likewise, the fact that the chamber went to 895 psig before it failed, with the failure origin in the forward cylinder, suggests that the lower-toughness aft cylinder was essentially free of defects.

(3) Chamber 674514

On 17 September 1963, chamber 674514 was burst tested because the forward dome was overstrength.

Chamber Component	Ultimate Tensile Strength	
	Minimum, ksi	Average, ksi
Forward Dome	183.3	183.7
Forward Cylinder	174.9	177.1
Aft Cylinder	172.0	173.4
Aft Flange	173.9	174.9

Prior to the room-temperature hydrotest, the chamber was subjected to one cycle of 645 psig for 86 sec. The chamber was then pressurized until it burst at 898 psig, 126 psig above the minimum acceptable burst pressure. This pressure represented an ultimate biaxial strength of

$$F_h = PR/t = 898 \times 22.13/0.098$$
$$= 202.8 \text{ ksi}$$

Deformation in the cylinders was recorded by strain gages. A maximum radial deformation of 0.367 in. was recorded in the forward cylinder; the maximum radial deformation in the aft cylinder was 0.336 in. The factor of safety was 1.34. Thus, there was no evidence that the motor was degraded by the presence of an overstrength component.

Rupture occurred longitudinally from the aft Y-joint through the forward Y-joint and through the forward dome. A second circumferential rip occurred in the aft barrel that extended approximately 330°. Although the origin of failure was not determined, the forward cylinder with the higher radial strain is suspect.

The precrack Charpy impact test data from the membrane wall of this chamber, as determined in Phases I and II are summarized in the following tabulation:

IV, E, Correlation of Fracture Toughness and Chamber Performance (cont.)

Chamber Component	Room Temperature Precrack Charpy Impact, in.-lb/in.^{2}
Forward Closure	419 to 451 Av (3) 436
Forward Cylinder	364 to 496 Av (9) 418*
Aft Cylinder	302 to 396 Av (12) 344*
Aft Flange	317 to 531 Av (3) 448

*Includes Phase I and Phase II data from both ends of the body cylinders.

Note that the Charpy data from the high-strength forward closure were not appreciably different from those of the other components. The fact that the chamber went to 898 psig before it failed indicates that the chamber was essentially free of defects.

b. Elevated-Temperature Hydroburst Tests

(1) Chamber 673122

On 15 October 1962, chamber 673122 was externally heated to 321°F (average) by quartz lamps to simulate aerodynamic heating during flight. Rupture occurred at 713-psig pressure; break wires indicated the fracture origin to be near the center of the aft cylinder. The burst pressure exceeded the minimum allowable by approximately 4%.

The fracture propagated in a ductile manner (shear-type fracture) fore and aft in a relatively straight line from the origin in the aft cylinder, and terminated in the forward and aft domes.

The precrack Charpy impact data from the body cylinders of chamber 673122 as obtained in Phases I and II of this contract, as well as some data taken at the time of the hydroburst test, are summarized in the following tabulation:

IV, E, Correlation of Fracture Toughness and Chamber Performance (cont.)

The fact that the chamber withstood two excursions to proof pressure with a total of 130 sec at pressure, demonstrated that there were no defects in the chamber of critical size at 640-psig pressure. Likewise, the fact that the chamber went to 895 psig before it failed, with the failure origin in the forward cylinder, suggests that the lower-toughness aft cylinder was essentially free of defects.

(3) Chamber 674514

On 17 September 1963, chamber 674514 was burst tested because the forward dome was overstrength.

Chamber Component	Ultimate Tensile Strength	
	Minimum, ksi	Average, ksi
Forward Dome	183.3	183.7
Forward Cylinder	174.9	177.1
Aft Cylinder	172.0	173.4
Aft Flange	173.9	174.9

Prior to the room-temperature hydrotest, the chamber was subjected to one cycle of 645 psig for 86 sec. The chamber was then pressurized until it burst at 898 psig, 126 psig above the minimum acceptable burst pressure. This pressure represented an ultimate biaxial strength of

$$F_h = PR/t = 898 \times 22.13/0.098$$
$$= 202.8 \text{ ksi}$$

Deformation in the cylinders was recorded by strain gages. A maximum radial deformation of 0.367 in. was recorded in the forward cylinder; the maximum radial deformation in the aft cylinder was 0.336 in. The factor of safety was 1.34. Thus, there was no evidence that the motor was degraded by the presence of an overstrength component.

Rupture occurred longitudinally from the aft Y-joint through the forward Y-joint and through the forward dome. A second circumferential rip occurred in the aft barrel that extended approximately 330°. Although the origin of failure was not determined, the forward cylinder with the higher radial strain is suspect.

The precrack Charpy impact test data from the membrane wall of this chamber, as determined in Phases I and II are summarized in the following tabulation:

IV, E, Correlation of Fracture Toughness and Chamber Performance (cont.)

Chamber Component	Room Temperature Precrack Charpy Impact, in.-lb/in.^{2}
Forward Closure	419 to 451 Av (3) 436
Forward Cylinder	364 to 496 Av (9) 418*
Aft Cylinder	302 to 396 Av (12) 344*
Aft Flange	317 to 531 Av (3) 448

*Includes Phase I and Phase II data from both ends of the body cylinders.

Note that the Charpy data from the high-strength forward closure were not appreciably different from those of the other components. The fact that the chamber went to 898 psig before it failed indicates that the chamber was essentially free of defects.

b. Elevated-Temperature Hydroburst Tests

(1) Chamber 673122

On 15 October 1962, chamber 673122 was externally heated to 321°F (average) by quartz lamps to simulate aerodynamic heating during flight. Rupture occurred at 713-psig pressure; break wires indicated the fracture origin to be near the center of the aft cylinder. The burst pressure exceeded the minimum allowable by approximately 4%.

The fracture propagated in a ductile manner (shear-type fracture) fore and aft in a relatively straight line from the origin in the aft cylinder, and terminated in the forward and aft domes.

The precrack Charpy impact data from the body cylinders of chamber 673122 as obtained in Phases I and II of this contract, as well as some data taken at the time of the hydroburst test, are summarized in the following tabulation:

IV, E, Correlation of Fracture Toughness and Chamber Performance (cont.)

Chamber Component	Precrack Charpy Impact Temperatures			
	-40°F	RT	200°F	320°F
Forward Cylinder Reinforced Section	352 to 359 Av (3) 355	334 to 578 Av (6) 460	289 to 875 Av (3) 638	1080 to 1330 Av (3) 1167
Membrane Wall	---	396 to 731 Av (19) 546	765 to 765 Av (2) 765	1170*
Aft Cylinder Reinforced Section	378 to 464 Av (3) 409	387 to 634 Av (6) 560	719 to 865 Av (3) 815	1130 to 1300 Av (3) 1200
Membrane Wall	---	441 to 672 Av (15) 545	723 to 908 Av (3) 801	1110 to 1315 Av (3) 1226

* One test.

Note that the body cylinders had approximately the same toughness

(2) Chamber 2192109

On 14 September 1964, chamber 2192109 was pressurized with preheated oil at 212°F (average) to simulate operating temperature. After a 570-psig hold for one minute without yielding, the chamber was pressurized until it ruptured at 728 psig. The origin of failure, as determined by break wire and accelerometer data, was located near the center of the aft barrel. The ultimate tensile stress for laboratory ambient temperature was calculated using the measured burst pressure, temperature and wall thickness near the origin of rupture.

$$F_{tu} = 177.0 \text{ ksi}$$

the factor of safety was 1.29.

The precrack Charpy impact data from the body cylinders of chamber 2192109 as obtained in Phases I and II are summarized in the following tabulation:

Chamber Component	Precrack Charpy Impact Temperature			
	-40°F	RT	200°F	320°F
Forward Cylinder				
Reinforced Section 0.19 in.	220 to 315 Av (3) 279	332 to 400 Av (2) 336	415 to 450 Av (3) 438	691 to 768 Av (3) 725
Membrane Wall 0.10 in.	---	242 to 454 Av (12) 364	---	---
Aft Cylinder				
Membrane Wall 0.10 in.	---	339 to 423 Av (6) 381	---	---

IV, E, Correlation of Fracture Toughness and Chamber Performance (cont.)

Note that the room-temperature toughness in the membrane wall (fracture origin) was approximately the same in both body cylinders and appreciably lower than the mean (480 in.-lb/in.^{2}). Note, also, that the toughness (438 in.-lb/in.^{2}) of the forward cylinder at the temperature of hydroburst, 212°F, was appreciably lower than the mean (650 in.-lb/in.^{2}) for that temperature. The fact that chamber 2192109 passed the proof test at room temperature indicates that the chamber was essentially free of defects.

SECTION V

SUMMARY AND CONCLUSIONS

A. SUMMARY

Material taken from second-stage 6Al-4V titanium Minuteman rocket motor cases was tested with precrack Charpy impact specimens to evaluate the following as factors affecting plane-stress crack toughness and/or chamber performance: (1) anisotropy and inhomogeneity, (2) forging practice, (3) interstitial-element chemistry, and (4) test temperature. The material was obtained from 14 hydroburst Minuteman chambers, nine of which were premature proof-test failures, four were successfully hydroburst chambers and one failed after 11 proof-test cycles. Closures, skirts and body cylinders from the 14 chambers provided data on 69 forgings involving three forging practices; viz, die, ring-roll, and extrusion. The small size of the precrack Charpy specimen permitted testing with the specimen oriented to propagate the crack in the chamber-axial direction, and with the specimen both in the 0.19-in.-thick reinforced section adjacent to the girth welds and in the 0.10-in.-thick walls on either side of the girth-weld reinforced sections. Selected forgings in each chamber were tested at -40, RT, 200, and 320°F. Particular attention was directed to the material in the immediate vicinity of fracture origins in an attempt to correlate fracture toughness and chamber performance.

1. Anisotropy and Inhomogeneity

Precrack Charpy specimens were cut to test crack propagation in the chamber-hoop and -axial directions. Marked anisotropy was noted in nine out of 13 body-cylinder forgings tested. Moreover, in four out of six components where secondary fracture occurred in the hoop direction, the W/A values in the hoop direction were either very low (as compared with a mean value of 477 in.-lb/in.^{2}) or lower than those propagating fracture in the chamber-axial direction. Precrack Charpy specimens also were taken from both ends of many of the body cylinders to determine if there was a variation in toughness from end-to-end in a given cylinder forging. In some individual cylinders, there appeared to be a marked difference from end-to-end in both the membrane wall and the reinforced sections. However, analysis of variance indicated that there was no significant difference between the ends of the cylinders.

2. Effect of Chemistry and Forging Practice

Multiple covariance analysis showed that there were significant differences in the means for the different types of forgings when tests were made of the membrane-wall material. Moreover, multiple regression and correlation analysis indicated that for Minuteman chemistry carbon and oxygen were the interstitial-solid-solution elements having the greatest effect on toughness. Least-square best-fit equations also were obtained from the

computer program relating interstitial content and W/A value. Analysis of variance to determine if there was a statistically significant difference between cylinder-forging W/A values showed a highly significant difference (significance level 0.0001). Also, it was found that there was a highly significant difference between W/A values obtained from the reinforced sections (specimens nominally 0.18 in. thick) and the membrane walls (specimens nominally 0.10 in. thick) of the cylinder forgings (significance level 0.0002).

3. Effect of Test Temperature

Marked temperature effects were observed in both precrack Charpy slow-bend and impact testing. The results indicated that testing for K_c at a single test temperature can be seriously misleading if service involves a range of temperature. In general, an increase in test temperature for Minuteman 6Al-4V titanium from -40 to 320°F resulted in a three-fold increase in plane-stress crack toughness; however, some heats are much less responsive to such a temperature increase than others. The forging-to-forging differences in response to test temperature makes testing of every forging necessary where toughness is a critical consideration.

4. Correlation of Toughness and Chamber Performance

Although there were marked differences in precrack Charpy impact W/A values from forging-to-forging in the Minuteman chambers, even the toughest of the forgings did not have sufficient plane-stress crack toughness to meet the leak-before-burst criterion. In one chamber (R369), which contained an initial flaw that very nearly penetrated the chamber wall, a calculation of the failure hoop stress that was based on the precrack Charpy W/A value and the measured crack length was in excellent agreement with the chamber hoop stress at the fracture origin. The measured W/A value was input to Irwin's flat-sheet analysis using the relationship established in Phase I between K_c and W/A; viz, $K_c = 100\ (W/A) + 6700$.

The usefulness of a leak-before-burst criterion was evaluated on the basis of chamber hoop stress (rather than yield strength). Fracture surfaces in the vicinity of the initiating defects indicated that the flat fracture associated with pop-in usually extended nearly to the OD free surface. Thus, the plane-strain pop-in instability typically enlarges the initial crack to a depth approaching the thickness of the material and, therefore, to a length of approximately twice the thickness. Whether the initial pop-in instability will immediately fail the chamber (at the hoop stress existing at the instant of pop-in) or be arrested, requiring additional pressurization to fail the chamber, depends on the plane-stress critical crack size at the pop-in stress. If the plane-stress critical crack length is greater than twice the wall thickness ($c > B$), the pop-in will be arrested.

V, A, Summary (cont.)

Unfortunately, none of the components containing fracture origins had sufficient plane-stress crack toughness to arrest pop-in and, therefore, the usefulness of a leak-before-burst criterion that was based on hoop stress was not proven.

An attempt was made to predict the hoop stress at failure on the basis of the known flaw dimensions and the mean K_{Ic} value as determined in Phase I from 109 forgings (39 ksi-in.$^{1/2}$ with a standard deviation of 1.6 ksi-in.$^{1/2}$). The prediction was either close or conservative in four out of six cases. The calculated K_{Ic} values that were based on the known hoop stress and the flaw dimensions in the discrepant cases were in one instance (36 ksi-in.$^{1/2}$) within two-sigma standard deviation, while the other (32 ksi-in.$^{1/2}$) was below the lower limit of a three-sigma standard deviation.

Four out of ten prematurely burst cases failed after the chamber was at proof pressure, and one failed on rising load after withstanding ten cycles of pressurization, including three cycles to higher pressure than the final burst pressure (chamber 673078). The latter was of particular interest because the flawed body cylinder had higher plane-strain crack toughness (K_{Ic} = 45.9 ksi-in.$^{1/2}$ as compared with a three-sigma upper limit of 43.8 that was based on the 109 forgings tested in Phase I) and higher-than-average W/A values (617 in.-lb/in.^{2} in the reinforced sections and 727 in.-lb/in.^{2} in the membrane wall). Thus, in five out of ten cases investigated, there was slow crack growth involved in the failure. The slow crack growth was very likely the result of cyclic loading in chamber 673078, and stress-corrosion cracking in the chambers which failed under sustained load (the proof-test environment was inhibited Los Angeles City water). One of the four chambers which failed after reaching proof pressure withstood the full 90 sec of sustained pressure, only to fail just after starting to unload. This case, therefore, had grown a crack during proof test that was just short of critical size at the end of the sustained-load portion of the proof test. If the crack had not continued to grow for a few seconds after starting to unload, the chamber would have passed the proof test while containing a near-critical crack.

B. CONCLUSIONS

1. Calculated values of plane-strain (K_{Ic}) crack toughness were based on the measured initial-flaw size and the hoop stress causing fracture of full-scale second-stage 6Al-4V titanium Minuteman rocket motor cases were consistent with the plane-strain crack toughness measured in the 109 forgings tested in Phase I of the data collection.

2. The plane-stress (K_c) crack toughness in Minuteman-chemistry 6Al-4V titanium is not sufficient to meet Irwin's leak-before-burst criterion, nor is it sufficient to meet a leak-before-burst criterion that is based on

V, B, Conclusion (cont.)

the hoop stress at proof pressure. Thus, while a given defect subjected to rising load may be arrested after a plane-strain-instability pop-in, it will fail the chamber at or before reaching the Minuteman proof pressure because of insufficient plane-stress (K_c) crack toughness.

3. The precrack Charpy impact test is a useful method for estimating the K_c value in 6Al-4V Minuteman titanium on the basis of the relationship

$$K_c = 100\ (W/A) + 6700$$

Precrack Charpy impact tests of 26 forgings gave a W/A sample mean of 477 in.-lb/in.^{2} with a standard deviation of 140 in.-lb/in.^{2}. The two-sigma spread of 197 to 757 in.-lb/in.^{2} was the result of large forging-to-forging differences in plane-stress crack toughness, which was in marked contrast to the two-sigma spread in plane-strain (K_{Ic}) crack toughness, 35.8 to 42.2 ksi-in.$^{1/2}$, as measured in 109 forgings.

4. Statistically, there were highly significant differences in precrack Charpy impact W/A values between forgings and forging practices. The response of forgings to test temperature was variable; a rise in test temperature from -40 to 320°F produced a three-fold increase in W/A value in some forgings but only a slight increase in others. Thus, testing for plane-stress crack toughness at a single temperature can be seriously misleading where service involves a range of temperature. For critical service applications, every forging should be fracture tested and at temperatures encompassing the full range anticipated in service.

APPENDIX I

TABULATION OF DATA

TABLE XVI

PRECRACK CHARPY IMPACT DATA - 6A1-4V TITANIUM

Minuteman Chamber S/N	Component	Specimen Location	Wall Thickness	-40	RT	200	320
R26	Dome		0.071		443 - 623 Avg(12) 494		
	Fwd Adaptor		0.109	243 - 264 Avg(3) 281	318 - 484 Avg(12) 426	469 - 505 Avg(3) 485	391 - 672 Avg(3) [illegible]9
	Fwd Cyl		0.102	715 - 728 Avg(2) 722	691 - 906 Avg(4) 806	1039 - 1237 Avg(3) 1154	1223 - 1378 Avg(3) 1308
	Aft Cyl		0.101	709 - 865 Avg(3) 791	663 - 815 Avg(2) 739	1052 - 1268 Avg(3) 1196	1254 - 1501 Avg(3) 1393
	Aft Flange		0.107	580 - 668 Avg(3) 617	719 - 883 Avg(3) 822	916 - 1090 Avg(3) 1013	1387 - 1712 Avg(3) 1511

TABLE XVII

PRECRACK CHARPY IMPACT DATA
MINUTEMAN CHAMBER R26 (44 IN. DIA)

Component	Specimen No.
Forward Dome	A1 - 12
Forward Adaptor	A13 - 24
Forward Cylinder	
At G1 Weld	A25 - 36
At G2 Weld	-
Aft Cylinder	
At G2 Weld	A37 - 48*
At G3 Weld	-
Aft Flange	A49 - 60

*Location in the cylinder not known; material taken adjacent to that used in Phase I.

TABLE XVII (cont.)

SPECIMEN NO.	WIDTH	DBN-cd	AREA	W/A	in.-lb	ft-lb	DEGREES	C D	Test Temp.
A-1	0.072	0.2567	0.0185	472	8.724	0.727	157.5	0.0708	RT
A-2	0.071	0.2259	0.0160	486	7.776	0.648	158.6	0.1018	RT
A-3	0.071	0.2486	0.0177	463	8.196	0.683	158.1	0.0562	RT
A-4	0.071	0.2602	0.0185	540	9.996	0.833	156.2	0.0699	RT
A-5	0.072	0.2459	0.0177	483	8.544	0.712	157.7	0.0806	RT
A-6	0.074	0.2354	0.0174	456	7.932	0.661	158.4	0.0693	RT
A-7	0.071	0.2554	0.0181	448	8.10	0.675	158.2	0.0704	RT
A-8	0.071	0.2579	0.0183	443	8.10	0.675	158.2	0.0701	RT
A-9	0.069	0.2393	0.0165	465	7.68	0.640	158.7	0.0869	RT
A-10	0.070	0.2180	0.0153	524	8.016	0.668	158.3	0.0866	RT
A-11	0.074	0.2366	0.0175	526	9.204	0.767	157.0	0.0620	RT
A-12	0.074	0.2550	0.0189	623	11.772	0.981	154.5	0.0501	RT
A-13	0.111	0.2532	0.0281	419	11.772	0.981	154.5	0.0504	RT
A-14	0.119	0.2385	0.0284	410	11.652	0.971	154.6	0.0673	RT
A-15	0.109	0.2598	0.0283	484	13.692	1.141	152.8	0.0677	RT
A-16	0.116	0.2492	0.0289	446	12.876	1.073	153.5	0.0556	RT
A-17	0.108	0.2390	0.0258	415	10.704	0.892	155.5	0.0773	RT
A-18	0.110	0.2342	0.0	443	11.436	0.953	154.8	0.0685	RT
A-19	0.109	0.2279	0.0248	449	11.124	0.927	155.1	0.0752	RT
A-20	0.109	0.2542	0.0277	437	12.108	1.004	154.2	0.0739	RT
A-21	0.109	0.2285	0.0249	443	11.028	0.919	155.2	0.0772	RT

TABLE XVII (cont.)

SPECIMEN NO.	WIDTH	DBN - cd	AREA	W/A	in.-lb	ft-lb	DEGREES	C D.	Test Temp.
A-22	0.108	0.2521	0.0272	318	8.64	0.720	157.6	0.0687	RT
A-23	0.109	0.1996	0.0218	445	9.696	0.808	156.5	0.1025	RT
A-24	0.109	0.2528	0.0276	407	11.232	0.936	155.0	0.0736	RT
A-25	0.101	0.2246	0.0227	691	15.696	1.308	151.1	0.0770	RT
A-26	0.101	0.2649	0.0268	797	21.36	1.78	146.5	0.0641	RT
A-27	0.102	0.2522	0.0257	906	23.28	1.94	145.2	0.0713	RT
A-28	0.102	0.2465	0.0251	808	20.28	1.69	147.3	0.0822	RT
A-29	0.102	0.2345	0.0239	728	17.40	1.45	149.7		-40°F
A-30	0.102	0.2620	0.0269	715	19.08	1.59	148.3		-40°F
A-31	0.102	0.2605	0.0266	1186	31.56	2.63	139.0		200°F
A-32	0.102	0.2516	0.0257	1237	31.80	2.65	139.7		200°F
A-33	0.102	0.2931	0.0299	1039	31.08	2.59	140.2		200°F
A-34	0.102	0.2594	0.0265	1223	32.40	2.70	139.4		320°F
A-35	0.102	0.2556	0.0261	1324	34.56	2.88	138.1		320°F
A-36	0.102	0.2577	0.0263	1378	36.24	3.02	137.1		320°F
A-37									RT
A-38	0.102	0.2460	0.0251	663	16.644	1.387	150.3	0.0820	RT
A-39	0.102	0.2539	0.0259	815	21.12	1.76	146.7	0.0510	RT
A-40	0.102	0.2664	0.0272	799	21.72	1.81	146.3		-40°F
A-41	0.102	0.2634	0.0269	709	19.08	1.59	148.3		-40°F
A-42	0.101	0.2612	0.0264	865	22.80	1.90	145.5		-40°F

TABLE XVII (cont.)

SPECIMEN NO.	WIDTH	DBN-cd	AREA	W/A	in.-lb	ft-lb	DEGREES	C D	Test Temp.
A-43	0.101	0.2485	0.0251	1267	31.80	2.65	139.7		200°F
A-44	0.101	0.2624	0.0265	1268	33.60	2.80	138.7		200°F
A-45	0.101	0.2654	0.0268	1052	28.20	2.35	142.0		200°F
A-46	0.101	0.2488	0.0251	1501	37.68	3.14	136.3		320°F
A-47	0.101	0.2422	0.0245	1254	30.72	2.56	140.4		320°F
A-48	0.101	0.2505	0.0253	1423	36.00	3.00	137.3		320°F
A-49	0.109	0.2639	0.0288	883	25.44	2.12	143.6	0.0647	RT
A-50	0.109	0.2690	0.0293	864	25.32	2.11	143.7	0.0606	RT
A-51	0.109	0.2637	0.0287	719	20.64	1.72	147.1	0.0635	RT
A-52	0.109	0.2491	0.0272	604	16.416	1.368	150.5		-40°F
A-53	0.106	0.2413	0.0256	580	14.856	1.238	151.8		-40°F
A-54	0.106	0.2494	0.0264	668	17.64	1.47	149.5		-40°F
A-55	0.107	0.2415	0.0258	1033	26.64	2.22	143.0		200°F
A-56	0.106	0.2569	0.0272	1090	29.64	2.47	141.1		200°F
A-57	0.106	0.2471	0.0262	916	24.00	2.00	144.7		200°F
A-58	0.108	0.2393	0.0258	1433	36.96	3.08	136.7		320°F
A-59	0.106	0.2484	0.0263	1387	36.48	3.04	137.0		320°F
A-60	0.106	0.2453	0.0260	1712	44.52	3.71	132.6		320°F
A-61	0.104	0.239	0.0248	264	6.54	0.545	160.0	0.079	-40°F
A-64	0.105	0.265	0.0278	257	7.15	0.596	159.3	0.053	-40°F
A-67	0.104	0.256	0.0266	243	6.47	0.539	160.1	0.052	-40°F

TABLE XVII (cont.)

SPECIMEN NO.	WIDTH	DBN-cd	AREA	W/A	in.-lb	ft-lb	DEGREES	C D	Test Temp.
A-62	0.105	0.259	0.0272	482	13.10	1.092	153.3	0.0614	200°F
A-65	0.104	0.248	0.0258	469	12.11	1.009	154.2	0.0708	200°F
A-68	0.105	0.278	0.0292	505	14.75	1.229	151.9	0.0411	200°F
A-63	0.104	0.258	0.0268	672	18.00	1.50	149.2	0.0608	320°F
A-66	0.105	0.284	0.0298	391	11.65	0.971	154.6	0.0351	320°F
A-69	0.105	0.246	0.0258	585	15.10	1.258	151.6	0.0700	320°F

TABLE XVIII

PRECRACK CHARPY IMPACT DATA - 6Al-4V TITANIUM

Minuteman S/N	Chamber Component	Specimen Location	Wall Thickness	Test Temperature, °F -40	RT	200	320
141	Dome		0.072	487 - 551 Avg(3) 524	527 - 609 Avg(3) 578	711 - 748 Avg(3) 725	799 - 886 Avg(3) 856
	Fwd Adaptor		0.108	297 - 345 Avg(3) 326	352 - 404 Avg(3) 377	520 - 552 Avg(3) 538	657 - 745 Avg(3) 701
	Fwd Cylinder		0.102	394 - 495 Avg(3) 454	515 - 590 Avg(3) 550	585 - 747 Avg(3) 691	830 - 1054 Avg(3) 952
	Aft Cylinder		0.100	525 - 601 Avg(3) 570	666 - 740 Avg(3) 713	888 - 901 Avg(3) 896	1184 - 1348 Avg(2) 1266
	Aft Flange		0.109	346 - 422 Avg(3) 395	379 - 496 Avg(3) 428	508 - 667 Avg(3) 613	789 - 1049 Avg(3) 908

TABLE XIX

PRECRACK CHARPY IMPACT DATA
MINUTEMAN CHAMBER R41 (44 IN. DIA)

Component	Specimen No.
Forward Dome	B1 - 12
Forward Adaptor	B13 - 24
Forward Cylinder	
At G1 Weld	B25 - 36*
At G2 Weld	-
Aft Cylinder	
At G2 Weld	B37 - 48*
At G3 Weld	-
Aft Flange	B49 - 60

*Location in the cylinder not known.

TABLE XIX (cont.)

SPECIMEN NO	WIDTH	DBN - cd	AREA	W/A	in.-lb	ft-lb	DEGREES	C D	Test Temp.
B-1	0.072	0.2581	0.0186	598	11.124	0.927	155.1	0.0541	RT
B-2	0.072	0.2706	0.0195	609	11.88	0.990	154.4	0.0436	RT
B-3	0.073	0.2498	0.0182	527	9.60	0.800	156.6	0.0614	RT
B-4	0.072	0.2539	0.0183	487	8.916	0.743	157.3		-40°F
B-5	0.071	0.2594	0.0184	533	9.804	0.817	156.4		-40°F
B-6	0.071	0.2510	0.0178	551	9.804	0.817	156.4		-40°F
B-7	0.071	0.2616	0.0186	748	13.92	1.160	152.6		200°F
B-8	0.071	0.2557	0.0182	711	12.444	1.037	153.9		200°F
B-9	0.072	0.2686	0.0193	715	13.80	1.150	152.7		200°F
B-10	0.071	0.2582	0.0183	884	16.176	1.348	150.7		320°F
B-11	0.071	0.2538	0.0180	799	14.388	1.199	152.2		320°F
B-12	0.073	0.2517	0.0184	886	16.296	1.358	150.6		320°F
B-13	0.108	0.2481	0.0268	374	9.996	0.833	156.2	0.0676	RT
B-14	0.109	0.2296	0.0250	352	8.808	0.734	157.4	0.0788	RT
B-15	0.109	0.2250	0.0245	404	9.888	0.824	156.3	0.0836	RT
B-16	0.109	0.2093	0.0228	337	7.680	0.640	158.7		-40°F
B-17	0.109	0.2160	0.0235	345	8.100	0.675	158.2		-40°F
B-18	0.108	0.2123	0.0229	297	6.804	0.567	159.7		-40°F
B-19	0.108	0.2520	0.0272	520	14.148	1.179	152.4		200°F
B-20	0.108	0.2445	0.0264	700	18.48	1.54	148.8		320°F
B-21	0.108	0.2491	0.0269	745	20.04	1.67	147.5		320°F

TABLE XIX (cont.)

SPECIMEN NO.	WIDTH	DBN-cd	AREA	W/A	in.-lb	ft-lb	DEGREES	C D	Test Temp.
B-22	0.108	0.2639	0.0285	542	15.456	1.288	151.3		200°F
B-23	0.107	0.2494	0.0267	552	14.748	1.229	151.9		200°F
B-24	0.107	0.2436	0.0261	657	17.16	1.43	149.9		320°F
B-25	0.104	0.2534	0.0264	545	14.388	1.199	152.2		RT
B-26	0.101	0.2478	0.0250	515	12.876	1.073	153.5		RT
B-27	0.101	0.2513	0.0254	590	14.976	1.248	151.7		RT
B-28	0.104	0.2412	0.0251	394	9.888	0.824	156.3		-40°F
B-29	0.101	0.2377	0.0240	495	11.88	0.990	154.4		-40°F
B-30	0.102	0.2263	0.0231	473	10.920	0.910	155.3		-40°F
B-31	0.101	0.2576	0.0260	585	15.216	1.268	151.5		200°F
B-32	0.102	0.2271	0.0232	740	17.16	1.43	149.9		200°F
B-33	0.101	0.2461	0.0249	747	18.60	1.55	148.7		200°F
B-34	0.101	0.2282	0.0230	830	19.08	1.59	148.3		320°F
B-35	0.103	0.2397	0.0247	1054	26.04	2.17	143.3		320°F
B-36	0.101	0.2503	0.0253	972	24.60	2.05	144.3		320°F
B-37	0.100	0.2479	0.0248	740	18.36	1.53	148.9		RT
B-38	0.100	0.2433	0.0243	666	16.176	1.348	150.7		RT
B-39	0.100	0.2515	0.0252	733	18.48	1.54	148.8		RT
B-40	0.100	0.2427	0.0243	601	14.616	1.218	152.0		-40°F
B-41	0.100	0.2541	0.0254	525	13.332	1.111	153.1		-40°F
B-42	0.100	0.2569	0.0257	583	14.976	1.248	151.7		-40°F

TABLE XIX (cont.)

SPECIMEN NO	WIDTH	DBN-cd	AREA	W/A	in.-lb	ft-lb	DEGREES	C D.	Test Temp.
B-43	0.100	0.2436	0.0244	900	21.96	1.83	142.1		200°F
B-44	0.100	0.2541	0.0254	888	22.56	1.88	145.7		200°F
B-45	0.100	0.2613	0.0261	901	23.52	1.96	145.0		200°F
B-46	0.100	0.2517	0.0252	1348	33.96	2.83	138.5		320°F
B-47	0.100	0.2299	0.0230	1184	27.24	2.27	142.6		320°F
B-48									
B-49	0.108	0.2266	0.0245	408	9.996	0.833	156.2		RT
B-50	0.109	0.2439	0.0266	379	10.092	0.841	156.1		RT
B-51	0.109	0.2553	0.0278	496	13.80	1.150	152.7		RT
B-52	0.111	0.2650	0.0294	416	12.228	1.019	154.1		-40°F
B-53	0.109	0.2438	0.0266	422	11.232	0.936	155.0		-40°F
B-54	0.108	0.2334	0.0252	346	8.724	0.727	157.5		-40°F
B-55	0.110	0.2621	0.0288	508	14.616	1.218	152.0		200°F
B-56	0.110	0.2440	0.0268	663	17.76	1.48	149.4		200°F
B-57	0.110	0.2518	0.0277	667	18.48	1.54	148.8		200°F
B-58	0.109	0.2412	0.0263	1049	27.60	2.30	142.4		320°F
B-59	0.109	0.2627	0.0286	789	22.56	1.88	145.7		320°F
B-60	0.109	0.2632	0.0287	886	25.44	2.12	143.6		320°F

TABLE XX

PRECRACK CHARPY IMPACT DATA - 6A1-4V TITANIUM

Minuteman S/N	Chamber Component	Specimen Location	Wall Thickness	Test Temperature, °F -40	RT	200	320
BL26	Fwd Closure	2-in. fwd of G1 weld	0.114	370 - 421 Avg(2) 395	519 - 580 Avg(3) 554	724 - 775 Avg(3) 750	973 - 1150 Avg(2) 1061
	Fwd	G1 reinforced section	0.180		405 - 432 Avg(2) 419		
	Fwd Cyl	G1 reinforced section	0.180		429 - 559 Avg(4) 486		
		2-in. aft of G1 weld	0.109		433 - 482 Avg(4) 456		
	Aft Cyl	2-in. fwd of G3 weld	0.107	317 - 331 Avg(3) 326	441 - 438 Avg(3) 425	561 - 570 Avg(3) 564	815 - 953 Avg(3) 864
		G3 reinforced section	0.175		418 - 541 Avg(4) 461		
	Aft closure	G3 reinforced section	0.180		380 - 623 Avg(4) 460		
		2-in. aft of G3 weld	0.114	393 - 450 Avg(3) 421	477 - 542 Avg(3) 518	637 - 715 Avg(3) 686	965 - 1024 Avg(3) 989

TABLE XXI

PRECRACK CHARPY IMPACT DATA
MINUTEMAN CHAMBER BL-26 (44 IN. DIA)

Component	Specimen No.
Forward Dome	-
Forward Adaptor	D1 - 14
Forward Cylinder	
At G1 Weld	D15 - 22
At G2 Weld	-
Aft Cylinder	
At G2 Weld	-
At G3 Weld	D23 - 38
Aft Flange	D39 - 54

TABLE XXI (cont.)

SPECIMEN NO.	WIDTH	DBN-cd	AREA	W/A	in.-lb	ft-lb	DEGREES	C D	Test Temp.
D-1	0.114	0.249	0.0284	370	10.50	0.875	155.7	0.071	-40°F
D-5	0.115	0.280	0.0322	421	13.57	1.131	152.9	0.040	-40°F
D-23	0.107	0.238	0.0255	331	8.45	0.704	157.8	0.080	-40°F
D-27	0.107	0.271	0.0290	317	9.20	0.767	157.0	0.049	-40°F
D-31	0.107	0.240	0.0257	329	8.45	0.704	157.8	0.060	-40°F
D-43	0.114	0.280	0.0319	393	12.55	1.046	153.8	0.040	-40°F
D-47	0.114	0.275	0.0314	421	13.21	1.101	153.2	0.046	-40°F
D-51	0.115	0.283	0.0325	450	14.62	1.218	152.0	0.037	-40°F
D-2	0.112	0.284	0.0318	562	17.88	1.49	149.3	0.037	RT
D-6	0.114	0.285	0.0325	580	18.84	1.57	148.5	0.035	RT
D-9	0.115	0.261	0.0300	519	15.58	1.298	151.2	0.059	RT
D-11	0.196 0.181	0.316	0.0596	757	45.12	3.76	132.2	-	RT
D-12	0.195 0.180	0.317	0.0594	741	44.04	3.67	132.8	-	RT
D-13	0.195 0.178	0.274	0.0511	432	22.08	1.84	146.0	0.043	RT
D-14	0.194 0.173	0.267	0.0477	405	19.32	1.61	148.2	0.049	RT
D-15	0.190 0.176	0.257	0.0470	559	26.28	2.19	143.2	0.061	RT
D-16	0.190 0.176	0.262	0.0479	514	24.60	2.05	144.3	0.056	RT
D-17	0.190 0.175	0.254	0.0464	442	20.52	1.71	147.2	0.064	RT
D-18	0.191 0.177	0.254	0.0467	429	20.04	1.67	147.5	0.063	RT
D-19	0.109	0.266	0.0290	452	13.10	1.092	153.3	0.056	RT

TABLE XXI (cont.)

SPECIMEN NO	WIDTH	DBN - cd	AREA	W/A	in. - lb	ft - lb	DEGREES	C D.	Test Temp.
D-20	0.109	0.280	0.0305	433	13.21	1.101	153.2	0.042	RT
D-21	0.109	0.264	0.0288	455	13.10	1.092	153.3	0.057	RT
D-22	0.109	0.276	0.0301	482	14.50	1.208	152.1	0.043	RT
D-24	0.107	0.280	0.0300	411	12.34	1.028	154.0	0.039	RT
D-28	0.107	0.271	0.0290	426	12.34	1.028	154.0	0.050	RT
D-32	0.107	0.279	0.0299	438	13.10	1.092	153.3	0.042	RT
D-35	0.185 0.166	0.272	0.0477	418	19.92	1.66	147.6	0.044	RT
D-36	0.185 0.168	0.268	0.0473	454	21.48	1.79	146.5	0.048	RT
D-37	0.185 0.168	0.270	0.0477	430	20.52	1.71	147.2	0.048	RT
D-38	0.187 0.172	0.277	0.0497	541	26.88	2.24	142.9	0.041	RT
D-39	0.187 0.176	0.238	0.0432	380	16.42	1.368	150.5	0.079	RT
D-40	0.187 0.184	0.276	0.0512	623	31.92	2.66	139.7	0.041	RT
D-41	0.187 0.177	0.263	0.0479	426	20.40	1.70	147.3	0.055	RT
D-42	0.187 0.176	0.264	0.0479	411	19.68	1.64	147.8	0.052	RT
D-44	0.114	0.283	0.0323	542	17.52	1.46	149.6	0.037	RT
D-48	0.114	0.264	0.0301	534	16.06	1.338	150.8	0.056	RT
D-52	0.114	0.275	0.0314	477	14.98	1.248	151.7	0.044	RT
D-3	0.113	0.267	0.0302	775	23.40	1.95	145.1	0.052	200°F
D-7	0.114	0.271	0.0309	750	23.16	1.93	145.3	0.048	200°F
D-10	0.114	0.263	0.0300	724	21.72	1.81	146.3	0.059	200°F

TABLE XXI (cont.)

SPECIMEN NO.	WIDTH	DBN-cd	AREA	W/A	in.-lb	ft-lb	DEGREES	C D	Test Temp.
D-25	0.106	0.252	0.0267	570	15.22	1.268	151.5	0.069	200°F
D-29	0.106	0.264	0.0280	561	15.70	1.308	151.1	0.057	200°F
D-33	0.106	0.250	0.0265	561	14.86	1.238	151.8	0.070	200°F
D-45	0.113	0.270	0.0305	637	19.44	1.62	148.1	0.052	200°F
D-49	0.113	0.278	0.0314	715	22.44	1.87	145.8	0.044	200°F
D-53	0.113	0.271	0.0306	706	21.60	1.80	146.4	0.050	200°F
D-4	0.115	0.271	0.0312	973	30.36	2.53	140.7	0.051	320°F
D-8	0.115	0.271	0.0312	1150	35.88	2.99	137.4	0.050	320°F
D-26	0.107	0.264	0.0282	953	25.88	2.24	142.9	0.058	320°F
D-30	0.107	0.274	0.0293	823	24.12	2.01	144.5	0.045	320°F
D-34	0.107	0.265	0.0284	815	23.16	1.93	145.3	0.056	320°F
D-46	0.114	0.281	0.0320	1024	32.76	2.73	139.2	0.037	320°F
D-50	0.114	0.275	0.0314	978	30.72	2.56	140.4	0.046	320°F
D-54	0.114	0.278	0.0317	965	30.60	2.55	140.5	0.041	320°F

TABLE XXII

PRECRACK CHARPY IMPACT DATA - 6A1-4V TITANIUM

Minuteman Chamber S/N	Component	Specimen Location	Wall Thickness	Test Temperature, °F -40	RT	200	320
2191456	Dome		0.070	453 - 464 Avg(3) 458	484 - 564 Avg(3) 530	612 - 672 Avg(3) 648	840 - 915 Avg(3) 885
	Fwd Adaptor		0.106	349 - 392 Avg(3) 367	411 - 435 Avg(3) 423	585 - 601 Avg(3) 592	725 - 848 Avg(3) 793
	Fwd Cyl	(a)	0.100	380 - 402 Avg(3) 389	418 - 537 Avg(3) 469	593 - 637 Avg(3) 610	842 - 977 Avg(3) 906
	Aft Cyl	(a)	0.101	618 - 693 Avg(3) 658	767 - 768 Avg(3) 767	1001 - 1063 Avg(3) 1038	1246 - 1482 Avg(3) 1353
	Aft Flange		0.107	532 - 576 Avg(3) 558	638 - 725 Avg(3) 674	864 - 935 Avg(3) 906	1160 - 1258 Avg(3) 1194

(a) Adjacent to material tested in Phase I.

TABLE XXIII

PRECRACK CHARPY IMPACT DATA
MINUTEMAN CHAMBER 2191456 (44 IN. DIA)

Component	Specimen No.
Forward Dome	C1 - 12
Forward Adaptor	C13 - 24
Forward Cylinder	
At G1 Weld	C25 - 36*
At G2 Weld	-
Aft Cylinder	
At G2 Weld	C37 - 48*
At G3 Weld	-
Aft Flange	C49 - 60

*Location in the cylinder not known; material taken adjacent to that used in Phase I.

TABLE XXIII (cont.)

SPECIMEN NO	WIDTH	DBN-cd	AREA	W A	in.-lb	ft-lb	DEGREES	C D	Test Temp.
C-1	0.069	0.2595	0.0179	564	10,092	0.841	156.1		RT
C-2	0.070	0.2597	0.0182	543	9.888	0.824	156.3		RT
C-3	0.072	0.2579	0.0186	484	9.000	0.750	157.2		RT
C-4	0.071	0.2569	0.0182	464	8.448	0.704	157.8		-40°F
C-5	0.069	0.2501	0.0173	453	7.836	0.653	158.5		-40°F
C-6	0.069	0.2540	0.0175	458	8.016	0.668	158.3		-40°F
C-7	0.069	0.2632	0.0182	672	12.228	1.019	154.1		200°F
C-8	0.069	0.2416	0.0167	660	11.028	0.919	155.2		200°F
C-9	0.069	0.2542	0.0175	612	10.704	0.892	155.5		200°F
C-10	0.069	0.2515	0.0174	840	14.616	1.218	152.0		320°F
C-11	0.069	0.2633	0.0182	915	16.644	1.387	150.3		320°F
C-12	0.069	0.2611	0.0180	899	16.176	1.348	150.7		320°F
C-13	0.106	0.2294	0.0243	411	9.996	0.833	156.2		RT
C-14	0.107	0.2554	0.0273	435	11.88	0.990	154.4		RT
C-15	0.107	0.2458	0.0263	423	11.124	0.927	155.1		RT
C-16	0.106	0.2605	0.0276	392	10.812	0.901	155.4		-40°F
C-17	0.106	0.2355	0.0250	349	8.724	0.727	157.5		-40°F
C-18	0.106	0.2426	0.0257	358	9.204	0.767	157.0		-40°F
C-19	0.106	0.2596	0.0275	601	16.536	1.378	150.4		200°F
C-20	0.106	0.2434	0.0258	590	15.216	1.268	151.5		200°F
C-21	0.105	0.2517	0.0264	585	15 456	1.288	151.3		200°F

TABLE XXIII (cont.)

SPECIMEN NO.	WIDTH	DBM-cd	AREA	W/A	in.-lb	ft-lb	DEGREES	C D	Test Temp.
C-22	0.105	0.2601	0.0273	848	23.16	1.93	145.3		320°F
C-23	0.105	0.2563	0.0269	807	21.72	1.81	146.3		320°F
C-24	0.105	0.2502	0.0263	725	19.08	1.59	148.3		320°F
C-25	0.099	0.2415	0.0239	418	9.996	0.833	156.2		RT
C-26	0.099	0.2580	0.0255	537	13.692	1.141	152.8		RT
C-27	0.099	0.2319	0.0230	452	10.404	0.867	155.8		RT
C-28	0.099	0.2641	0.0261	402	10.500	0.875	155.7		-40°F
C-29	0.099	0.2535	0.0251	386	9.696	0.808	156.5		-40°F
C-30	0.099	0.2572	0.0255	380	9.696	0.808	156.5		-40°F
C-31	0.099	0.2233	0.0221	593	13.104	1.092	153.3		200°F
C-32	0.099	0.2422	0.0240	600	14.388	1.199	152.2		200°F
C-33	0.100	0.2370	0.0237	637	15.096	1.258	151.6		200°F
C-34	0.100	0.2576	0.0258	977	25.20	2.10	143.8		320°F
C-35	0.100	0.2416	0.0242	898	21.72	1.81	146.3		320°F
C-36	0.100	0.2383	0.0238	842	20.04	1.67	147.5		320°F
C-37	0.101	0.2526	0.0255	767	19.56	1.63	148.0		RT
C-38	0.101	0.2493	0.0252	767	19.32	1.61	148.2		RT
C-39	0.101	0.2448	0.0247	768	18.96	1.58	148.4		RT
C-40	0.103	0.2755	0.0284	663	18.84	1.57	148.5		-40°F
C-41	0.101	0.2482	0.0251	693	17.40	1.45	149.7		-40°F
C-42	0.101	0.2493	0.0252	618	15.576	1.298	151.2		-40°F

TABLE XXIII (cont.)

SPECIMEN NO	WIDTH	DBN-cd	AREA	W.A	in.-lb	ft-lb	DEGREES	C D	Test Temp.
C-43	0.101	0.2563	[illegible].0259	1001	25.92	2.16	143.4		200°F
C-44	0.100	0.2627	[illegible].0263	1063	27.96	2.33	142.2		200°F
C-45	0.100	0.2502	0.0250	1051	26.28	2.19	143.2		200°F
C-46	0.100	0.2648	0.0265	1331	35.28	2.94	137.7		320°F
C-47	0.100	0.2614	0.0261	1246	32.52	2.71	139.3		320°F
C-48	0.100	0.2678	0.0268	1482	39.72	3.31	135.2		320°F
C-49	0.107	0.2441	0.0261	638	16.644	1.387	150.3		RT
C-50	0.106	0.2575	0.0273	725	19.80	1.65	147.7		RT
C-51	0.107	0.2568	0.0275	657	18.12	1.51	149.1		RT
C-52	0.108	0.2586	0.0279	532	14.856	1.238	151.8		-40°F
C-53	0.106	0.2579	0.0273	566	15.456	1.288	151.3		-40°F
C-54	0.108	0.2620	0.0283	576	16.296	1.358	150.6		-40°F
C-55	0.106	0.2571	0.0273	919	25.08	2.09	143.9		200°F
C-56	0.107	0.2458	0.0263	935	24.60	2.05	144.3		200°F
C-57	0.107	0.2440	0.0261	864	22.56	1.88	145.7		200°F
C-58	0.108	0.2512	0.0271	1258	34.08	2.84	138.4		320°F
C-59	0.107	0.2548	0.0273	1160	31.68	2.64	139.8		320°F
C-60	0.108	0.2753	0.0297	1164	34.56	2.88	138.1		320°F

TABLE XXIV

PRECRACK CHARPY IMPACT DATA - 6Al-4V TITANIUM

Minuteman Chamber S/N	Component	Specimen Location	Wall Thickness	Test Temperature, °F -40	RT	200	320
1369	Fwd Skirt		0.107		615 - 636 Avg(3) 629		
	Fwd Closure	3-in. fwd of G1 weld	0.116		423 - 48 Avg(3) 446		
		G1 reinforced section	0.190		356 - 39. Avg(3) 374	471 - 486 Avg(3) 477	659 - 806 Avg(3) 749
	Fwd Cyl	G1 reinforced section	0.185	205 - 231 Avg(2) 218	286 - 303 Avg(3) 295	343 - 409 Avg(3) 385	550 - 568 Avg(3) 558
		3-in. aft of G1 weld	0.107		316 - 330 Avg(3) 324		
		3-in. fwd of G2 weld	0.108		332 - 349 Avg(3) 342		
		G2 reinforced section	0.185		207 - 216 Avg(2) 211		
	Aft Cyl	G2 reinforced section	0.180		359 - 385 Avg(3) 374		
		3-in. aft of G2 weld	0.104		432 - 489 Avg(3) 455		
		3-in. fwd of G3 weld	0.106		472 - 514 Avg(3) 490		
		G3 reinforced section	0.180	268 - 292 Avg(3) 280	350 - 377 Avg(3) 368	465 - 599 Avg(3) 523	756 - 869 Avg(3) 810

TABLE XXIV (cont.)

Minuteman Chamber S/N	Component	Specimen Location	Wall Thickness	Test Temperature, °F -40	RT	200	320
R369	Aft Closure	G3 reinforced section	0.190	297 - 335 Avg(3) 316	344 - 381 Avg(3) 366	512 - 548 Avg(3) 529	728 - 829 Avg(3) 765
		3-in. aft of G3 weld	0.114		487 - 496 Avg(3) 492		
	Aft Skirt		0.117		606 - 628 Avg(3) 615		

TABLE XXV

PRECRACK CHARPY IMPACT DATA
MINUTEMAN CHAMBER R369 (52 IN. DIA)

Component	Specimen No.
Forward Skirt	L1 - 3
Forward Closure	L4 - 18
Forward Cylinder	
At G1 Weld	L19 - 33
At G2 Weld	L34 - 39
Aft Cylinder	
At G2 Weld	L40 - 45
At G3 Weld	L46 - 60
Aft Closure	L61 - 75
Aft Skirt	L76 - 78

TABLE XXV (cont.)

SPECIMEN NO.	WIDTH	DBN - cd	AREA	W/A	in. - lb	ft-lb	DEGREES	C.D.	Test Temp.
L-7	0.193 0.186	0.315	0.0597	527	31.44	2.62	140.0		-40°F
L-11	0.194 0.188	0.315	0.0602	543	32.64	2.72	139.3		-40°F
L-15	0.194 0.188	0.316	0.0604	628	37.92	3.16	136.2		-40°F
L-19	0.191 0.182	0.314	0.0586	571	33.48	2.79	138.8		-40°F
L-23	0.189 0.176	0.242	0.0442	231	10.19	0.849	156.0	0.073	-40°F
L-27	0.191 0.180	0.237	0.0440	205	9.00	0.750	157.2	0.080	-40°F
L-49	0.189 0.175	0.240	0.0437	292	12.77	1.064	153.6	0.074	-40°F
L-53	0.187 0.175	0.205	0.0371	280	10.40	0.867	155.8	0.111	-40°F
L-57	0.188 0.178	0.207	0.0377	268	10.09	0.841	156.1	0.110	-40°F
L-61	0.193 0.186	0.251	0.0476	315	14.98	1.248	151.7	0.065	-40°F
L-65	0.193 0.186	0.240	0.0445	297	13.21	1.101	153.2	0.076	-40°F
L-69	0.193 0.187	0.252	0.0479	335	16.06	1.338	150.8	0.065	-40°F
L-1	0.107	0.258	0.0276	635	17.52	1.46	149.6	0.059	RT
L-2	0.106	0.265	0.0281	636	17.88	1.49	149.3	0.050	RT
L-3	0.107	0.255	0.0273	615	16.78	1.398	150.2	0.062	RT
L-4	0.115	0.266	0.0306	486	14.86	1.238	151.8	0.053	RT
L-5	0.116	0.258	0.0299	423	12.66	1.055	153.7	0.060	RT
L-6	0.117	0.266	0.0309	428	13.21	1.101	153.2	0.049	RT
L-8	0.194 0.188	0.253	0.0483	368	17.76	1.48	149.4	0.064	RT
L-12	0.193 0.187	0.248	0.0471	356	16.78	1.398	150.2	0.070	RT

TABLE XXV (cont.)

SPECIMEN NO.	WIDTH	DBN - cd	AREA	W/A	in.-lb	ft-lb	DEGREES	C D	Test Temp.
L-16	0.193 0.188	0.255	0.0486	398	19.32	1.61	148.2	0.062	RT
L-20	0.191 0.183	0.257	0.0481	297	14.27	1.189	152.3	0.059	RT
L-24	0.189 0.179	0.243	0.0447	286	12.77	1.064	153.6	0.073	RT
L-28	0.191 0.181	0.243	0.0452	303	13.69	1.141	152.8	0.074	RT
L-31	0.107	0.259	0.0277	325	9.00	0.750	157.2	0.060	RT
L-32	0.107	0.255	0.0273	330	9.00	0.750	157.2	0.061	RT
L-33	0.107	0.252	0.0270	316	8.54	0.712	157.7	0.066	RT
L-34	0.107	0.263	0.0281	349	9.80	0.817	156.4	0.055	RT
L-35	0.108	0.252	0.0272	346	9.40	0.783	156.8	0.066	RT
L-36	0.108	0.268	0.0289	332	9.60	0.800	156.6	0.048	RT
L-37	0.190 0.183			CRACKED THROUGH					
L-38	0.189 0.180	0.160	0.0295	207	6.12	0.510	160.5	0.156	RT
L-39	0.188 0.177	0.239	0.0436	216	9.40	0.783	156.8	0.077	RT
L-40	0.186 0.175	0.252	0.0455	377	17.16	1.43	149.9	0.064	RT
L-41	0.187 0.174	0.247	0.0446	385	17.16	1.43	149.9	0.069	RT
L-42	0.187 0.174	0.250	0.0451	359	16.18	1.348	150.7	0.067	RT
L-43	0.104	0.261	0.0271	443	12.00	1.000	154.3	0.056	RT
L-44	0.104	0.245	0.0255	432	11.02	0.919	155.2	0.073	RT
L-45	0.104	0.260	0.0270	489	13.21	1.101	153.2	0.057	RT
L-46	0.106	0.255	0.0270	485	13.10	1.092	153.3	0.062	RT
L-47	0.106	0.258	0.0273	472	12.88	1.073	153.5	0.060	RT

TABLE XXV (cont.)

SPECIMEN NO.	WIDTH	DBN - cd	AREA	W/A	in.-lb	ft-lb	DEGREES	C.D.	Test Temp.
L-48	0.106	0.264	0.0280	514	14.39	1.199	152.2	0.052	RT
L-50	0.189 0.176	0.206	0.0376	376	14.15	1.179	152.4	0.111	RT
L-54	0.188 0.176	0.222	0.0404	377	15.22	1.268	151.5	0.094	RT
L-58	0.188 0.175	0.225	0.0408	350	14.27	1.189	152.3	0.089	RT
L-62	0.193 0.185	0.216	0.0408	344	14.04	1.170	152.5	0.101	RT
L-66	0.193 0.185	0.248	0.0469	381	17.88	1.49	149.3	0.069	RT
L-70	0.193 0.187	0.205	0.0390	372	14.50	1.208	152.1	0.111	RT
L-73	0.114	0.263	0.0300	487	14.62	1.218	152.0	0.055	RT
L-74	0.114	0.265	0.0302	492	14.86	1.238	151.8	0.053	RT
L-75	0.114	0.265	0.0302	496	14.98	1.248	151.7	0.052	RT
L-76	0.117	0.271	0.0317	628	19.92	1.66	147.6	0.090	RT
L-77	0.117	0.261	0.0305	610	18.60	1.55	148.7	0.052	RT
L-78	0.117	0.264	0.0309	606	18.72	1.56	148.6	0.054	RT
L-9	0.193 0.186	0.249	0.0472	473	22.32	1.86	145.9	0.068	200°F
L-13	0.194 0.184	0.255	0.0482	471	22.68	1.89	145.6	0.061	200°F
L-17	0.193 0.187	0.251	0.0477	486	23.16	1.93	145.3	0.066	200°F
L-21	0.190 0.181	0.229	0.0425	404	17.16	1.43	149.9	0.088	200°F
L-25	0.190 0.180	0.191	0.0353	343	12.11	1.009	154.2	0.125	200°F
L-29	0.192 0.182	0.251	0.0469	409	19.20	1.60	148.3	0.065	200°F
L-51	0.194 0.174	0.269	0.0495	599	29.64	2.47	141.1	0.048	200°F

TABLE XXV (cont.)

SPECIMEN NO.	WIDTH	DBN - cd	AREA	W/A	in.-lb	ft-lb	DEGREES	C.D.	Test Temp.
L-55	0.188 0.176	0.229	0.0417	506	21.12	1.76	146.7	0.085	200°F
L-59	0.188 0.174	0.228	0.0413	465	19.20	1.60	148.3	0.087	200°F
L-63	0.193 0.186	0.249	0.0472	526	24.84	2.07	144.1	0.068	200°F
L-67	0.193 0.183	0.248	0.0466	512	23.88	1.99	144.8	0.068	200°F
L-71	0.192 0.186	0.249	0.0471	548	25.80	2.15	143.5	0.069	200°F
L-10	0.194 0.188	0.263	0.0502	782	39.24	3.27	135.4	0.055	320°F
L-14	0.194 0.188	0.231	0.0441	659	29.04	2.42	141.5	0.083	320°F
L-18	0.193 0.187	0.250	0.0475	806	38.28	3.19	136.0	0.065	320°F
L-22	0.190 0.179	0.202	0.0373	550	20.52	1.71	147.2	0.115	320°F
L-26	0.192 0.184	0.237	0.0446	557	24.84	2.07	144.1	0.080	320°F
L-30	0.192 0.185	0.240	0.0452	568	25.68	2.14	143.6	0.078	320°F
L-52	0.188 0.176	0.251	0.0457	804	36.72	3.06	136.9	0.064	320°F
L-56	0.188 0.176	0.247	0.0450	869	39.12	3.26	135.5	0.067	320°F
L-60	0.189 0.177	0.248	0.0454	756	34.32	2.86	139.3	0.066	320°F
L-64	0.193 0.187	0.252	0.0479	829	39.72	3.31	135.2	0.066	320°F
L-68	0.192 0.185	0.236	0.0445	728	32.40	2.70	139.4	0.082	320°F
L-72	0.193 0.187	0.247	0.0469	739	34.68	2.89	138.1	0.073	320°F

TABLE XXVI

PRECRACK CHARPY IMPACT DATA - 6Al-4V TITANIUM

Minuteman Chamber S/N	Component	Specimen Location	Wall Thickness	Test Temperature, °F -40	RT	200	320
R490	Fwd Skirt		0.108		471 - 570 Avg(3) 516		
	Fwd Closure	3-in. fwd of G1 weld	0.114		367 - 387 Avg(3) 376		
		G1 reinforced section	0.178	270 - 296 Avg(3) 284	350 - 436 Avg(3) 388	474 - 612 Avg(3) 520	636 - 780 Avg(3) 706
	Fwd Cyl	G1 reinforced section	0.180		346 - 421 Avg(3) 378		
		3-in. aft of G1 weld	0.107		343 - 435 Avg(3) 393		
		3-in. fwd of G2 weld	0.109		321 - 466 Avg(3) 410		
		ditto hoop	0.109		654 - 703 Avg(3) 680		
		G2 reinforced section	0.182	237 - 267 Avg(3) 256	323 - 366 Avg(3) 347	428 - 599 Avg(3) 509	556 - 706 Avg(3) 644
	Aft Cyl	G2 reinforced section	0.185		315 - 380 Avg(3) 343	377 - 478 Avg(3) 427	636 - 668 Avg(3) 656
		G2 weld (hoop)	0.195	1250 - 1530 Avg(3) 1363	1656 - 1836 Avg(3) 1721	1840 - 2040 Avg(3) 1960	2160 - 2320 Avg(3) 2253
		3-in. aft of G2 weld	0.109		379 - 388 Avg(3) 382		
		ditto hoop	0.110		403 - 439 Avg(3) 426		

TABLE XXVI (cont.)

Minuteman Chamber S/N	Component	Specimen Location	Wall Thickness	Test Temperature, °F -40	RT	200	320
R490	Aft Cyl (continued)	3-in. fwd of G3 weld	0.107		256 - 311 Avg(3) 284		
		G3 reinforced section	0.182		260 - 303 Avg(3) 289		
	Aft Closure	G3 reinforced section	0.184	189 - 324 Avg(3) 274	425 - 453 Avg(3) 440	479 - 584 Avg(3) 523	
		3-in. aft of G3 weld	0.118		479 - 481 Avg(2) 480		
	Aft Skirt	-	0.112		543 - 545 Avg(2) 544		

TABLE XXVII

PRECRACK CHARPY IMPACT DATA
MINUTEMAN CHAMBER R490 (52 IN. DIA)

Component	Specimen No.
Forward Skirt	M1 - 3
Forward Closure	M4 - 17
Forward Cylinder	
At G1 Weld	M18 - 23
At G2 Weld	M24 - 41 M54 - 65*
Aft Cylinder	
At G2 Weld	M42 - 53 M66 - 71
At G3 Weld	M72 - 77
Aft Closure	M78 - 92
Aft Skirt	M93 - 95

TABLE XXVII (cont.)

SPECIMEN NO	WIDTH	DBN - cd	AREA	W/A	in. - lb	ft-lb	DEGREES	C D	Test Temp.
M-7	0.172	0.249	0.0428	270	11.54	0.962	154.7	0.069	-40°F
M-10	0.176	0.224	0.0394	285	11.23	0.936	155.0	0.095	-40°F
M-14	0.179	0.265	0.0474	296	14.04	1.170	152.5	0.054	-40°F
M-30	0.183	0.235	0.0430	237	10.19	0.849	156.0	0.080	-40°F
M-34	0.180	0.275	0.0495	267	13.21	1.101	153.2	0.043	-40°F
M-38	0.177	0.284	0.0503	265	13.33	1.111	153.1	0.036	-40°F
M-42	0.184	0.054	0.0099	192.7	1.908	0.159	166.2	0.263	-40°F
M-46	0.184	0.096	0.0177	170.8	3.024	0.252	164.5	0.219	-40°F
M-50	0.182	0.250	0.0455	261	11.88	0.990	154.4	0.068	-40°F
M-54	0.197	0.282	0.0556	1310	73.08	6.09	119.1	0.040	-40°F
M-58	0.197	0.227	0.0447	1250	56.04	4.67	126.3	0.093	-40°F
M-62	0.195	0.266	0.0519	1536	79.32	6.61	116.2	0.054	-40°F
M-78	0.186	0.287	0.0534	189	10.09	0.841	156.1	0.032	-40°F
M-82	0.186	0.255	0.0474	308	14.62	1.218	152.0	0.064	-40°F
M-86	0.186	0.241	0.0448	324	14.50	1.208	152.1	0.077	-40°F
M-1	0.107	0.281	0.0301	570	17.16	1.43	149.9	0.049	RT
M-2	0.108	0.271	0.0291	507	14.75	1.229	151.9	0.048	RT
M-3	0.108	0.267	0.0288	471	13.57	1.131	152.9	0.052	RT
M-4	0.113	0.278	0.0314	367	11.54	0.962	154.7	0.042	RT
M-5	0.114	0.287	0.0327	374	12.23	1.019	154.1	0.033	RT

TABLE XXVII (cont.)

SPECIMEN NO	WIDTH	DBN-cd	AREA	W/A	in.-lb	ft-lb	DEGREES	C D	Test Temp.
M-6	0.115	0.272	0.0313	386.9	12.11	1.009	154.2	0.049	RT
M	0.175	0.280	0.0490	377	18.48	1.54	148.8	0.039	RT
M-11	0.178	0.273	0.0495	436	21.60	1.80	146.4	0.046	RT
M-15	0.179	0.256	0.0458	350	16.05	1.338	150.8	0.064	RT
M-18	0.179	0.263	0.0471	346	16.30	1.358	150.6	0.055	RT
M-19	0.182	0.274	0.0499	420.8	21.00	1.75	146.8	0.044	RT
M-20	0.182	0.256	0.0466	368	17.16	1.43	149.9	0.063	RT
M-21	0.105	0.277	0.0291	343	10.00	0.833	156.2	0.042	RT
M-22	0.107	0.274	0.0293	401	11.77	0.981	154.5	0.046	RT
M-23	0.107	0.272	0.0291	435	12.66	1.055	153.7	0.048	RT
M-24	0.108	0.270	0.0292	682 *	19.92	1.66	147.6	0.046	RT
M-25	0.109	0.282	0.0307	703 *	21.60	1.80	146.4	0.039	RT
M-26	0.109	0.285	0.0311	654 *	20.34	1.695	147.3	0.034	RT
M-27	0.109	0.179	0.0195	321	6.27	0.523	160.3	0.140	RT
M-28	0.109	0.258	0.0281	466	13.10	1.092	153.3	0.062	RT
M-29	0.109	0.271	0.0295	444	13.10	1.092	153.3	0.046	RT
M-31	0.181	0.252	0.0456	352	16.06	1.338	150.8	0.067	RT
M-39	0.182	.259	0.0471	323	15.22	1.268	151.5	0.059	RT
M-35	0.182	0.246	0.0448	366	16.42	1.368	150.5	0.073	RT
M-43	0.184	0.256	0.0471	315	14.86	1.238	151.8	0.064	RT
M-47	0.186	0.246	0.0458	333.9	15.34	1.278	151.4	0.072	RT

*Crack propagating in the chamber-hoop direction.

TABLE XXVII (cont.)

SPECIMEN NO.	WIDTH	DBN-cd	AREA	W/A	in.-lb	ft-lb	DEGREES	C D	Test Temp.
M-51	0.185	0.261	0.0483	380	18.36	1.53	148.9	0.058	RT
M-53	0.195	0.287	0.0560	1656	92.76	7.73	111.4	0.035	RT
M-59	0.195	0.282	0.0552	1672	92.28	7.69	111.6	0.037	RT
M-63	0.194	0.296	0.0574	1836	105.4	8.78	105.2	0.024	RT
M-66	0.109	0.274	0.0299	379	11.34	0.945	154.9	0.046	RT
M-67	0.109	0.275	0.0300	388	11.65	0.971	154.6	0.045	RT
M-68	0.109	0.267	0.029[illegible]	379	11.03	0.919	155.2	0.053	RT
M-69	0.109	0.272	0.0296	439 *	13.00	1.083	153.4	0.047	RT
M-70	0.110	0.260	0.0286	403 *	11.54	0.962	154.7	0.060	RT
M-71	0.110	0.252	0.0277	437 *	12.11	1.009	154.2	0.064	RT
M-72	0.106	0.243	0.0258	256	6.61	0.551	159.9	0.075	RT
M-73	0.107	0.185	0.0198	284	5.63	0.469	161.1	0.114	RT
M-74	0.107	0.254	0.0272	311	8.45	0.704	157.8	0.065	RT
M-75	0.180	0.273	0.0491	260	12.77	1.064	153.6	0.045	RT
M-76	0.185	0.275	0.0509	303	15.46	1.288	151.3	0.045	RT
M-77	0.180	0.276	0.0497	303	15.10	1.258	151.6	0.051	RT
M-78	0.184	0.192	0.0353	1091	27.60	2.30	142.4	0.127	RT
M-79	0.185	0.287	0.0531	453	24.06	2.005	144.7	0.032	RT
M-83	0.185	0.275	0.0509	441	22.44	1.87	145.8	0.047	RT
M-87	0.184	0.274	0.0504	425	21.42	1.785	146.5	0.047	RT
M-90	0.117	0.275	0.0322	123	3.98	0.332	163.2	0.043	RT

*Crack propagating in the chamber-hoop direction.

TABLE XXVII (cont.)

SPECIMEN NO.	WIDTH	DBN - cd	AREA	W/A	in.-lb	ft-lb	DEGREES	C D	Test Temp.
M-91	0.119	0.268	0.0319	481	15.34	1.278	151.4	0.063	RT
M-92	0.119	0.238	0.0283	479	13.57	1.131	152.9	0.081	RT
M-93	0.112	0.198	0.0221	543	12.00	1.000	154.3	0.120	RT
M-94	0.112	0.273	0.0305	545	16.64	1.387	150.3	0.046	RT
M-95	0.112	0.272	0.0304	141	4.30	0.358	162.8	0.048	RT
M-8	0.175	0.256	0.0448	474	21.24	1.77	146.6	0.0634	200°F
M-12	0.178	0.271	0.0482	612	29.52	2.46	141.2	0.0465	200°F
M-16	0.179	0.260	0.0465	475	22.08	1.84	146.0	0.0583	200°F
M-32	0.180	0.264	0.0475	599	28.44	2.37	141.8	0.0499	200°F
M-36	0.176	0.252	0.0444	501	22.26	1.855	145.9	0.0586	200°F
M-40	0.179	0.230	0.0412	428	17.64	1.47	149.5	0.0866	200°F
M-44	0.183	0.243	0.0445	377	16.78	1.398	150.2	0.0765	200°F
M-48	0.184	0.255	0.0469	427	20.04	1.67	147.5	0.0658	200°F
M-52	0.185	0.247	0.0457	478	21.84	1.82	146.2	0.0673	200°F
M-56	0.195	0.276	0.0538	1840	99.24	8.27	107.7	0.0423	200°F
M-60	0.198	0.285	0.0564	2040	115.3	9.61	101.0	0.0335	200°F
M-64	0.196	0.252	0.0494	2000	99.00	8.25	107.8	0.0656	200°F
M-80	0.188	0.233	0.0438	584	25.56	2.13	143.1	0.0797	200°F
M-84	0.188	0.229	0.0430	505	21.72	1.81	146.3	0.0902	200°F
M-88	0.188	0.208	0.0391	479	18.72	1.56	148.6	0.1107	200°F

TABLE XXVII (cont.)

SPECIMEN NO	WIDTH	DBN - cd	AREA	W/A	in.-lb	ft-lb	DEGREES	C D	Test Temp.
M-9	0.175	0.236	0.0413	636	26.28	2.19	143.2	0.0813	320°F
M-13	0.179	0.253	0.0453	780	35.34	2.945	137.7	0.0644	320°F
M-17	0.181	0.255	0.0462	701	32.40	2.70	139.4	0.0603	320°F
M-33	0.180	0.261	0.0470	671	31.56	2.63	138.9	0.0567	320°F
M-37	0.178	0.250	0.0445	706	31.44	2.62	140.0	0.0618	320°F
M-41	0.181	0.202	0.0366	556	20.34	1.695	147.3	0.1168	320°F
M-45	0.184	0.242	0.0443	636	28.32	2.36	141.9	0.0713	320°F
M-49	0.184	0.268	0.0493	664	32.76	2.73	139.2	0.0476	320°F
M-53	0.186	0.246	0.0458	668	30.60	2.55	140.5	0.0688	320°F
M-57	0.198	0.278	0.0550	2160	118.9	9.91	99.5	0.0371	320°F
M-61	0.197	0.266	0.0524	2320	121.6	10.13	98.4	0.0517	320°F
M-65	0.194	0.271	0.0526	2280	120.2	10.02	98.9	0.0470	320°F

TABLE XXVIII

PRECRACK CHARPY IMPACT DATA - 6Al-4V TITANIUM

Minuteman Chamber S/N	Component	Specimen Location	Wall Thickness	Test Temperature, °F -40	RT	200	320
R512	Fwd Skirt		0.109		693 - 776 Avg(3) 737		
	Fwd Closure	3-in. fwd of G1 weld	0.121		535 - 554 Avg(3) 542		
		G1 reinforced section	0.189	364 - 411 Avg(3) 390	433 - 493 Avg(3) 467	528 - 760 Avg(3) 623	827 - 972 Avg(3) 908
	Fwd Cyl	G1 reinforced section	0.186		362 - 456 Avg(3) 420		
		3-in. aft of G1 weld	0.107		468 - 540 Avg(3) 509		
		3-in. fwd of G2 weld	0.108		526 - 532 Avg(3) 529		
		Ditto hoop			388 - 468 Avg(3) 436		
		G2 reinforced section	0.186	265 - 309 Avg(3) 292	340 - 409 Avg(3) 368	468 - 538 Avg(3) 508	708 - 733 Avg(2) 720
	Aft Cyl	G2 reinforced section	0.185	248 - 257 Avg(3) 254	316 - 341 Avg(3) 326	429 - 487 Avg(3) 463	626 - 662 Avg(2) 644
		3-in. aft of G2 weld	0.109		386 - 443 Avg(3) 414		
		Ditto hoop	0.107		414 - 539 Avg(3) 467		

TABLE XXVIII (cont.)

Minuteman Chamber S/N	Component	Specimen Location	Wall Thickness	Test Temperature, °F -40	RT	200	320
R512	Aft Cyl (continued)	3-in. fwd of G3 weld	0.110		405 - 438 Avg(3) 424		
		G3 reinforced section	0.187		368 - 372 Avg(3) 370		
	Aft Closure	G3 reinforced section	0.180	430 - 496 Avg(3) 468	577 - 661 Avg(3) 607	670 - 722 Avg(3) 689	895 - 1075 Avg(3) 978
		3-in. aft of G3 weld	0.111		670 - 701 Avg(3) 683		
	Aft Skirt	-	0.118		558 - 778 Avg(3) 668		

TABLE XXIX

PRECRACK CHARPY IMPACT DATA
MINUTEMAN CHAMBER R512 (52-IN.-DIA)

Component	Specimen No.
Forward Skirt	P1 - 3
Forward Closure	P4 - 18
Forward Cylinder	
At G1 Weld	P19 - 24
At G2 Weld	P25 - 38
Aft Cylinder	
At G2 Weld	P40 - 54
At G3 Weld	P55 - 60
Aft Closure	P61 - 75
Aft Skirt	P76 - 78

TABLE XXIX (cont.)

SPECIMEN NO.	WIDTH	DBN-cd	AREA	W/A	in.-lb	ft-lb	DEGREES	C D	Test Temp.
P-28	0.190 0.172	0.255	0.0462	265	12.23	1.019	154.1	0.060	-40°F
P-32	0.192 0.175	0.274	0.0503	303	15.22	1.268	151.5	0.043	-40°F
P-36	0.192 0.180	0.266	0.0497	309	15.34	1.278	151.4	0.051	-40°F
P-40	0.194 0.180	0.271	0.0507	256	13.00	1.083	153.4	0.045	-40°F
P-44	0.195 0.181	0.239	0.0449	248	11.12	0.927	155.1	0.077	-40°F
P-48	0.195 0.182	0.255	0.0481	257	12.34	1.028	154.0	0.060	-40°F
P-7	0.184	0.2560	0.0471	395	18.60	1.55	148.7		-40°F
P-11	0.190	0.2268	0.0431	364	15.696	1.308	151.1		-40°F
P-15	0.190	0.2397	0.0455	411	18.72	1.56	148.6		-40°F
P-61	0.177	0.2370	0.0419	430	18.00	1.50	149.2		-40°F
P-65	0.181	0.2330	0.0422	478	20.16	1.68	147.4		-40°F
P-69	0.181	0.2460	0.0445	496	22.08	1.84	146.0		-40°F
P-1	0.109	0.2604	0.0284	693	19.68	1.64	147.8		RT
P-2	0.109	0.2539	0.0277	741	20.52	1.71	147.2		RT
P-3	0.109	0.2592	0.0283	776	21.96	1.83	146.1		RT
P-4	0.121	0.2537	0.0307	535	16.416	1.368	150.5		RT
P-5	0.120	0.2528	0.0303	554	16.776	1.398	150.2		RT
P-6	0.121	0.2623	0.0317	537	17.016	1.418	150.0		RT
P-8	0.185	0.2392	0.0443	474	21.00	1.75	146.8		RT
P-12	0.190	0.2263	0.0430	433	18.60	1.55	148.7		RT

TABLE XXIX (cont.)

SPECIMEN NO	WIDTH	DBN-cd	AREA	W/A	in.-lb	ft-lb	DEGREES	C.D.	Test Temp.
P-16	0.189	0.2513	0.0475	493	23.40	1.95	145.1		RT
P-19	0.186	0.2435	0.0453	362	16.416	1.368	150.5		RT
P-20	0.187	0.2492	0.0466	443	20.64	1.72	147.1		RT
P-21	0.185	0.2473	0.0458	456	20.88	1.74	146.9		RT
P-22	0.106	0.2643	0.0280	468	13.104	1.092	153.3		RT
P-23	0.107	0.2572	0.0275	519	14.268	1.189	152.3		RT
P-25	0.108	0.274	0.0296	526	15.58	1.298	151.2	0.046	RT
P-26	0.108	0.271	0.0293	532	15.58	1.298	151.2	0.049	RT
P-27	0.108	0.273	0.0295	528	15.58	1.298	151.2	0.046	RT
P-29	0.190 0.180	0.255	0.0472	356	16.78	1.398	150.2	0.060	RT
P-33	0.191 0.179	0.255	0.0472	340	16.06	1.338	150.8	0.060	RT
P-37	0.192 0.184	0.270	0.0508	409	20.76	1.73	147.0	0.047	RT
P-41	0.194 0.187	0.218	0.0415	316	13.10	1.092	153.3	0.098	RT
P-45	0.195 0.186	0.232	0.0442	320	14.15	1.179	152.4	0.085	RT
P-49	0.194 0.186	0.250	0.0475	341	16.18	1.348	150.7	0.068	RT
P-52	0.108	0.272	0.0294	412	12.11	1.009	154.2	0.048	RT
P-53	0.109	0.262	0.0286	386	11.03	0.919	155.2	0.056	RT
P-54	0.109	0.267	0.0291	443	12.88	1.073	153.5	0.050	RT
P-79	0.107	0.273	0.0292	452 *	13.21	1.101	153.2	0.045	RT
P-80	0.106	0.283	0.0300	468 *	14.04	1.170	152.5	0.034	RT
P-81	0.106	0.260	0.276	388 *	10.70	0.892	155.5	0.057	RT

*Crack propagating in the chamber hoop-direction

TABLE XXIX (cont.)

SPECIMEN NO.	WIDTH	DBN - cd	AREA	W/A	in.-lb	ft-lb	DEGREES	C D.	Test Temp.
P-82	0.108	0.268	0.0289	539 *	15.58	1.298	151.2	0.049	RT
P-83	0.107	0.268	0.0287	449 *	12.88	1.073	153.5	0.053	RT
P-84	0.107	0.261	0.279	414 *	11.54	0.962	154.7	0.059	RT
P-24	0.107	0.2653	0.0284	540	15.336	1.278	151.4		RT
P-55	0.110	0.2471	0.0272	405	11.028	0.919	155.2		RT
P-56	0.110	0.2648	0.0291	431	12.552	1.046	153.8		RT
P-57	0.110	0.2524	0.0278	436	12.108	1.009	154.2		RT
P-58	0.187	0.2190	0.0410	368	15.096	1.258	151.6		RT
P-59	0.189	0.2451	0.0463	370	17.148	1.429	149.9		RT
P-60	0.187	0.2398	0.0448	372	16.664	1.387	150.3		RT
P-62	0.173	0.2429	0.0420	583	24.48	2.04	144.4		RT
P-66	0.180	0.2531	0.0456	661	30.12	2.51	140.8		RT
P-70	0.181	0.2341	0.0424	577	24.48	2.04	144.4		RT
P-73	0.111	0.2512	0.0279	701	19.56	1.63	148.0		RT
P-74	0.111	0.2629	0.0292	670	19.56	1.63	148.0		RT
P-75	0.111	0.2611	0.0290	677	19.62	1.635	147.9		RT
P-76	0.118	0.2658	0.0314	558	17.52	1.46	149.6		RT
P-77	0.118	0.2649	0.0313	667	20.88	1.74	146.9		RT
P-78	0.118	0.2605	0.0307	778	23.88	1.99	144.8		RT

*Crack propagating in the chamber hoop-direction

TABLE XXIX (cont.)

SPECIMEN NO.	WIDTH	DBN-cd	AREA	W/A	in.-lb	ft-lb	DEGREES	C.D.	Test Temp.
P-30	0.190 0.180	0.244	0.0451	468	21.12	1.76	146.7	0.073	200°F
P-34	0.191 0.180	0.249	0.0462	538	24.84	2.07	144.1	0.069	200°F
P-38	0.191 0.183	0.255	0.0477	518	24.72	2.06	144.2	0.062	200°F
P-42	0.194 0.187	0.242	0.0461	487	22.44	1.87	145.8	0.073	200°F
P-46	0.194 0.184	0.213	0.0403	429	17.28	1.44	149.8	0.104	200°F
P-50	0.194 0.184	0.259	0.0490	478	23.40	1.95	145.1	0.058	200°F
P-9	0.186	0.2379	0.0442	581	25.68	2.14	143.5		200°F
P-13	0.188	0.2118	0.0398	528	21.00	1.75	146.8		200°F
P-17	0.190	0.2638	0.0501	760	38.10	3.175	136.1		200°F
P-63	0.174	0.2379	0.0414	675	27.96	2.33	142.2		200°F
P-67	0.180	0.2273	0.0409	722	29.52	2.46	141.2		200°F
P-71	0.181	0.2325	0.0421	670	28.20	2.35	142.0		200°F
P-10	0.189	0.2453	0.0464	972	45.12	3.76	132.2		320°F
P-14	0.189	0.2323	0.0439	827	36.30	3.025	137.1		320°F
P-18	0.190	0.2573	0.0489	926	45.30	3.775	132.1		320°F
P-64	0.182	0.2186	0.0398	1075	42.78	3.565	133.5		320°F
P-68	0.181	0.2126	0.0385	895	34.44	2.87	138.2		320°F
P-72	0.182	0.2319	0.0422	963	40.62	3.385	134.7		320°F
P-31	0.192 0.176	0.255	0.0469	733	34.4	2.87	138.2		320°F

TABLE XXIX (cont.)

SPECIMEN NO.	WIDTH	DBN · cd	AREA	W/A	in.-lb	ft-lb	DEGREES	C.D.	Test Temp.
P-35	0.192 0.177	0.255	0.0469	733	34.4	2.87	138.2	0.063	320°F
P-43	0.195 0.181	0.245	0.0461	662	30.5	2.54	140.6	0.071	320°F
P-47	0.195 0.181	0.220	0.0414	626	25.9	2.16	143.4	0.099	320°F

TABLE XXX

PRECRACK CHARPY IMPACT DATA - 6A1-4V TITANIUM

Minuteman Chamber S/N	Component	Specimen Location	Wall Thickness	Test Temperature, °F -40	RT	200	320
R516	Fwd Skirt	-	0.104		645 - 663 Avg(3) 655		
	Fwd Closure	2-in. fwd of G1 weld	0.115		371 - 473 Avg(3) 420		
		G1 reinforced section	0.185	287 - 355 Avg(3) 311	356 - 428 Avg(3) 394	489 - 573 Avg(3) 528	670 - 975 Avg(3) 795
	Fwd Cyl	G1 reinforced section	0.185		373 - 644 Avg(3) 465		
		2-in. aft of G1 weld	0.107		404 - 428 Avg(3) 415		
		3-in. fwd of G2 weld	0.106		315 - 375 Avg(3) 349		
		Ditto hoop	0.104		393 - 501 Avg(3) 459		
		G2 reinforced section	0.182	214 - 272 Avg(3) 252	328 - 405 Avg(3) 358	390 - 458 Avg(3) 434	647 - 709 Avg(3) 671
	Aft Cyl	G2 reinforced section	0.187	339 - 345 Avg(3) 341	389 - 457 Avg(3) 429	526 - 576 Avg(3) 555	687 - 796 Avg(3) 746
		3-in. aft of G2 weld	0.107		384 - 482 Avg(3) 444		
		Ditto hoop	0.105		345 - 400 Avg(3) 374		

TABLE XXX (cont.)

Minuteman Chamber S/N	Component	Specimen Location	Wall Thickness	Test Temperature, °F -40	RT	200	320
R516	Aft Cyl (continued)	3-in. fwd of G3 weld	0.109		426 - 493 Avg(3) 469		
		G3 reinforced section	0.190		338 - 381 Avg(3) 362		
	Aft Closure	G3 reinforced section	0.190	320 - 381 Avg(3) 355	384 - 392 Avg(3) 389	546 - 644 Avg(3) 591	774 - 826 Avg(3) 798
		3-in. aft of G3 weld	0.118		500 - 526 Avg(3) 510		
	Aft Skirt	-	0.116		530 - 555 Avg(3) 542		

TABLE XXXI

PRECRACK CHARPY IMPACT DATA
MINUTEMAN CHAMBER R516 (52 IN. DIA)

Component	Specimen No.
Forward Skirt	R1 - 3
Forward Closure	R4 - 18
Forward Cylinder	
At G1 Weld	R19 - 24
At G2 Weld	R25 - 42
Aft Cylinder	
At G2 Weld	R43 - 60
At G3 Weld	R61 - 66
Aft Closure	R67 - 81
Aft Skirt	R82 - 84

TABLE XXXI (cont.)

SPECIMEN NO.	WIDTH	DBW - cd	AREA	W/A	in.-lb	ft-lb	DEGREES	C D	Test Temp.
R-7	0.191 0.172	0.274	0.0497	355	17.64	1.47	149.5	0.043	-40°F
R-11	0.192 0.172	0.267	0.0481	287	13.80	1.150	152.7	0.046	-40°F
R-15	0.193 0.173	0.275	0.0503	291	14.62	1.218	152.0	0.042	-40°F
R-31	0.187 0.167	0.282	0.0499	214	10.70	0.892	155.5	0.037	-40°F
R-35	0.190 0.168	0.276	0.0494	270	13.33	1.111	153.1	0.041	-40°F
R-39	0.191 0.170	0.293	0.0529	272	14.39	1.199	152.2	0.024	-40°F
R-43	0.189 0.178	0.285	0.0523	340	17.76	1.48	149.4	0.033	-40°F
R-47	0.191 0.181	0.289	0.0538	339	18.24	1.52	149.0	0.029	-40°F
R-51	0.190 0.179	0.260	0.0480	345	16.54	1.378	150.4	0.056	-40°F
R-67	0.193 0.179	0.262	0.0487	320	15.58	1.298	151.2	0.057	-40°F
R-71	0.194 0.182	0.269	0.0506	363	18.36	1.53	148.9	0.050	-40°F
R-75	0.197 0.187	0.274	0.0526	381	20.04	1.67	147.5	0.045	-40°F
R-1	0.104	0.264	0.0275	656	18.00	1.50	149.2	0.045	RT
R-2	0.104	0.267	0.0277	645	17.88	1.49	149.3	0.053	RT
R-3	0.105	0.270	0.0284	663	18.84	1.57	148.5	0.051	RT
R-4	0.115	0.269	0.0309	473	14.62	1.218	152.0	0.050	RT
R-5	0.115	0.276	0.0317	417	13.21	1.101	153.2	0.042	RT
R-6	0.115	0.258	0.0297	371	11.03	0.919	155.2	0.060	RT
R-8	0.191 0.176	0.199	0.0365	356	13.00	1.083	153.4	0.118	RT
R-12	0.191 0.176	0.230	0.0422	398	16.78	1.398	150.2	0.088	RT

TABLE XXXI (cont.)

SPECIMEN NO	WIDTH	DBN-cd	AREA	W/A	in.-lb	ft-lb	DEGREES	C.D	Test Temp.
R-16	0.192 0.181	0.265	0.0494	428	21.12	1.76	146.7	0.051	RT
R-19	0.191 0.180	0.243	0.0451	644	29.04	2.42	141.5	0.075	RT
R-20	0.190 0.182	0.262	0.0487	377	18.36	1.53	148.9	0.057	RT
R-21	0.190 0.179	0.261	0.0482	373	18.00	1.50	149.2	0.058	RT
R-22	0.108	0.262	0.0283	412	11.65	0.971	154.6	0.057	RT
R-23	0.107	0.254	0.0272	428	11.65	0.971	154.6	0.066	RT
R-24	0.107	0.260	0.0278	404	11.23	0.936	155.0	0.060	RT
R-25	0.103	0.267	0.0275	393 *	10.81	0.901	155.4	0.054	RT
R-26	0.104	0.277	0.0288	483 *	13.92	1.160	152.6	0.042	RT
R-27	0.105	0.271	0.0285	501 *	14.27	1.189	152.3	0.049	RT
R-28	0.104	0.245	0.0255	315	8.02	0.668	158.3	0.072	RT
R-29	0.106	0.265	0.0281	356	10.00	0.833	156.2	0.055	RT
R-30	0.106	0.257	0.0272	375	10.19	0.849	156.0	0.062	RT
R-32	0.190 0.173	0.243	0.0441	405	17.88	1.49	149.3	0.086	RT
R-36	0.190 0.174	0.241	0.0439	328	14.39	1.199	152.2	0.077	RT
R-40	0.190 0.176	0.239	0.0437	340	14.86	1.238	151.8	0.077	RT
R-44	0.190 0.186	0.261	0.0491	457	22.44	1.87	145.8	0.057	RT
R-48	0.190 0.184	0.254	0.0475	440	20.88	1.74	146.9	0.065	RT
R-52	0.190 0.184	0.236	0.0441	389	17.16	1.43	149.9	0.082	RT
R-55	0.106	0.260	0.0276	384	10.60	0.883	155.6	0.060	RT
R-56	0.108	0.267	0.0288	467	13.45	1.121	153.0	0.050	RT

*Crack propagating in the chamber hoop-direction.

TABLE XXXI (cont.)

SPECIMEN NO.	WIDTH	D&W - cd	AREA	W/A	in.-lb	ft-lb	DEGREES	C.D.	Test Temp.
R-57	0.109	0.276	0.0301	482	14.50	1.208	152.1	0.045	RT
R-58	0.104	0.264	0.0275	345 *	9.50	0.792	156.7	0.055	RT
R-59	0.105	0.279	0.0293	376 *	11.03	0.919	155.2	0.041	RT
R-60	0.105	0.263	0.0276	400 *	11.03	0.919	155.2	0.056	RT
R-61	0.109	0.266	0.0290	426	12.34	1.028	154.0	0.052	RT
R-62	0.109	0.260	0.0283	488	13.80	1.150	152.7	0.060	RT
R-63	0.110	0.267	0.0294	493	14.50	1.208	152.1	0.053	RT
R-64	0.193 0.177	0.238	0.0440	338	14.88	1.248	151.7	0.080	RT
R-65	0.195 0.185	0.249	0.0473	381	18.00	1.50	149.2	0.069	RT
R-66	0.195 0.185	0.252	0.0479	368	17.64	1.47	149.5	0.067	RT
R-68	0.193 0.186	0.236	0.0447	384	17.16	1.43	149.9	0.083	RT
R-72	0.194 0.185	0.233	0.0442	391	17.28	1.44	149.8	0.085	RT
R-76	0.195 0.187	0.261	0.0499	392	19.56	1.63	148.0	0.058	RT
R-79	0.119	0.270	0.0321	526	16.90	1.408	150.1	0.049	RT
R-80	0.118	0.272	0.0321	504	16.18	1.348	150.7	0.047	RT
R-81	0.118	0.262	0.0309	500	15.46	1.288	151.3	0.058	RT
R-82	0.116	0.279	0.0324	530	17.16	1.43	149.9	0.042	RT
R-83	0.116	0.277	0.0321	542	17.40	1.45	149.7	0.044	RT
R-84	0.116	0.255	0.0296	555	16.42	1.368	150.5	0.064-	RT

*Cracking propagating in the chamber hoop-direction.

TABLE XXXI (cont.)

SPECIMEN NO	WIDTH	DBN - cd	AREA	W/A	in.-lb	ft-lb	DEGREES	C D	Test Temp.
R-9	0.192 0.177	0.252	0.0465	573	26.64	2.42	141.5	0.066	200°F
R-13	0.193 0.180	0.217	0.0405	489	19.80	1.65	147.7	0.102	200°F
R-17	0.193 0.177	0.237	0.0438	523	22.92	1.91	145.5	0.077	200°F
R-33	0.191 0.174	0.231	0.0422	458	19.32	1.61	148.2	0.086	200°F
R-37	0.190 0.174	0.233	0.0424	453	19.20	1.60	148.3	0.086	200°F
R-41	0.191 0.176	0.188	0.0345	390	13.45	1.121	153.0	0.030	200°F
R-45	0.191 0.184	0.253	0.0474	562	26.64	2.22	143.0	0.066	200°F
R-49	0.190 0.184	0.244	0.0456	576	26.28	2.19	143.2	0.077	200°F
R-53	0.190 0.184	0.243	0.0454	526	23.88	1.99	144.8	0.076	200°F
R-69	0.194 0.184	0.241	0.0455	546	24.84	2.07	144.1	0.078	200°F
R-73	0.196 0.187	0.249	0.0477	584	27.84	2.32	142.3	0.071	200°F
R-77	0.195 0.186	0.264	0.0503	644	32.40	2.70	139.4	0.057	200°F
R-10	0.192 0.174	0.253	0.0463	975	45.12	3.76	132.2	0.065	320°F
R-14	0.194 0.177	0.217	0.0403	670	27.0	2.25	142.8	0.103	320°F
R-18	0.193 0.173	0.212	0.0388	739	28.68	2.39	141.7	0.107	320°F
R-34	0.191 0.169	0.240	0.0432	647	27.96	2.33	142.2	0.081	320°F
R-38	0.192 0.172	0.250	0.0455	709	32.28	2.69	139.5	0.068	320°F
R-42	0.192 0.172	0.252	0.0459	656	30.12	2.51	140.6	0.066	320°F
R-46	0.191 0.181	0.262	0.0487	754	36.72	3.06	136.9	0.058	320°F
R-50	0.190 0.180	0.265	0.0490	796	39.00	3.25	135.6	0.053	320°F

TABLE XXXI (cont.)

SPECIMEN NO	WIDTH	DBN - cd	AREA	W/A	in.-lb	ft-lb	DEGREES	C.D.	Test Temp.
R-54	0.190 0.182	0.231	0.0430	687	29.52	2.46	141.2	0.088	320°F
R-70	0.195 0.182	0.255	0.0481	793	38.16	3.18	136.1	0.065	320°F
R-74	0.197 0.188	0.258	0.0497	826	41.04	3.42	134.5	0.062	320°F
R-78	0.190 0.184	0.243	0.0454	774	35.16	2.93	137.8	0.076	320°F

TABLE XXXII

PRECRACK CHARPY IMPACT DATA - 6A1-4V TITANIUM

Minuteman Chamber S/N	Component	Specimen Location	Wall Thickness	Test Temperature, °F -40	RT	200	320
R543	Fwd Skirt	-	0.114		700 - 732 Avg(3) 714		
	Fwd Closure	3-in. fwd of G1 weld	0.114		448 - 504 Avg(3) 484		
		G1 reinforced section	0.185	286 - 424 Avg(3) 346	427 - 480 Avg(3) 447	528 - 683 Avg(3) 619	839 - 928 Avg(3) 872
	Fwd Cyl	G1 reinforced section	0.185	262 - 353 Avg(3) 307	394 - 436 Avg(3) 419	522 - 592 Avg(3) 554	820 - 917 Avg(3) 861
		3-in. aft of G1 weld	0.106		401 - 500 Avg(3) 447		
		Ditto hoop			361 - 507 Avg(3) 450		
		3-in. fwd of G2 weld	0.105		431 - 496 Avg(3) 445		
		G2 reinforced section	0.182		289 - 393 Avg(3) 352		
	Aft Cyl	G2 reinforced section	0.185		247 - 302 Avg(3) 280		
		3-in. aft of G2 weld	0.107		360 - 371 Avg(2) 366		
		3-in. fwd of G3 weld	0.104		336 - 351 Avg(3) 343		
		Ditto Hoop	0.105		546 - 646 Avg(3) 602		

TABLE XXXII (cont.)

Minuteman Chamber S/N	Component	Specimen Location	Wall Thickness	Test Temperature, °F -40	RT	200	320
R543	Aft Cyl (continued)	G3 reinforced section	0.185	226 - 252 Avg(3) 236	269 - 361 Avg(3) 303	331 - 473 Avg(2) 402	516 - 599 Avg(3) 565
	Aft Closure	G3 reinforced section	0.190	333 - 352 Avg(3) 341	435 - 475 Avg(3) 458	625 - 677 Avg(3) 648	798 - 1052 Avg(3) 930
		3-in. aft of G3 weld	0.118		491 - 583 Avg(3) 554		
	Aft Skirt	-	0.113		722 - 770 Avg(3) 753		

TABLE XXXIII

PRECRACK CHARPY IMPACT DATA
MINUTEMAN CHAMBER R543 (52-IN. DIA)

Component	Specimen No.
Forward Skirt	S1 - 3
Forward Closure	S4 - 18
Forward Cylinder	
At G1 Weld	S19 - 33 S82 - 84
At G2 Weld	S34 - 39
Aft Cylinder	
At G2 Weld	S40 - 45
At G3 Weld	S46 - 60 S79 - 81
Aft Closure	S61 - 75
Aft Skirt	S76 - 78

TABLE XXXIII (cont.)

SPECIMEN NO.	WIDTH	DBN - cd	AREA	W/A	in.-lb	ft-lb	DEGREES	C D	Test Temp.
S-7	0.187 0.174	0.254	0.0458	286	13.10	1,092	153.3	0.065	-40°F
S-11	0.188 0.179	0.268	0.0492	424	20.88	1.74	146.9	0.049	-40°F
S-15	0.189 0.177	0.256	0.0468	328	15.34	1.278	151.4	0.062	-40°F
S-19	0.186 0.177	0.225	0.0408	262	10.70	0.892	155.5	0.090	-40°F
S-23	0.189 0.185	0.242	0.0457	307	14.04	1.170	152.5	0.073	-40°F
S-27	0.189 0.184	0.251	0.0468	353	16.54	1.378	150.4	0.075	-40°F
S-49	0.190 0.186	0.246	0.0462	252	11.65	0.971	154.6	0.070	-40°F
S-53	0.190 0.180	0.188	0.0348	230	8.02	0.668	158.3	0.129	-40°F
S-57	0.193 0.183	0.245	0.0461	226	10.40	0.867	155.8	0.071	-40°F
S-61	0.193 0.184	0.260	0.0516	333	17.16	1.43	149.9	0.055	-40°F
S-65	0.195 0.187	0.268	0.0512	352	18.00	1.50	149.2	0.050	-40°F
S-69	0.193 0.183	0.259	0.0487	337	16.42	1.368	150.5	0.059	-40°F
S-1	0.113	0.259	0.0293	700	20.52	1.71	147.2	0.058	RT
S-2	0.114	0.262	0.0299	710	21.24	1.79	146.5	0.054	RT
S-3	0.114	0.259	0.0295	732	21.60	1.80	146.4	0.060	RT
S-4	0.115	0.272	0.0314	504	15.82	1.318	151.0	0.046	RT
S-5	0.114	0.261	0.0298	499	14.86	1.238	151.8	0.058	RT
S-6	0.113 0.113	0.268	0.0303	448	13.58	1.131	152.9	0.049	RT
S-8	0.189 0.177	0.259	0.0474	435	20.64	1.72	147.1	0.037	RT
S-12	0.190 0.175	0.237	0.0433	427	18.48	1.54	148.8	0.079	RT

TABLE XXXIII (cont.)

SPECIMEN NO.	WIDTH	DBN - cd	AREA	W/A	in.-lb	ft-lb	DEGREES	C.D.	Test Temp.
S-16	0.191 0.179	0.254	0.0470	480	22.56	1.88	145.7	0.062	RT
S-20	0.187 0.180	0.239	0.0439	394	17.28	1.44	149.8	0.078	RT
S-24	0.190 0.184	0.238	0.0445	426	18.96	1.58	148.4	0.078	RT
S-28	0.189 0.183	0.240	0.0446	436	19.44	1.62	148.1	0.076	RT
S-31	0.105	0.259	0.0272	401	10.92	0.910	155.3	0.056	RT
S-32	0.106	0.269	0.0285	440	12.55	1.046	153.8	0.049	RT
S-33	0.107	0.269	0.0288	500	14.39	1.199	152.2	0.048	RT
S-34	0.102	0.263	0.0268	351	9.40	0.783	156.8	0.054	RT
S-35	0.105	0.278	0.0292	489	14.27	1.189	152.3	0.039	RT
S-36	0.106	0.274	0.0290	496	14.39	1.199	152.2	0.043	RT
S-37	0.186 0.180	0.248	0.0454	289	13.10	1.092	153.3	0.067	RT
S-38	0.189 0.174	0.247	0.0446	373	16.64	1.387	150.3	0.070	RT
S-39	0.190 0.175	0.237	0.0433	393	17.02	1.418	150.0	0.080	RT
S-40	0.185 0.177	0.215	0.0389	247	9.60	0.800	156.6	0.100	RT
S-41	0.189 0.182	0.238	0.0441	302	13.33	1.111	153.1	0.078	RT
S-42	0.190 0.181	0.211	0.0391	290	11.34	0.945	154.9	0.105	RT
S-43	0.106	0.078	0.0083	171	1.416	0.138	166.6	0.238	RT
S-44	0.107	0.280	0.0300	360	10.81	0.901	155.4	0.038	RT
S-45	0.107	0.262	0.0280	371	10.40	0.867	155.8	0.055	RT
S-46	0.103	0.275	0.0283	336	9.50	0.792	156.7	0.042	RT
S-47	0.105	0.243	0.0255	342	8.72	0.727	157.5	0.072	RT

TABLE XXXIII (cont.)

SPECIMEN NO.	WIDTH	DBN-cd	AREA	W/A	in.-lb	ft-lb	DEGREES	C.D.	Test Temp.
S-48	0.104	0.271	0.0282	351	9.89	0.824	156.3	0.045	RT
S-50	0.193 0.188	0.247	0.0471	361	17.02	1.418	150.0	0.069	RT
S-54	0.194 0.179	0.233	0.0435	278	12.11	1.009	154.2	0.082	RT
S-58	0.193 0.181	0.187	0.0350	269	9.40	0.783	156.8	0.128	RT
S-62	0.194 0.186	0.245	0.0466	464	21.60	1.80	146.4	0.067	RT
S-66	0.194 0.185	0.240	0.0455	475	21.60	1.80	146.4	0.077	RT
S-70	0.194 0.187	0.248	0.0472	435	20.52	1.71	147.2	0.071	RT
S-73	0.116	0.267	0.0310	491	15.22	1.268	151.5	0.051	RT
S-74	0.118	0.272	0.0321	583	18.72	1.56	148.6	0.043	RT
S-75	0.118	0.264	0.0316	577	18.24	1.52	149.0	0.054	RT
S-76	0.113	0.269	0.0304	766	23.28	1.94	145.2	0.050	RT
S-77	0.113	0.274	0.0310	770	23.88	1.99	144.8	0.046	RT
S-78	0.114	0.273	0.0311	722	22.44	1.87	145.8	0.046	RT
S-79	0.104	0.247	0.0257	546*	14.04	1.170	152.5	0.073	RT
S-80	0.105	0.274	0.0288	613*	17.64	1.47	149.5	0.046	RT
S-81	0.105	0.272	0.0286	646*	18.48	1.54	148.8	0.044	RT
S-82	0.105	0.264	0.0277	481*	13.33	1.111	153.1	0.053	RT
S-83	0.105	0.272	0.0286	361*	13.92	1.160	152.6	0.046	RT
S-84	0.105	0.264	0.0277	507*	14.04	1.170	152.5	0.054	RT

*Crack propagating in the chamber hoop-direction.

TABLE XXXIII (cont.)

SPECIMEN NO.	WIDTH	DBN-cd	AREA	W/A	in.-lb	ft-lb	DEGREES	C.D.	Test Temp.
S-9	0.188 0.176	0.253	0.0460	683	31.44	2.62	140.0	0.064	200°F
S-13	0.188 0.175	0.237	0.0430	647	27.84	2.32	142.3	0.080	200°F
S-17	0.192 0.179	0.260	0.0482	528	25.44	2.12	143.8	0.055	200°F
S-21	0.189 0.176	0.232	0.0423	522	22.08	1.84	146.0	0.084	200°F
S-25	0.190 0.185	0.239	0.0448	549	24.60	2.05	144.3	0.075	200°F
S-29	0.189 0.179	0.250	0.0460	592	27.24	2.27	142.6	0.065	200°F
S-51	0.192 0.187	0.241	0.0457	473	21.60	1.80	146.4	0.074	200°F
S-55	0.187 0.177	0.314	0.0571	691	39.48	3.29	135.3		200°F
S-59	0.193 0.182	0.195	0.0366	331	12.11	1.009	154.2	0.120	200°F
S-63	0.194 0.187	0.256	0.0488	642	31.32	2.61	140.1	0.062	200°F
S-67	0.193 0.185	0.261	0.0493	677	33.36	2.78	138.9	0.055	200°F
S-71	0.194 0.187	0.256	0.0488	625	30.48	2.54	140.6	0.060	200°F
S-10	0.188 0.175	0.258	0.0468	928	43.44	3.62	133.2	0.063	320°F
S-14	0.188 0.176	0.243	0.0442	839	37.08	3.09	136.7	0.076	320°F
S-18	0.192 0.181	0.255	0.0476	850	40.44	3.37	134.8	0.063	320°F
S-22	0.190 0.183	0.234	0.0436	820	35.76	2.98	137.5	0.082	320°F
S-26	0.190 0.184	0.245	0.0458	846	38.76	3.23	135.8	0.072	320°F
S-30	0.188 0.179	0.247	0.0453	917	41.52	3.46	134.2	0.071	320°F
S-52	0.191 0.185	0.248	0.0466	579	27.00	2.25	142.8	0.069	320°F
S-56	0.193 0.183	0.239	0.0449	516	23.16	1.93	145.3	0.077	320°F

TABLE XXXIII (cont.)

SPECIMEN NO.	WIDTH	DBN-cd	AREA	W/A	in.-lb	ft-lb	DEGREES	C D	Test Temp.
S-60	0.190 0.177	0.236	0.0433	599	25.92	2.16	143.4	0.081	320°F
S-64	0.194 0.186	0.235	0.0447	1052	47.04	3.92	131.2	0.083	320°F
S-68	0.193 0.185	0.262	0.0495	941	46.56	3.88	131.5	0.057	320°F
S-72	0.194 0.186	0.245	0.0466	798	37.20	3.10	136.6	0.074	320°F

TABLE XXXIV

PRECRACK CHARPY IMPACT DATA - 6A1-4V TITANIUM

Minuteman Chamber S/N	Component	Specimen Location	Wall Thickness	Test Temperature, °F -40	RT	200	320
673078	Fwd Closure	2-in. fwd of G1 weld	0.108		563 - 704 Avg(3) 645		
		G1 reinforced section	0.173	318 - 324 Avg(3) 320	374 - 414 Avg(3) 397	640 - 715 Avg(2) 678	902 - 998 Avg(3) 935
	Fwd Cyl	G1 reinforced section	0.172	368 - 435 Avg(2) 401	530 - 564 Avg(3) 543	631 - 710 Avg(2) 670	784 - 1230 Avg(3) 1021
		2-in. aft of G1 weld	0.101		518 - 701 Avg(3) 630		
		2-in. fwd of G2 weld	0.097		655 - 824 Avg(3) 727		
		G2 reinforced section	0.172		442 - 738 Avg(3) 617		
	Aft Cyl	G2 reinforced section	0.168		422 - 482 Avg(3) 456		
		2-in. aft of G2 weld	0.100		446 - 494 Avg(3) 476		
		2-in. fwd of G3 weld	0.098		555 - 643 Avg(3) 608		
		G3 reinforced section	0.167	343 - 404 Avg(3) 380	462 - 512 Avg(3) 484	676 - 815 Avg(3) 733	895 - 1081 Avg(3) 994
	Aft Closure	G3 reinforced section	0.176	398 - 488 Avg(3) 456	603 - 827 Avg(3) 706	862 - 990 Avg(3) 908	908 - 1174 Avg(3) 1061

TABLE XXXIV

Minuteman Chamber S/N	Component	Specimen Location	Wall Thickness	Test Temperature, °F -40	RT	200	320
673078	Aft Closure (continued)	2-in. aft of G3 weld	0.106		570 - 650 Avg(3) 622		
		Near secondary hoop-direction fracture	0.108		567 - 642 Avg(3) 614		
		Ditto	0.105		492 - 539 Avg(3) 519		

TABLE XXXV

PRECRACK CHARPY IMPACT DATA
MINUTEMAN CHAMBER 673078 (.44 IN. DIA)

Component	Specimen No.
Forward Dome	-
Forward Adaptor	E1 - 14
Forward Cylinder	
At G1 Weld	E16 - 30
At G2 Weld	E31 - 36
Aft Cylinder	
At G2 Weld	E37 - 42
At G3 Weld	E43 - 57
Aft Flange	E58 - 72 E73 - 78*

*Specimens taken at intersection of primary fracture (axial) and secondary fracture (hoop) in aft flange.

TABLE XXXV (cont.)

SPECIMEN NO.	WIDTH	DBN-cd	AREA	W/A	in.-lb	ft-lb	DEGREES	C D.	Test Temp.
E-5	0.175	0.271	0.0475	318	15.10	1.258	151.6	0.044	-40°F
E-13	0.175	0.249	0.0437	318	13.92	1.160	152.6	0.065	-40°F
E-17	0.175	0.277	0.0485	435	21.12	1.76	146.7	0.038	-40°F
E-21	0.171	0.264	0.0452	368	16.64	1.387	150.3	0.051	-40°F
E-25	0.173	0.178	0.0308	271	8.36	0.697	157.9	0.136	-40°F
E-59	0.177	0.268	0.0475	488	23.16	1.93	145.3	0.047	-40°F
E-63	0.178	0.273	0.0487	483	23.52	1.96	145.0	0.042	-40°F
E-67	0.178	0.267	0.0476	398	18.96	1.58	148.4	0.048	-40°F
E-8	0.175	0.248	0.0435	403	17.52	1.46	149.6	0.0636	RT
E-12	0.174	0.257	0.0448	374	16.78	1.398	150.2	0.0604	RT
E-20	0.171	0.270	0.0462	530	24.48	2.04	144.4	0.0448	RT
E-9	0.174	0.2169	0.0377	324	12.228	1.019	154.1		-40°F
E-47	0.167	0.2376	0.0397	404	16.056	1.338	150.8		-40°F
E-51	0.171	0.2191	0.0375	343	12.876	1.073	153.5		-40°F
E-55	0.169	0.2271	0.0384	393	15.096	1.258	151.6		-40°F
E-1	0.108	0.2560	0.0276	704	19.44	1.62	148.1		RT
E-2	0.108	0.2462	0.0266	563	14.976	1.248	151.7		RT
E-3	0.108	0.2495	0.0269	669	18.00	1.50	149.2		RT

TABLE XXXV (cont.)

SPECIMEN NO.	WIDTH	DBN-cd	AREA	W/A	in.-lb	ft-lb	DEGREES	C.D.	Test Temp.
E-4	0.173	0.2296	0.0397	414	16.416	1.368	150.5		RT
E-16	0.172	0.2544	0.0438	564	24.72	2.06	144.2		RT
E-28	0.102	0.2679	0.0273	701	19.14	1.595	148.3		RT
E-29	0.101	0.2525	0.0255	518	13.212	1.101	153.2		RT
E-30	0.100	0.2394	0.0239	672	16.056	1.338	150.8		RT
E-31	0.097	0.2619	0.0254	655	16.644	1.387	150.3		RT
E-32	0.097	0.2700	0.0262	824	21.60	1.80	146.4		RT
E-33	0.098	0.2610	0.0256	703	18.00	1.50	149.2		RT
E-35	0.172	0.2692	0.0463	671	31.08	2.59	140.2		RT
E-37	0.167	0.2162	0.0361	482	17.40	1.45	149.1		RT
E-38	0.168	0.2009	0.0338	422	14.268	1.189	152.3		RT
E-39	0.171	0.2563	0.0438	464	20.34	1.695	147.3		RT
E-40	0.100	0.2428	0.0243	494	12.00	1.000	154.3		RT
E-41	0.100	0.2469	0.0247	446	11.028	0.919	155.2		RT
E-42	0.100	0.2458	0.0246	488	12.00	1.000	154.3		RT
E-43	0.097	0.2654	0.0257	643	16.536	1.378	150.4		RT
E-44	0.098	0.2566	0.0251	625	15.696	1.308	151.1		RT
E-45	0.098	0.2350	0.0230	555	12.768	1.064	153.6		RT
E-46	0.166	0.2503	0.0415	512	21.24	1.77	146.6		RT
E-54	0.168	0.2261	0.0380	477	18.12	1.51	149.1		RT
E-58	0.174	0.2419	0.0421	687	28.92	2.41	141.6		RT

TABLE XXXV (cont.)

SPECIMEN NO.	WIDTH	DBN-cd	AREA	W/A	in.-lb	ft-lb	DEGREES	C-D	Test Temp.
E-70	0.106	0.2510	0.0266	650	17.28	1.44	149.8		RT
E-71	0.107	0.2508	0.0268	645	17.28	1.44	149.8		RT
E-72	0.106	0.2501	0.0265	570	15.096	1.258	151.6		RT
E-73	0.108	0.2605	0.0281	632	17.76	1.48	149.4		RT
E-74	0.108	0.2511	0.0271	642	17.40	1.45	149.7		RT
E-75	0.107	0.2445	0.0262	567	14.856	1.238	151.8		RT
E-76	0.105	0.2587	0.0272	525 *	14.268	1.189	152.3		RT
E-77	0.105	0.2510	0.0264	492 *	12.996	1.083	153.4		RT
E-78	0.105	0.2437	0.0256	539 *	13.80	1.150	152.7		RT
E-24	0.122	0.270	0.0465	534	24.84	2.07	144.1	0.0436	RT
E-34	0.174	0.276	0.0481	738	35.52	2.96	137.6	0.0364	RT
E-36	0.173	0.237	0.0410	442	18.12	1.51	149.1	0.0766	RT
E-50	0.172	0.258	0.0444	462	20.52	1.71	147.2	0.0557	RT
E-62	0.177	0.298	0.0528	827	43.68	3.64	133.0	0.0197	RT
E-66	0.177	0.255	0.0452	603	27.24	2.27	142.6	0.0502	RT
E-6	0.176	0.266	0.0468	712	33.48	2.79	138.8	0.0496	200°F
E-10	0.172	0.254	0.0437	640	27.96	2.33	142.2	0.0625	200°F
E-18	0.177	0.250	0.0443	631	27.96	2.33	142.2	0.0622	200°F
E-22	0.171	0.252	0.0431	710	30.60	2.55	140.5	0.0630	200°F
E-52	0.173	0.273	0.0472	719	33.96	2.83	138.5	0.0417	200°F

*Crack propagating in the chamber hoop-direction.

TABLE XXXV (cont.)

SPECIMEN NO	WIDTH	DBN - cd	AREA	W/A	in.-lb	ft-lb	DEGREES	C D	Test Temp.
E-56	0.174	0.257	0.0448	676	30.30	2.525	140.7	0.0598	200°F
E-64	0.177	0.258	0.0457	873	39.90	3.325	135.1	0.0541	200°F
E-48	0.166	0.2640	0.0438	815	35.70	2.975	137.5		200°F
E-60	0.176	0.2564	0.0451	990	44.64	3.72	132.5		200°F
E-68	0.175	0.2406	0.0421	862	36.30	3.025	137.1		200°F
E-7	0.174	0.267	0.0464	998	46.32	3.86	131.6	0.051	320°F
E-11	0.173	0.277	0.0479	902	43.20	3.60	133.3	0.041	320°F
E-14	0.179	0.254	0.0455	916	41.70	3.475	134.1	0.063	320°F
E-19	0.173	0.284	0.0491	1230	60.60	5.05	124.2	0.033	320°F
E-23	0.171	0.287	0.0491	1050	51.41	4.284	128.6	0.033	320°F
E-26	0.172	0.228	0.0392	784	30.72	2.56	140.4	0.090	320°F
E-57	0.173	0.274	0.0474	895	42.42	3.535	133.7	0.044	320°F
E-65	0.175	0.285	0.0499	1100	55.18	4.598	126.7	0.031	320°F
E-69	0.175	0.285	0.0499	908	45.30	3.775	132.1	0.031	320°F
E-49	0.169	0.2443	0.0413	1081	44.64	3.72	132.5		320°F
E-53	0.169	0.2458	0.0415	1005	41.70	3.475	134.1		320°F
E-61	0.176	0.2597	0.0457	1174	53.64	4.47	127.5		320°F

TABLE XXXVI

PRECRACK CHARPY IMPACT DATA - 6A1-4V TITANIUM

Minuteman Chamber S/N	Component	Specimen Location	Wall Thickness	Test Temperature, °F -40	RT	200	320
673095	Fwd Closure	2-in fwd of G1 weld	0.106		476 - 613 Avg(3) 529		
		G1 reinforced section	0.174	331 - 413 Avg(3) 376	484 - 650 Avg(3) 546	589 - 685 Avg(3) 635	908 - 1424 Avg(2) 1166
	Fwd Cyl	G1 reinforced section	0.175	225 - 393 Avg(3) 328	543 - 674 Avg(3) 603	708 - 769 Avg(3) 749	837 - 1030 Avg(3) 919
		2-in. aft of G1 weld	0.101		608 - 783 Avg(3) 684		
		2-in. fwd of G2 weld	0.101		452 - 677 Avg(3) 598		
		G2 reinforced section	0.178		541 - 696 Avg(3) 634		
	Aft Cyl	G2 reinforced section	0.174		352 - 444 Avg(3) 386		
		2-in. aft of G2 weld	0.102		334 - 401 Avg(4) 379		
		Ditto Hoop	0.102		280 - 325 Avg(3) 301		
		2-in. fwd of G3 weld	0.099		355 - 419 Avg(3) 389		
		G3 reinforced section	0.179	208 - 253 Avg(3) 336	352 - 392 Avg(3) 375	532 - 577 Avg(3) 559	752 - 1038 Avg(3) 850
	Aft Closure	G3 reinforced section	0.164	252 - 266 Avg(2) 259	351 - 400 Avg(3) 377	470 - 576 Avg(3) 538	761 - 765 Avg(2) 763
		2-in. aft of G3 weld	0.103		418 - 498 Avg(3) 458		

TABLE XXXVII

PRECRACK CHARPY IMPACT DATA
MINUTEMAN CHAMBER 673095 (44 IN. DIA)

Component	Specimen No.
Forward Dome	-
Forward Adapter	F1 - 15
Forward Cylinder	
At G1 Weld	F16 - 30
At G2 Weld	F31 - 36
Aft Cylinder	
At G2 Weld	F37 - 46
At G3 Weld	F47 - 61
Aft Flange	F62 - 76

TABLE XXXVII (cont.)

SPECIMEN NO.	WIDTH	DBN - cd	AREA	W/A	in.-lb	ft-lb	DEGREES	C D	Test Temp.
F-4	0.172	0.234	0.0403	413	16.63	1.387	150.3	0.082	-40°F
F-8	0.174	0.235	0.0410	383	15.70	1.308	151.1	0.080	-40°F
F-12	0.176	0.231	0.0407	331	13.46	1.121	153.0	0.086	-40°F
F-16	0.174	0.220	0.0383	225	8.63	0.720	157.6	0.091	-40°F
F-20	0.175	0.237	0.0415	393	16.30	1.358	150.6	0.073	-40°F
F-24	0.175	0.255	0.0447	365	16.30	1.358	150.6	0.062	-40°F
F-50	0.174	0.276	0.0486	247	12.00	1.000	154.3	0.040	-40°F
F-54	0.178	0.055	0.0098	253	2.48	0.207	165.3	0.262	-40°F
F-58	0.179	0.218	0.0390	208	8.10	0.675	158.2	0.095	-40°F
F-62	0.155	0.244	0.0379	266	10.10	0.841	156.1	0.070	-40°F
F-66	0.168	0.315	0.0530	313	1.66	0.138	166.6		-40°F
F-70	0.165	0.238	0.0393	252	9.89	0.824	156.3	0.077	-40°F
F-1	0.106	0.222	0.0235	497	14.04	1.170	152.5	0.095	RT
F-2	0.106	0.240	0.0254	613	15.58	1.298	151.2	0.075	RT
F-3	0.106	0.278	0.0295	476	14.04	1.170	152.5	0.038	RT
F-5	0.172	0.262	0.0451	484	21.84	1.82	146.2	0.051	RT
F-9	0.172	0.288	0.0496	650	32.22	2.685	139.5	0.024	RT
F-13	0.175	0.262	0.0459	504	23.15	1.93	145.3	0.054	RT
F-17	0.174	0.253	0.0440	543	23.88	1.99	144.8	0.064	RT
F-21	0.176	0.285	0.0502	674	33.84	2.82	138.6	0.034	RT

TABLE XXXVII (cont.)

SPECIMEN NO.	WIDTH	DBN-cd	AREA	W/A	in.-lb	ft-lb	DEGREES	C.D.	Test Temp.
F-25	0.176	0.268	0.0472	592	27.96	2.33	142.2	0.050	RT
F-28	0.101	0.259	0.0262	608	15.94	1.328	150.9	0.056	RT
F-29	0.101	0.276	0.0279	662	18.48	1.54	148.8	0.039	RT
F-30	0.101	0.279	0.0282	783	22.08	1.84	146.0	0.037	RT
F-31	0.099	0.246	0.0244	452	11.03	0.919	155.2	0.069	RT
F-32	0.101	0.289	0.0292	666	19.44	1.62	148.1	0.026	RT
F-33	0.102	0.224	0.0218	677	14.75	1.229	151.9	0.090	RT
F-34	0.178	0.254	0.0452	666	30.12	2.51	140.8	0.064	RT
F-35	0.178	0.229	0.0408	541	22.08	1.84	146.0	0.089	RT
F-36	0.178	0.288	0.0513	696	35.70	2.975	137.5	0.030	RT
F-37	0.172	0.263	0.0453	352	15.94	1.328	150.9	0.052	RT
F-38	0.176	0.278	0.0489	444	21.72	1.81	146.3	0.041	RT
F-39	0.174	0.266	0.0463	362	16.78	1.398	150.2	0.054	RT
F-40	0.103	0.271	0.0280	401	11.23	0.936	155.0	0.042	RT
F-41	0.101	0.265	0.0268	384	10.30	0.858	155.9	0.051	RT
F-42	0.101	0.256	0.0248	334	8.28	0.690	158.0	0.059	RT
F-43	0.097	0.257	0.0250	396	9.89	0.824	156.3	0.058	RT
F-44	0.102	0.254	0.0260	299 *	7.78	0.648	158.6	0.061	RT
F-45	0.102	0.235	0.0240	280 *	6.71	0.559	159.8	0.082	RT
F-46	0.102	0.244	0.0249	325 *	8.10	0.675	158.2	0.710	RT
F-47	0.099	0.253	0.0251	355	8.92	0.743	157.3	0.0610	RT

*Crack propagating in the chamber hoop-direction.

TABLE XXXVII (cont.)

SPECIMEN NO.	WIDTH	DBN-cd	AREA	W/A	in.-lb	ft-lb	DEGREES	C D	Test Temp.
F-48	0.099	0.284	0.0281	419	11.77	0.981	154.5	0.033	RT
F-49	0.098	0.278	0.0273	392	10.70	0.892	155.5	0.0346	RT
F-51	0.176	0.249	0.0439	352	15.46	1.288	151.3	0.0634	RT
F-55	0.179	0.249	0.0446	382	17.02	1.418	150.0	0.050	RT
F-59	0.179	0.265	0.0475	392	18.60	1.55	148.7	0.0513	RT
F-63	0.156	0.260	0.0406	351	14.27	1.189	152.3	0.057	RT
F-67	0.171	0.261	0.0447	400	17.8	1.49	149.3	0.0519	RT
F-71	0.165	0.248	0.0409	381	15.58	1.298	151.2	0.070	RT
F-74	0.102	0.265	0.0270	498	13.45	1.121	153.0	0.0518	RT
F-75	0.103	0.256	0.0264	459	12.11	1.009	154.2	0.0592	RT
F-76	0.104	0.234	0.0244	418	10.19	0.849	156.0	0.0795	RT
F-6	0.174	0.256	0.0445	685	30.48	2.54	140.6	0.0632	200°F
F-10	0.170	0.228	0.0388	589	22.86	1.905	145.5	0.0905	200°F
F-14	0.176	0.271	0.0477	631	30.12	2.51	140.8	0.0504	200°F
F-18	0.176	0.237	0.0417	708	29.52	2.46	141.2	0.0817	200°F
F-22	0.176	0.259	0.0457	769	35.16	2.93	137.8	0.0589	200°F
F-26	0.176	0.280	0.0493	769	37.92	3.16	136.2	0.0374	200°F
F-52	0.177	0.261	0.0462	532	24.60	2.05	144.3	0.0579	200°F
F-56	0.178	0.276	0.0492	568	27.96	2.33	142.2	0.0399	200°F
F-60	0.179	0.246	0.0441	577	25.44	2.12	143.8	0.0688	200°F

TABLE XXXVII (cont.)

SPECIMEN NO.	WIDTH	DBN-cd	AREA	W/A	in.-lb	ft-lb	DEGREES	C D.	Test Temp.
F-64	0.158	0.224	0.0354	470	16.64	1.387	150.3	0.0933	200°F
F-68	0.169	0.268	0.0453	576	26.10	2.175	143.3	0.0475	200°F
F-72	0.167	0.258	0.0431	568	24.48	2.04	144.4	0.0632	200°F
F-7	0.173	0.260	0.0450	1424	51.41	4.284	128.6	0.060	320°F
F-11	0.172	0.288	0.0495	908	44.94	3.745	132.3	0.028	320°F
F-15	0.175	0.113	0.0198	606	12.00	1.000	154.3	0.200	320°F
F-19	0.176	0.197	0.0347	837	29.04	2.42	141.5	0.121	320°F
F-23	0.177	0.262	0.0464	891	41.34	3.445	134.3	0.056	320°F
F-27	0.178	0.268	0.0477	1030	49.14	4.095	130.1	0.049	320°F
F-53	0.178	0.279	0.0497	752	37.38	3.115	136.5	0.039	320°F
F-57	0.178	0.274	0.0488	759	37.02	3.085	136.7	0.047	320°F
F-61	0.178	0.264	0.0470	1038	48.78	4.065	130.3	0.052	320°F
F-65	0.164	0.086	0.0141	445	6.28	0.523	160.3	0.232	320°F
F-69	0.166	0.261	0.0433	765	33.12	2.76	139.0	0.060	320°F
F-73	0.167	0.277	0.0462	761	35.16	2.93	137.8	0.039	320°F

TABLE XXXVIII

PRECRACK CHARPY IMPACT DATA - 6A1-4V TITANIUM

Minuteman Chamber S/N	Component	Specimen Location	Wall Thickness	Test Temperature, °F -40	RT	200	320
673122	Fwd Closure	2-in. fwd of G1 weld	0.102		532 - 631 Avg(3) 573		
		G1 reinforced section	0.177	280 - 452 Avg(3) 375	656 - 693 Avg(3) 679	753 - 1100 Avg(3) 964	1250 - 1340 Avg(3) 1293
	Fwd Cyl	G1 reinforced section	0.171		334 - 578 Avg(3) 439		
		2-in. Aft of G1 weld	0.102		396 - 412 Avg(3) 406		
		2-in. fwd of G2 weld	0.100		498 - 588 Avg(3) 549		
		G2 reinforced section	0.170	352 - 359 Avg(3) 355	408 - 554 Avg(3) 484	289 - 875 Avg(3) 638	1080 - 1330 Avg(3) 1167
	Aft Cyl	G2 reinforced section	0.171	378 - 464 Avg(3) 409	593 - 634 Avg(3) 619	719 - 865 Avg(3) 815	1130 - 1300 Avg(3) 1200
		2-in. aft of G2 weld	0.097		550 - 620 Avg(3) 585		
		2-in. fwd of G3 weld	0.094		441 - 548 Avg(3) 484		
		G3 reinforced section	0.170		387 - 631 Avg(3) 507		
	Aft Closure	G3 reinforced section	0.179	169 - 468 Avg(3) 329	601 - 640 Avg(3) 624	770 - 1060 Avg(3) 874	1140 - 1200 Avg(3) 1163
		2-in. aft of G3 weld	0.106		487 - 519 Avg(3) 503		

TABLE XXXIX

PRECRACK CHARPY IMPACT DATA
MINUTEMAN CHAMBER 673122 (44-IN. DIA)

Component	Specimen No.
Forward Dome	-
Forward Adaptor	G1 - 15
Forward Cylinder	
At G1 Weld	G16 - 21
At G2 Weld	G22 - 36
Aft Cylinder	
At G2 Weld	G37 - 51
At G3 Weld	G52 - 57
Aft Flange	G58 - 72

TABLE XXXIX (cont.)

SPECIMEN NO.	WIDTH	DBN-cd	AREA	W/A	in.-lb	ft-lb	DEGREES	C D	Test Temp.
G-4	0.177	0.218	0.0386	280	10.81	0.901	155.4	0.095	-40°F
G-8	0.178	0.266	0.0474	392	18.60	1.55	148.7	0.049	-40°F
G-12	0.180	0.261	0.0470	452	21.24	1.77	146.6	0.053	-40°F
G-25	0.173	0.276	0.0478	354	16.90	1.408	150.1	0.040	-40°F
G-29	0.170	0.280	0.0477	352	16.78	1.398	150.2	0.035	-40°F
G-33	0.174	0.282	0.0491	359	17.64	1.47	149.5	0.034	-40°F
G-37	0.174	0.272	0.0473	378	17.88	1.49	149.3	0.043	-40°F
G-41	0.171	0.260	0.0445	464	20.64	1.72	147.1	0.054	-40°F
G-45	0.171	0.250	0.0428	386	16.54	1.378	150.4	0.064	-40°F
G-58	0.176	0.275	0.0490	169	8.28	0.690	158.0	0.042	-40°F
G-62	0.178	0.278	0.0495	468	23.16	1.93	145.3	0.036	-40°F
G-66	0.178	0.269	0.0480	350	16.78	1.398	150.2	0.048	-40°F
G-1	0.102	0.230	0.0235	557	13.10	1.092	153.3	0.0840	RT
G-2	0.102	0.289	0.0295	532	15.70	1.308	151.1	0.0265	RT
G-3	0.103	0.282	0.0291	631	18.36	1.53	148.9	0.0307	RT
G-5	0.176	0.252	0.0443	693	30.72	2.56	142.7	0.0594	RT
G-9	0.176	0.272	0.0479	656	31.44	2.62	140.0	0.0437	RT
G-13	0.178	0.254	0.0452	688	31.08	2.59	140.2	0.0622	RT
G-16	0.172	0.243	0.0419	578	24.24	2.02	144.6	0.0733	RT
G-17	0.171	0.260	0.0445	404	18.00	1.50	149.2	0.0551	RT

TABLE XXXIX (cont.)

SPECIMEN NO	WIDTH	DBN-cd	AREA	W/A	in.-lb	ft-lb	DEGREES	C.D.	Test Temp.
G-18	0.170	0.263	0.0448	334	14.98	1.248	151.7	0.0523	RT
G-19	0.101	0.271	0.0274	410	11.23	0.936	155.0	0.0439	RT
G-20	0.103	0.277	0.0286	396	11.34	0.945	154.9	0.0369	RT
G-21	0.102	0.265	0.0270	412	11.12	0.927	155.1	0.0504	RT
G-22	0.100	0.278	0.0278	498	16.64	1.387	150.3	0.0374	RT
G-23	0.100	0.288	0.0288	562	16.18	1.348	150.7	0.0277	RT
G-24	0.101	0.280	0.0283	588	16.64	1.387	150.3	0.0342	RT
G-26	0.171	0.256	0.0438	408	17.88	1.49	149.3	0.0582	RT
G-30	0.170	0.274	0.0466	554	25.80	2.15	143.5	0.0401	RT
G-34	0.170	0.277	0.0472	491	23.16	1.93	145.3	0.0402	RT
G-38	0.172	0.273	0.0470	631	29.64	2.47	141.1	0.0461	RT
G-42	0.171	0.269	0.0460	634	29.16	2.43	141.4	0.0457	RT
G-46	0.169	0.265	0.0449	593	26.64	2.22	143.0	0.0494	RT
G-49	0.097	0.278	0.0270	550	14.86	1.238	151.8	0.0381	RT
G-50	0.097	0.283	0.0275	620	17.04	1.42	149.9	0.0323	RT
G-51	0.097	0.282	0.0274	586	16.06	1.338	150.8	0.0372	RT
G-52	0.093	0.271	0.0252	441	11.12	0.927	155.1	0.0442	RT
G-53	0.094	0.272	0.0256	464	11.88	0.990	154.4	0.0433	RT
G-54	0.095	0.263	0.0250	548	13.69	1.141	152.8	0.0517	RT
G-55	0.166	0.273	0.0453	387	17.52	1.46	149.6	0.0426	RT
G-56	0.170	0.253	0.0430	502	21.60	1.80	146.4	0.0626	RT

TABLE XXXIX (cont.)

SPECIMEN NO.	WIDTH	DBN - cd	AREA	W/A	in.-lb	ft-lb	DEGREES	C D.	Test Temp.
G-57	0.173	0.277	0.0480	631	30.30	2.525	140.7	0.0484	RT
G-59	0.180	0.270	0.0486	640	31.08	2.59	140.2	0.0379	RT
G-63	0.179	0.280	0.0502	631	31.68	2.64	139.8	0.0350	RT
G-67	0.178	0.271	0.0483	601	29.04	2.42	141.5	0.0444	RT
G-70	0.104	0.281	0.0293	487	14.27	1.189	152.3	0.0337	RT
G-71	0.107	0.285	0.0305	519	15.82	1.318	151.0	0.0314	RT
G-72	0.107	0.280	0.0300	503	15.10	1.258	151.6	0.0359	RT
G-6	0.178	0.258	0.0460	753	34.62	2.885	138.1	0.0570	200°F
G-10	0.178	0.270	0.0481	1040	50.26	4.188	129.2	0.0448	200°F
G-14	0.179	0.281	0.0503	1100	55.37	4.614	126.6	0.0352	200°F
G-27	0.172	0.261	0.0449	750	33.66	2.805	138.7	0.0574	200°F
G-31	0.171	0.260	0.0445	289	12.88	1.073	153.5	0.0553	200°F
G-35	0.172	0.290	0.0499	875	43.68	3.64	133.0	0.0268	200°F
G-39	0.173	0.271	0.0469	862	40.44	3.37	134.8	0.0447	200°F
G-43	0.175	0.248	0.0434	865	37.56	3.13	136.4	0.0724	200°F
G-47	0.174	0.245	0.0427	719	30.72	2.56	140.4	0.0720	200°F
G-60	0.179	0.276	0.0495	770	38.10	3.175	136.1	0.0392	200°F
G-64	0.179	0.280	0.0502	791	39.72	3.31	135.2	0.0358	200°F
G-68	0.179	0.279	0.0500	1060	52.99	4.416	127.8	0.0375	200°F

TABLE XXXIX (cont.)

SPECIMEN NO	WIDTH	DBN - cd	AREA	W/A	in.-lb	ft-lb	DEGREES	C.D.	Test Temp.
G-7	0.178	0.274	0.0488	1250	60.84	5.07	124.1	0.044	320°F
G-11	0.180	0.261	0.0470	1340	63.12	5.26	123.1	0.056	320°F
G-15	0.179	0.292	0.0523	1290	67.44	5.62	121.3	0.027	320°F
G-28	0.172	0.284	0.0488	1080	52.99	4.416	127.8	0.035	320°F
G-32	0.170	0.267	0.0454	1090	49.56	4.13	129.7	0.050	320°F
G-36	0.171	0.288	0.0492	1330	65.28	5.44	122.2	0.030	320°F
G-40	0.173	0.273	0.0472	1300	61.51	5.126	123.8	0.043	320°F
G-44	0.173	0.272	0.0465	1170	54.41	4.534	127.1	0.046	320°F
G-48	0.172	0.273	0.0470	1130	53.18	4.432	127.7	0.042	320°F
G-61	0.180	0.287	0.0517	1140	59.23	4.936	124.8	0.029	320°F
G-65	0.179	0.281	0.0503	1150	57.94	4.828	125.4	0.034	320°F
G-69	0.178	0.241	0.0429	1200	51.60	4.30	128.5	0.075	320°F

TABLE XL

PRECRACK CHARPY IMPACT DATA - 6A1-4V TITANIUM

Minuteman Chamber S/N	Component	Specimen Location	Wall Thickness	Test Temperature, °F -40	RT	200	320
674514	Fwd Closure	2-in. fwd of G1 weld	0.106		419 - 451 Avg(3) 436		
		G1 reinforced section	0.175	315 - 354 Avg(3) 329	479 - 480 Avg(2) 480	510 - 634 Avg(4) 549	725 - 927 Avg(3) 857
	Fwd Cyl	G1 reinforced section	0.175	206 - 241 Avg(3) 223	268 - 383 Avg(3) 309	344 - 451 Avg(3) 392	606 - 784 Avg(3) 677
		2-in. aft of G1 weld	0.100		426 - 496 Avg(3) 467		
	Aft Cyl	20-in. aft of G2 weld	0.098		295 - 324 Avg(3) 306		
		Ditto Hoop	0.098		274 - 320 Avg(3) 304		
		2-in. fwd of G3 weld	0.100		302 - 362 Avg(3) 340		
		G3 reinforced section	0.170	244 - 381 Avg(4) 316	274 - 524 Avg(5) 376	390 - 657 Avg(4) 562	906 - 989 Avg(2) 948
	Aft Closure	G3 reinforced section		348 - 367 Avg(3) 354	534 - 702 Avg(3) 591	617 - 811 Avg(4) 714	836 - 983 Avg(3) 907
		2-in. aft of G3 weld	0.100		317 - 531 Avg(3) 448		

TABLE XLI

PRECRACK CHARPY IMPACT DATA
MINUTEMAN CHAMBER 674514 (44-IN. DIA)

Component	Specimen No.
Forward Dome	-
Forward Adaptor	H1 - 15 H70 - 74
Forward Cylinder	
At G1 Weld	H16 - 30 H75 - 83
At G2 Weld	-
Aft Cylinder	
At G2 Weld	H61 - 66*
At G3 Weld	H84 - 89 H46 - 60
Aft Flange	H31 - 45 H90 - 95

*Specimens taken at intersection of primary fracture (axial) and secondary fracture (hoop) in aft cylinder, approx. midway between G2 and G3 welds.

TABLE XLI (cont.)

SPECIMEN NO.	WIDTH	DBN - cd	AREA	W/A	in.-lb	ft-lb	DEGREES	C D	Test Temp.
H-75	0.176 0.162	0.253	0.0428	206	8.81	0.734	157.4	0.065	-40°F
H-79	0.177 0.158	0.265	0.0444	241	10.70	0.892	155.5	0.053	-40°F
H-83	0.177 0.157	0.266	0.0444	221	9.80	0.817	156.4	0.052	-40°F
H-84	0.174 0.163	0.260	0.0438	244	10.70	0.892	155.5	0.058	-40°F
H-90	0.177 0.159	0.275	0.0462	348	16.06	1.338	150.8	0.043	-40°F
H-4	0.177	0.2441	0.0432	317	13.692	1.141	152.8		-40°F
H-9	0.174	0.2144	0.0373	354	13.212	1.101	153.2		-40°F
H-13	0.175	0.2401	0.0420	315	13.212	1.101	153.2		-40°F
H-19	0.176	0.2780	0.0489	366	17.88	1.49	149.3		-40°F
H-24	0.177	0.2889	0.0511	321	16.416	1.368	150.5		-40°F
H-39	0.174	0.2403	0.0418	367	15.336	1.278	151.4		-40°F
H-43	0.175	0.2204	0.0386	348	13.452	1.121	153.0		-40°F
H-46	0.171	0.2610	0.0446	323	14.388	1.199	152.2		-40°F
H-50	0.174	0.2542	0.0442	318	14.04	1.170	152.5		-40°F
H-54	0.174	0.2602	0.0453	381	17.28	1.44	149.8		-40°F
H-1	0.107	0.2531	0.0271	451	12.228	1.019	154.1		RT
H-2	0.106	0.2293	0.0243	419	10.188	0.849	156.0		RT
H-3	0.106	0.2442	0.0259	438	11.34	0.945	154.9		RT
H-6	0.176	0.2431	0.0428	479	20.52	1.71	147.2		RT
H-10	0.174	0.2386	0.0415	480	19.92	1.66	147.6		RT

TABLE XLI (cont.)

SPECIMEN NO.	WIDTH	DBN-cd	AREA	W/A	in.-lb	ft-lb	DEGREES	C.D.	Test Temp.
H-21	0.176	0.2272	0.0400	465	18.60	1.55	148.7		RT
H-25	0.174	0.2466	0.0429	383	16.416	1.368	150.5		RT
H-28	0.100	0.2440	0.0244	496	12.108	1.009	154.2		RT
H-29	0.100	0.2590	0.0259	426	11.028	0.919	155.2		RT
H-30	0.100	0.2560	0.0256	478	12.228	1.019	154.1		RT
H-31	0.098	0.2582	0.0253	317	8.016	0.668	158.3		RT
H-32	0.101	0.2552	0.0258	531	13.692	1.141	152.8		RT
H-33	0.104	0.2591	0.0269	496	13.332	1.111	153.1		RT
H-40	0.172	0.2390	0.0411	534	21.96	1.83	146.1		RT
H-44	0.173	0.2280	0.0394	536	21.12	1.76	146.7		RT
H-47	0.168	0.2384	0.0401	296	11.88	0.990	154.4		RT
H-51	0.173	0.2541	0.0440	524	23.04	1.92	145.4		RT
H-55	0.173	0.2569	0.0444	492	21.84	1.82	146.2		RT
H-58	0.100	0.2084	0.0208	362	7.524	0.627	158.9		RT
H-59	0.100	0.2368	0.0237	302	7.152	0.596	159.3		RT
H-60	0.100	0.2228	0.0223	356	7.932	0.661	158.4		RT
H-61	0.098	0.2109	0.0207	324	6.708	0.559	159.8		RT
H-62	0.098	0.1641	0.0161	295	4.752	0.396	162.2		RT
H-63	0.097	0.2686	0.0261	298	7.776	0.648	158.6		RT
H-64	0.098	0.2062	0.0202	320 *	6.468	0.539	160.1		RT
H-65	0.098	0.2564	0.0251	319 *	8.016	0.668	158.3		RT

*Crack propagating in the chamber hoop-direction.

TABLE XLI (cont.)

SPECIMEN NO.	WIDTH	DBN-cd	AREA	W/A	in.-lb	ft-lb	DEGREES	C D.	Test Temp.
H-66	0.097	0.2486	0.0241	274 *	6.612	0.551	159.9		RT
H-16	0.177								
H-17	0.177								
H-76	0.201 0.193	0.275	0.0542	268	14.50	1.208	152.1	0.043	RT
H-80	0.202 0.184	0.252	0.0486	277	13.45	1.121	153.0	0.065	RT
H-85	0.199 0.189	0.262	0.0508	295	14.98	1.248	151.7	0.057	RT
H-88	0.199 0.186	0.217	0.0418	274	11.44	0.953	154.8	0.102	RT
H-91	0.179 0.165	0.273	0.0470	702	33.00	2.75	139.1	0.047	RT
H-70	0.177 0.167	0.249	0.0428	510	21.84	1.82	146.2	0.070	200°F
H-72	0.176 0.168	0.245	0.0421	516	21.72	1.81	146.3	0.075	200°F
H-77	0.176 0.163	0.123	0.0208	344	7.152	0.596	159.3	0.195	200°F
H-81	0.177 0.163	0.232	0.0394	383	15.10	1.258	151.6	0.088	200°F
H-86	0.174 0.164	0.227	0.0384	390	14.98	1.248	151.7	0.092	200°F
H-92	0.179 0.166	0.248	0.0428	642	27.48	2.29	142.5	0.071	200°F
H-94	0.178 0.168	0.268	0.0464	784	36.36	3.03	137.1	0.052	200°F
H-7	0.175	0.2246	0.0393	721	28.32	2.36	141.9		200°F
H-11	0.174	0.2216	0.0386	634	24.48	2.04	144.4		200°F
H-14	0.174	0.2384	0.0415	536	22.26	1.855	145.9		200°F
H-22	0.174	0.2773	0.0483	701	33.84	2.82	138.6		200°F
H-26	0.176	0.2194	0.0386	451	17.40	1.45	149.7		200°F

TABLE XLI (cont.)

SPECIMEN NO.	WIDTH	DBN - cd	AREA	W/A	in. - lb	ft - lb	DEGREES	C.D.	Test Temp.
H-41	0.174	0.2454	0.0427	811	34.62	2.885	138.1		200°F
H-45	0.174	0.2567	0.0447	617	27.60	2.30	142.4		200°F
H-48	0.171	0.2693	0.0461	657	30.30	2.525	140.7		200°F
H-52	0.173	0.2379	0.0412	555	22.86	1.905	145.5		200°F
H-56	0.173	0.2669	0.0462	644	29.76	2.48	141.0		200°F
H-8	0.174	0.2289	0.0398	986	39.24	3.27	135.4		320°F
H-12	0.175	0.2411	0.0422	894	37.74	3.145	136.3		320°F
H-15	0.176	0.2387	0.0420	709	29.76	2.48	141.0		320°F
H-23	0.175	0.2753	0.0482	957	46.14	3.845	131.7		320°F
H-27	0.173	0.2358	0.0408	606	24.72	2.06	144.2		320°F
H-42	0.173	0.2381	0.0412	836	34.44	2.87	138.2		320°F
H-49	0.172	0.2650	0.0456	989	45.12	3.76	132.2		320°F
H-53	0.173	0.2659	0.0460	1424	65.52	5.46	122.1		320°F
H-57	0.172	0.2083	0.0358	560	20.04	1.67	147.5	0.186	320°F
H-71	0.177 0.164	0.225	0.0384	725	27.84	2.32	142.3	0.093	320°F
H-73	0.176 0.165	0.269	0.0459	918	42.12	3.51	133.9	0.050	320°F
H-74	0.176 0.164	0.245	0.0417	927	38.64	3.22	135.9	0.072	320°F
H-78	0.177 0.158	0.267	0.0447	784	35.04	2.92	137.9	0.053	320°F
H-82	0.178 0.158	0.238	0.0400	642	25.68	2.14	143.6	0.080	320°F
H-87	0.175 0.159	0.261	0.0436	906	39.48	3.29	135.3	0.058	320°F

TABLE XLI (cont.)

SPECIMEN NO.	WIDTH	DBN - cd	AREA	W/A	in.-lb	ft-lb	DEGREES	C D	Test Temp.
H-89	0.173 0.156	0.193	0.0317	514	16.30	1.358	150.6	0.126	320°F
H-93	0.180 0.165	0.266	0.0459	983	45.12	3.76	132.2	0.053	320°F
H-95	0.179 0.164	0.262	0.0449	901	40.44	3.37	134.8	0.057	320°F

TABLE XLII

PRECRACK CHARPY IMPACT DATA - 6A1-4V TITANIUM

Minuteman Chamber S/N	Component	Specimen Location	Wall Thickness	Test Temperature, °F -40	RT	200	320
2192109	Fwd Skirt		0.113		481 - 508 Avg(3) 498		
	Fwd Closure	2-in. fwd of G1 weld	0.113		413 - 493 Avg(3) 461		
		G1 reinforced section	0.185	269 - 349 Avg(3) 319	422 - 532 Avg(3) 474	499 - 595 Avg(3) 551	887 - 1019 Avg(3) 947
	Fwd Cyl	G1 reinforced section	0.185	220 - 315 Avg(3) 279	332 - 400 Avg(2) 366	415 - 450 Avg(3) 438	691 - 768 Avg(3) 725
		2-in. aft of G1 weld	0.107		289 - 387 Avg(3) 331		
		Near hoop-fracture junction	0.105		242 - 276 Avg(3) 263		
		Ditto, Hoop direction	0.106		340 - 381 Avg(3) 365		

TABLE XLIII

PRECRACK CHARPY IMPACT DATA
MINUTEMAN CHAMBER 2192109 (52-IN.DIA)

Component	Specimen No.
Forward Skirt	K1 - 3
Forward Closure	K4 - 18
Forward Cylinder	
At G1 Weld	K19 - 33
At G2 Weld	K34 - 39*
Aft Cylinder	
At G2 Weld	-
At G3 Weld	-
Aft Closure	-
Aft Skirt	-

*Specimens located at intersection of primary axial fracture and secondary hoop fracture.

TABLE XLIII (cont.)

SPECIMEN NO.	WIDTH	DBN-cd	AREA	W/A	in.-lb	ft-lb	DEGREES	C.D	Test Temp.
K-7	0.185 0.170	0.287	0.0509	269	13.69	1.141	152.8	0.031	-40°F
K-11	0.190 0.177	0.270	0.0495	349	17.28	1.44	149.8	0.050	-40°F
K-15	0.191 0.179	0.270	0.0500	340	17.02	1.418	150.0	0.048	-40°F
K-19	0.189 0.181	0.279	0.0516	220	11.34	0.945	154.9	0.029	-40°F
K-23	0.193 0.187	0.274	0.0521	315	16.42	1.368	150.5	0.045	-40°F
K-27	0.193 0.185	0.287	0.0542	301	16.30	1.358	150.6	0.032	-40°F
K-1	0.112	0.272	0.0304	481	14.62	1.218	152.0	0.046	RT
K-2	0.113	0.265	0.0299	505	15.10	1.258	151.6	0.054	RT
K-3	0.113	0.280	0.0316	508	16.06	1.338	150.8	0.040	RT
K-4	0.113	0.275	0.0311	493	15.34	1.278	151.4	0.046	RT
K-5	0.113	0.262	0.0296	413	12.23	1.019	154.1	0.057	RT
K-6	0.113	0.262	0.0296	478	14.15	1.179	152.4	0.054	RT
K-8	0.188 0.176	0.284	0.0517	532	27.48	2.29	142.5	0.032	RT
K-12	0.190 0.180	0.255	0.0472	422	19.92	1.66	147.6	0.064	RT
K-16	0.191 0.181	0.261	0.0485	468	22.68	1.89	145.6	0.060	RT
K-20	0.190 0.183	0.155	0.0289	217	6.28	0.523	160.3	0.164	RT
K-24	0.188	0.258	0.0486	400	19.44	1.62	148.1	0.060	RT
K-28	0.192 0.184	0.266	0.0501	332	16.64	1.387	150.3	0.052	RT
K-31	0.105	0.267	0.0280	289	8.10	0.675	158.2	0.053	RT
K-32	0.107	0.266	0.0285	387	11.03	0.919	155.2	0.052	RT

TABLE XLIII (cont.)

SPECIMEN NO.	WIDTH	DBN-cd	AREA	W/A	in.-lb	ft-lb	DEGREES	C D	Test Temp.
K-33	0.108	0.258	0.0279	316	8.81	0.734	157.4	0.061	RT
K-34	0.104	0.231	0.0240	242	5.80	0.483	160.9	0.088	RT
K-35	0.105	0.265	0.0278	276	7.68	0.640	158.7	0.054	RT
K-36	0.105	0.270	0.0284	270	7.68	0.640	158.7	0.049	RT
K-37	0.106	0.279	0.0296	373 *	11.03	0.919	155.2	0.040	RT
K-38	0.106	0.268	0.0284	381 *	10.81	0.901	155.4	0.052	RT
K-39	0.106	0.277	0.0294	340 *	10.00	0.833	156.2	0.040	RT
K-9	0.189 0.180	0.257	0.0474	595	28.20	2.35	142.0	0.062	200°F
K-13	0.190 0.182	0.225	0.0419	558	23.40	1.95	145.1	0.095	200°F
K-17	0.191 0.182	0.249	0.0464	499	23.16	1.93	145.3	0.071	200°F
K-21	0.192 0.184	0.230	0.0432	450	19.44	1.62	148.1	0.089	200°F
K-25	0.194 0.187	0.225	0.0429	448	19.20	1.60	148.3	0.094	200°F
K-29	0.192 0.186	0.203	0.0384	415	15.94	1.328	150.9	0.115	200°F
K-10	0.190 0.180	0.277	0.0512	1019	52.2	4.35	128.2	0.041	320°F
K-14	0.191 0.176	0.252	0.0462	887	41.0	3.42	134.5	0.064	320°F
K-18	0.191 0.179	0.261	0.0483	934	45.1	3.76	132.2	0.058	320°F
K-22	0.193 0.180	0.231	0.0431	768	33.1	2.76	139.0	0.088	320°F
K-26	0.193 0.188	0.238	0.0453	715	32.4	2.70	139.4	0.079	320°F
K-30	0.193 0.182	0.240	0.0450	691	31.1	2.59	140.2	0.077	320°F

*Crack propagating in the chamber hoop-direction.

APPENDIX II

TRANSITION CURVES
(W/A vs TEMPERATURE)

6Al-4V Titanium 160 ksi Yield Strength
39 ksi-in.$^{1/2}$ Plane-Strain Fracture Toughness

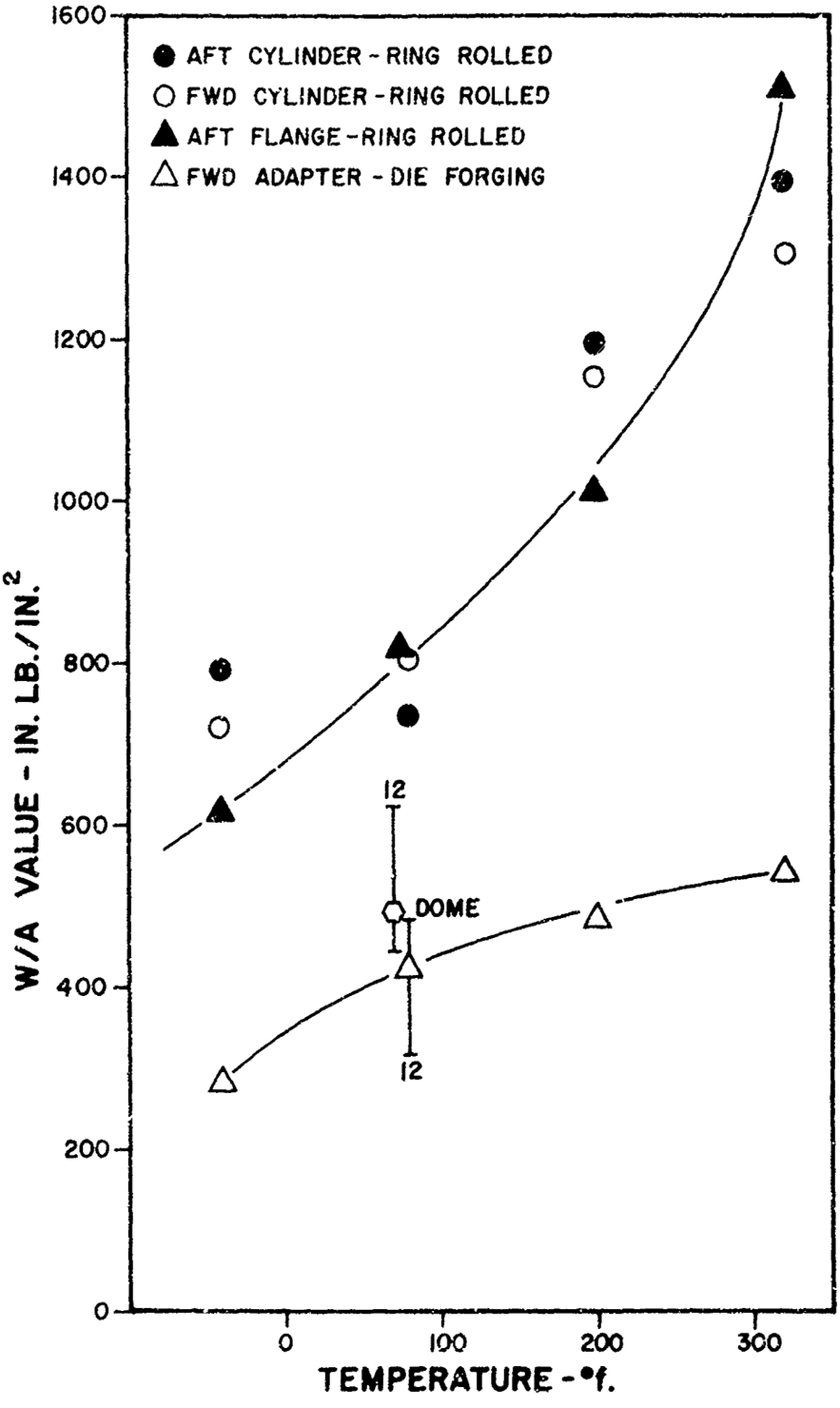

Figure 25. Chamber R26

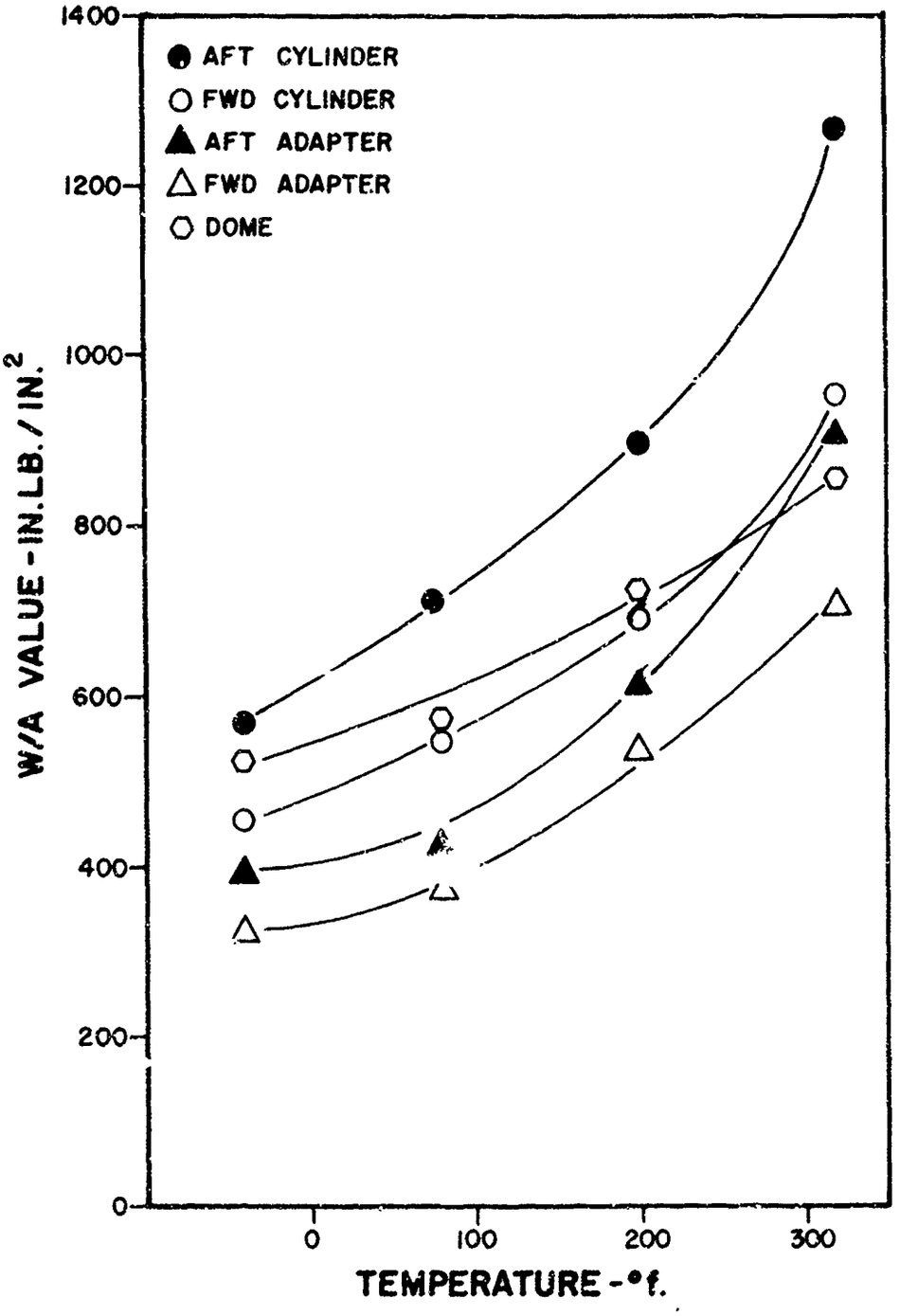

Figure 26. Chamber R41

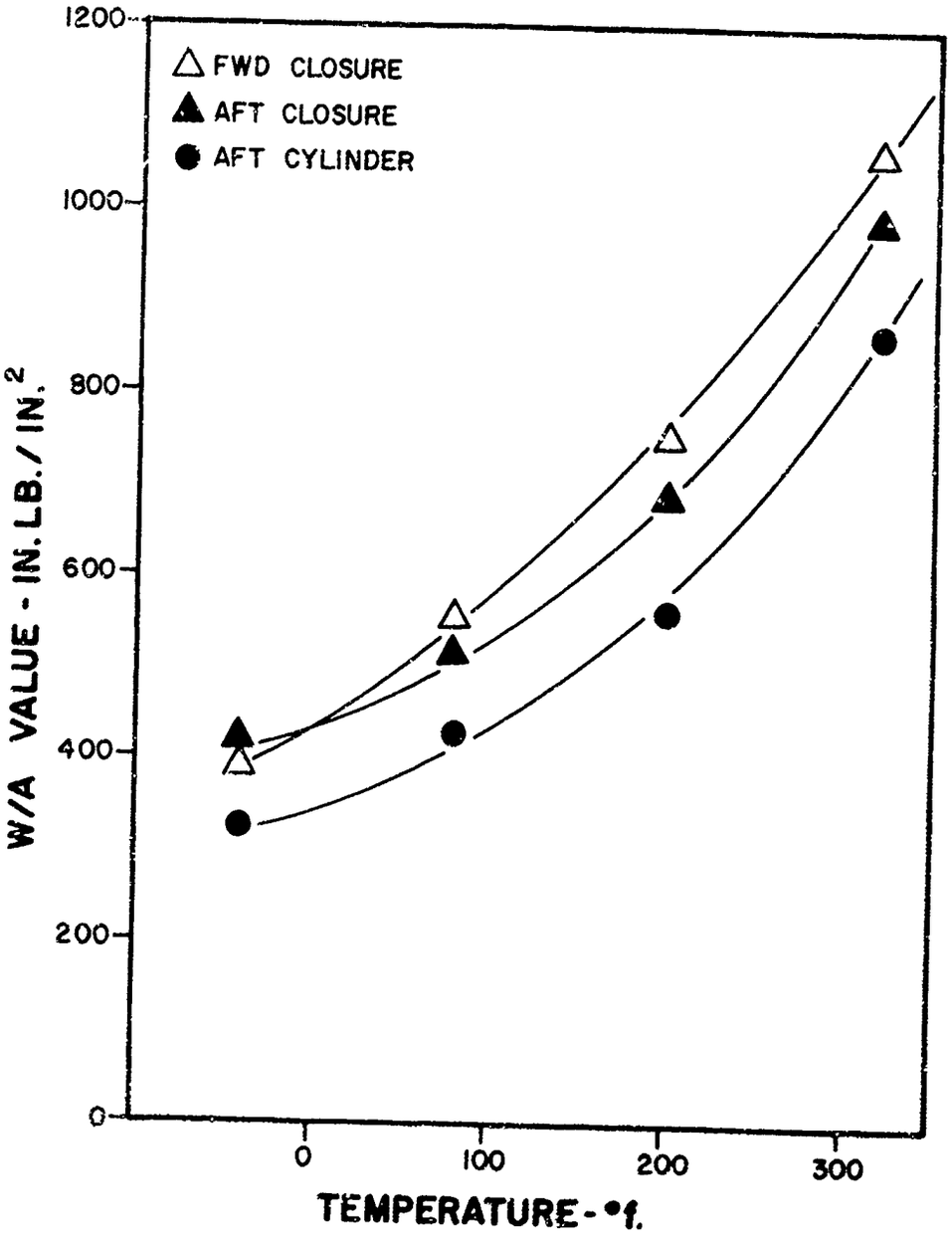

Figure 27. Chamber BL26

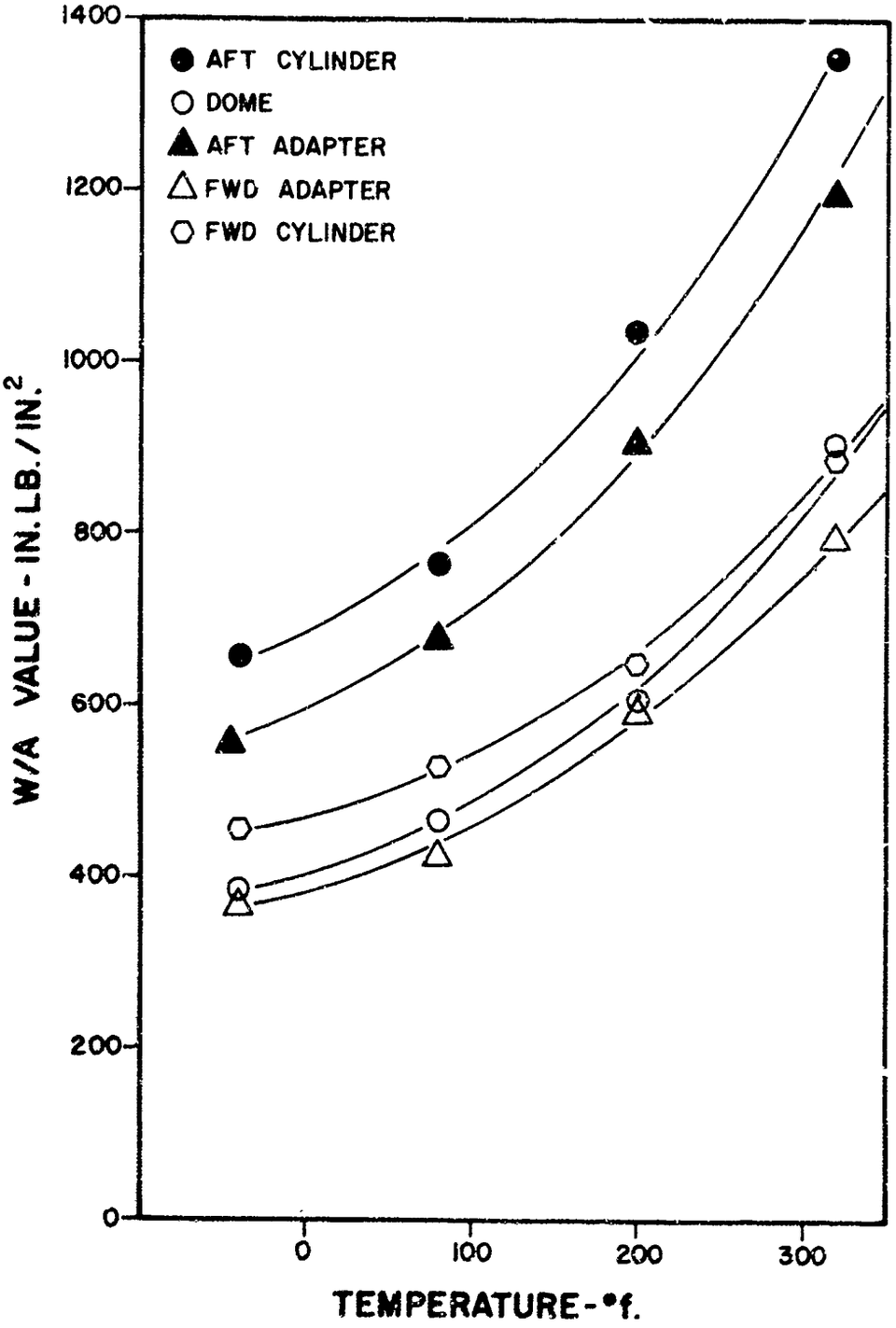

Figure 28. Chamber 2191456

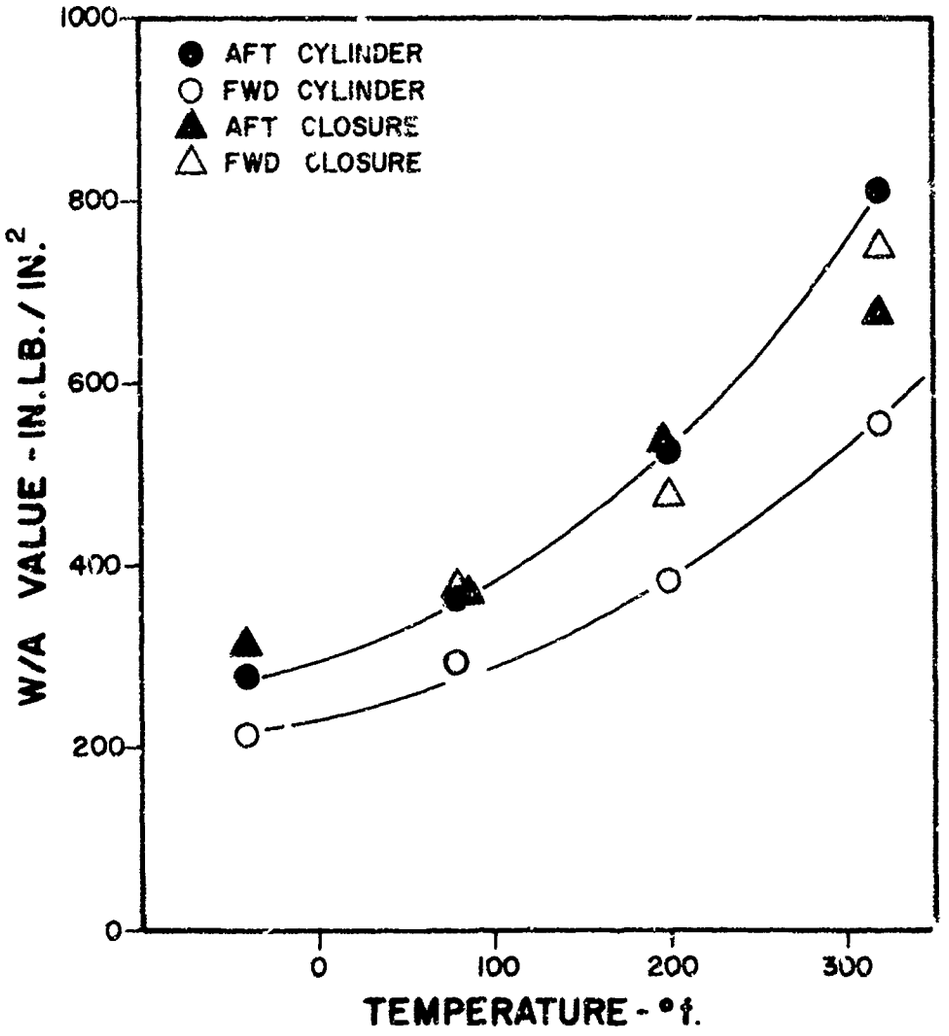

Figure 29. Chamber R369

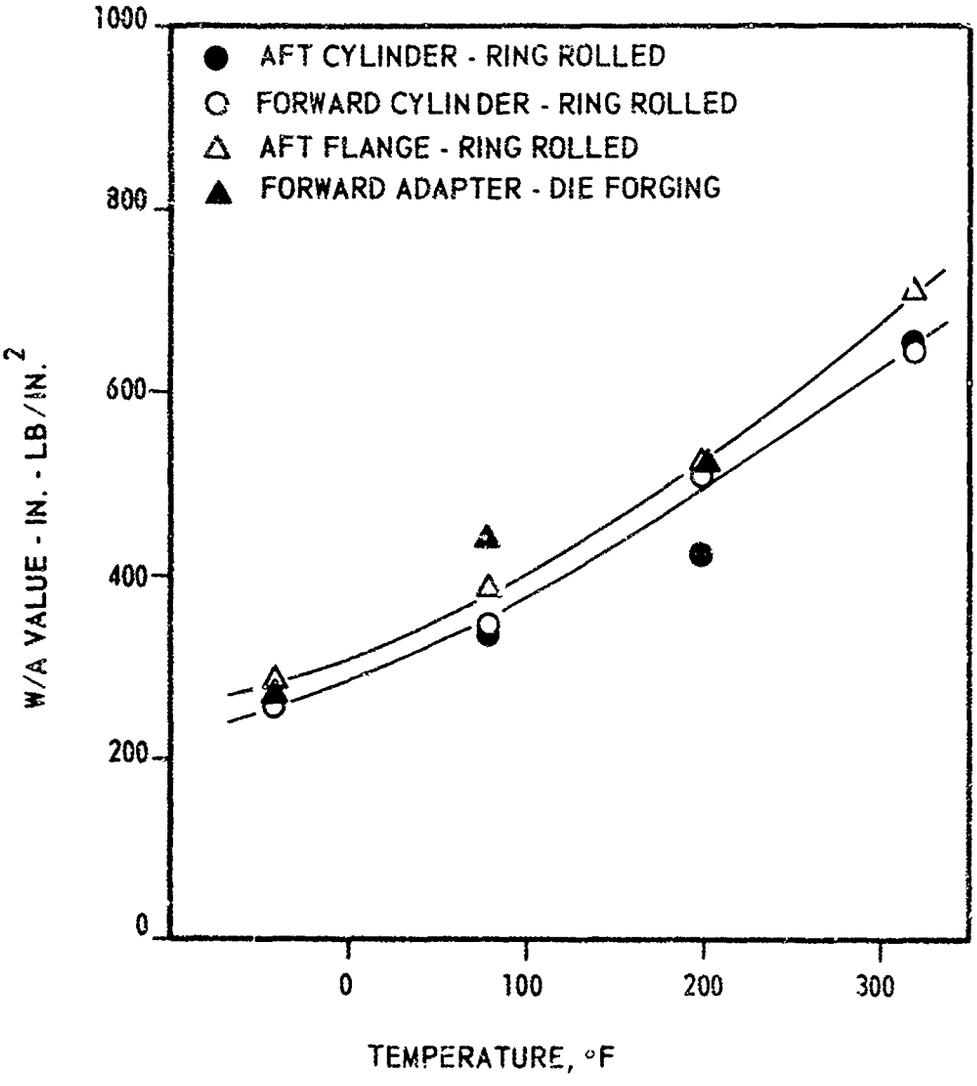

Figure 30. Chamber R490

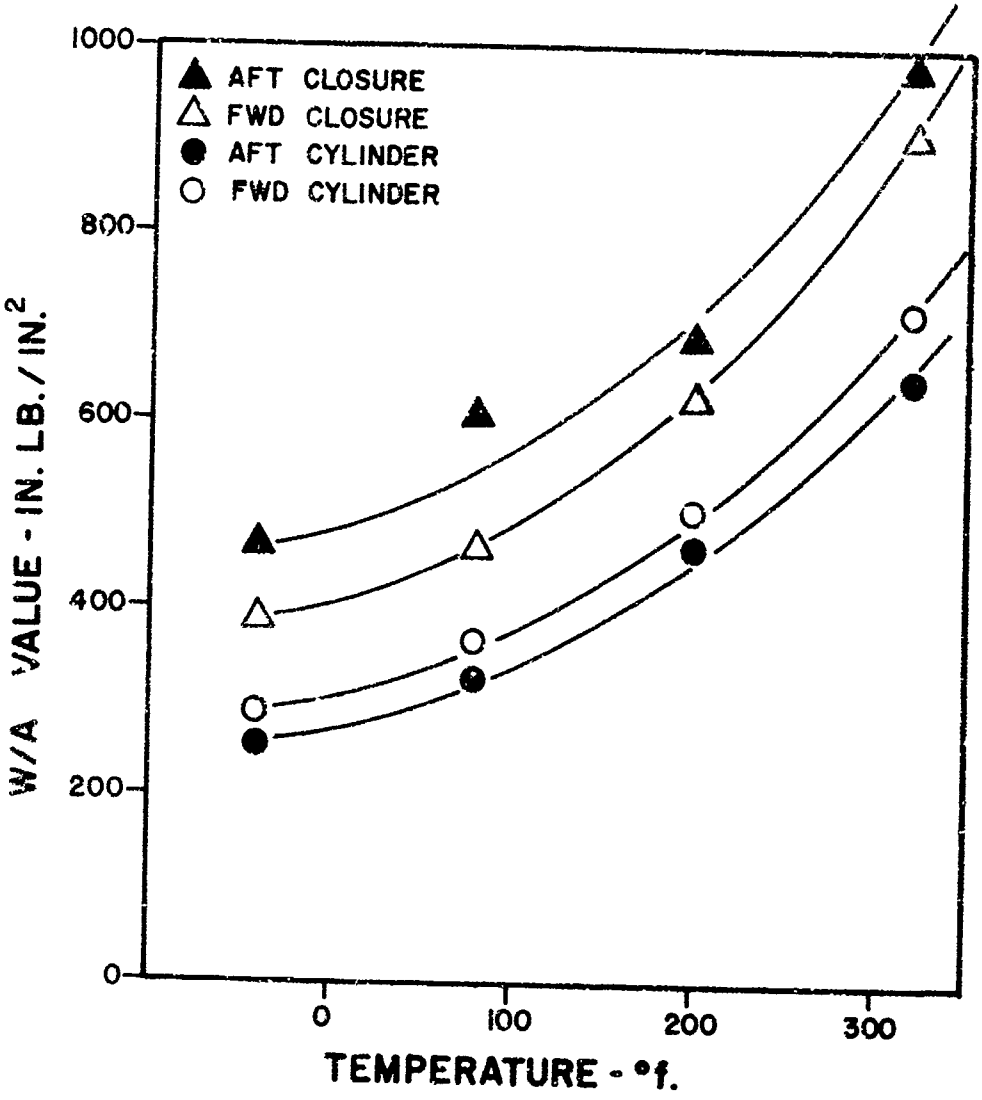

Figure 31. Chamber R512

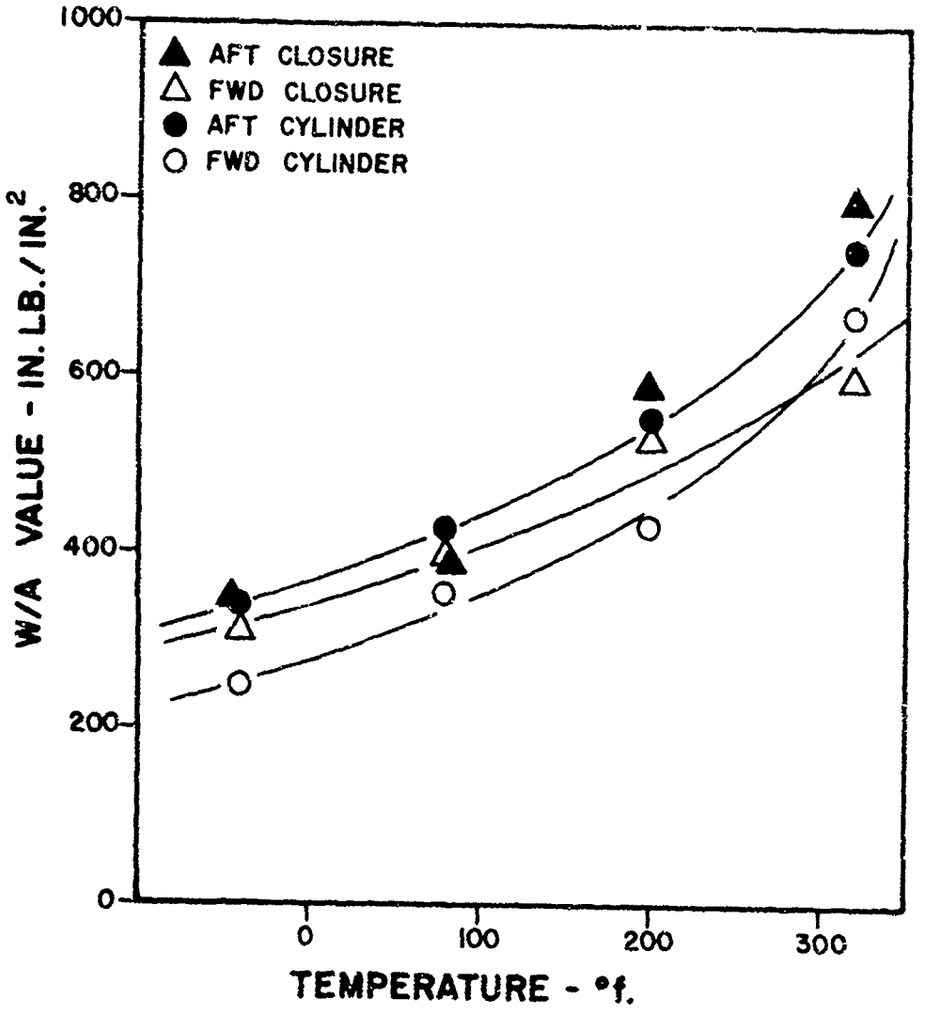

Figure 32. Chamber R516

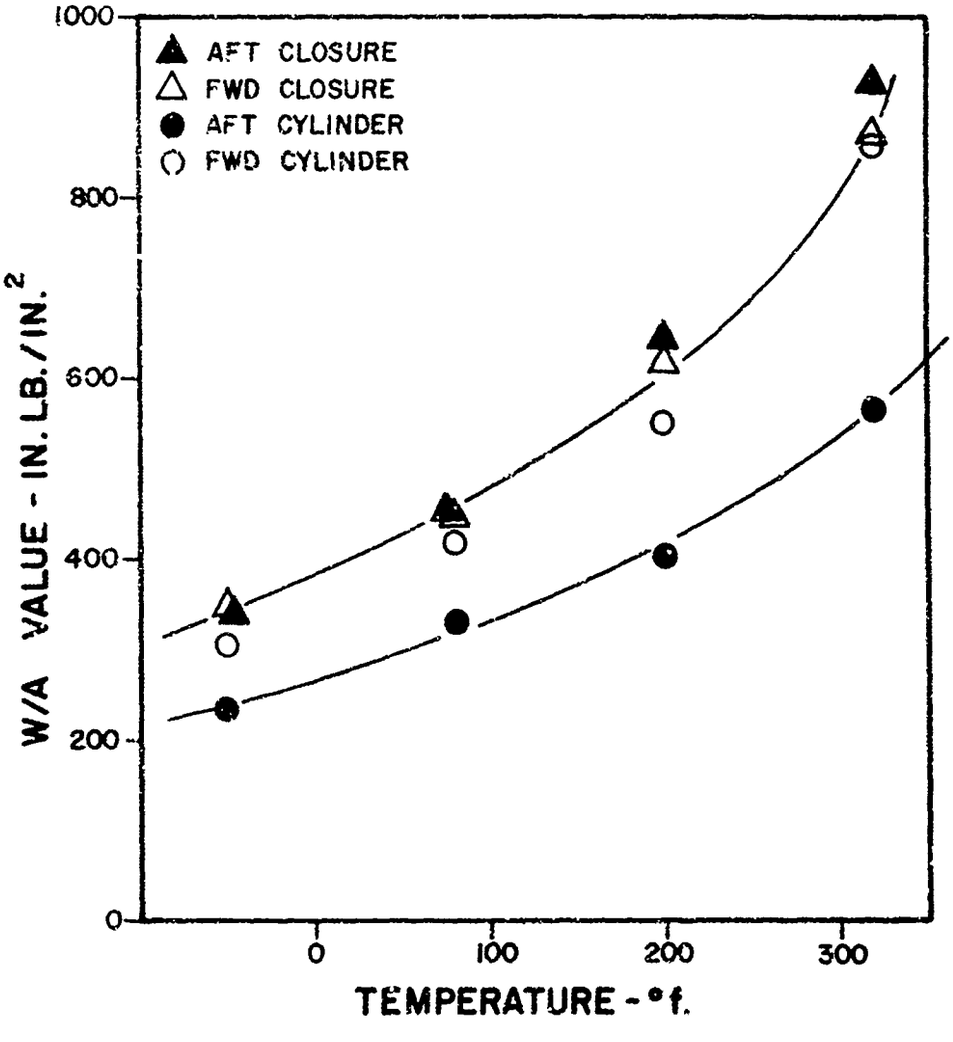

Figure 33. Chamber R543

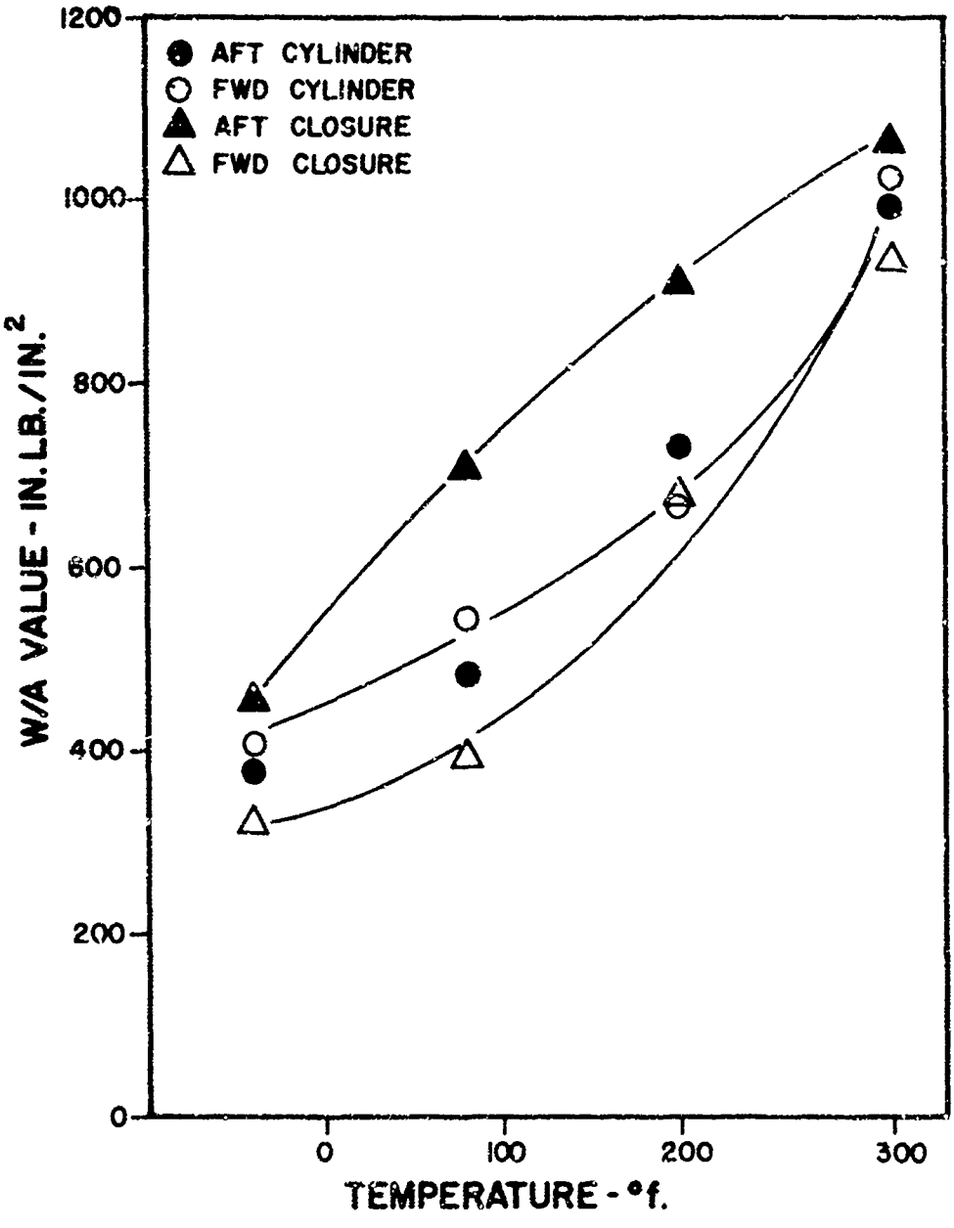

Figure 34. Chamber 673078

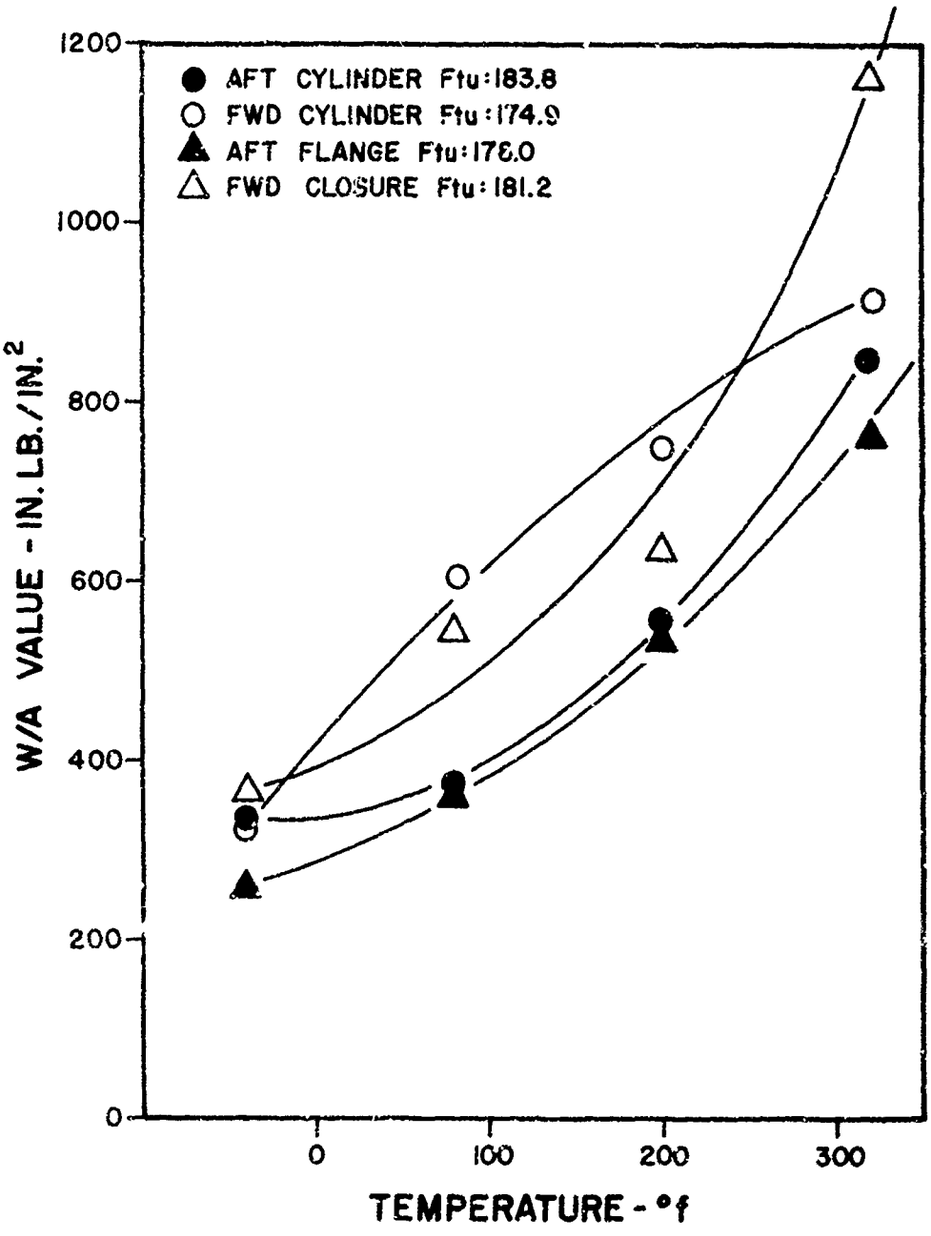

CYLINDERS RING ROLLED BY LADISH
CLOSURES DIE FORGED BY LADISH

Figure 35. Chamber 673095

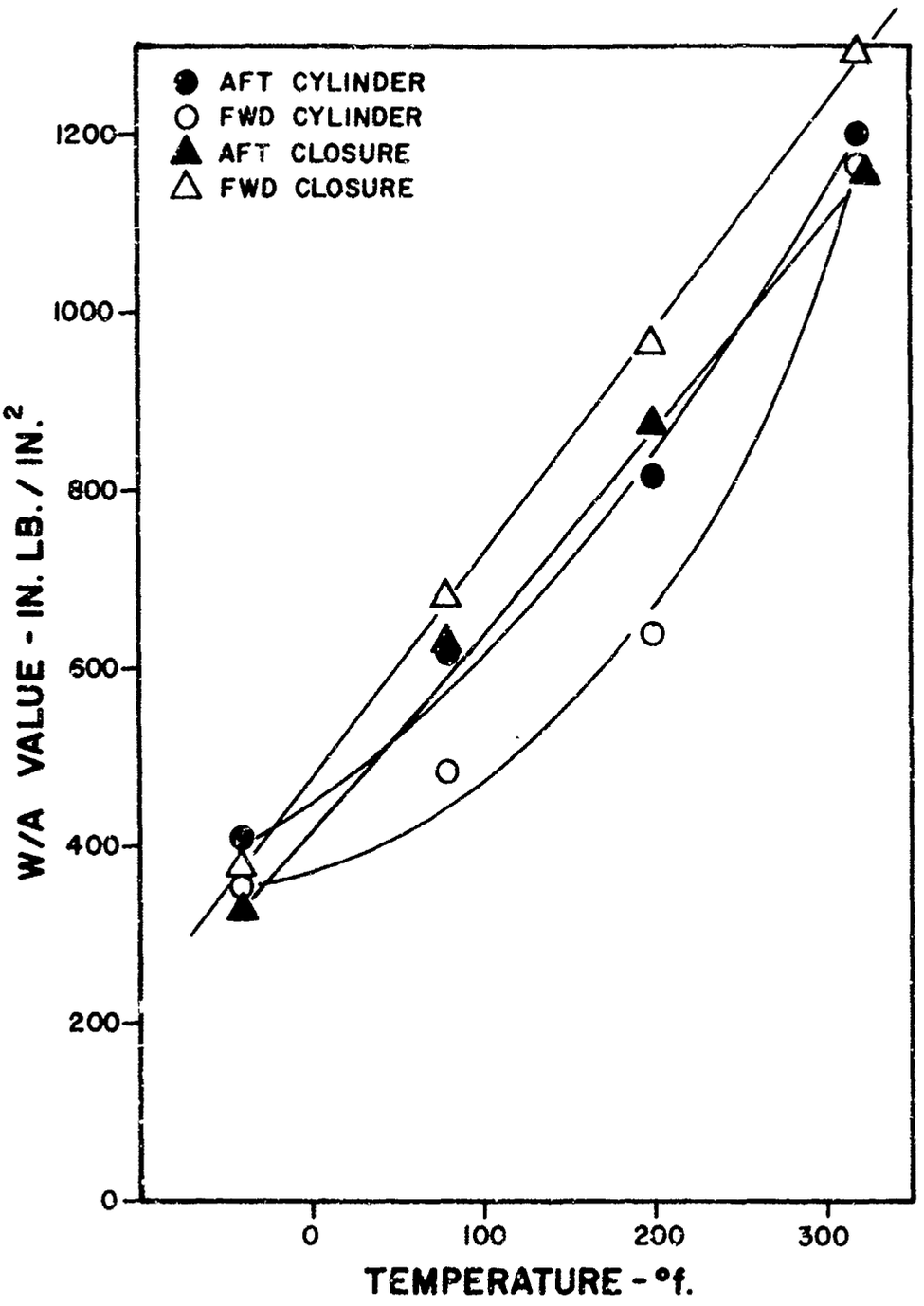

Figure 36. Chamber 673122

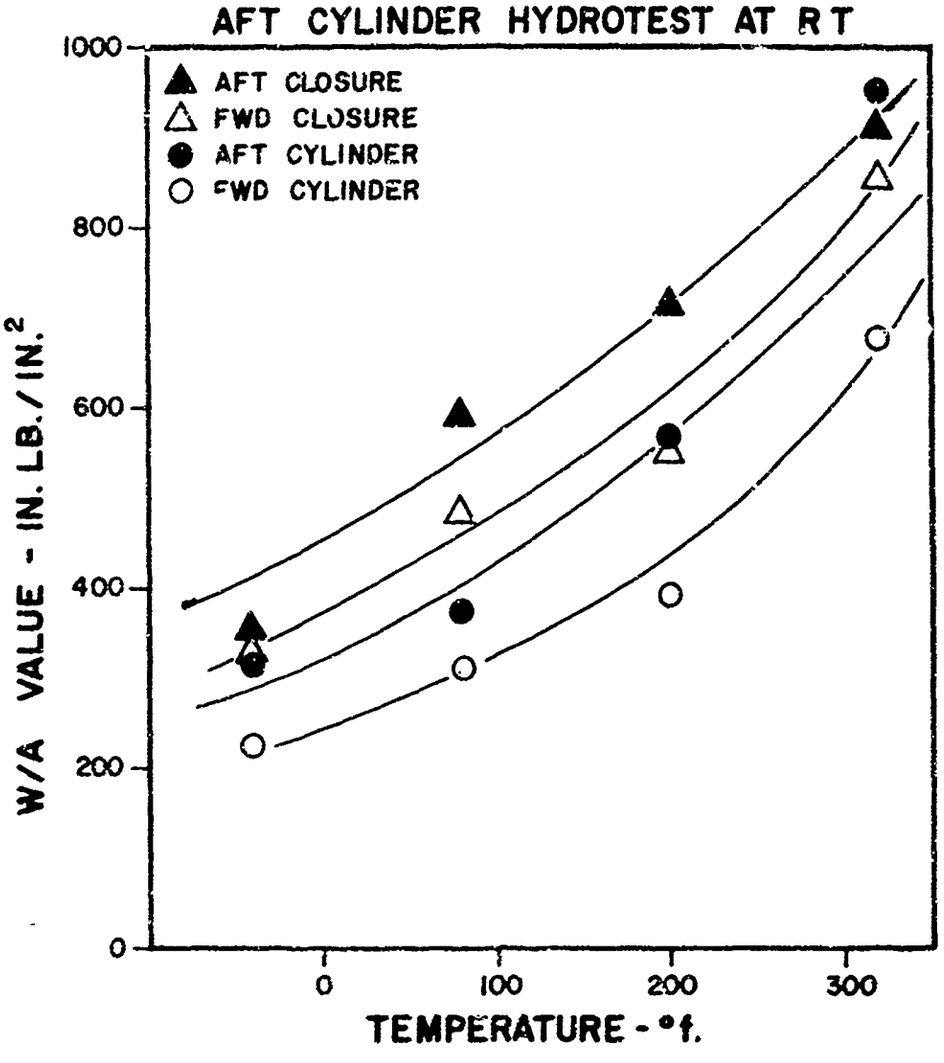

Figure 37. Chamber 674514

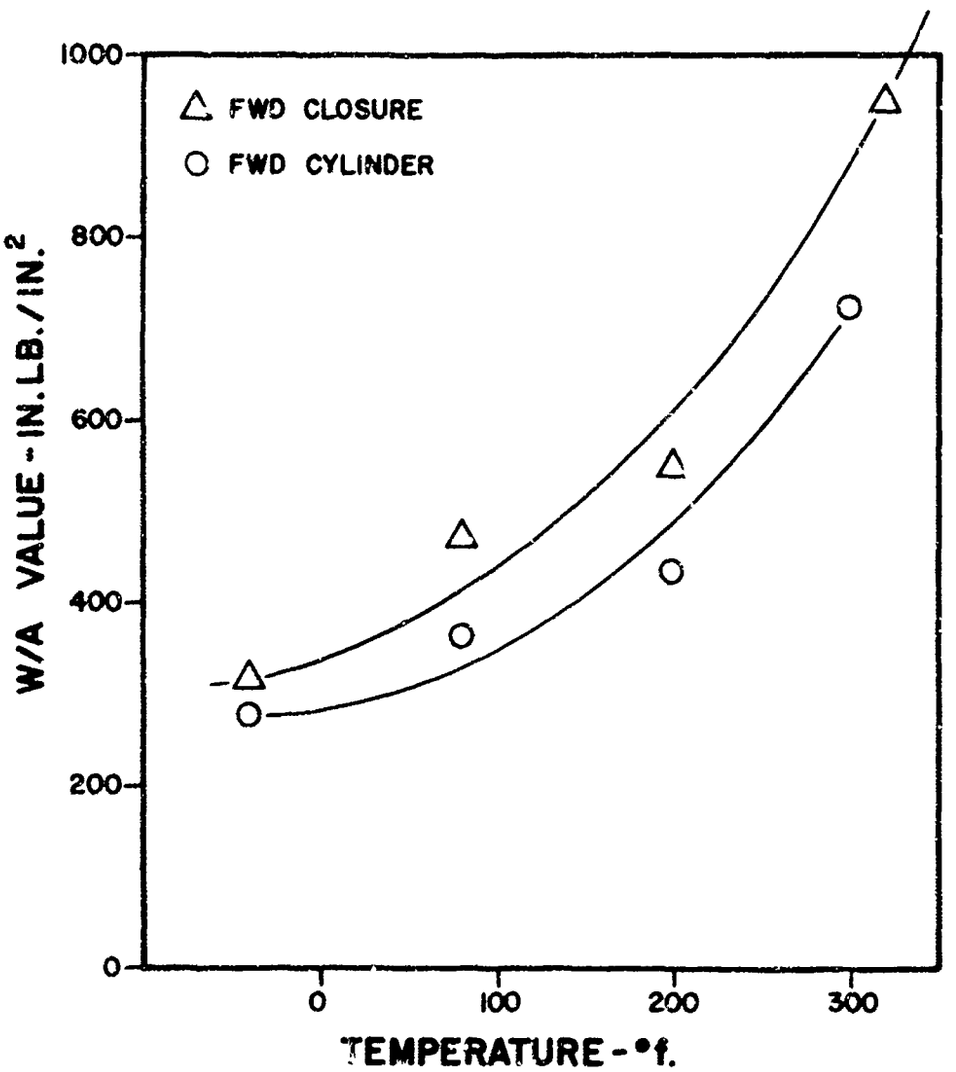

Figure 38. Chamber 2192109

Unclassified
Security Classification

DOCUMENT CONTROL DATA - R&D
(Security classification of title, body of abstract and indexing annotation must be entered when the overall report is classified)

1 ORIGINATING ACTIVITY (Corporate author) Aerojet-General Corporation Sacramento, California 95813	2a REPORT SECURITY CLASSIFICATION Unclassified 2b GROUP N/A

3 REPORT TITLE

Tensile Properties and Fracture Toughness of 6Al-4V Titanium

4 DESCRIPTIVE NOTES (Type of report and inclusive dates)

April 1968 to March 1969

5 AUTHOR(S) (Last name, first name, initial)

Hartbower, C. E., Reuter, W. G., and Crimmins, P. P.

6 REPORT DATE	7a TOTAL NO OF PAGES	7b NO. OF REFS
March 1969	201	20

8a CONTRACT OR GRANT NO	9a ORIGINATOR'S REPORT NUMBER(S)
F33615-67-C-1358 b PROJECT NO 7381 c Task 738106 d	N/A 9b OTHER REPORT NO(S) (Any other numbers that may be assigned this report) AFML-TR-68-163, Vol II

10 AVAILABILITY/LIMITATION NOTICES

This document is subject to special export controls and each transmittal to foreign governments or foreign nationals may be made only with prior approval of the Air Force Materials Laboratory (MAAE), Wright-Patterson Air Force Base, Ohio 45433

11 SUPPLEMENTARY NOTES	12 SPONSORING MILITARY ACTIVITY
	Air Force Materials Laboratory

13 ABSTRACT

(See Attached)

DD FORM 1 JAN 64 1473

Unclassified
Security Classification

Unclassified

Security Classification

14 KEY WORDS	LINK A		LINK B		LINK C	
	ROLE	WT	ROLE	WT	ROLE	WT
6Al-4V Titanium MIL-HDBK-5 Data Fracture Toughness Fracture Testing Chamber Performance						

INSTRUCTIONS

1. ORIGINATING ACTIVITY: Enter the name and address of the contractor, subcontractor, grantee, Department of Defense activity or other organization *(corporate author)* issuing the report.

2a. REPORT SECURITY CLASSIFICATION. Enter the overall security classification of the report. Indicate whether "Restricted Data" is included. Marking is to be in accordance with appropriate security regulations.

2b. GROUP: Automatic downgrading is specified in DoD Directive 5200.10 and Armed Forces Industrial Manual. Enter the group number. Also, when applicable show that optional markings have been used for Group 3 and Group 4 as authorized.

3. REPORT TITLE: Enter the complete report title in all capital letters. Titles in all cases should be unclassified. If a meaningful title cannot be selected without classification, show title classification in all capitals in parenthesis immediately following the title.

4. DESCRIPTIVE NOTES: If appropriate, enter the type of report, e.g., interim, progress, summary, annual, or final. Give the inclusive dates when a specific reporting period is covered.

5. AUTHOR(S): Enter the name(s) of author(s) as shown on or in the report. Enter last name, first name, middle initial. If military, show rank and branch of service. The name of the principal author is an absolute minimum requirement.

6. REPORT DATE: Enter the date of the report as day, month, year, or month, year. If more than one date appears on the report, use date of publication.

7a. TOTAL NUMBER OF PAGES: The total page count should follow normal pagination procedures, i.e., enter the number of pages containing information.

7b. NUMBER OF REFERENCES: Enter the total number of references cited in the report.

8a. CONTRACT OR GRANT NUMBER: If appropriate, enter the applicable number of the contract or grant under which the report was written.

8b, 8c, & 8d. PROJECT NUMBER: Enter the appropriate military department identification, such as project number, subproject number, system numbers, task number, etc.

9a. ORIGINATOR'S REPORT NUMBER(S): Enter the official report number by which the document will be identified and controlled by the originating activity. This number must be unique to this report.

9b. OTHER REPORT NUMBER(S): If the report has been assigned any other report numbers *(either by the originator or by the sponsor)*, also enter this number(s).

10. AVAILABILITY/LIMITATION NOTICES: Enter any limitations on further dissemination of the report, other than those imposed by security classification, using standard statements such as:

(1) "Qualified requesters may obtain copies of this report from DDC."

(2) "Foreign announcement and dissemination of this report by DDC is not authorized."

(3) "U. S. Government agencies may obtain copies of this report directly from DDC. Other qualified DDC users shall request through _____."

(4) "U. S. military agencies may obtain copies of this report directly from DDC. Other qualified users shall request through _____."

(5) "All distribution of this report is controlled. Qualified DDC users shall request through _____."

If the report has been furnished to the Office of Technical Services, Department of Commerce, for sale to the public, indicate this fact and enter the price, if known.

11. SUPPLEMENTARY NOTES: Use for additional explanatory notes.

12. SPONSORING MILITARY ACTIVITY: Enter the name of the departmental project office or laboratory sponsoring *(paying for)* the research and development. Include address.

13 ABSTRACT: Enter an abstract giving a brief and factual summary of the document indicative of the report, even though it may also appear elsewhere in the body of the technical report. If additional space is required, a continuation sheet shall be attached.

It is highly desirable that the abstract of classified reports be unclassified. Each paragraph of the abstract shall end with an indication of the military security classification of the information in the paragraph, represented as *(TS), (S), (C), or (U)*

There is no limitation on the length of the abstract. However, the suggested length is from 150 to 225 words.

14. KEY WORDS: Key words are technically meaningful terms or short phrases that characterize a report and may be used as index entries for cataloging the report. Key words must be selected so that no security classification is required. Identifiers, such as equipment model designation, trade name, military project code name, geographic location, may be used as key words but will be followed by an indication of technical context. The assignment of links, rules, and weights is optional.

Unclassified

Security Classification